INVESTIGATION OF PHYTOCHEMICALS FROM

CALOPHYLLUM SPECIES FOR THEIR CYTOTOXIC

AND ANTIOXIDANT ACTIVITIES

HEMAROOPINI A/P SUBRAMANIAM

MASTER OF SCIENCE

FACULTY OF SCIENCE

UNIVERSITI TUNKU ABDUL RAHMAN

MAY 2017

INVESTIGATION OF PHYTOCHEMICALS FROM *CALOPHYLLUM* SPECIES FOR THEIR CYTOTOXIC AND ANTIOXIDANT ACTIVITIES

By

HEMAROOPINI A/P SUBRAMANIAM

A dissertation submitted to the Department of Chemical Science

Faculty of Science,

Universiti Tunku Abdul Rahman,

in partial fulfillment of the requirements for the degree of

Master of Science

May 2017

Specially dedicated to
my beloved family

ABSTRACT

INVESTIGATION OF PHYTOCHEMICALS FROM *CALOPHYLLUM* SPECIES FOR THEIR CYTOTOXIC AND ANTIOXIDANT ACTIVITIES

Hemaroopini a/p Subramaniam

Chemical investigation on the stem barks of three *Calophylum* species, namely *C. teysmannii*, *C. andersonii* and *C. soulattri* has resulted in the isolation of a new chromanone acid, caloteysmannic acid (**71**), a new phloroglucinol derivative, calosubellinone (**78**) along with other eight known compounds, namely isocalolongic acid (**72**), calolongic acid (**73**), stigmasterol (**74**), friedelin (**75**), friedelinol (**76**), protocatechuic acid (**77**), garsubellin B (**79**) and soulattrone A (**80**). All these compounds were identified based on modern spectroscopic methods including 1D NMR (^{1}H and ^{13}C), 2D NMR (HMQC and HMBC), UV-Vis, IR and mass spectrometry.

Study on the stem bark extracts of *C. teysmannii* furnished compounds **71**-**74**, *C. andersonii* afforded compounds **75**-**77**, and *C. soulattri* yielded compounds **78**-**80**. All the crude extracts and pure compounds obtained were screened for their cytotoxic activity against HeLa, MDA-MB-231, LS174T and T98G cancer cell lines, and HEK293 normal human cell line via MTT colourimetric assay, in addition to DPPH assay.

The assay results revealed that there is a substantial correlation between the chemical classes of test compounds and their cytotoxicity. The cytotoxic activity of compounds against the four cancer cell lines was reported to show decreasing cytotoxic effect in the following order: chromanone acids **71**, **72** & **73** > simple phenolic compound **77** > phloroglucinol derivatives **77** & **78** > terpenoids **74**, **75**, **76** & **80**. Chromanone acids **71**, **72** and **73** showed promising cytotoxic effects on HeLa, MDA-MB-231, LS174T and T98G cancer cell lines with IC_{50} values in the range of 4.2 to 11.8 μg/mL. Moreover, they were found to exhibit good cancer-specific cytotoxicity with IC_{50} value against normal human HEK293 cells which was at least 5-fold higher than that of cancer cells. On top of that, compounds **71**, **72** and **73** also showed comparable growth inhibitory activities with the positive control, cisplatin towards LS174T and T98G cancer cells.

Based on the DPPH results, in general, the test compounds displayed their antioxidant potency in the following decreasing order of radical scavenging activity: simple phenolic compound > phloroglucinol derivatives > terpenoids > chromanone acids. Protocatechuic acid (**77**) showed the highest antioxidant activity with IC_{50} value of 4.0 μg/mL which was identical to that of positive control, vitamin C. Besides, calosubellinone (**78**) also showed strong radical scavenging activity (IC_{50} = 8.5 μg/mL) comparable to the positive control, kaempferol (IC_{50} = 8.0 μg/mL).

ACKNOWLEDGEMENT

First and foremost, I would like to express my sincere gratitude to the Almighty for his blessings that has allowed me to achieve this milestone. I am deeply indebted to my supervisor Dr Lim Chan Kiang for his warm hospitality, constructive criticism and encouragements during the write up of this dissertation. Through his supervision, I have gained precious experience in learning of various scientific techniques and knowledge throughout my postgraduate study. His guidance has significantly expanded my research capabilities as he constantly challenged my scope of knowledge in the field of chemistry. I would also like to extend my appreciation to my co-supervisor, Dr Say Yee How for his guidance throughout this research project pertaining to bioassay screening.

A huge thanks to the academic and laboratory staffs of Faculty of Science for their guidance and assistance. Thanks to fellow postgraduates students for their support and encouragement.

Last but not the least, I would like to express my sincere appreciation to my parents and sister, without whom I would not have come this far. Thank you for believing in me and constantly pushing me beyond my capabilities.

APPROVAL SHEET

This dissertation/thesis entitled "**INVESTIGATION OF PHYTOCHEMICALS FROM *CALOPHYLLUM* SPECIES FOR THEIR CYTOTOXIC AND ANTIOXIDANT ACTIVITIES"** was prepared by **HEMAROOPINI A/P SUBRAMANIAM** and submitted as partial fulfillment of the requirements for the degree of Master of Science at Universiti Tunku Abdul Rahman.

Approved by:

_____

(Dr. LIM CHAN KIANG)   Date:…………………..

Assistant Professor/Supervisor

Department of Chemical Science

Faculty of Science

Universiti Tunku Abdul Rahman

_____

(Dr. SAY YEE HOW)   Date:…………………..

Associate Professor/Co-supervisor

Department of Biomedical Science

Faculty of Science

Universiti Tunku Abdul Rahman

FACULTY OF SCIENCE

UNIVERSITI TUNKU ABDUL RAHMAN

Date: _____

SUBMISSION OF DISSERTATION

It is hereby certified that **HEMAROOPINI A/P SUBRAMANIAM** (ID No: **14ADM04870**) has completed this dissertation entitled "**INVESTIGATION OF PHYTOCHEMICALS FROM *CALOPHYLLUM* SPECIES FOR THEIR CYTOTOXIC AND ANTIOXIDANT ACTIVITIES**" under the supervision of Dr. Lim Chan Kiang (Supervisor) from the Department of Chemical Science, Faculty of Science, and Dr. Say Yee How (Co-Supervisor) from the Department of Biomedical Science, Faculty of Science.

I understand that University will upload softcopy of my dissertation in pdf format into UTAR Institutional Repository, which may be made accessible to UTAR community and public.

Yours truly,

_____

(Hemaroopini a/p Subramaniam)

DECLARATION

I hereby declare that the dissertation is based on my original work except for quotations and citations which have been duly acknowledged. I also declare that it has not been previously or concurrently submitted for any other degree at UTAR or other institutions.

Name _____

(HEMAROOPINI A/P SUBRAMANIAM)

Date _____

TABLE OF CONTENTS

LIST OF TABLES

LIST OF FIGURES

LIST OF SYMBOLS/ABBREVIATIONS

^{1}H	Proton
1D-NMR	One Dimensional Nuclear Magnetic Resonance
2D-NMR	Two Dimensional Nuclear Magnetic Resonance
^{13}C	Carbon
Å	Angstrom
β	Beta
δ	Chemical shift
δ_C	Chemical shift of carbon
δ_H	Chemical shift of proton
λ_{max}	Maximum wavelength
μg	Microgram
μL	Microliter
Acetone-d_6	Deuterated acetone
ATPase	Adenosine triphosphatase
brs	Broad singlet
c	Concentration of sample in g/mL
CC	Column chromatography
$CDCl_3$	Deuterated chloroform
d	Doublet
DCM	Dichloromethane
dd	Doublet of doublet
DMSO	Dimethylsulfoxide

DPPH	1,1-diphenyl-2-picrylhydrazyl
EIMS	Electron Ionization Mass Spectrometry
EtOAc	Ethyl acetate
FTIR	Fourier-Transform Infrared Spectroscopy
GC-MS	Gas Chromatography-Mass Spectrometry
HEK293	Human embryonic kidney cells
HeLa	Cervical carcinoma
HMBC	Heteronuclear Multiple Bond Coherence
HMQC	Heteronuclear Multiple Quantum Coherence
HPLC	High Performance Liquid Chromatography
HREIMS	High Resolution Electrospray Ionization Mass Spectrometry
Hz	Hertz
IC_{50}	Half maximal inhibitory concentration
ICAM-1	Intercellular adhesion molecule 1
IL-6	Interleukin 6
IL-8	Interleukin 8
IR	Infrared
J	Coupling constant in Hertz
K^+	Potassium ion
K	Kelvin
KBr	Potassium bromide
LC-MS	Liquid Chromatography-Mass Spectrometry
LS174T	Colorectal carcinoma

m	Multiplet
m/z	Mass-to-charge ratio
MDA-MB-231	Breast adenocarcinoma
MeOH	Methanol
mM	Milimoles
Mo-Kα	Molybdenum – K-alpha
mol	Mole
mp	Melting point
MTT	3-(4,5-dimethylthiazol-2-yl)-2,5-diphenyltetrazolium bromide
Na^+	Sodium ion
nm	Nanometer
NMR	Nuclear Magnetic Resonance
O-H	Oxygen-Hydrogen (or Hydroxyl)
ppm	Part per million
qd	Quartet of doublets
R_f	Retention factor
s	Singlet
Si	Silica
t	Triplet
T98G	Ganglioblastoma
TLC	Thin Layer Chromatography
TMS	Tetramethylsilane
UV-Vis	Ultraviolet-Visible

CHAPTER 1

INTRODUCTION

1.1 General Introduction

Nature has been discovered as a remarkable source of therapeutic agents since the evolution of human intellect. Where there is life, there are diseases and death. In the dire need to halt the severity of illness and death, human beings are depending on forests for remedial measures whereby plants are prepared in the form of decoctions or poultice to accelerate healing. Over the years, plant remedies came to surface from the remnants found at the ancient dwellings.

The earliest use of medicinal plants was evident in "Rig Veda", which is the oldest repository of human knowledge being written around 3000-2500 BC, followed by the evolution of Ayurveda, the precursor of Indian medicine around 2000 BC (Chintalapally and Rao, 2016). On the other hand, China has been a great contributor to the herbal medicine development around the world mainly due to its profound historical background in herbal medicine. The catalog of Chinese herbs recorded in Shen Nung Pen Tsao Ching, to be highlighted particularly, is believed to be the oldest record which has then been successively revised and extended in different dynasties of China (Talapatra and Talapatra, 2015). Along with the rise of the later empires, this remedial knowledge was further expanded, moving towards Egypt, Greece

and to other parts of the world, having an indisputable influence on human therapy until today.

Today, natural product chemistry studies mainly the secondary metabolites derived from living organisms through isolation, structural identification and chemical characterization of organic compounds. This area is predominantly focused on the chemistry of compounds in addition to the screening for their biological activities. With the advancement of technology and man-power development, various well-established methods for extraction and isolation of natural products are made available today. Hence, this area of chemistry has exclusively broadened the horizons for plant-based drug development.

The more interesting side of natural products is that, apart from acting as new drug in unmodified state, natural products can also be used as chemical "building blocks" to synthesize more complex molecules. For example, diosgenin is isolated from *Dioscorea floribunda* and it can be chemically modified for the production of oral contraceptives (Sarker and Nahar, 2012)

Natural products are extensively studied in the search for new therapeutic agents which are highly demanded to combat the increasing problems of incurable diseases, emergence of new diseases, antibiotic resistance, and not forgetting the toxicity of several existing medical products (Zhang and Demain, 2005). Therefore, natural products together with other approaches may expand the molecular armamentarium for therapeutic choices, and give way for the finding of new undiscovered routes in drug discovery.

1.2 Cancer and Natural Products as Anticancer Agents

Cancer is a group of diseases characterized by the uncontrolled growth and spread of abnormal cells that can lead to death. The causes of cancer can be due to external or internal factors. External factors include infectious organisms, tobacco and lifestyle practices, and internal factors such as hormones, inherited genetic mutations and immune condition. These factors may act collectively or in sequence to cause cancer. The general conventional methods used for the treatment of cancer are surgery, chemotherapy and radiation (American Cancer Society, 2016).

In the global context, cancer has been the major cause of death, with lung, stomach, colorectal and breast cancers being the leading types of cancer with high mortality rate (World Health Organisation, 2011). Hence, extensive study has been conducted to discover antitumour agents from natural products to fight against cancer cells.

Despite the existence of a number of anticancer drugs and treatments, there is still a critical need for less toxic and abusive drugs. The major concern and objective of research in development of cancer drug is to discover new drugs that act specifically on cancer cells, without imposing any harms to normal healthy cells, thereby reducing the undesired side effects. From the repertoire of existing plant derived drugs, vinblastine and vincristine isolated from the Madagascar periwinkle *Catharanthus roseus* (Roepke et al., 2010) have been the best known natural drugs in the clinical use for the treatment of cancer.

Hence, the search of anticancer agents from plant sources has been continued to discover more tolerable drugs with minimal side effects.

1.3 Future Prospects of Natural Products in Therapy

Today, natural products are widely used worldwide for medical purposes and continue to be a profound medicinal practice in various parts of the world due to the fact that natural products are less toxic compared to the conventional drugs. Among developing nations, particularly those in Latin America, Asia, Africa and the Middle East, 70% to 95% of the population are depending on these traditional remedies for primary health management. The global market for traditional medicines was reported at US$ 83 billion in 2008, with a rapid rate of growth. In some industrialized countries the practice of traditional medication is equally substantial. France, Canada, Italy and Germany for example, reported that about 70% to 90% of their populations utilize traditional medicines for their health care (World Health Organisation, 2011).

A study conducted by WHO's Roll Back Malaria programme reported that in Mali, Zambia, Ghana and Nigeria, approximately 60% of febrile cases among children, predominantly caused by malaria, are treated using herbal remedies at home (World Health Organisation, 2002). Information gathered by UNAIDS disclosed that most of the HIV/AIDS patients in developing countries use traditional remedies to manage opportunistic infections (Joint United Nations Programme on HIV/AIDS, 2003). Other ailments usually

treated with traditional medicines include bronchitis, diarrhea, headaches, microbial infections, sickle-cell anaemia, hypertension, diabetes, burns, rashes, insomnia and menopause (Calixto, 2000). In the future, natural products will continue to flourish as valuable source of therapeutic agents due to the high demand for primary health care of world population.

1.4 Botany of Plant Species Studied

1.4.1 The Family Guttiferae

The Guttiferae family has received enormous attention from the scientific community due to its astounding therapeutic potentials. Guttiferae belongs to the tropical family of trees and shrubs, consisting of approximately 50 genera with around 1200 species, distributed in the warm damp tropics of the world. This family of trees was reported to be a rich source of secondary metabolites, of which xanthones, coumarins, benzophenones and bioflavonoids are the major classes of compounds (Melo et al., 2014).

1.4.2 The Genus *Calophyllum*

The name *Calophyllum* refers to beautiful leaf in the Greek language. This genus comprises of approximately 180-200 species, belonging to the Guttiferae family. *Calophyllum* is greatly distributed in the tropical Asia,

5

India, East Africa and Latin America (Antonio et al., 2014). This genus is known by the local people as "*Bintangor*" in Malaysia, "*Poonagam*" in India and "*Guanandi*" around Latin America (Orwa et al., 2009). Their growth environments vary, covering a large number of habitats including ridges in mountain forests, coastal swamps and lowland jungle (Dweck and Meadows, 2002). The genus *Calophyllum* is known to be used as traditional medicines to treat various ailments. The more widely used species is *C. inophyllum*, whereby the fruit oil has been used to treat rheumatism, gonorrhea, and itching, the gum extracted from the stems is used to treat ulcers, a decoction from the bark is used for hemorrhage and ulcer, together with other therapeutic uses such as antiseptic, expectorant, diuretic, and purgative (Filho et al., 2009). In addition, this genus is known to be used in various other fields. For instance, the wood of *C. inophyllum* is used in carpentry and constructions, whereas oil from the seed is used in soap and cosmetic manufacturing (Orwa et al., 2009).

1.4.3 *Calophyllum teysmannii*

The taxonomy of *Calophyllum teysmannii* is presented in Table 1.1.

Table 1.1: Taxonomy of *Calophyllum teysmannii*

Kingdom	: Plantae
Phylum/Division	: Magnoliophyta
Class	: Eudicots
Order	: Malphighiales
Family	: Guttiferae
Genus	: *Calophyllum*
Species	: *C. teysmannii*

C. teysmannii was named after J.E. Teysmann, a dutch gardener and horticulturist at Bogor Botanical Garden who had collected many plants in Indonesia. *Calophyllum teysmannii* is an evergreen tree, capable of growing from 3 to 40 metres tall. Its bole, which is very often with short spreading buttresses or spurs up to 70 cm tall, is up to 95 cm in diameter and has stilt roots. The bark of this plant has rough, narrow and shallow fissures with brown to grey-brown complexion. When cut, it releases a clear yellowish brown exudate. The leaves are obovate-shaped, and are distinct with a notch at the apex. The margine of the leaves are thickened and of lighter colour when it is dried. The flower of *Calophyllum teysmannii* usually has four or zero petals and its fruit is ovoid-globose, relatively smooth when dry.

This plant is distributed in Malay Peninsula and Borneo. It is widely dispersed in places such as peat swamps, flat-lying mixed dipterocarp forest, secondary forest on mangroves, kerangas vegetation and ridges in lower montane rain forest at elevations up to 1,220 metres (Stevens, 1980).

Figure 1.1: Stem of *Calophyllum teysmannii*

Figure 1.2: Leaves of *Calophyllum teysmannii*

1.4.4 *Calophyllum andersonii*

The taxonomy of *Calophyllum andersonii* is presented in Table 1.2.

Table 1.2: Taxonomy of *Calophyllum andersonii*

Kingdom	: Plantae
Phylum/Division	: Magnoliophyta
Class	: Eudicots
Order	: Malphighiales
Family	: Guttiferae
Genus	: *Calophyllum*
Species	: *C. andersonii*

Calophyllum andersonii is named after J.A.R. Anderson, who is renowned for his research on the peat swamps of northwestern Borneo, in which this species is greatly distributed. This species grows 3-40 metres tall, having short, plump terminal bugs. The flowers have four petals and fruits with a well-developed outer layer and stone walls of 0.8 mm thickness. *C. andersonii* is rather similar to *C. teysmannii,* but differs in the morphology of leaves and fruits in which leaves of *C. andersonii* are less rigid, and the midrib is not raised. In addition, the fruits of *C. andersonii* are smaller than that of *C. teysmannii* which bears larger fruits with rounded apex. The other significant difference between these two species is that the filaments of *C. andersonii* papillate toward the apex, a character that is not observed in *C. teysmannii* (Stevens, 1980).

9

1.4.5 *Calophyllum soulattri*

The taxonomy of *Calophyllum soulattri* is presented in Table 1.3.

Table 1.3: Taxonomy of *Calophyllum soulattri*

Kingdom	: Plantae
Phylum/Division	: Magnoliophyta
Class	: Eudicots
Order	: Malphighiales
Family	: Guttiferae
Genus	: *Calophyllum*
Species	: *C. soulattri*

Calophyllum soulattri or also known as Nicobar canoe tree is a tall, evergreen tree capable of growing to a height of 30 metres. It is also sometimes grown as a shade tree and ornamental. This species looks very much like *Calophyllum inophyllum* in terms of its flowers and fruits except that the leaves are narrower. The bole of this plant, which is rarely buttressed or spurred, is up to 70 cm in diameter. The timber of this plant is what makes it special. It is widely exploited from the wild for timber, which is exported in large quantities to be used for masts, spars and planking. Its latex is used as poison and the roots are used to treat ailments such as rheumatic pains. Furthermore, oil extracted from the seeds of this plant is used for the treatment of rheumatism and skin infections. *C. soulattri* is highly distributed in regions of

Southeast Asia, for instance Nicobar and Andaman Islands, Cambodia, Vietnam, Thailand, Indonesia, Malaysia, Philippines, Australia and the Solomon Islands. It is widely dispersed in places such as lowland or lower montane rainforest or sometimes in swamp forest at elevations up to 1,700 metres, alluvial sites and along rivers (Stevens, 1980).

Figure 1.3: Stem, leaves and flowers of *Calophyllum soulattri*

1. 5 Remarks on Plants Selection

Plants from the genus *Calophyllum* are revealed to be a rich source of xanthones, chromanones, coumarins, triterpenoids and bioflavonoids, many of which were reported to exhibit interesting biological activities. Hence, in this study, three *Calophyllum* species namely *C. teysmannii*, *C. andersonii* and *C. soulattri* were chosen for their chemical and biological studies with the aim to discover new and known compounds with anticancer and antioxidant properties from these plant species.

Although the three plant species selected have been previously studied for their chemical profiles by other research groups, the difference in geographic location of plant collected has distinguished my works from the other research groups as climate and soil factors might result in significant variation of chemical composition having in the same plant species at different geographic locations.

On top of that, the three plants from the same genus were chosen in this study with the aim to obtain chemical derivatives which have close structural similarity for structure-activity (SAR) study, since different plant species from the identical genus are chemotaxonomically related.

1.6 Objectives of Study

(a) To extract and isolate chemical compounds from the stem bark of *Calophyllum teysmannii*, *Calophyllum andersonii* and *Calophyllum soulattri.*

(b) To elucidate and identify the chemical structures of the isolated compounds through modern spectroscopic methods.

(c) To evaluate the cytotoxic and antioxidant activities of crude extracts and isolated compounds via MTT and DPPH assays, respectively.

CHAPTER 2

LITERATURE REVIEW

2.1 Chemistry of *Calophyllum* Species

Extensive phytochemical studies conducted on the genus *Calophyllum* have revealed it to be a rich source of xanthones, triterpenoids, coumarins and flavonoids.

2.1.1 Xanthones

An investigation on the acetone extract of the roots of *Calophyllum blancoi* has afforded five pyranoxanthones, 3-hydroxyblancoxanthone (**1**), blancoxanthone (**2**), and acetyl blancoxanthone (**3**), pyranojacaeubin (**4**) and caloxanthone (**5**) (Shen et al., 2005).

On the other hand, a phytochemical study conducted on the ethanolic extract of the twigs of *Calophyllum inophyllum* furnished two new prenylated xanthones, namely caloxanthone P (**6**) and caloxanthone O (**7**) (Dai et al., 2010).

Furthermore, a phytochemical investigation done on the petroleum ether extract of bark of *Calophyllum thorelii* gave a new tetracyclic xanthone, oxy-thorelione A (**8**) (Nguyen et al., 2012).
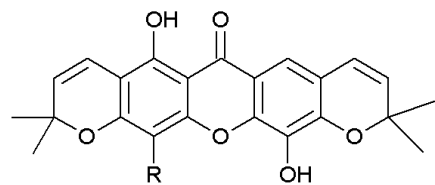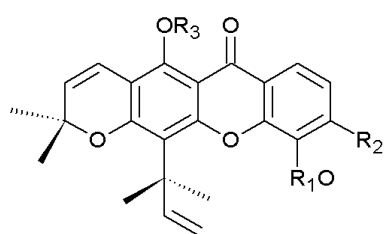
(**1**) R₁=H; R₂=OH; R₃=H
(**2**) R₁=H; R₂=H; R₃=H
(**3**) R₁=Ac; R₂=H; R₃=H

(**4**) R = H
(**5**) R = prenyl
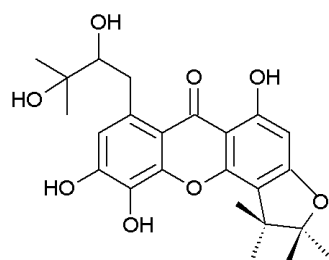
(**6**)
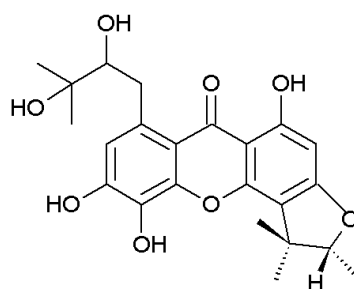
(**7**)
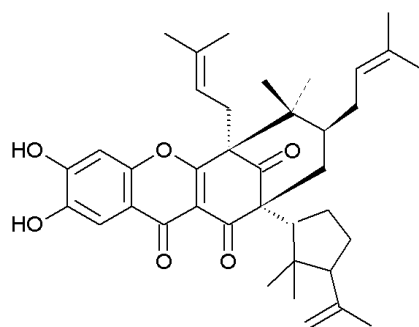
(**8**)

Figure 2.1: Structures of xanthones isolated from *Calophyllum* species

2.1.2 Triterpenoids

Three friedelane-type triterpenoids were reported for their isolation from the ethyl acetate extract of leaves of *Calophyllum inophyllum*. The triterpenoids were identified as 27-hydroxyacetate canophyllic acid (**9**), 3-oxo-27-hydroxyacetate friedelan-28-oic acid (**10**) and 3,4-secofriedelan-3,28-dioic acid (**11**) (Laure et al., 2005).

In addition to that, research carried out by Li and co-workers on the stems and leaves of *Calophyllum inophyllum* afforded a friedelane-type triterpene, 3β-23-epoxy-friedelan-28-oic acid (**12**) together with other triterpenoids, canophyllal (**13**), canophyllic acid (**14**), epifriedelanol (**15**), 3-oxo-friedelan-28-oic acid (**16**), canophyllol (**17**) and oleanolic acid (**18**) (Li et al., 2010).

(**9**) R=H (α); OH (β)
(**10**) R=O

(**11**)
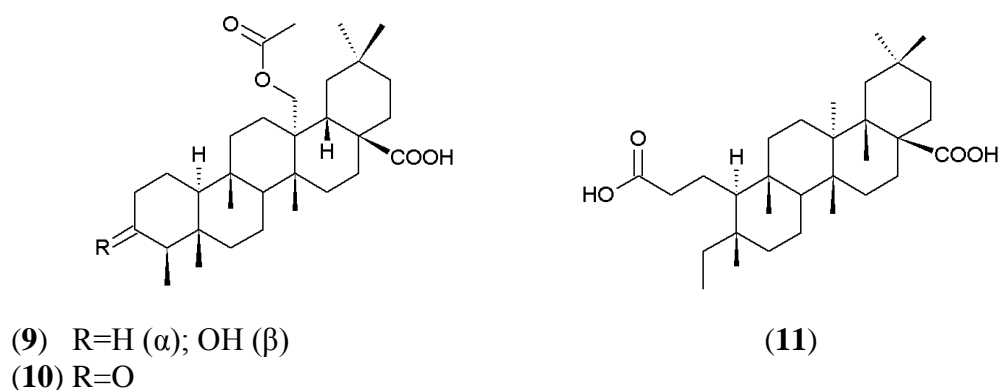
Figure 2.2: Structures of triterpenoids isolated from *Calophyllum* species
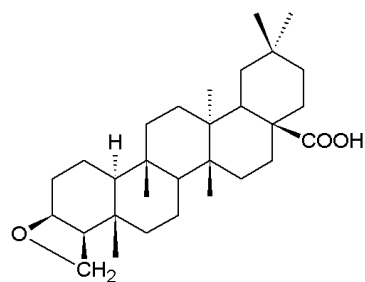
(**12**)   (**13**) R₁=O; R₂=CHO
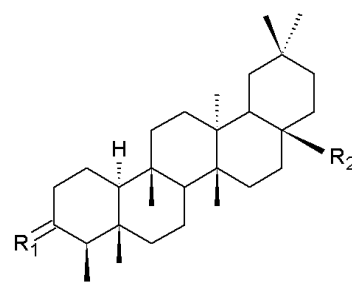
(**14**) R₁=β-OH; R₂=COOH
(**15**) R₁=β-OH; R₂=CH₃
(**16**) R₁=O; R₂=COOH
(**17**) R₁=O; R₂=CH₂OH
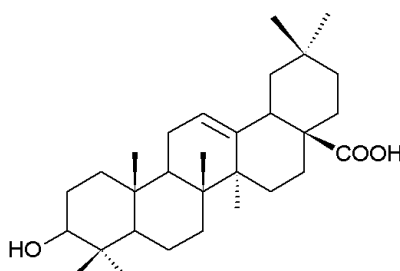
(**18**)

Figure 2.3: Structures of triterpenoids isolated from *Calophyllum* species (continued)

2.1.3 Coumarins

In year 1996, McKee and co-researchers conducted a phytochemical study on different parts of *Calophyllum lanigerum* and *Calophyllum teysmannii*. This research afforded three pyranocoumarins, namely calanolide E2 (**19**), cordatolide E (**20**) and pseudocordatolide C (**21**) from the latex, leaves and

stem bark of *Calophyllum lanigerum*, respectively. On the other hand, the leaves of *Calophyllum teysmannii* afforded calanolide F (**22**).

In year 2003, research carried out by Ito and co-workers on the acetone extract of stem bark of *Calophyllum brasiliense* furnished three 4-substituted coumarins named brasimarins A (**23**), B (**24**) and C (**25**).

Furthermore, a phytochemical study conducted on the hexane extract of stem bark of *Calophyllum soulattri* furnished a pyranocoumarin, soulamarin (**26**) (Ee et al., 2011)
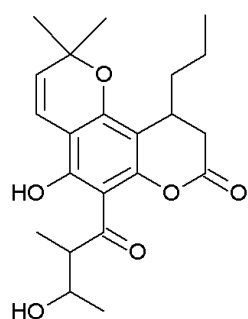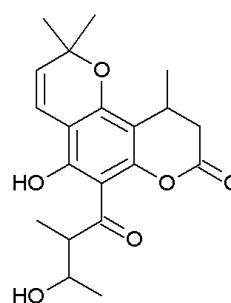
(**19**)   (**20**)
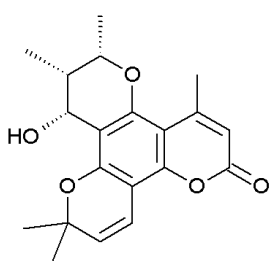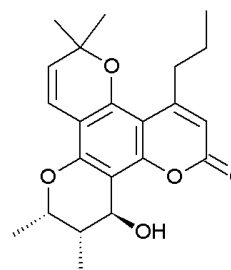
(**21**)   (**22**)

Figure 2.4: Structures of coumarin derivatives isolated from *Calophyllum* species
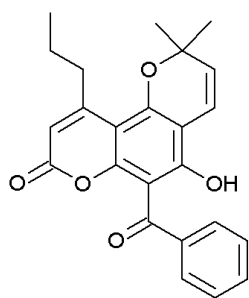
(23)
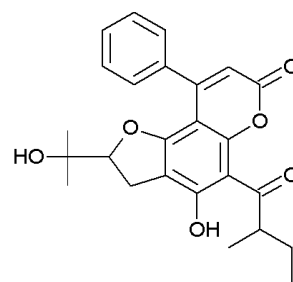
(24)
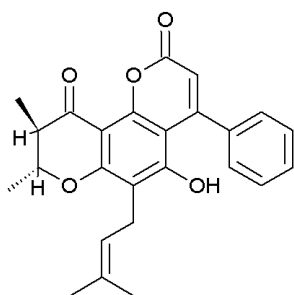
(25)
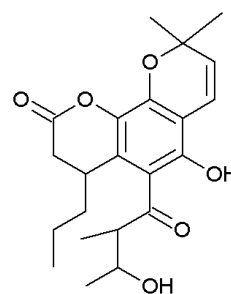
(26)

Figure 2.5: Structures of coumarin derivatives isolated from *Calophyllum* species (continued)

2.1.4 Flavonoids

In year 1984, Dharmaratne and co-researchers reported the isolation of two neoflavonoids, namely thwaitesic acid **(27)** and isothwaitesic acid **(28)** from the petrol extract of leaves of *Calophyllum lankaensis*.

In addition to that, seven biflavonoids were reported for their isolation from the leaves of *Calophyllum venulosum* through column chromatography. The

biflavonoids were identified as pyranoamentoflavone 7, 4'''-dimethyl ether (**29**), pyranoamentoflavone 7, 4'-dimethyl ether (**30**), 6''-(3-methyl-2-butenyl) amentoflavone (**31**), 6''-(2-hydroxy-3-methyl-3-butenyl)amentoflavone (**32**), pyranoamentoflavone (**33**), amentoflavone (**34**) and 2,3 dihydroamentoflavone (**35**) (Cao et al., 1997).
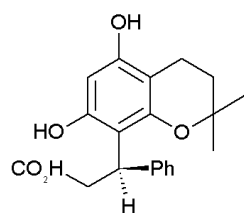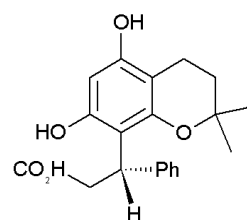
(*27*)   (*28*)
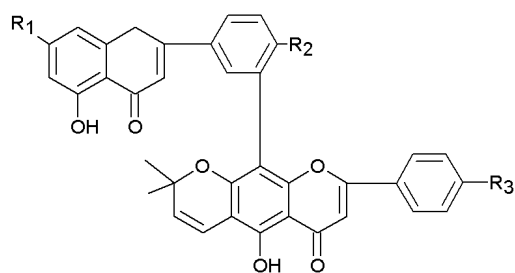
(**29**) R$_1$=OMe; R$_2$=OH; R$_3$=OMe

(**30**) R$_1$=OMe; R$_2$=OMe; R$_3$=OH

(**31**) R=

(**32**) R=
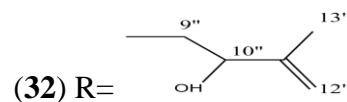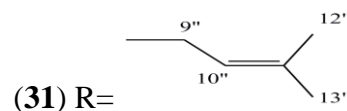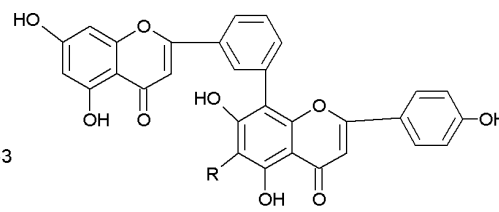
Figure 2.6: Structures of flavonoids isolated from *Calophyllum* species
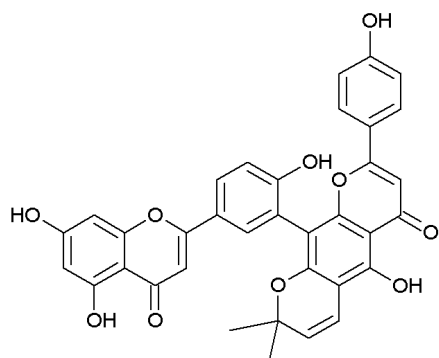
(33)
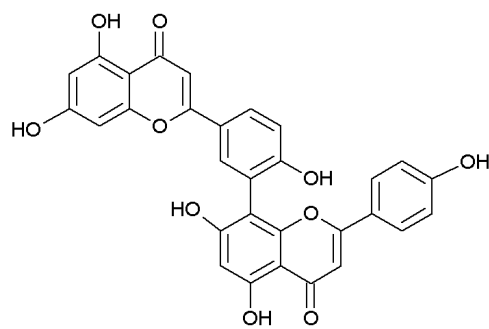
(34)
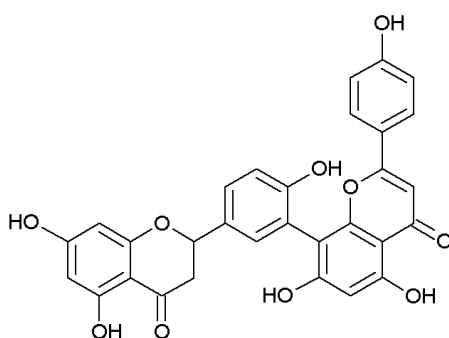
(35)

Figure 2.7: Structures of flavonoids isolated from *Calophyllum* species (continued)

2.2 Biological Activities of *Calophyllum* Species

Calophyllum species are well known for their medicinal uses and have been used traditionally in folk medicine. As such, this genus has sparked great interest among researchers to study the biological properties of the compounds isolated from this genus. Isolation of novel and new structural compounds

from different species of *Calophyllum* has provided interesting chemical diversity for more extensive research to unveil the biological potentials having in this genus.

Acquired immune deficiency syndrome or better known as AIDS has been one of the most feared diseases caused by human immunodeficiency virus (HIV). In the midst of finding a cure for this syndrome, a series of coumarins, namely calanolide A (**36**), calanolide B (**37**), calanolide C (**38**), 12-acetoxycalanolide (**39**), 12-methoxycalanolide A (**40**) and 12-methoxycalanolide B (**41**) were isolated through anti-HIV bioassay-guided fractionation of fruit and twig extracts of *Calophyllum lanigerum*. Compounds **36** and **37** were completely protective against HIV-1 replication and cytopathicity with EC_{50} values of 0.1 and 0.4 μM, respectively, but both were inactive against HIV-2. Furthermore, compound **36** was active against the AZT-resistant G-9106 and pyridinone-resistant A17 strain of HIV-1 (Kashman, 1992).

Due to alarming issues of antimicrobial drug resistance, the exploitation of natural products for new drugs with better therapeutic efficacy is urgently needed. In line with this, various species of *Calophyllum* have been screened for their antimicrobial properties. In a study conducted in Sri Lanka, a series of xanthones isolated from *Calophyllum moonii* and *Calophyllum lankensis* were screened for antimicrobial activity, particularly against methicillin-resistant *Staphylococcus aureus* (MRSA). Trapezifolixanthone (**42**), thwaitesixanthone (**43**), calothwaitesixanthone (**44**), 6-deoxy-γ-mangostin (**45**), calozeyloxanthone (**46**), batukinaxanthone (**47**) and calabaxanthone (**48**)

21

have been tested for antibacterial activity on 17 strains of MRSA, in which the inhibition of *S. aureus* was seen only with compound **44** with MIC value of 8.3 μg/mL in comparison with the positive control, vancomycin and gentamicin with the MIC values of 2 and 1 μg/mL, respectively (Dharmaratne et al., 1999).

Besides bacterial infections, the recurrence of fungal infection is also one of the medical conditions that need attention due to the resistance of fungus to various existing antifungal agents. In the search for natural products with antifungal property, six xanthones, namely caledonixanthones E (**49**), caloxanthones F (**50)** and G (**51**), dehydrocycloguanandin (**52**), 6-hydroxy-5-methoxyxanthone (**53**) and 7-hydroxy-8-methoxyxanthone (**54**) were isolated from the stem bark of *Calophyllum caledonicum,* and screened for their antifungal activities against *Aspergillus fumigatus* and *Candida albicans*. Among these compounds, compound **49** was revealed to exhibit strong antifungal activity with MIC value of 8 μg/mL, comparable to that of the positive control used, amphotericin B (Morel et al., 2002).

In year 2004, Hay and co-workers isolated seven xanthones, namely demethylcalabaxanthone (**55**), caloxanthone C (**56**), calozeyloxanthone (**46**), calothwaitesixanthone (**44**), dombakinaxanthone **(57)** 6-deoxy-γ-mangostin (**45**) and macluraxanthone (**58**) from the root bark of *Calophyllum caledonicum*. These compounds were screened for their antimalarial activity against chloroquino-resistant strains of *Plasmodium falciparum*. Compounds **44**, **45** and **56** showed potent antimalarial activity with IC$_{50}$ values of 0.9, 1.0

and 0.8 μg/mL, respectively compared with the standard chloroquine of 0.03 μg/mL.

Furthermore, the formation of advanced glycation end-products (AGEs) may trigger the development of degenerative disorders such as atherosclerosis and Alzheimer's disease. The families of Calophyllaceae and Clusiaceae have been indicated to possess compounds like polyphenols which are capable of inhibiting the formation of AGEs. In a research conducted by Ferchichi et al. (2012), the bioguided fractionation of methanol leaf extract of *Calophyllum flavoramulum* furnished 3-methoxy-2-hydroxyxanthone (**59**), canophyllol (**17**) 3,4-dihydroxy-tetrahydrofuran-3-carboxylic acid (**60**), amentoflavone (**34**) quercitrin (**61**), apelactone (**62**) and 3,4-dihydroxybenzoic acid (**63**). From this series of compounds, compounds **34** and **59** were found to show strong anti-AGEs activities with IC_{50} values of 0.05 and 0.06 mM, respectively, and moderate anti-AGEs activities were observed for compounds **61** and **62** with both IC_{50} values of 0.5 mM.

Apart from these bioactivities, *Calophyllum* species were also being extensively screened for their anticancer activities. Compounds, notably xanthones isolated from *Calophyllum* species were reported to exhibit moderate to strong cytotoxic activities on various cancer cell lines. Repeated chromatographic isolation and purification on the dichloromethane extracts of stem bark of *Calophyllum inophyllum* and *Calophyllum soulattri* yielded a series of xanthones. *Calophyllum inophyllum* afforded inophinnin (**64**) and inophinone (**65**)**,** whereas *Calophyllum soulattri* afforded soulattrin (**66**) and

phylattrin (**67**). Trapezifolixanthone (**42**), pyranojacareubin (**68**), rheediaxanthone A (**69**), macluraxanthone (**58**), 4-hydroxyxanthone (**70**) and caloxanthone C (**55**) were also isolated from both the *Calophyllum* species. These compounds were tested for cytotoxicity on B-lymphocytes (Raji), colon carcinoma cells (LS174T), human neuroblastoma cells (IMR-32) and skin carcinoma cells (SK-ML-28). Among these compounds, compound **66** showed the most potent cytotoxic activity against all the four cancer cell lines with IC_{50} values of 1.01, 1.25, 0.27 and 0.57 μg/mL, respectively (Mah et al., 2015).
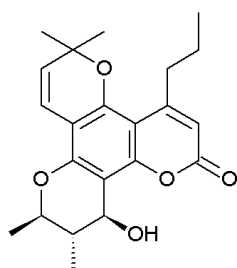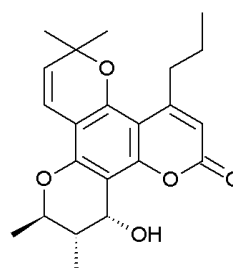
(**36**)   (**37**)

Figure 2.8: Structures of bioactive compounds isolated from *Calophyllum* species
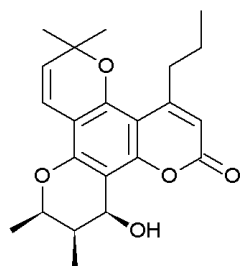
(**38**)
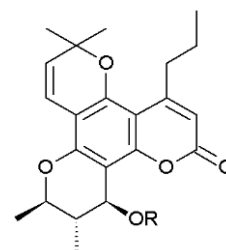
(**39**) R=Ac
(**40**) R=CH₃
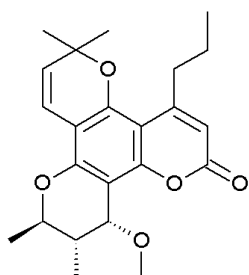
(**41**)
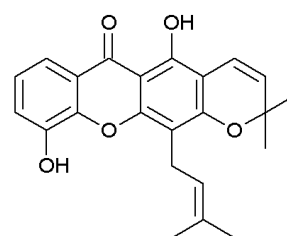
(**42**)
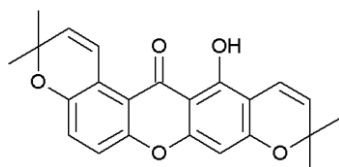
(**43**)
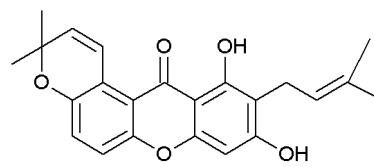
(**44**)
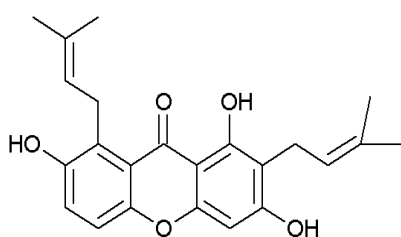
(**45**)
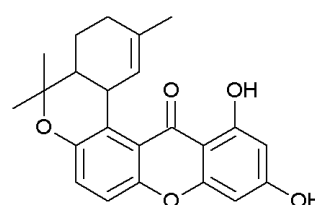
(**46**)

Figure 2.9: Structures of bioactive compounds isolated from *Calophyllum* species (continued)
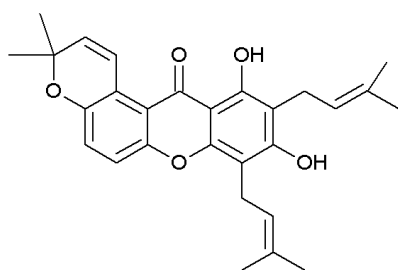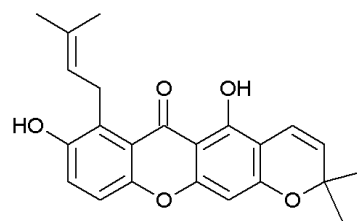
(**47**)   (**48**)
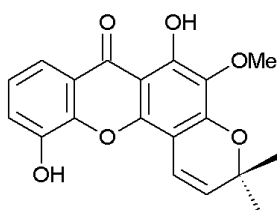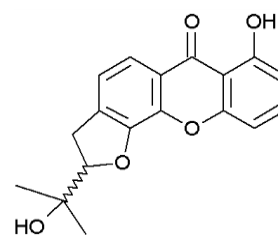
(**49**)   (**50**)
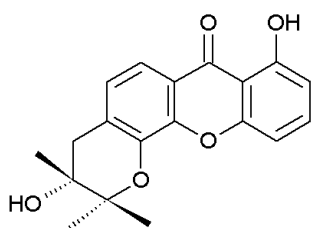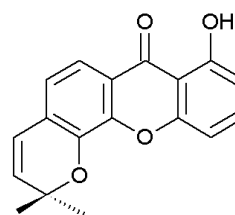
(**51**)   (**52**)

Figure 2.10: Structures of bioactive compounds isolated from *Calophyllum*
species (continued)
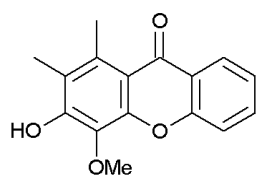
(53)
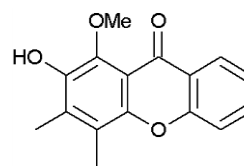
(54)
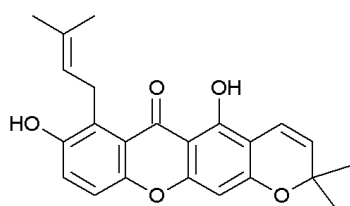
(55)
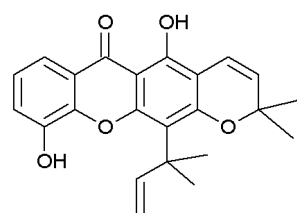
(56)
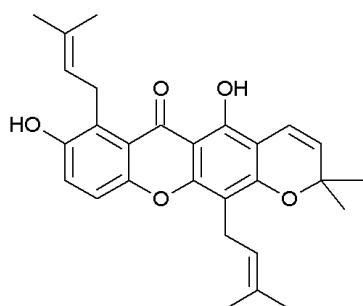
(57)
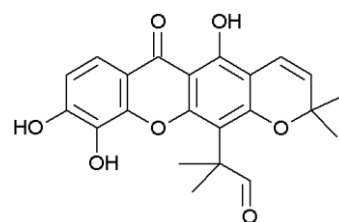
(58)

Figure 2.11: Structures of bioactive compounds isolated from *Calophyllum* species (continued)
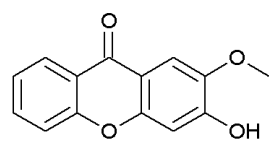
(59)
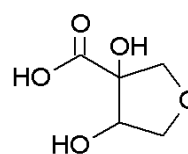
(60)
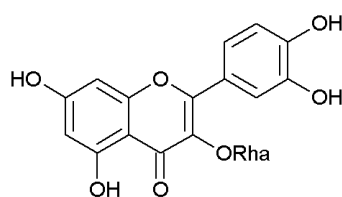
(61)
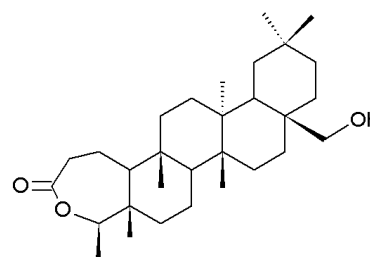
(62)
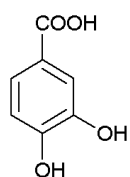
(63)
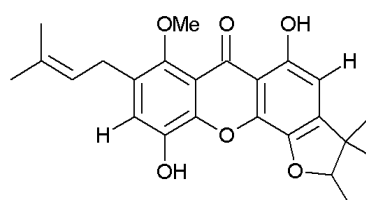
(64)

Figure 2.12: Structures of bioactive compounds isolated from *Calophyllum* species (continued)
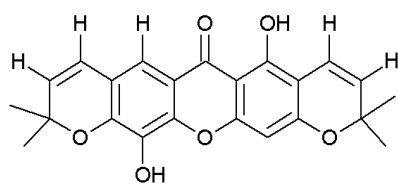
(**65**)
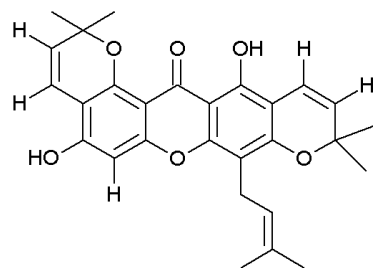
(**66**)
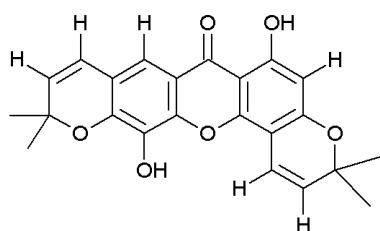
(**67**)
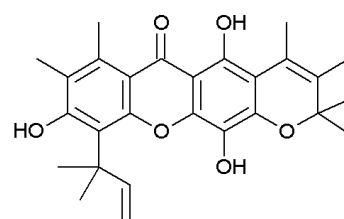
(**68**)
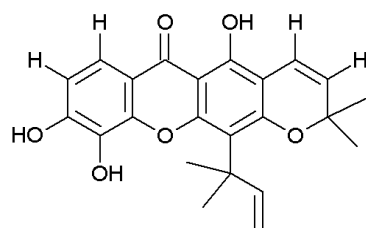
(**69**)
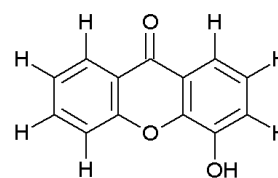
(**70**)

Figure 2.13: Structures of bioactive compounds isolated from *Calophyllum* species (continued)

2.2.1 Summary of Literature Investigation on the Chemistry and Biological Activities of *Calophyllum* Species

The types of secondary metabolites isolated from *Calophyllum* species and their biological properties are summarized in Table 2.1.

Table 2.1: Summary of chemistry and biological activities of *Calophyllum* species

Plant species	Compounds isolated	Biological activities	Literature reference
C. apetalum	- Coumarins - Triterpenoids - Chromanone acids - Xanthones	- Antitumour	- Govindachari et al., 1967 - Nigam and Mitra, 1969 - Inuma et al., 1997
C. blancoi	- Xanthones - Chromanone acids	- Anti-corona virus - Anticancer	- Shen et al., 2005 - Stout and Sears, 1968
C. brasilience	- Chromanone acids - Xanthones - Phenolic acids - Triterpenoids - Biflavonoids - Steroids - Terpenes - Coumarins	- Antibacterial - Anticancer - Antiulcerogenic - Antifungal - Analgesic - Anti-HIV - Leishmanicidal - Antiviral - Antimicrobial	- Leonti et al., 2001 - Sartori et al.,1999 - Souza et al., 2009 - Ito et al., 2002

C. caledonicum	- Xanthones
	- Chromanone acids
		- Antimalarial
		- Antifungal
		- Antiplasmodial
			- Morel et al.,
			  2000
			- Hay et al., 2003
			- Hay et al., 2004
			- Morel et al.,
			  2002

C. canum	- Xanthones	-	- Carpenter et al., 1969
C. chapelieri	- Chromanone acids	-	- Guerreiro et al., 1971
C. cordato- oblongum	- Xanthones - Pyranocoumarins - Chromanone acids - Triterpenoids	- Anti-HIV	- Dharmaratne et al., 1999

C. dispar	- Coumarins	- Molluscicidal
		- Piscicidal
		- Anti-HIV
		- Cytotoxic
			- Kashman et
			  al., 1992
			- Spino et al.,
			  1998
			- Guilet et al.,
			  2001

C. dryobalanoides	- Xanthones - Flavonoids - Triterpenoids - Chromanone acids	-	- Vo, 1997 - Ha et al., 2012

C. enervosum	- Xanthones
	- Polyisoprenylated
	  ketones
	- Benzophenones
	- Flavonoids
		- Antimicrobial	- Taher et al.,
			  2005

C. flavoramulum	- Flavonoids - Biflavonoids - Xanthones - Benzoic acids	- Anti-AGE - Antioxidant - Antidiabetic	- Ferchichi et al., 2012
C. gracilipes	- Xanthones	- Cytotoxic	- Nasir et al., 2013
C. inophyllum	- Xanthones - Triterpenes - Coumarins - Benzopyrano derivatives - Flavonoids	- Antioxidant - Anticancer - Anti-HIV - Antimicrobial - Anti-dyslipidemic	- Bruneton, 1993 - Breck and Stout, 1969 - Kawazu et al., 1968
C. lanigerum	- Coumarins	- Anti-HIV	- McKee et al., 1996
C. macrocarpum	- Flavonoids - Chromanone acids - Triterpenoids	-	- Ampofo and Waterman, 1986
C. panciflorum	- Biflavonoids	- Anti-tumor	- Ito et al., 1999
C. papuanum	- Chromanone acids	-	- Stout et al., 1968
C. pinetorum	- Flavonoids - Xanthones - Chromanone acids	-	- Roig, 1988 - Piccinelli et al., 2013
C. polyanthum	- Pyranocoumarins - Chromanone acids	- Anti-HIV	- Ma et al., 2004
C. soulattri	- Coumarins - Terpenoids	- Anti-HIV - Cytotoxic	- Sartori et al., 1999 - Nigam et al., 1988

C. sundaicum	- Xanthones
	- Polyprenylated
	  acylphloro-
	  glucinols
		- Anti-
		  depressant
		- Anticancer
		- Anti-HIV
			- Taher et al.,
			  2005
			- Velioglu et al.,
			  1998

C. teysmannii	- Coumarins
	- Xanthones
	- Triterpenes
		- Anti-HIV	- Pengsuparp
			  et al., 1996
			- McKee et al.,
			  1996
			- Maia et al.,2005

C. thorelii	- Xanthones - Benzophenones	- Cytotoxic	- Nguyen et al., 2012
C. tomentosum	- Xanthones - Triterpenes	-	- Banerji et al., 1994
C. venulosum	- Biflavonoids	-	- Chao et al., 1997

C. walkeri	- Flavonoids
	- Chromanones
	- Xanthones
	- Terpenoids
		-	- Ampofo and
			  Waterman, 1986
			- Dahanayake et
			  al., 1974

CHAPTER 3

MATERIALS AND METHODOLOGY

3.1 Plant Materials

Three *Calophyllum* species, namely *C. teysmannii, C. andersonii* and *C. soulattri* were collected from the jungle in Landeh, Sarawak for this research project. The plants collected were identified by the botanist Mr. Tinjan Anak Kuda from the Forest Department of Sarawak. Voucher specimens (UITM 3006, UITM 3009 and UITM 3010) were deposited at the herbarium of Universiti Teknologi MARA, Sarawak.

3.2 Chemical Reagants and Solvents

The solvents and materials used in this project are summarized in Tables 3.1 to 3.8.

Table 3.1: Deuterated solvents used for NMR analysis

Solvents	Source, Country
Deuterated chloroform	Acros Organics, Belgium
Acetone-d_6	Acros Organics, Belgium
Methanol-d_4	Acros Organics, Belgium

Table 3.2: Solvents and materials used in the extraction, isolation and purification of chemical constituents

Solvents/Materials	Source, Country
n-Hexane	Merck, Germany
Dichloromethane	Fisher Scientific, United Kingdom
Ethyl acetate	Lab Scan, Ireland
Acetone	QReC, Malaysia
Methanol	Mallinckrodit Chemicals, Phillisburg
Silica gel (60 Å)	Nacalai Tesque, Japan
Sephadex®LH-20	GE Healthcare, United States
Sodium sulphate anhydrous	John Kollin Corporation, United States

Table 3.3: Solvents and materials used for TLC analysis

Solvents/Materials	Source, Country
TLC silica gel 60 F254	Merck, Germany
Acetone	QReC, Malaysia
Dichloromethane	QReC, Malaysia
Ethyl acetate	Fisher Scientific, United Kingdom
n-Hexane	R&M Chemicals, United Kingdom
Iodine	Fisher Scientific, United Kingdom
Ferric chloride	Uni-Chem, India

Table 3.4: Solvents and cuvette used for UV-Vis analysis

Solvents/Materials	Source, Country
Chloroform	Fisher Scientific, United Kingdom
Cuvette (quartz)	Sigma Aldrich, United States

Table 3.5: HPLC grade solvents and material used for LC- and GC-MS analyses

Solvents/Materials	Source, Country
Acetonitrile	Fisher Scientific, United Kingdom
Methanol	Fisher Scientific, United Kingdom
Nylon syringe filter (0.5 μm)	Titan 2, United States

Table 3.6: Material used for IR analysis

Materials	Source, Country
Potassium bromide	Merck, Germany

Table 3.7: Chemical reagents and materials used for bioassay

Chemical reagents/Materials	Source, Country
DMEM	Sigma-Aldrich, United States
RPMI 1640	Sigma-Aldrich, United States
Fetal bovine serum	Sigma-Aldrich, United States
Thiazolyl blue tetrazolium bromide, 98%	Merck
Dimethyl sulfoxide (DMSO)	Fisher Scientific, United Kingdom
96-well plate	Techno Plastic, Switzerland
HeLa cell line	America Type Culture Collection (ATCC), United States
MDA-MB-231 cell line	America Type Culture Collection (ATCC), United States
LS174T cell line	America Type Culture Collection (ATCC), United States
T98G cell line	America Type Culture Collection (ATCC), United States
HEK293 cell line	America Type Culture Collection (ATCC), United States

Table 3.8: Chemical reagents and materials used for antioxidant assay

Chemical reagents/Materials	Source, Country
Kaempferol	Sigma-Aldrich, United States
Ascorbic acid (Vitamin C)	Sigma-Aldrich, United States
1,1-Diphenyl-2-picryhydrazyl (DPPH)	Sigma-Aldrich, United States
96-well plate	Techno Plastic, Switzerland

3.3 Extraction, Isolation and Purification of Chemical Constituents from Plant Materials

Dried and ground stem bark of *Calophyllum teysmanni* (2.0 kg), *Calophyllum andersonii* (1.0 kg) and *Calophyllum soulattri* (1.5 kg) were separately subjected to sequential solvent extraction by soaking them in closed containers with selected solvents of varying polarity, started with dichloromethane, followed by ethyl acetate and lastly methanol, and the soaking was repeated twice for each solvent, with occasional shaking for two days at room temperature. The crude solvent extracts were then filtered and the filtrates were subjected to evaporation under reduced pressure at 40 °C using a rotary evaporator to give dry crude dichloromethane, ethyl acetate and methanol extracts for each plant sample.

3.4 Chromatographic Methods

3.4.1 Silica Gel Column Chromatography

The sample was prepared via dry packing method in which the sample was firstly dissolved in an appropriate amount of solvent. Subsequently, the sample solution was added dropwise and mixed evenly with a minimal amount of silica gel. The wet mixture was left overnight at ambient temperature, allowing it to completely dry. Different sizes of glass columns with internal diameter of 25, 30 and 80 mm were used in this project for purification of compounds. Preparation of column packing was done using a sintered glass column and the packing material used was Merck Kieselgel 60, 230-400 Mesh (40-60 microns). In a separate beaker, silica gel was mixed with hexane to form a slurry. The slurry was then introduced into the column to a desired height. It was left to settle down. Then, the column was tapped with a rubber tubing to facilitate compact packing. Once the stationary phase was densely packed, the dried sample mixture was introduced onto the packed column. A thin layer of sodium sulphate was added on top of the sample layer.

Subsequently, a series of mobile phase in increasing polarity (hexane/dichloromethane/ethyl acetate/acetone/methanol) were added into the column in order to elute compounds out from the column. Gradient or isocratic elution was used to separate the mixture of compounds. Collection of

eluents from the column was done according to separated colour bands or volumes.

3.4.2 Size Exclusion Column Chromatography

Selected fractions obtained from silica gel column chromatography were further purified via size-exclusion chromatography, in which compounds were separated based on the differences in their sizes and molecular weights. Sephadex LH-20 was mixed with suitable amount of methanol. Then, the slurry was poured into a glass column. The packed column was left overnight before it was used. Sample solution was prepared by dissolving the sample in methanol. The sample solution was then introduced dropwisely into the packed column. Separation of the compounds was done by eluting the column with a mixture of methanol and dichloromethane (9:1). Collection of eluents from the column was done according to separated colour bands or volumes.

3.4.3 Thin Layer Chromatography (TLC)

TLC analysis was performed using precoated aluminium sheets of 8 cm $\times$ 4 cm coated with silica gel 60 F_{254}. Firstly, baseline and solvent front lines were drawn respectively across the plate approximately 0.5 cm from the bottom and top of TLC plate. Sample in the solution form was loaded onto the baseline of TLC plate with the aid of a microcapillary tube. The plate was then placed into

a developing chamber containing an appropriate solvent mixture as mobile phase. The TLC plate was allowed to develop until the solvent moves up to solvent front line.

3.5 TLC Visualization Methods

3.5.1 UV Light

The developed spots on the TLC plate were visualized under UV light at 254 nm and 365 nm, respectively. All the spots observed were circled lightly with a pencil. Each spot showed a retention factor (R_f) which is equal to the distance travelled by the compound over the distance travelled by the solvent. As shown below, the formula to calculate the R_f value of each analyte:

$$R_f = \frac{\text{distance travelled by the compound (cm)}}{\text{distance of the solvent front (cm)}}$$

3.5.2 Iodine Vapour Stain

Iodine vapour detection was performed in a closed chamber saturated with iodine vapour. A chamber was assembled by introducing approximately 1.5 g of iodine crystals into a closed container. It was allowed to be saturated with iodine vapour. The developed TLC plate was placed into the chamber. After

10 minutes, the plate was carefully removed from the chamber. The brown spots formed on the TLC plate were circled immediately with a pencil as the iodine spots might dissipate over time.

3.5.3 Ferric Chloride Solution

Ferric chloride solution was prepared by dissolving 1.0 g ferric chloride in 100 mL methanol. The solution was sprayed on the developed TLC plate to give coloured complexes. Dark blue or greenish spots indicate the presence of phenolic compounds whereas hydroxamic acids give a red spot on the TLC plates.

(i) UV (254 nm)	(ii) UV (365 nm)	(iii) Iodine Vapour	(iv) FeCl$_3$ Solution
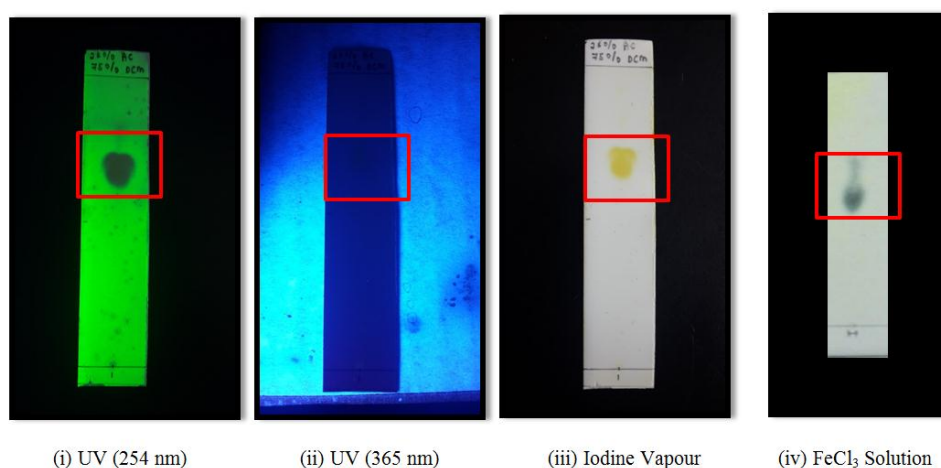
Figure 3.1: TLC plates viewed via different detection methods

3.6 Instruments

3.6.1 Nuclear Magnetic Resonance (NMR) Spectrometer

^{1}H and ^{13}C NMR spectra were determined on a JEOL JNM-ECX 400 MHz spectrometer, in CDCl$_3$, CD$_3$OD or acetone-d_6. Chemical shifts were expressed in δ (ppm) values relative to tetramethylsilane (TMS) as the internal standard.

3.6.2 Fourier Transform Infrared (IR) Spectrometer

Infrared spectra were obtained using a Perkin Elmer 2000-FTIR spectrophotometer, in KBr pellet.

3.6.3 Ultraviolet-Visible (UV-Vis) Spectrophotometer

Ultraviolet spectra were recorded on a double-beam Perkin Elmer Lambda (25/35/45) UV-Vis spectrophotometer.

3.6.4 Mass Spectrometry (MS)

EIMS and HR-EIMS were recorded on an Agilent 5975C MSD (Agilent Technologies, Santa Clara, CA, US) and Thermo Finnigan MAT95XL (Thermo Fisher, Bremen, Germany) mass spectrometers, respectively.

3.6.5 Melting Point Apparatus

Melting points of compounds were determined using a Stuart SMP 10 melting point apparatus.

3.6.6 Polarimeter

The specific rotation of chiral compounds was determined on a Jasco 43 Europe P-2000 digital polarimeter.

3.6.7 X-Ray Diffractometer

Diffraction data for the crystalline compound were collected on an Agilent SuperNova Dual diffractometer (Agilent Technologies, Santa Clara, CA, US) equipped with a graphite monochromated Mo-Kα radiation source (λ= 0.71073 A°) at 100(2) K.

3.7 Biological Assays

3.7.1 Cytotoxic Assay

The cytotoxic assay was conducted on four human cancer cell lines which are HeLa (cervical carcinoma), MDA-MB-231 (breast adenocarcinoma), LS174T (colorectal carcinoma) and T98G (ganglioblastoma). The cytotoxicity of the samples were also screened on human normal cell line, HEK293 (human embryonic kidney cells). The cell lines were obtained from American Type Culture Collection, USA.

3.7.1.1 Cell Culture

HeLa, MDA-MB-231, LS174T and HEK293 cell lines were cultured in Dulbecco's Modified Eagle's Medium (DMEM) while T98G in Modified Eagle's Medium (MEM). The cancer cell lines were supplemented with 5% Fetal Bovine Serum (FBS) and 1% penicillin-streptomycin, and were maintained at 37 °C in 5% CO_2 incubator.

3.7.1.2 MTT Assay

The master stock of sample and positive controls (doxorubicin and cisplatin) were prepared at concentration of 5 mg/mL by dissolving 5 mg of test

compound in 1 mL of DMSO. The stock solution was then filtered using a 0.22 μm syringe filter. Serial dilution of the master stock solution in their respective growth medium provided six sample solutions at concentrations of 3.13, 6.25, 12.50, 25.00, 50.00 and 100.00 μg/mL.

Cells were grown in a 96-well microplate by seeding each well with 100 μl of cells (1 x 10^4 cells/mL). After 24 hours incubation, growth medium was removed from the wells and each well was then treated with 100 μl of different concentrations of sample solutions, whereas controls were prepared using untreated cell population in 100 μl growth medium. The plate was then incubated for 72 hours in 5% CO_2 incubator at 37 °C. The assay was conducted in triplicates for each sample.

The cell viability was evaluated using the colourimetric 3-(4,5-dimethylthiazol-2-yl)-2,5-diphenyltetrazolium bromide (MTT) assay. After 72 hours incubation, 20 μl of 5 mg/mL MTT solution were added into each well and further incubated for 4 hours at 37 °C in 5% CO_2 incubator. After 4 hours, the supernatant was discarded and replaced with 100 μl of DMSO. Cell viability was determined by measuring optical density at 550 nm using a microplate reader (Bio-Rad Laboratories, Hercules, CA, USA).

The cell viability was calculated using the formula below:

$$\text{Cell viability (\%)} = (a\text{-}b)/(c\text{-}b) \times 100$$

Where a= average absorbance of cell treated with test compound

b= average absorbance of blank medium

c= average absorbance of cell control

3.7.2 Antioxidant Assay

3.7.2.1 DPPH Assay

Firstly, the crude extracts, isolated compounds and standard compounds (kaempferol and ascorbic acid) were dissolved separately in methanol to prepare master stocks at concentration of 2 mg/mL. All the master stocks were sonicated for five minutes. Then, DPPH solution was prepared at a concentration of 2 mg/mL and all the prepared solutions were stored in a 4 $^{\circ}$C chiller.

A 96-well plate was used to perform this assay. Serial dilution of the master stocks was performed using methanol to prepare sample solutions at different concentrations of 240, 120, 60, 30, 15, 7.5 and 3.75 µg/mL. A volume of 10 µl of DPPH solution was then added into each well followed by further dilution with methanol. The positive controls used in this assay were kaempferol and

ascorbic acid. Meanwhile, the negative control or blank was prepared to contain only methanol and DPPH solution. The plate was then wrapped with aluminium foil after addition of the reagents. It was incubated at room temperature for 30 minutes. At the end of incubation period, measurement of absorbance was done at 520 nm. A microplate reader (Model 680, Bio-Rad Laboratories, Hercules, CA, USA) was used to measure the absorbance of the sample solutions in each well. The results were then interpreted through Microplate Manager®, Version 5.2.1 software. The assay was performed in triplicate and then the average absorbance of each concentration was determined.

The inhibition rates of the test compounds were calculated based on the formula shown below:

DPPH free radical scavenging activity (%) $= 1 - (A_s / A_c) \times 100$

Where A_s = absorbance of sample

A_c = absorbance of control

Based on the resulting data, a graph of inhibition rate against the sample concentration was plotted. The concentration of sample required to cause 50% inhibition to the DPPH radical scavenging activity (IC_{50}) was obtained from the graph.

CHAPTER 4

RESULTS AND DISCUSSION

4.1 Extraction and Isolation of Chemical Constituents from *Calophyllum teysmannii*

Dried and ground stem bark of *Calophyllum teysmannii* (2.0 kg) after being successively extracted with dichloromethane, ethyl acetate and methanol yielded crude extracts weighing 297.9, 38.6 and 145.2 g, respectively. The summary of the weight and percentage of yield of crude extracts are shown in Table 4.1.

Table 4.1: Extract yields of *Calophyllum teysmannii*

Crude Extract	Weight (g)	Percentage of yield (%)*
Dichloromethane	297.9	14.9
Ethyl acetate	38.6	1.9
Methanol	145.2	7.3

* Percentage of yield was calculated based on the weight of the dried extract against dry weight of ground stem bark of *Calophyllum teysmannii* (2.0 kg) multiplied by 100%.

About 100 g of dichloromethane extract was subjected to Si gel CC (40-63 μm, 8.5 x 50 cm, 600 g) packed in *n*-hexane and eluted with *n*-hexane-dichloromethane mixtures of increasing polarity (90:10, 80:20, 70:30, 60:40, 50:50, 40:60, 30:70, 20:80, 10:90, 0:100), followed by increasing

concentration of EtOAc in dichloromethane (10:90, 20:80, 30:70, 40:60, 50:50, 60:40, 70:30, 80:20, 90:10, 100:0) to give 29 fractions (HEAA1-29). Fraction HEAA14 (6.2 g) was fractionated by Si gel CC (40-63 μm, 3.5 x 50 cm, 150 g) with a gradient of *n*-hexane-acetone (90:10, 80:20, 70:30, 60:40, 50:50, 40:60, 30:70, 20:80, 10:90, 0:100) to give 20 subfractions (HEAB1-20). Subfractions HEAB14-15 (0.75 g) were combined and further recrystallized in MeOH to afford caloteysmannic acid (**71**, 696 mg) as yellow cubic crystals. From subfractions HEAB4-7, isocalolongic acid (**72**, 1250 mg) was obtained. Meanwhile, fractions HEAA15-17 (4.8 g) was rechromatographed over Si gel CC (40-63 μm, 3.5 x 50 cm, 150 g) eluted with *n*-hexane-EtOAc (90:10, 80:20, 70:30, 60:40, 50:50, 40:60, 30:70, 20:80, 10:90, 0:100) to yield stigmasterol (**74**, 7 mg).

On the other hand, about 35 g of ethyl acetate extract was subjected to Si gel CC (40-63 μm, 8.5 x 50 cm, 600 g) packed in *n*-hexane and eluted with *n*-hexane-dichloromethane mixtures of increasing polarity (90:10, 80:20, 70:30, 60:40, 50:50, 40:60, 30:70, 20:80, 10:90, 0:100), followed by increasing concentration of EtOAc in dichloromethane (10:90, 20:80, 30:70, 40:60, 50:50, 60:40, 70:30, 80:20, 90:10, 100:0) to give 25 fractions (HEAG1-25). Fractions HEAG4-5 (6.2 g) was fractionated by Si gel CC (40-63 μm, 3.5 x 50 cm, 150 g) with a gradient of *n*-hexane-acetone (90:10, 80:20, 70:30, 60:40, 50:50, 40:60, 30:70, 20:80, 10:90, 0:100) to give 14 subfractions (HEAK 1-14). Subfraction HEAK8 (0.75 g) was further fractionated by Si gel CC (40-63 μm, 3.5 x 50 cm, 150 g) with a gradient of *n*-hexane-acetone (90:10, 80:20, 70:30, 60:40, 50:50, 40:60, 30:70, 20:80, 10:90, 0:100) to afford calolongic

acid (**73**, 9 mg). Meanwhile, purification of methanol extract via column chromatography failed to give any pure compound. The isolation of compounds is outlined in Figure 4.1.
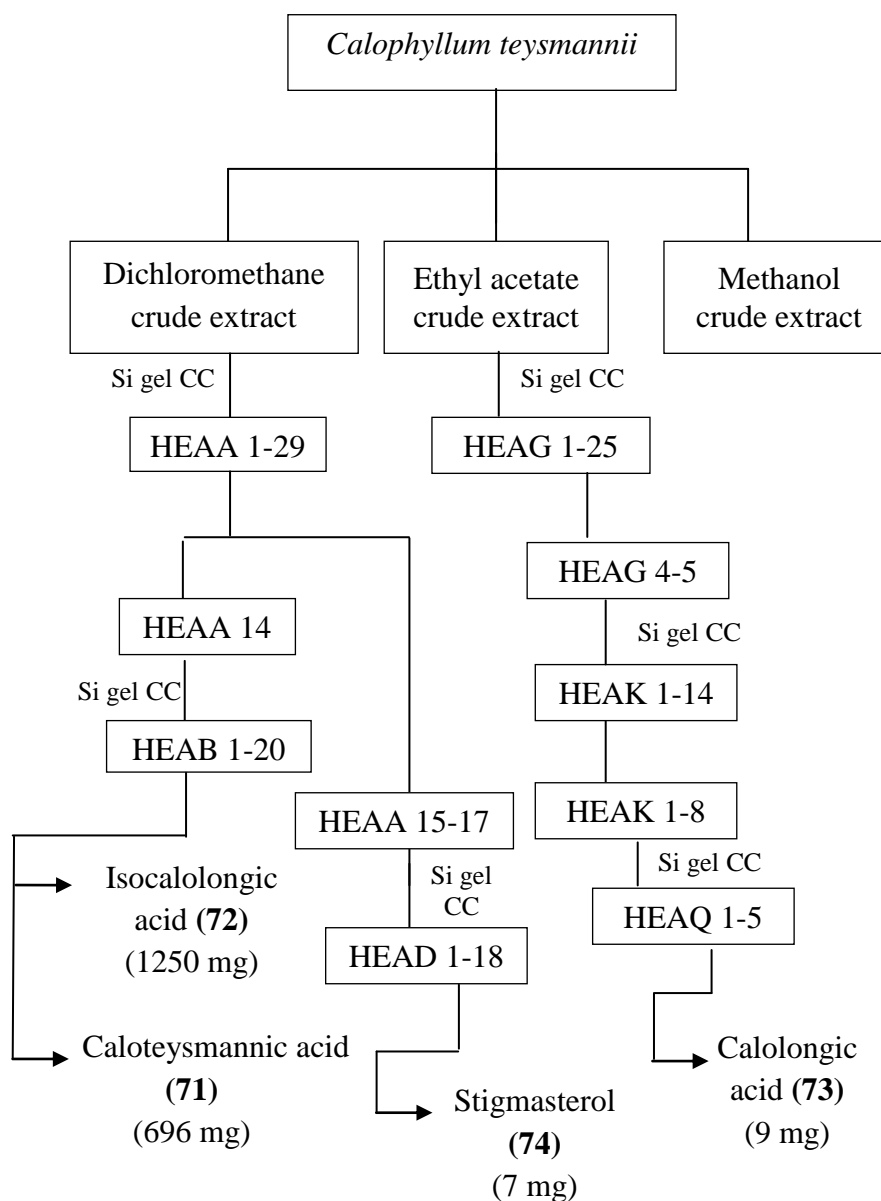
Figure 4.1: Isolation of compounds from the stem bark extracts of
Calophyllum teysmannii

4.1.1 Characterization of Caloteysmannic Acid (71)
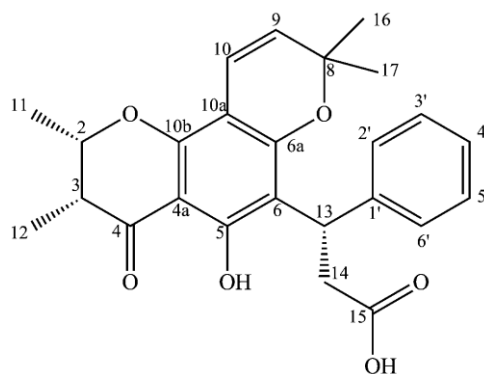
(**71**)

Compound **71** was obtained as yellow cubic crystals, mp 159–161 °C. It has a specific rotation, $[\alpha]_D$ of −156.0° (MeOH, c 0.05). It appeared as a dark reddish-pink spot on the developed TLC, under UV light at wavelength of 254 nm, and gave brown spot when treated with iodine vapour. Furthermore, the phenolic nature of this compound was indicated by a positive result revealed in the $FeCl_3$ test. This compound showed retention factor, R_f value of 0.71 via a mobile phase of 75% dichloromethane and 25% acetone.

The molecular formula of compound **71** was deduced as $C_{25}H_{26}O_6$ from the HR-EIMS ($[M]^{+\cdot}$ at m/z 422.17299) (Figure 4.3) and EIMS ($[M]^{+\cdot}$ at m/z 422) (Figure 4.4) The UV absorption maxima at 271.2 and 367.2 nm (Figure 4.5) suggested the presence of a pyranochromanone moiety that is typical to isocalolongic acid (Guerreiro et al., 1973), apetalic acid (Plattner et al., 1974), chapelieric acid (Gunatilaka et al., 1984), and other chromanone derivatives. The IR spectrum (Figure 4.6) exhibited absorption bands at 3346 (O-H stretch)

2948 (C-H stretch), 1619 (C=C stretch), 1387 (C-H bend) and 1133 (C-O stretch) cm^{-1}.

The ^{1}H and ^{13}C NMR spectra of **71** (Figures 4.7 and 4.8) revealed the presence of a 2,3-dimethylchromanone core [δ_H 4.62 (1H, qd, J = 6.7 and 3.1 Hz, H-2), 2.62 (1H, qd, J = 7.3 and 3.1 Hz, H-3), 1.34 (3H, d, J = 6.7 Hz, H-11) and 1.09 (3H, d, J = 7.3 Hz, H-12); δ_C 201.4 (C-4), 76.5 (C-2), 44.0 (C-3), 15.8 (C-11) and 9.0 (C-12)], a chelated hydroxyl group [δ_H 12.96 (s, 5-OH)], and a 2,2-dimethylpyran ring [δ_H 6.49 (1H, d, J = 10.4 Hz, H-10), 5.53 (1H, d, J = 10.4 Hz, H-9), 1.42 (3H, s, H-16) and 1.18 (3H, s, H-17); δ_C 126.3 (C-9), 115.6 (C-10), 78.3 (C-8), 27.6 (C-16) and 27.3 (C-17)]. Meanwhile, the resonances for a methine [δ_H 5.09 (1H, t, J = 8.0 Hz, H-13); δ_C 35.0 (C-13)], a methylene [δ_H 3.34 (1H, dd, J = 15.9, 8.5 Hz, H$_a$-14) and 3.12 (1H, dd, J = 15.9, 7.3 Hz, H$_b$-14); δ_C 36.4 (C-14)], a carboxyl group (δ_C 173.3, C-15), and a mono-substituted benzene ring [δ_H 7.40 (2H, d, J = 7.3 Hz, H-2' & H-6'), 7.21 (2H, t, J = 7.3 Hz, H-3' & H-5') and 7.09 (1H, t, J = 7.3 Hz, H-4'); δ_C 143.9 (C-1'), 127.9 (C-3' & C-5'), 127.8 (C-2' & C-6') and 125.9 (C-4')] indicated the presence of 3-phenylpropanoic acid side chain.

In the HMBC spectrum (Figure 4.10), key correlations from a pair of olefinic protons H-9 to C-8 (δ_C 78.3) and C-10a (δ_C 101.6); H-10 to C-6a (δ_C 159.6) and C-8 (δ_C 78.3) suggested the 2,2-dimethylpyran ring was angularly fused to the 2,3-dimethylchromanone nucleus at carbon positions C-6a and C-10a. Moreover, the HMBC correlations from H-13 to C-1' (δ_C 143.9), C-2' (δ_C 127.8), C-5 (δ_C 161.6), C-6 (δ_C 111.8), C-6' (δ_C 127.8), C-14 (δ_C 36.4) and C-

15 (δ_C 173.3); H-14 to C-1' (δ_C 143.9), C-6 (δ_C 111.8), C-13 (δ_C 35.0) and C-15 (δ_C 173.3) suggested the presence of 3-phenylpropanoic acid unit which was attached to the pyranochromanone core at carbon position C-6. On the basis of the above spectral evidence, caloteysmannic acid was established to have structure **71** which had not been previously reported.

Compound **71** was found to have three asymmetric centres at carbons C-2, C-3 and C-13 which could lead to a total of eight possible stereoisomers. The stereochemical assignment of this compound was done based on the NMR and X-ray crystallographic analyses. The *cis* coupling of protons H-2 and H-3 was evidenced from the coupling constant of 3.1 Hz observable in both proton signals of H-2 and H-3 at δ_H 4.62 and 2.62, respectively (Stout et al., 1968). This is consistent with axial-equatorial arrangement for protons H-2 and H-3 meaning that the configuration of 2,3-dimethylchromanone ring could be either 2*S*,3*R* or 2*R*,3*S* (Ha et al., 2012).

The crystal structure of **71** (Figure 4.2) was determined by X-ray diffraction analysis which further confirmed the compound to have absolute configuration of 2*S*,3*R* at asymmetric carbons C-2 and C-3. Apart from that, the asymmetric carbon C-13 located at the side chain moiety was deduced to have *S* configuration. Based on the spectral evidence, compound **71** was identified as (*S*)-3-[(2*S*,3*R*)-5-hydroxy-2,3,8,8-tetramethyl-4-oxo-2,3,4,8 tetrahydropyrano [2,3-*f*]chromen-6-yl]-3-phenylpropanoic acid which is a new compound with its trivial name given as caloteysmannic acid (**71**).
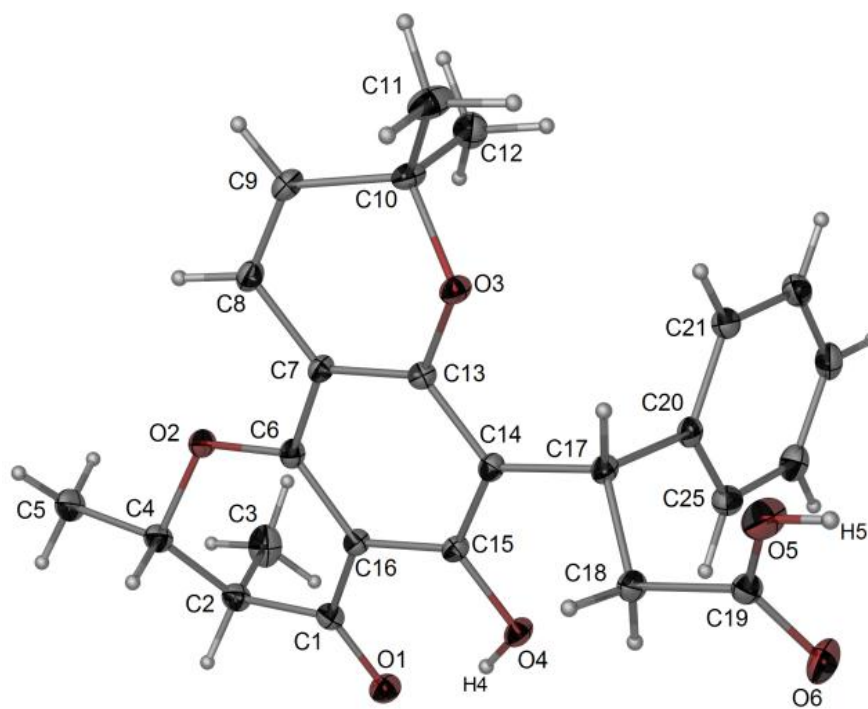
Figure 4.2: X-ray crystal structure of compound 71
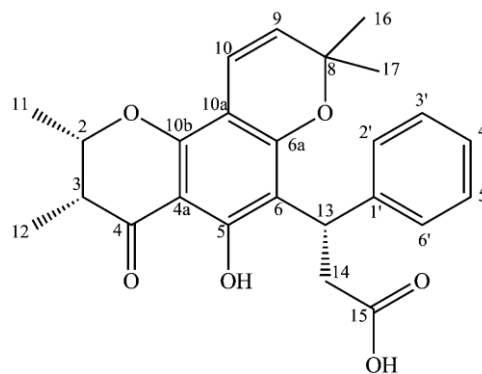
(**71**)

Table 4.2: Summary of NMR data and assignment of caloteysmannic acid (71)

Position	δ_H (ppm)	δ_C (ppm)	HMBC
2	4.62 (1H, qd, J = 6.7, 3.1 Hz)	76.5	-
3	2.62 (1H, qd, J = 7.3, 3.1 Hz)	44.0	C- 4
4	-	201.4	-
4a	-	100.9	-
5	-	161.6	-
6	-	111.8	-
6a	-	159.6	-
8	-	78.3	-
9	5.53 (1H, d, J = 10.4 Hz)	126.3	C- 8 & 10a
10	6.49 (1H, d, J = 10.4 Hz)	115.6	C- 6a & 8
10a	-	101.6	-
10b	-	155.3	-
11	1.34 (3H, d, J = 6.7 Hz)	15.8	C- 2 & 3
12	1.09 (3H, d, J = 7.3 Hz)	9.0	C- 2, 3 & 4
13	5.09 (1H, t, J = 8.0 Hz)	35.0	C- 1', 2', 5, 6, 6', 14 & 15
14	3.34 (H$_a$, dd, J = 15.9, 8.5 Hz) 3.12 (H$_b$, dd, J = 15.9, 7.3 Hz)	36.4	C- 1', 6, 13 & 15 C- 1', 6, 13 & 15
15	-	173.3	-
16	1.42 (3H, s)	27.6	C- 8, 9 & 17
17	1.18 (3H, s)	27.3	C- 8, 9 & 16
1'	-	143.9	-
2' & 6'	7.40 (2H, d, J = 7.3 Hz)	127.8	C- 3', 5' & 13
3' & 5'	7.21 (2H, t, J = 7.3 Hz)	127.9	C- 1', 2' & 6'
4'	7.09 (1H, t, J = 7.3 Hz)	125.9	C- 2', 3', 5' & 6'
5-OH	12.96 (1H, s)	-	C- 4a, 5 & 6
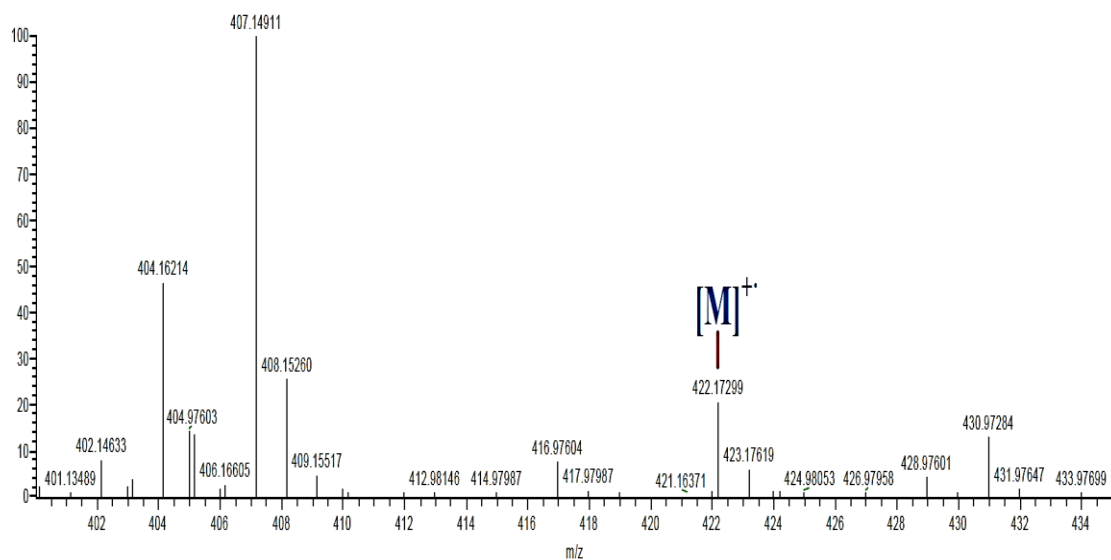
Figure 4.3: HREIMS spectrum of caloteysmannic acid (71)
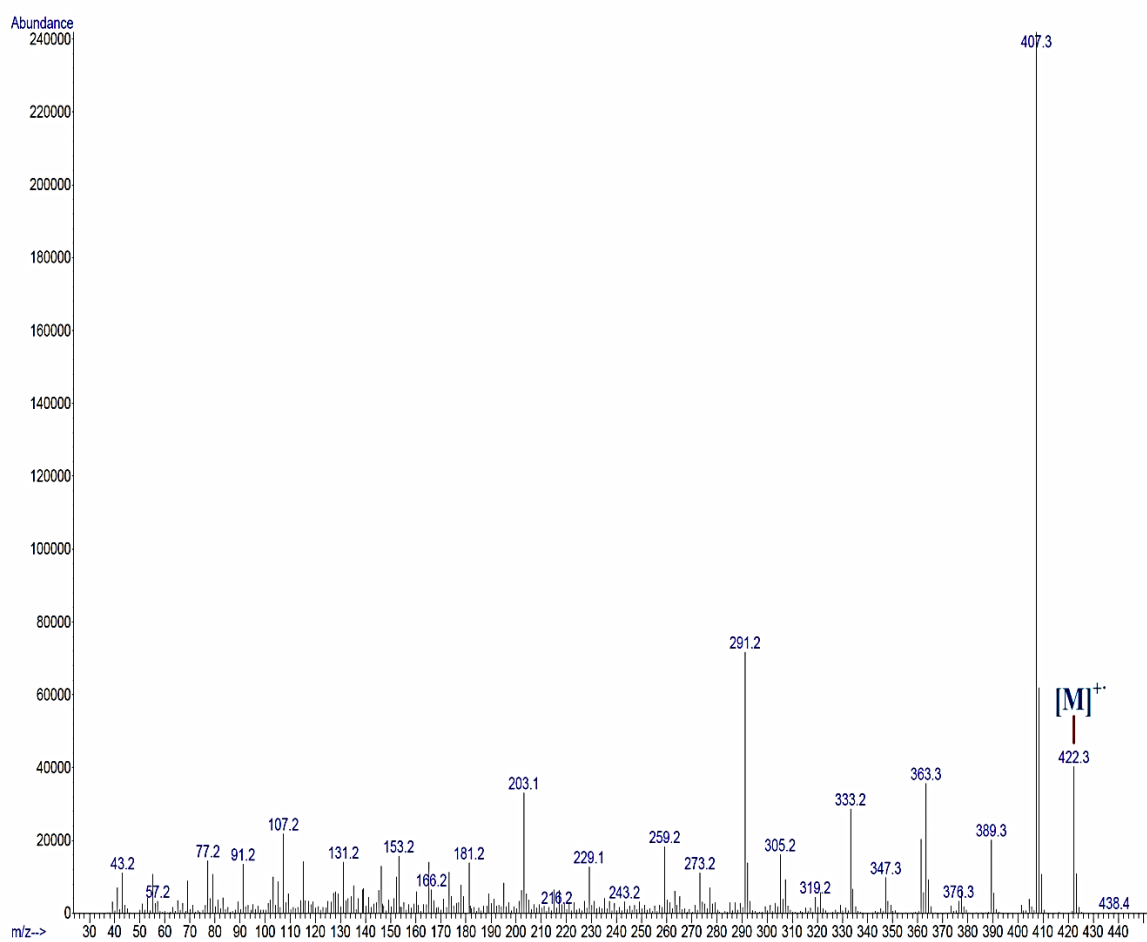
Figure 4.4: EIMS spectrum of caloteysmannic acid (71)

56
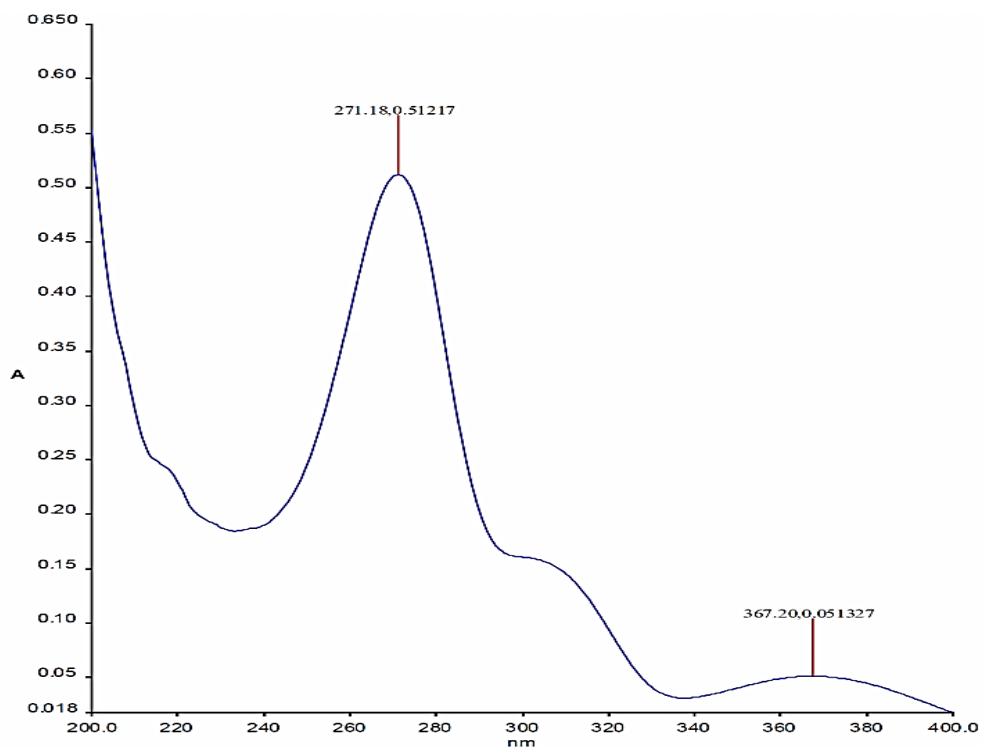
Figure 4.5: UV-Vis spectrum of caloteysmannic acid (71)
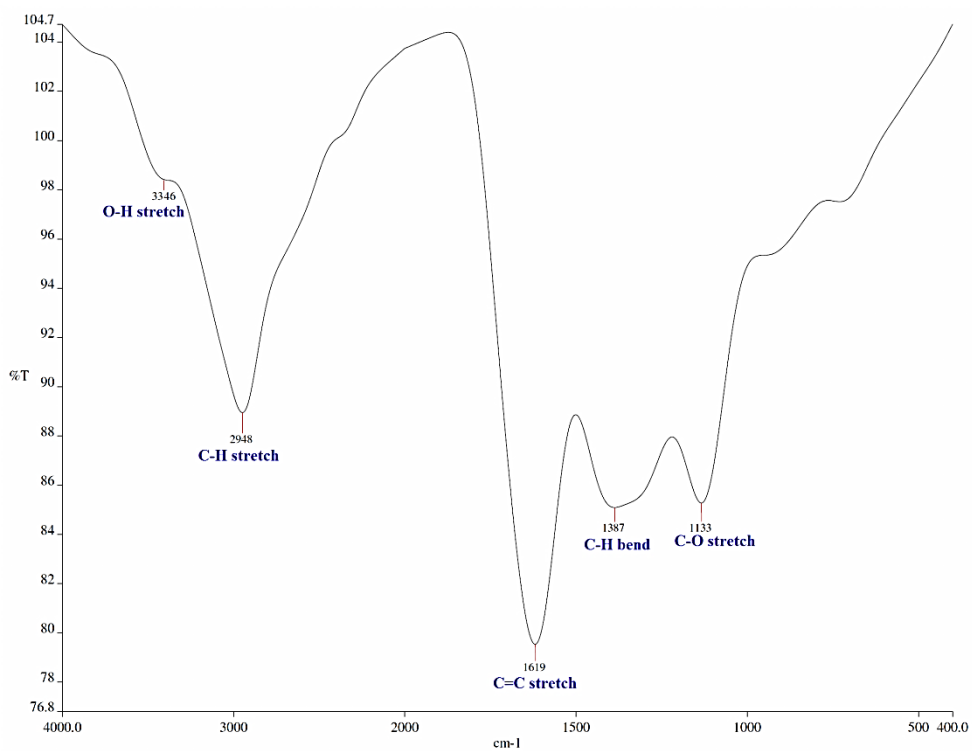
Figure 4.6: IR spectrum of caloteysmannic acid (71)
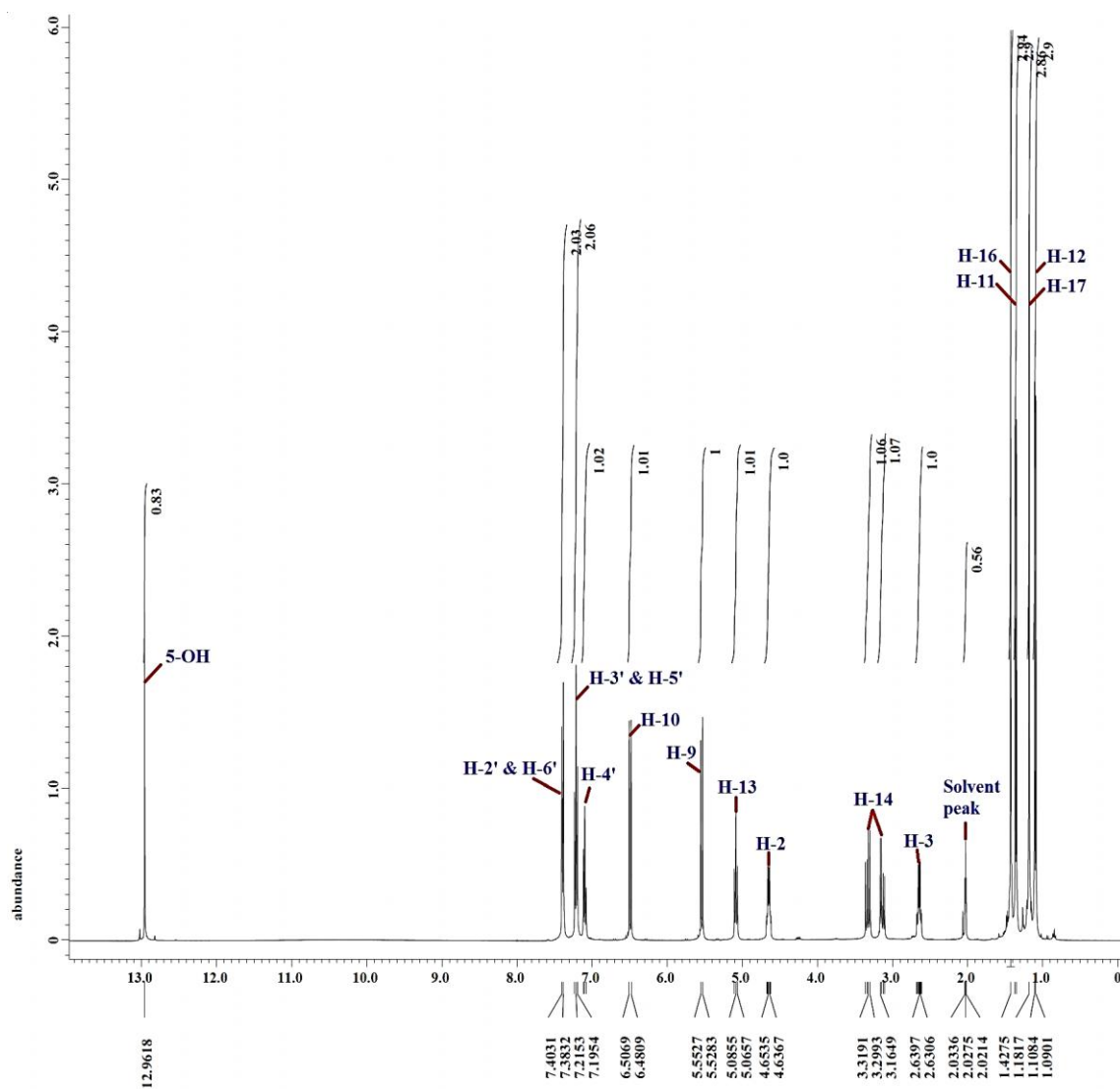
Figure 4.7: ¹H NMR spectrum of caloteysmannic acid (71) (400 MHz, acetone-*d₆*)
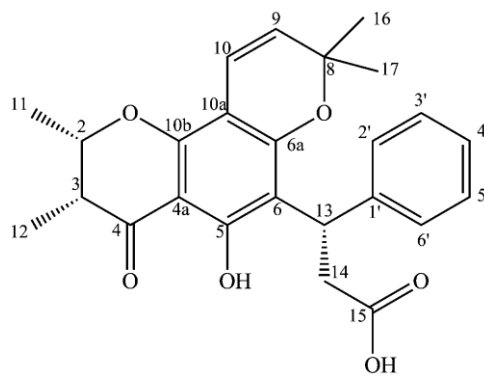
(**71**)
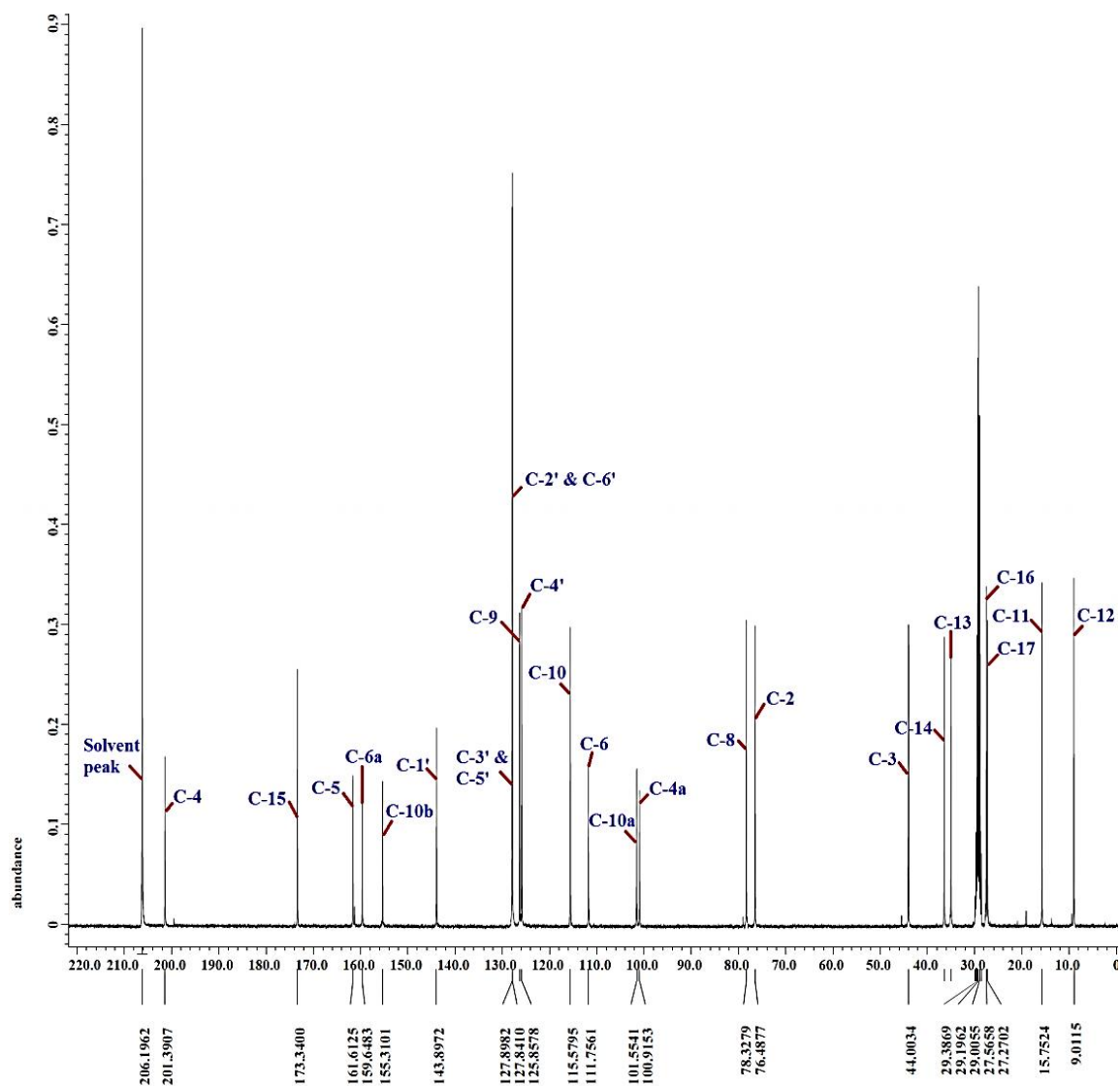
Figure 4.8: ^{13}**C NMR spectrum of caloteysmannic acid (71) (100 MHz, acetone-d_6)**
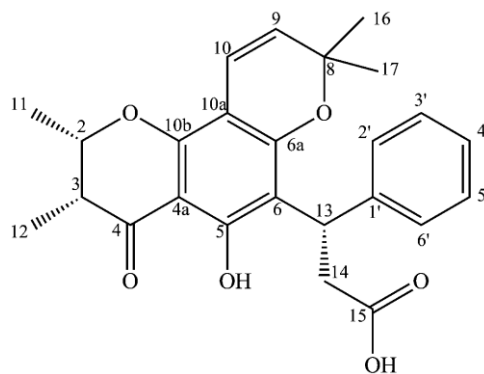
(**71**)
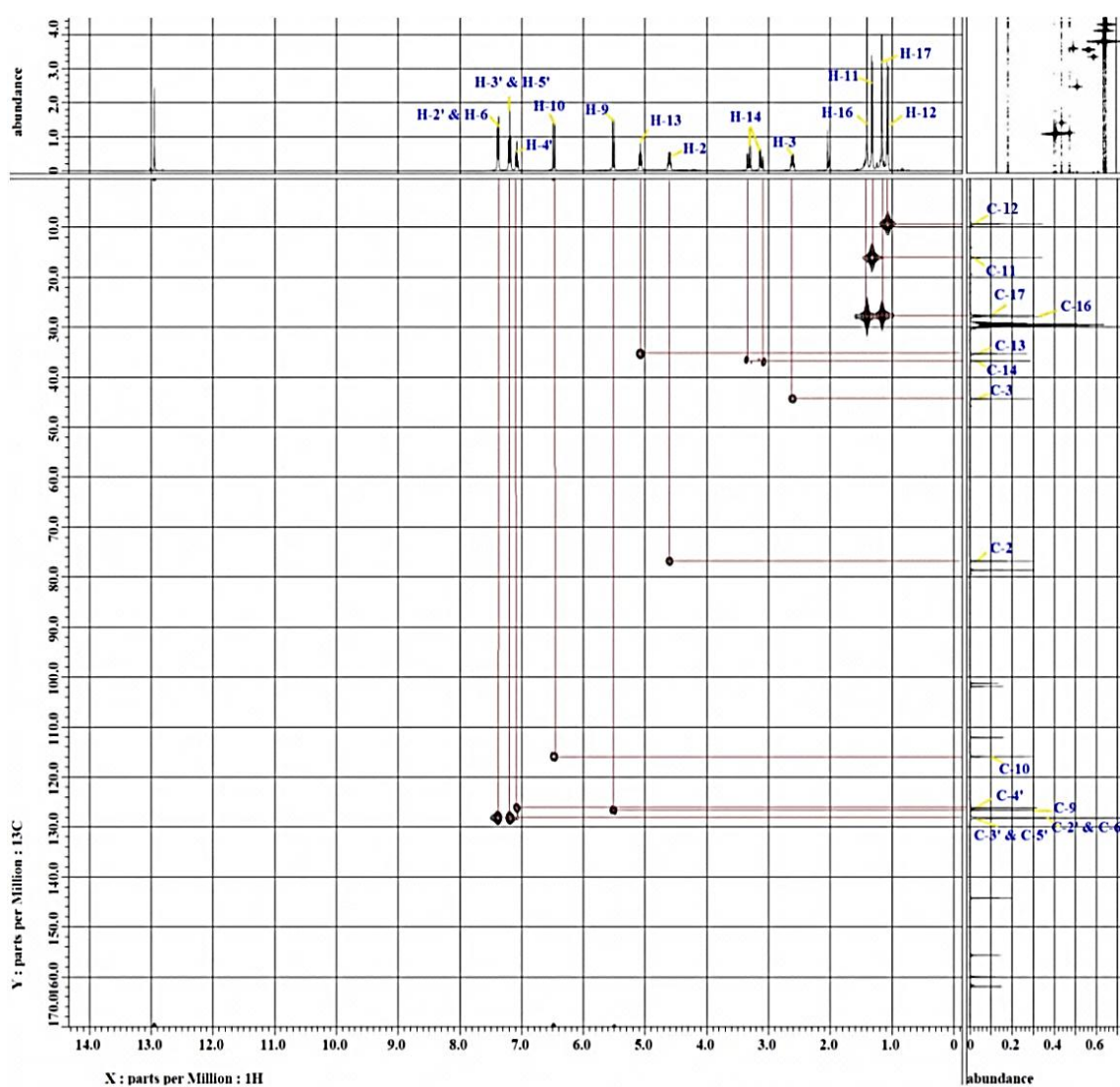
Figure 4.9: HMQC spectrum of caloteysmannic acid (71)
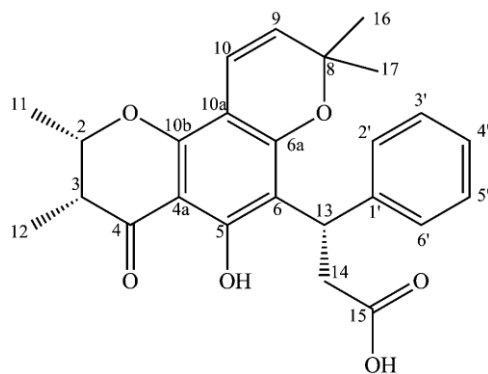
Figure 4.10: HMBC spectrum of caloteysmannic acid (71)

4.1.2 Characterization of Isocalolongic Acid (72)
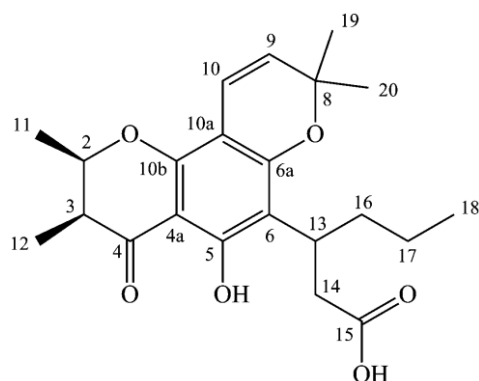
(**72**)

Compound **72** was isolated as yellow gum giving a specific rotation, $[\alpha]_D$ of

−50.0° (MeOH, *c* 0.05) (Lit. −48.3°, Guerreiro et al., 1973). It appeared as a

dark reddish-pink spot on the developed TLC when irradiated by UV light at

wavelength of 254 nm, and gave brown spot when treated with iodine vapour.

Moreover, compound **72** gave a dark blue spot when treated with $FeCl_3$

solution, due to its phenolic nature. This compound exhibited retention factor,

R_f value of 0.44 via a mobile phase of 90% dichloromethane and 10% acetone.

The molecular formula of compound **72** was deduced as $C_{22}H_{28}O_6$ from the

EIMS ([M]$^{+\cdot}$ at m/z 388) (Figure 4.11). Compound **72** showed absorption

maxima at 213.2, 271.5 and 366.5 nm (Figure 4.12) for a typical

pyranochromanone derivative (Guerreiro et al., 1973; Plattner et al., 1974;

Gunalatika et al., 1984). Meanwhile the IR spectrum (Figure 4.13) revealed

absorption bands at 3319 (O-H stretch), 2937 (C-H stretch), 1630 (C=C

stretch), 1373 (C-H bend) and 1139 (C-O stretch) cm^{-1}.

The ^{1}H and ^{13}C NMR spectra of **72** (Figures 4.14 and 4.15) indicated the presence of a 2,3-dimethylchromanone core [δ_H 4.61 (1H, qd, J = 6.7 and 3.1 Hz, H-2), 2.60 (1H, qd, J = 7.4 and 3.1 Hz, H-3), 1.35 (3H, d, J = 6.7 Hz) and 1.08 (3H, d, J = 7.4 Hz, H-12); δ_C 201.4 (C-4), 76.4 (C-2), 44.0 (C-3), 15.8 (C-11) and 9.0 (C-12)], a chelated hydroxyl group [δ_H 12.76 (s, 5-OH)] along with a 2,2-dimethylpyran ring [δ_H 6.50 (1H, d, J = 10.1 Hz, H-10), 5.54 (1H, d, J = 10.4 Hz, H-9), 1.42 (3H, s, H-19) and 1.41 (3H, s, H-20); δ_C 126.1 (C-9), 115.7 (C-10), 78.1 (C-8), 27.8 (C-19) and 27.7 (C-20)]. Apart from that, the presence of a 3-substituted hexanoic acid side chain was revealed by the resonances of a methine [δ_H 3.71 (1H, m, H-13); δ_C 30.0 (C-13)], three methylene [δ_H 2.69 (2H, m, H-14), 1.84 (1H, m, H$_a$-16), 1.53 (1H, m, H$_b$-16), 1.14 (2H, m, H-17); δ_C 38.2 (C-14), 35.2 (C-16), 20.9 (C-17)], a methyl [δ_H 0.81 (3H, t, J = 7.4 Hz, H-18; δ_C 13.8 (C-18)] and a carboxyl group [δ_C 174.4 (C-15)]. The *cis*-2,3-dimethyl substitution in the chromanone ring was evidenced from the resonances of proton H-2 (4.61, qd, J = 6.7 and 3.1 Hz) and H-3 (2.60, qd, J = 7.4 and 3.1 Hz). The lower J = 3.1 Hz for both signals of protons H-2 and H-3 represents axial-equatorial arrangement for H-3 and H-2 (Stout et al., 1968). Proton H-2 at δ_H 4.61 with J =3.1 Hz was indicative of (2e, 3a) dimethyl substitution (Ha et al., 2012).

The HMBC correlations (Figure 4.17) observed between proton H-9 and C-8 (δ_C 126.1), C-10a (δ_C 101.2), C-19 (δ_C 27.8) & C-20 (δ_C 27.7); H-10 and C-6a (δ_C 160.1), C-8 (δ_C 78.1), C-10a (δ_C 101.2) & C-10b (δ_C 155.1) indicated the angular attachment of the dimethylpyran moiety to the chromanone nucleus at carbon positions C-6a and C-10a. Diagnostic correlations observed between

proton H-14 and C-6 (δ_C 110.6), C-13 (δ_C 30.0), C-15 (δ_C 174.4) & C-16 (δ_C 35.2); H-16 and C-6 (δ_C 110.6) & C-17 (δ_C 20.9) confirmed the presence of 3-substituted hexanoic acid unit which was linked to carbon C-6 of the dimethylchromanone nucleus. On the basis of the above spectral evidence, compound **72** was deduced as isocalolongic acid. The NMR data and assignment of compound **72** are summarized in Table 4.3. This compound was previously reported for its isolation from *Calophyllum brasiliense* (Plattner et al., 1974).
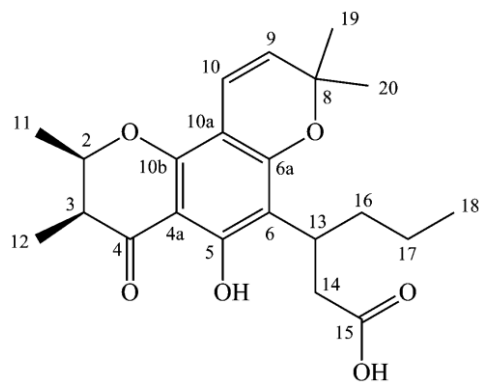
(**72**)

Table 4.3: Summary of NMR data and assignment of isocalolongic acid (72)

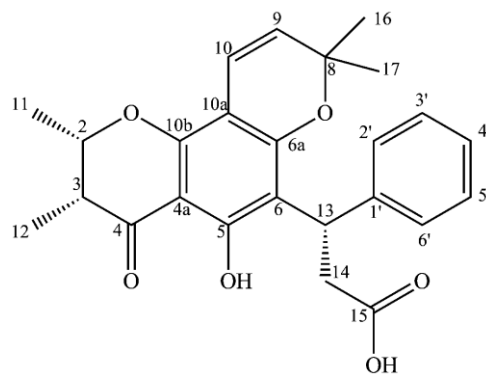| Position	δ_H (ppm)	δ_C (ppm)	HMBC
2	4.61 (1H, qd, J = 6.7, 3.1 Hz)	76.4	C-12
3	2.60 (1H, qd, J = 7.4, 3.1 Hz)	44.0	C- 4 & 12
4	-	201.4	-
4a	-	100.8	-
5	-	162.3	-
6	-	110.6	-
6a	-	160.1	-
8	-	78.1	-
9	5.54 (1H, d, J = 10.1 Hz)	126.1	C-8, 10a, 19 & 20
10	6.50 (1H, d, J = 10.1 Hz)	115.7	C-6a, 8, 10a & 10b
10a	-	101.2	-
10b	-	155.1	-
11	1.35 (3H, d, J = 6.7 Hz)	15.8	C-2 & 3
12	1.08 (3H, d, J = 7.4 Hz)	9.0	C-2, 3 & 4
13	3.71 (1H, m)	30.0	C-5, 6, 6a, 14 & 16
14	2.69 (2H, m)	38.2	C-6, 13, 15 & 16
15	-	174.4	-
16	1.84 (H_a, m)	35.2	C-6 & 17
	1.53 (H_b, m)		
17	1.14 (2H, m)	20.9	C-18
18	0.81 (3H, t, J = 7.4 Hz)	13.8	C-16 & 17
19	1.42 (3H, s)	27.8	C-8, 9 & 20
20	1.41 (3H, s)	27.7	C-8, 9 & 19
5-OH	12.76 (1H, s)	-	C-4a, 5 & 6
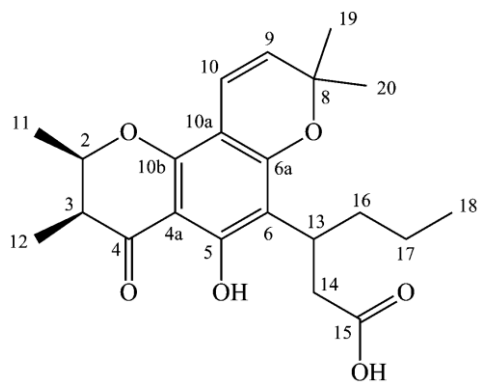
(**72**)
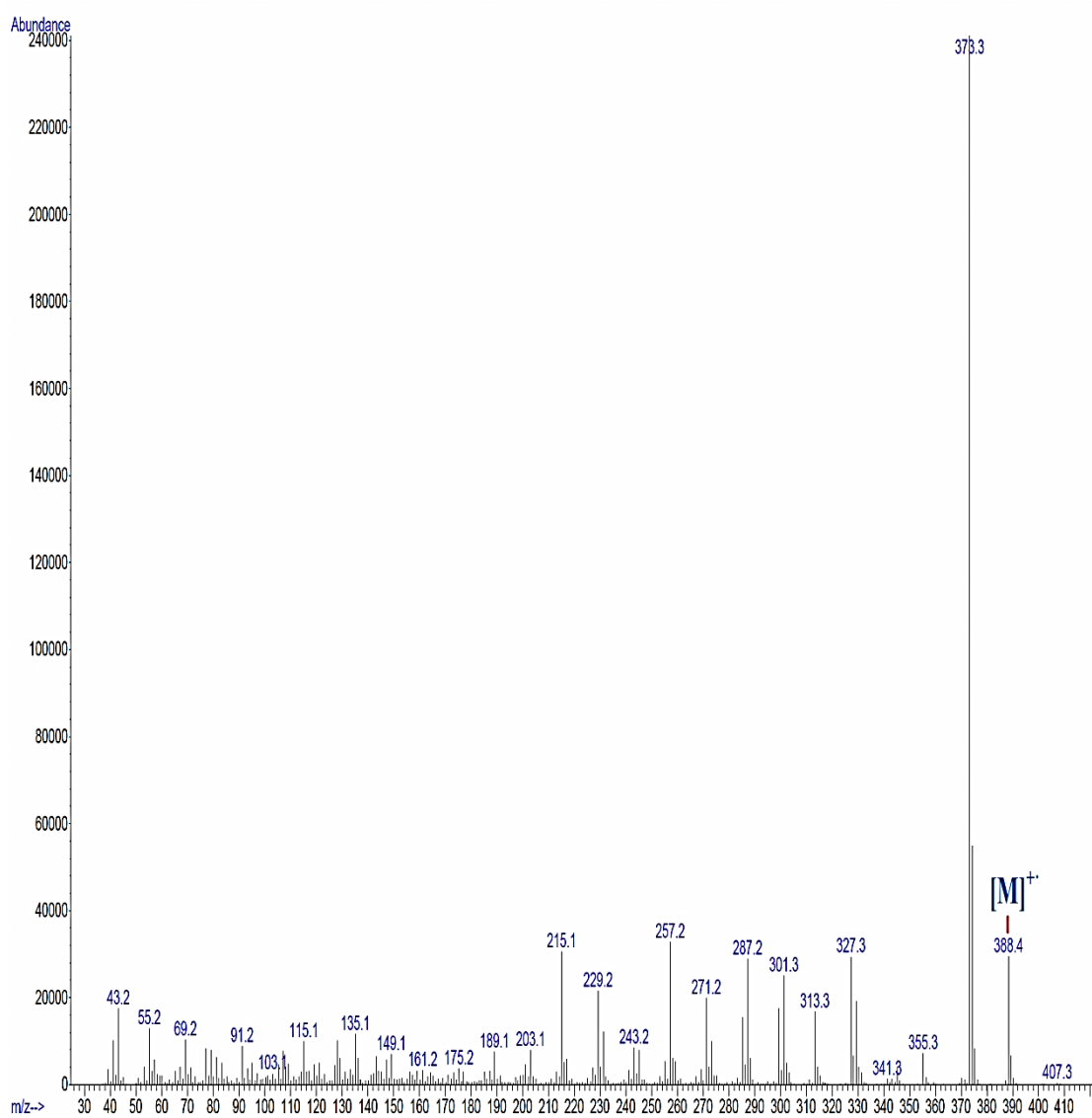
Figure 4.11: EIMS spectrum of isocalolongic acid (72)
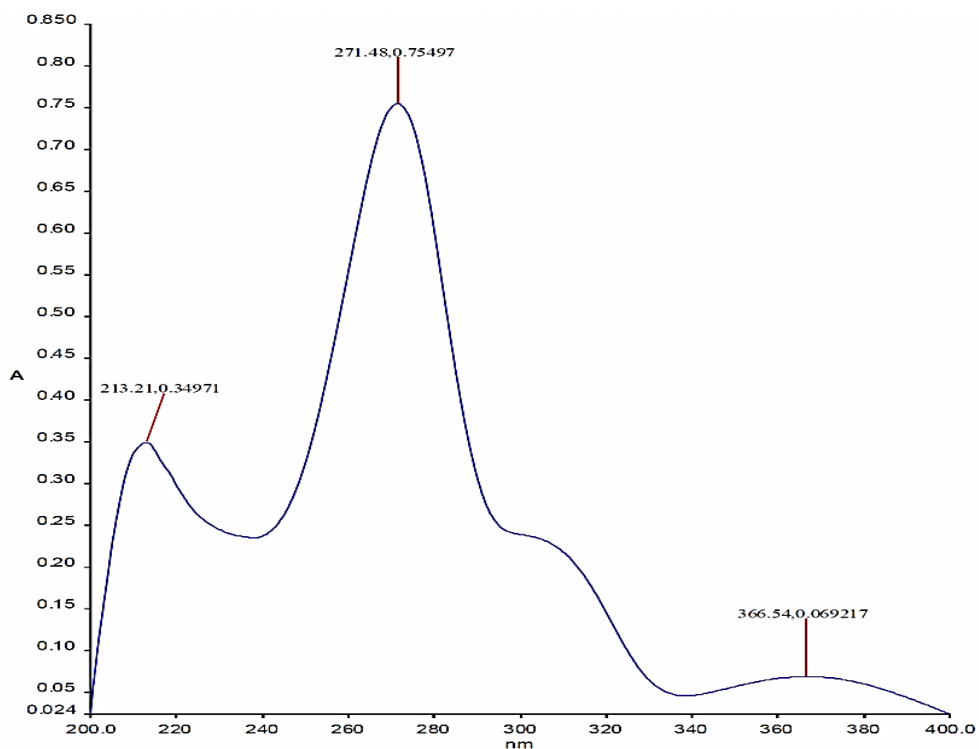
Figure 4.12: UV-Vis spectrum of isocalolongic acid (72)
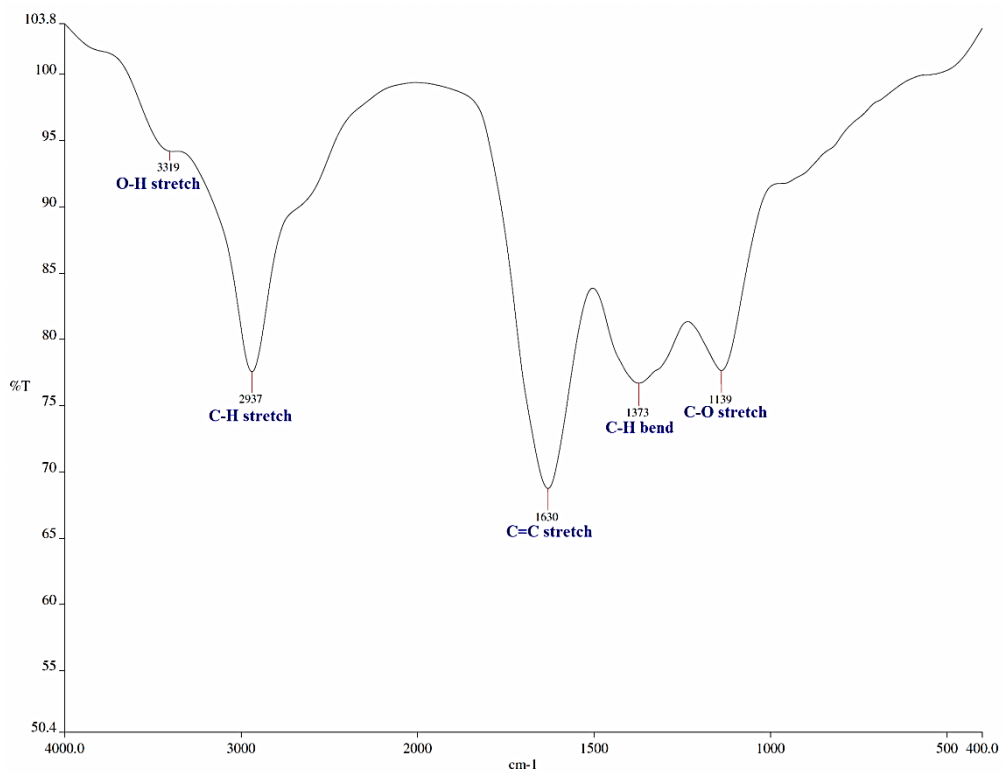
Figure 4.13: IR spectrum of isocalolongic acid (72)
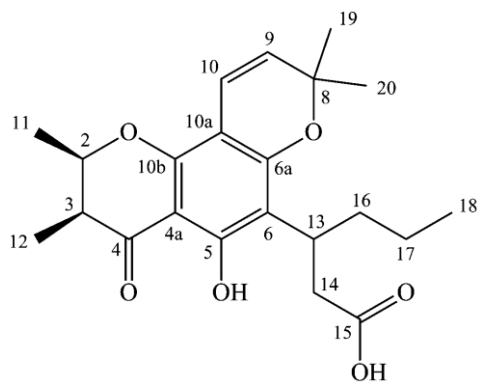
(**72**)
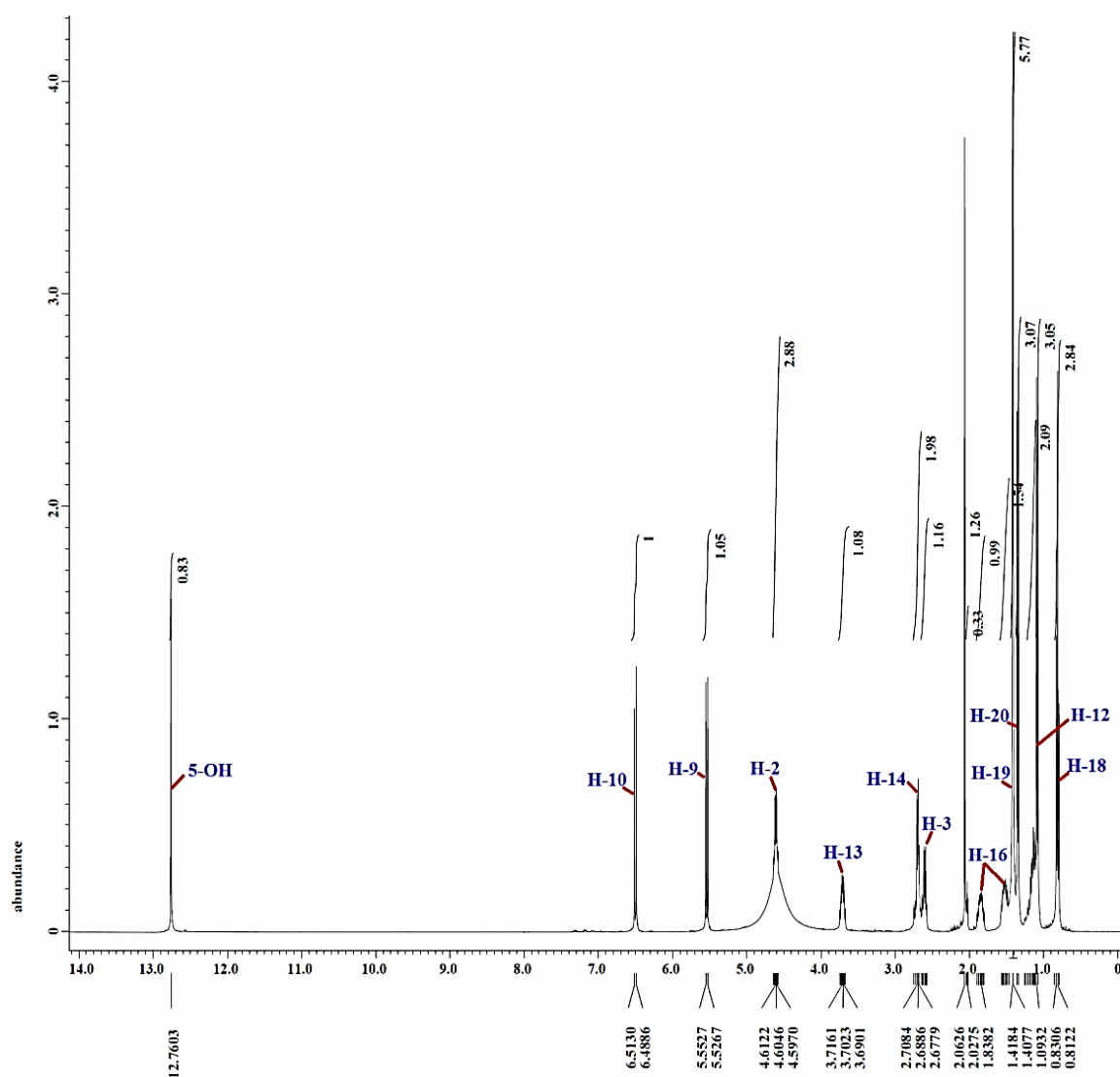
Figure 4.14: ^{1}H NMR spectrum of isocalolongic acid (**72**) (400 MHz, acetone-d_6)
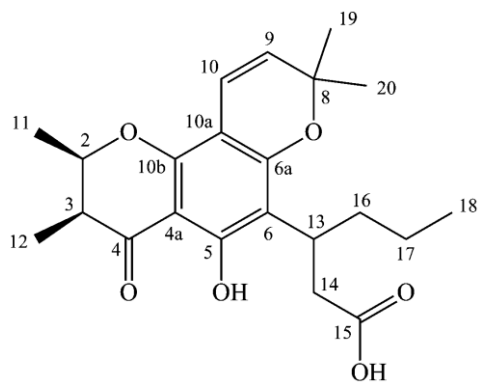
(**72**)
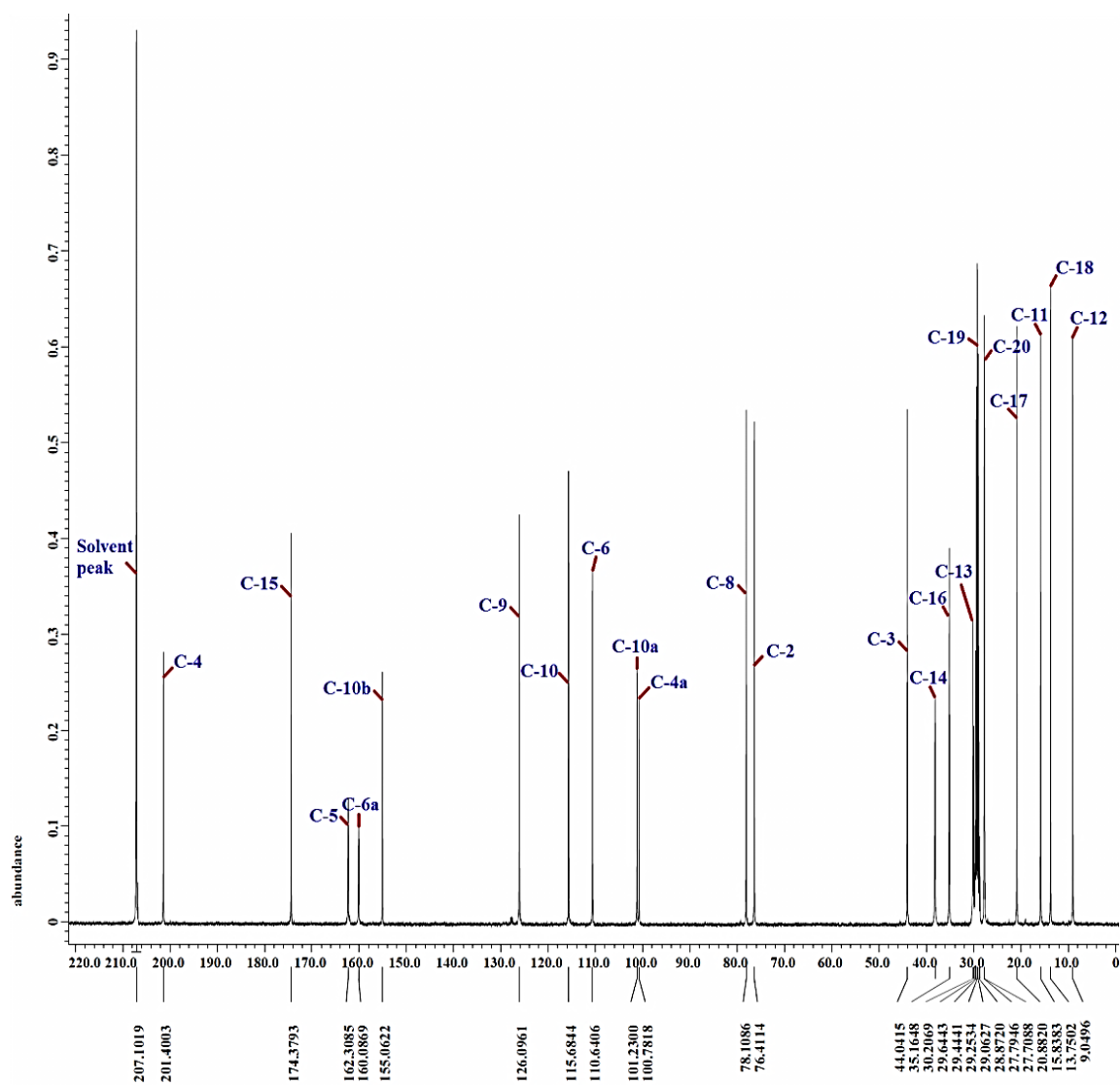
Figure 4.15: ^{13}**C NMR spectrum of isocalolongic acid (72) (100 MHz, acetone,** d_6**)**
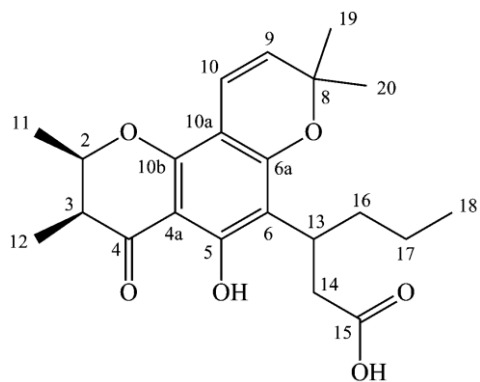
(**72**)
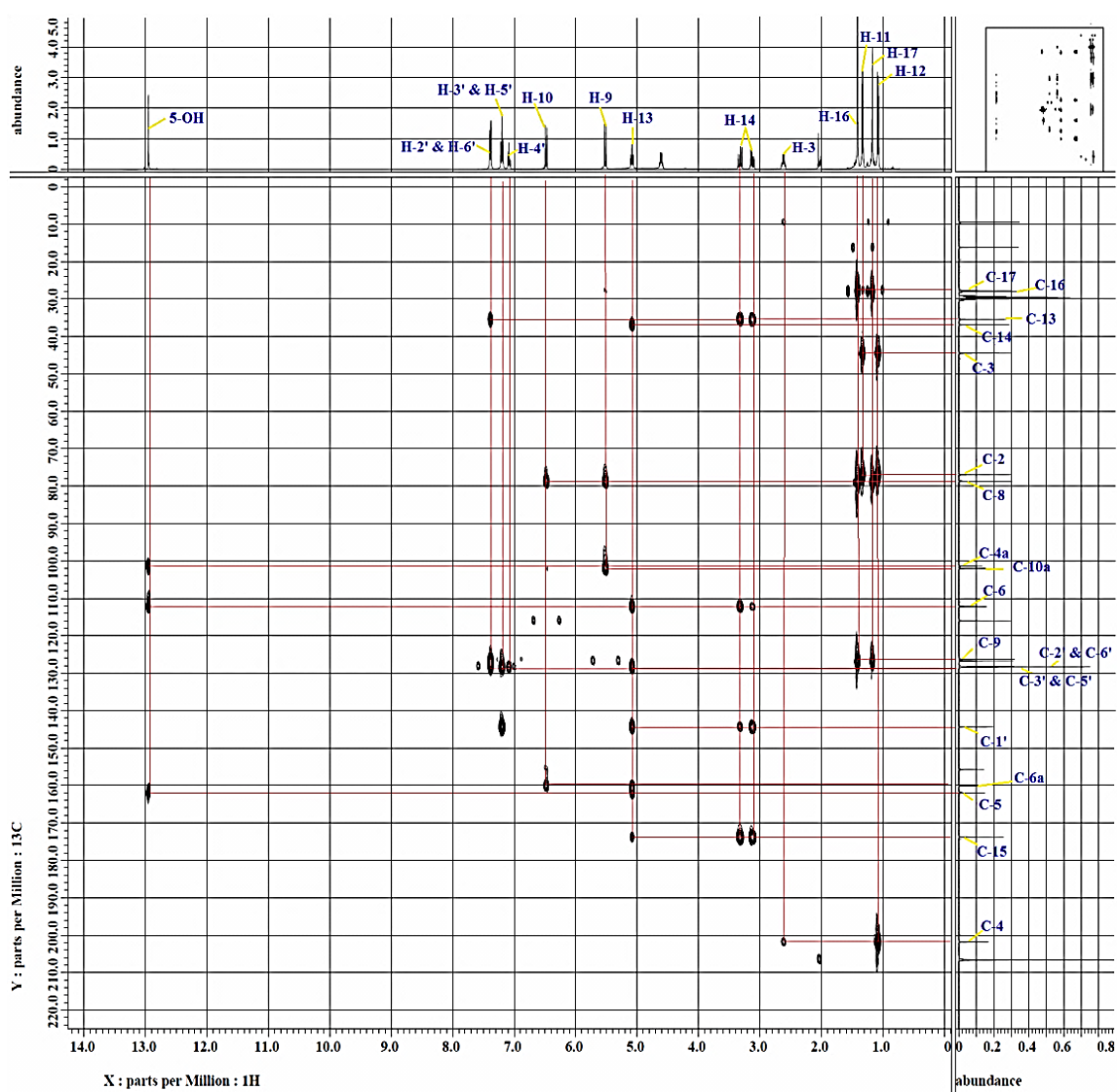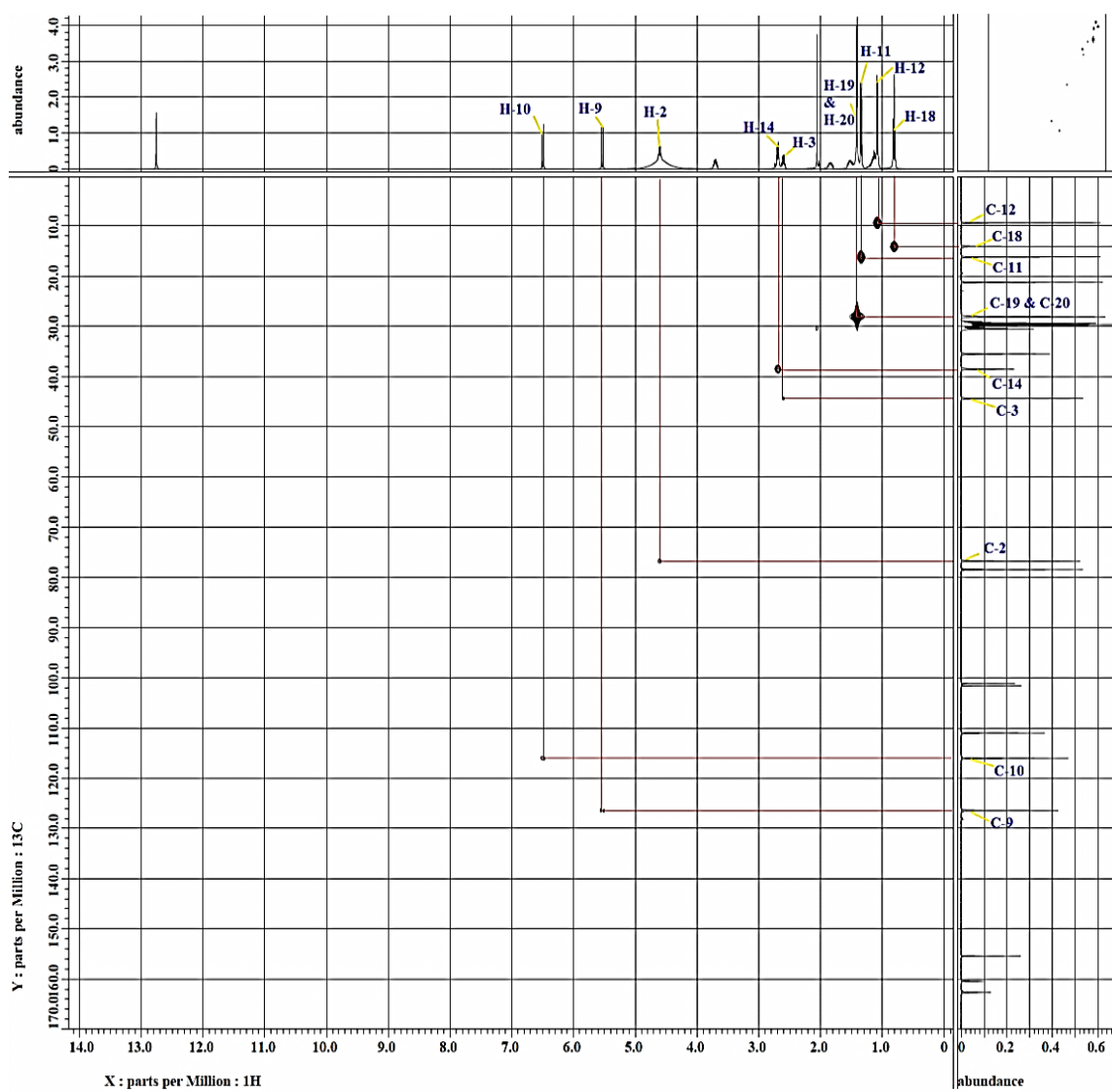
Figure 4.16: HMQC spectrum of isocalolongic acid (72)
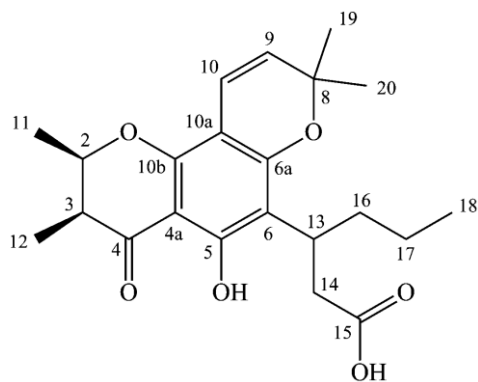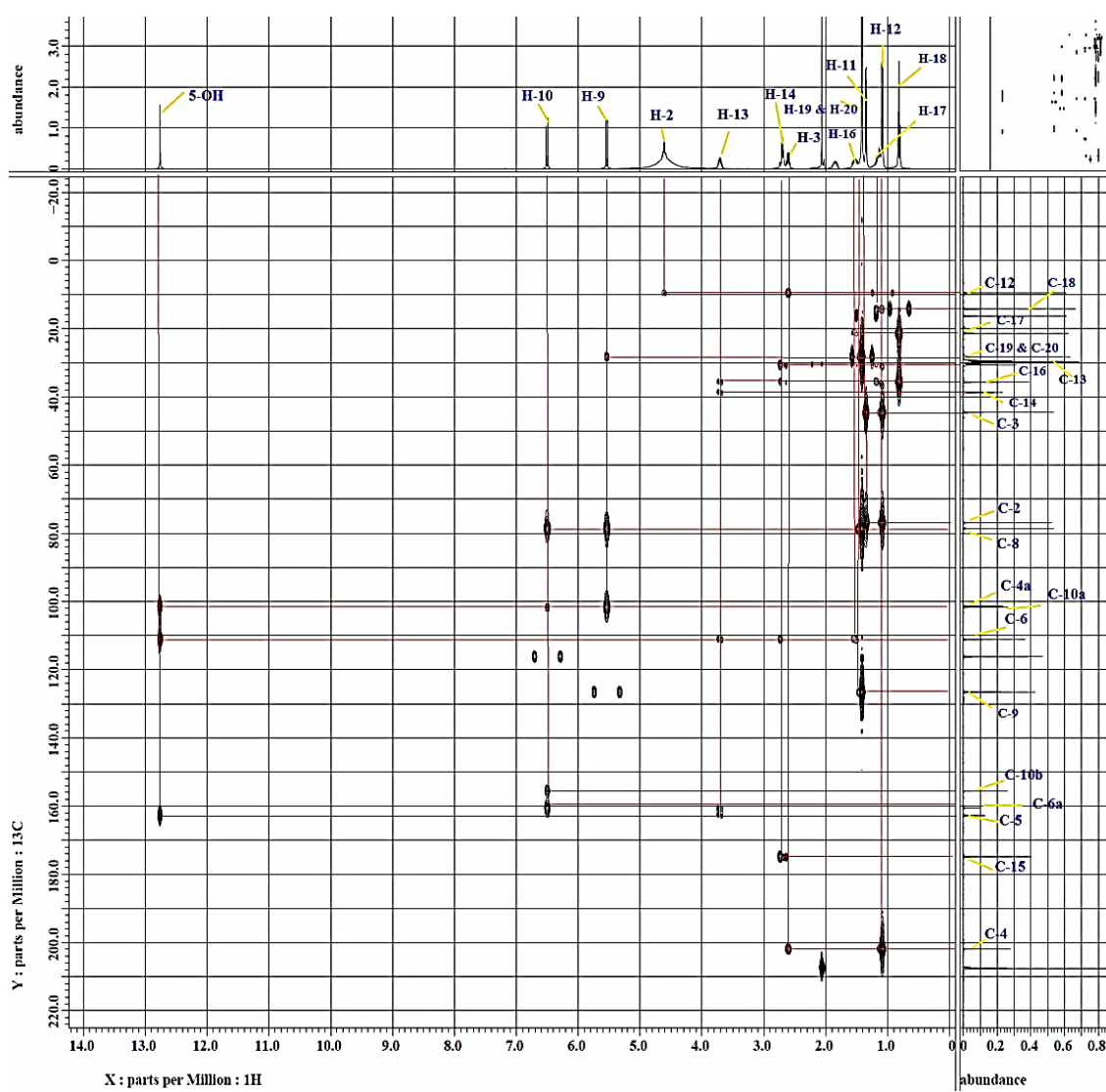
Figure 4.17: HMBC spectrum of isocalolongic acid (72)

4.1.3 Characterization of Calolongic Acid (73)
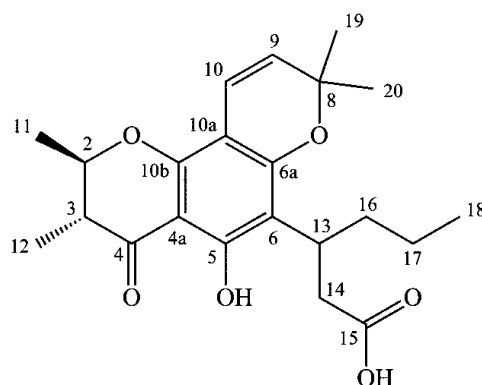
(**73**)

Compound **73** was obtained as yellow gum with a specific rotation $[\alpha]_D$ of $-36.0°$ (MeOH, c 0.05) (Lit $-28.3°$, Huerta-Reyes et al., 2004). This compound gave a dark reddish-pink spot on the developed TLC, under UV light at wavelength of 254 nm, and was stained brown when placed it in iodine chamber. The phenolic nature of this compound was indicated by the positive $FeCl_3$ test. A retention factor, R_f value of 0.74 was obtained via a mobile phase of 70% dichloromethane and 30% acetone.

The molecular formula of compound **73** was determined as $C_{22}H_{28}O_6$ from the EIMS ($[M]^{+\cdot}$ at m/z 388) (Figure 4.18). This compound gave UV absorption maxima at 243.9 nm (Figure 4.19) while the IR spectrum (Figure 4.20) showed absorption bands at 3442 (O-H stretch), 2939 (C-H stretch), 1621 (C=C stretch) and 1151 (C-O stretch) cm^{-1}.

Compound **73** and **72** were diastereomers. The structure of compound **73** was similar to that of isocalolongic acid (**72**) except for the relative spatial arrangement of 2,3-dimethyl substitution in the chromanone ring. Compound **73** showed H-2 resonance at δ_H 4.16 (1H, dq, J = 11.0, 6.1 Hz) indicating a *trans*-2,3-dimethyl substitution. The large coupling constant of 11.0 Hz was consistent with *trans* diaxial protons or (2e,3e) dimethyl substitution (Stout et al., 1968). On the contrary, compound **72** gave relatively a more deshielded H-2 resonance at δ_H 4.61 (1H, qd, J = 6.7, 3.1 Hz). The small coupling constant of 3.1 Hz was indicative of *cis* or (2e,3a) dimethyl substitution (Ha et al., 2012). The ^{1}H and ^{13}C NMR spectra of compound **73** (Figures 4.21 and 4.22) were closely resembled to that of compound **72** except for the signals due to 2,3-dimethyl substituted ring. The NMR data and HMBC assignment of compound **73** are summarized in Table 4.4. This compound was reported to have been previously isolated from *Calophyllum brasiliense* (Plattner et al., 1974).
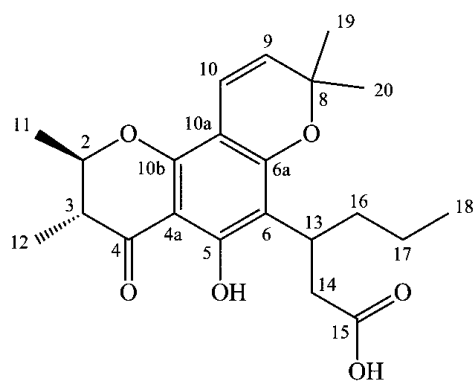
(**73**)

Table 4.4: Summary of NMR data and assignment of calolongic acid (73)

Position	δ_H (ppm)	δ_C (ppm)	HMBC
2	4.16 (1H, dq, J = 11.0, 6.1 Hz)	78.8	-
3	2.54 (1H, dq, J = 11.0, 7.3 Hz)	45.7	C-2, 4 & 12
4	-	198.8	-
4a	-	101.7	-
5	-	162.1	-
6	-	110.3	-
6a	-	160.0	-
8	-	78.1	-
9	5.45 (1H, d, J = 10.1 Hz)	125.9	C-8, 10a, 19 & 20
10	6.52 (1H, d, J = 10.1 Hz)	115.9	C-6a, 8 & 10b
10a	-	101.1	-
10b	-	155.2	-
11	1.49 (3H, d, J = 6.1 Hz)	19.8	C-2 & 3
12	1.19 (3H, d, J = 7.3 Hz)	10.2	C-2, 3 & 4
13	3.70 (1H, m)	30.3	-
14	2.84 (1H, dd, J = 15.9, 8.0 Hz) 2.74 (1H, dd, J = 15.9, 7.3 Hz)	38.3	C-6, 13, 15 & 16
15	-	179.1	-
16	1.84 (1H, m) 1.53 (1H, m)	35.3	C-6
17	1.15 (2H, m)	21.0	C-16 & 18
18	0.84 (3H, t, J = 7.3 Hz)	14.2	C-16 & 17
19	1.42 (3H, s)	28.4	C-8, 9 & 20
20	1.42 (3H, s)	28.3	C-8, 9 & 19
5-OH	12.69 (1H, s)	-	C-4a, 5 & 6
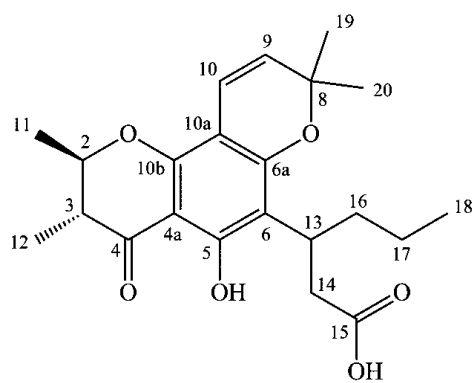
(**73**)
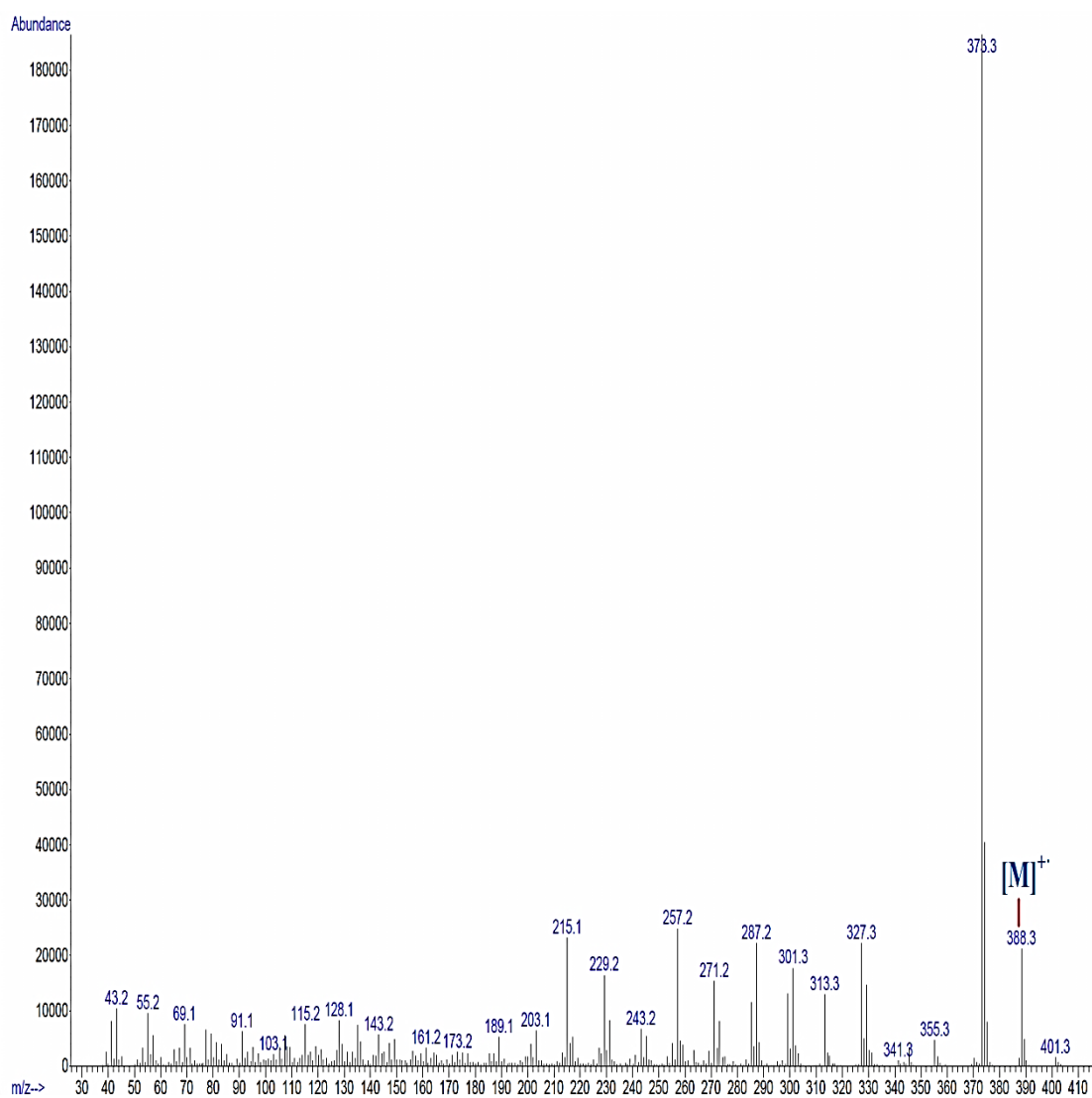
Figure 4.18: EIMS spectrum of calolongic acid (73)
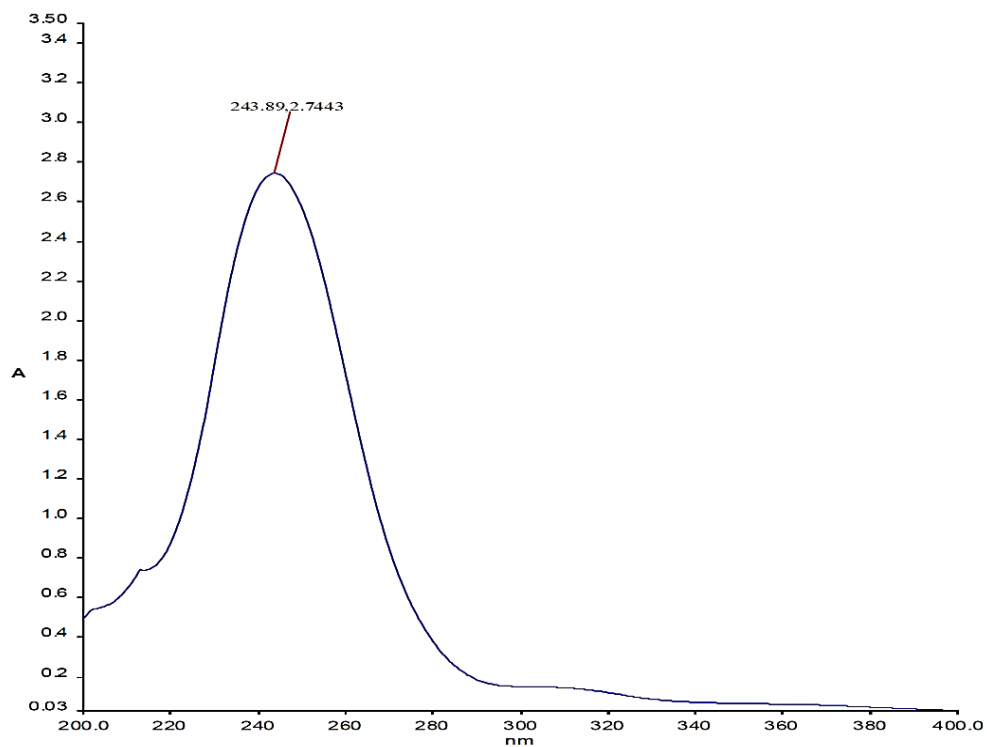
Figure 4.19: UV-Vis spectrum of calolongic acid (73)
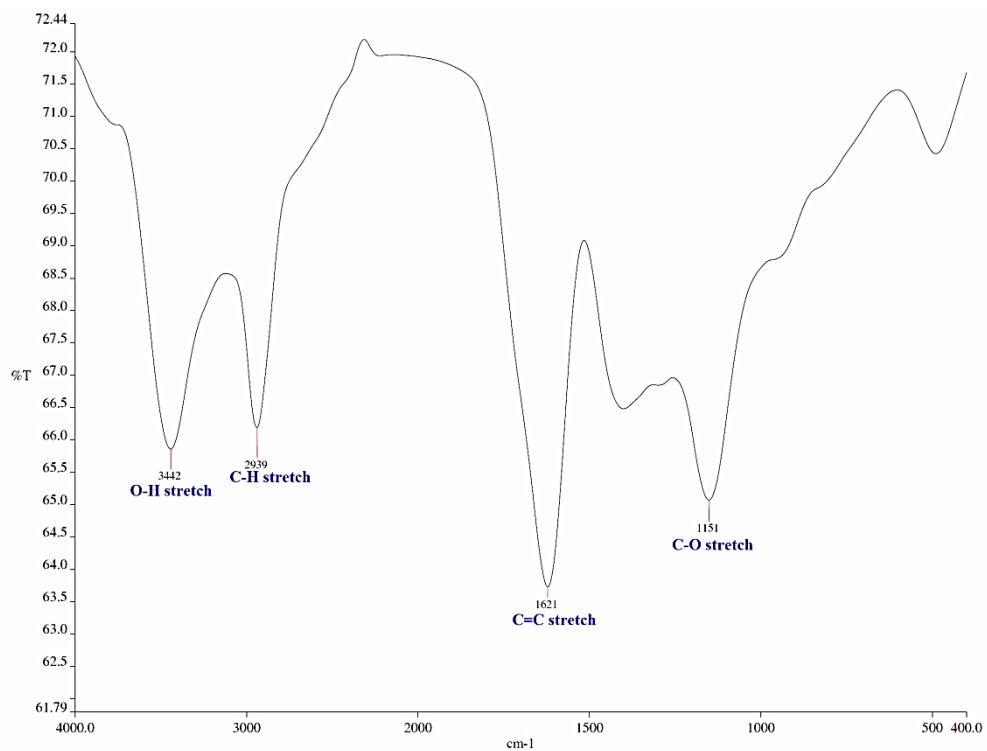
Figure 4.20: IR spectrum of calolongic acid (73)
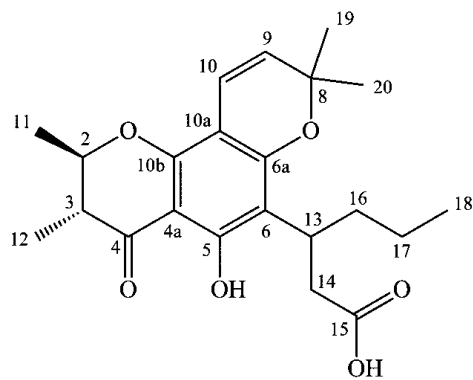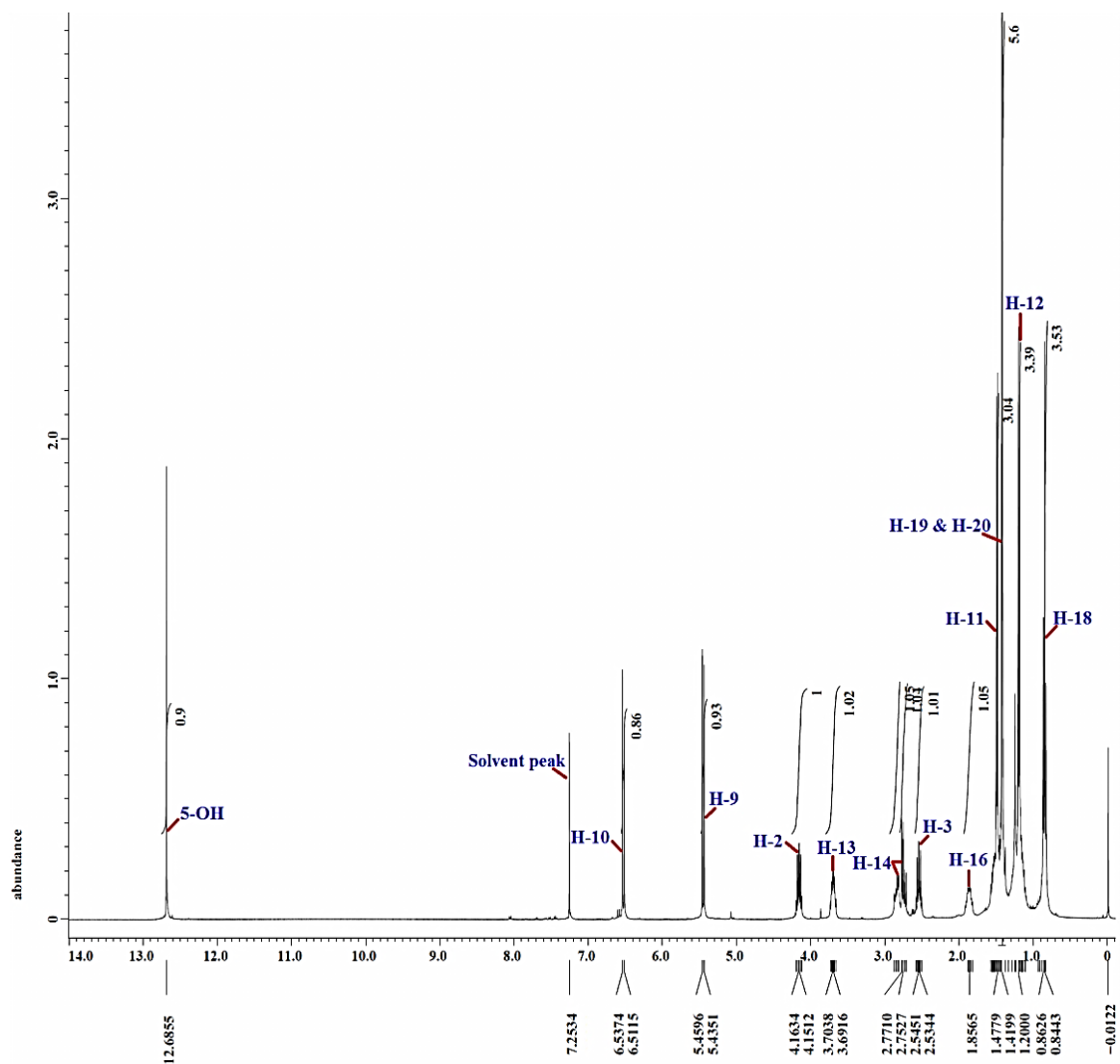
Figure 4.21: ^{1}H NMR spectrum of calolongic acid (**73**) (400 MHz, acetone-d_6)
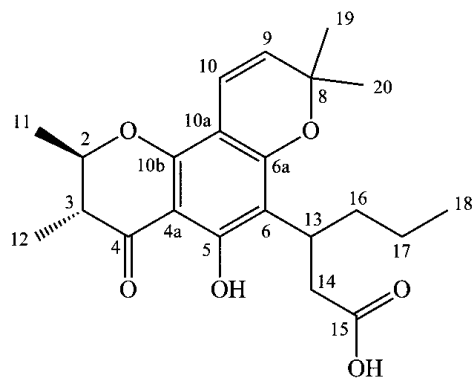
(**73**)
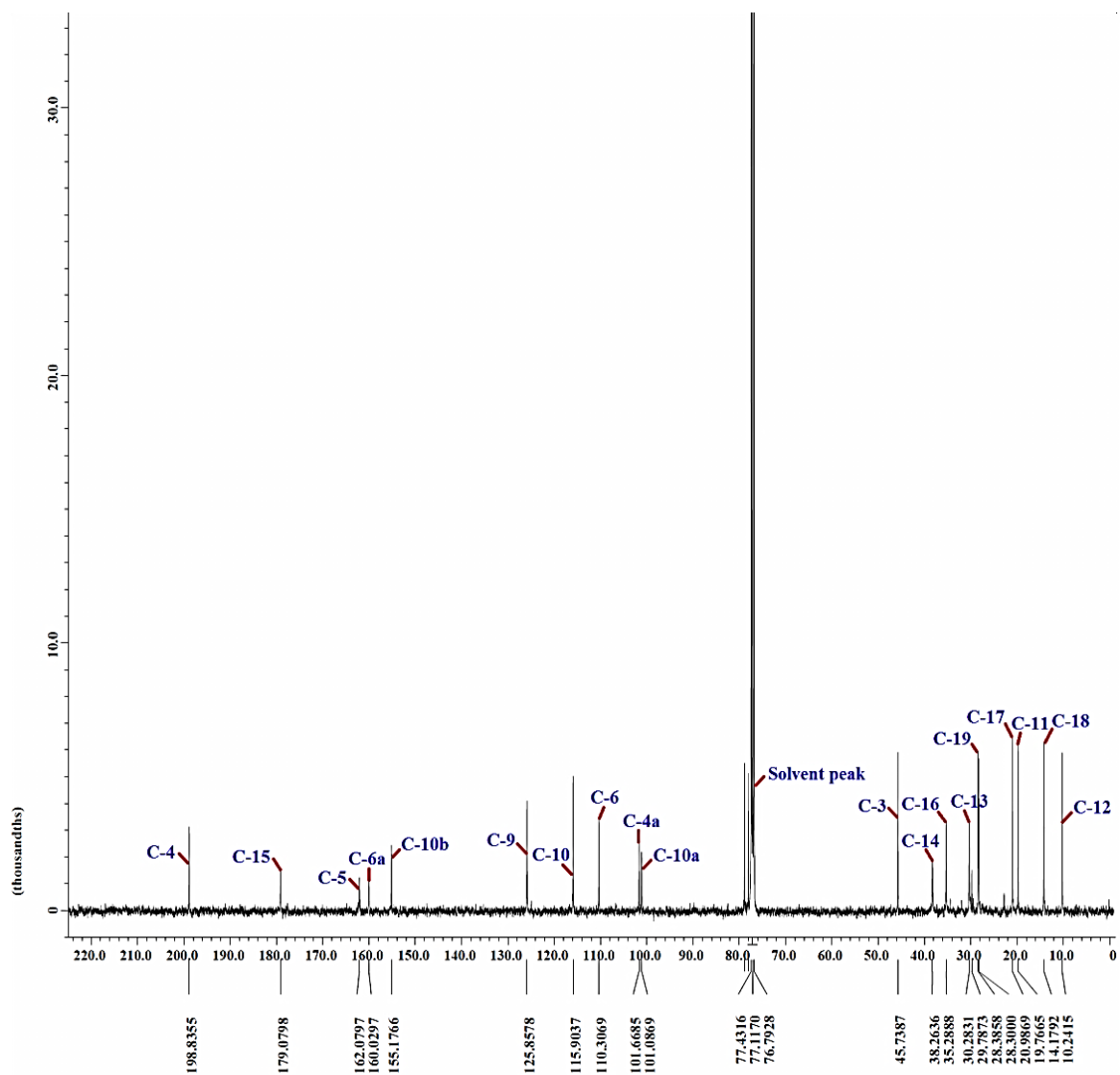
Figure 4.22: ^{13}C NMR spectrum of calolongic acid (**73**) (100 MHz, acetone-d_6)
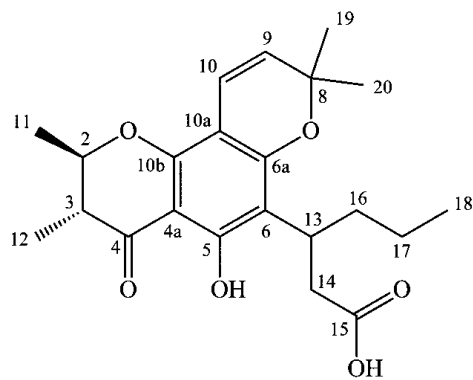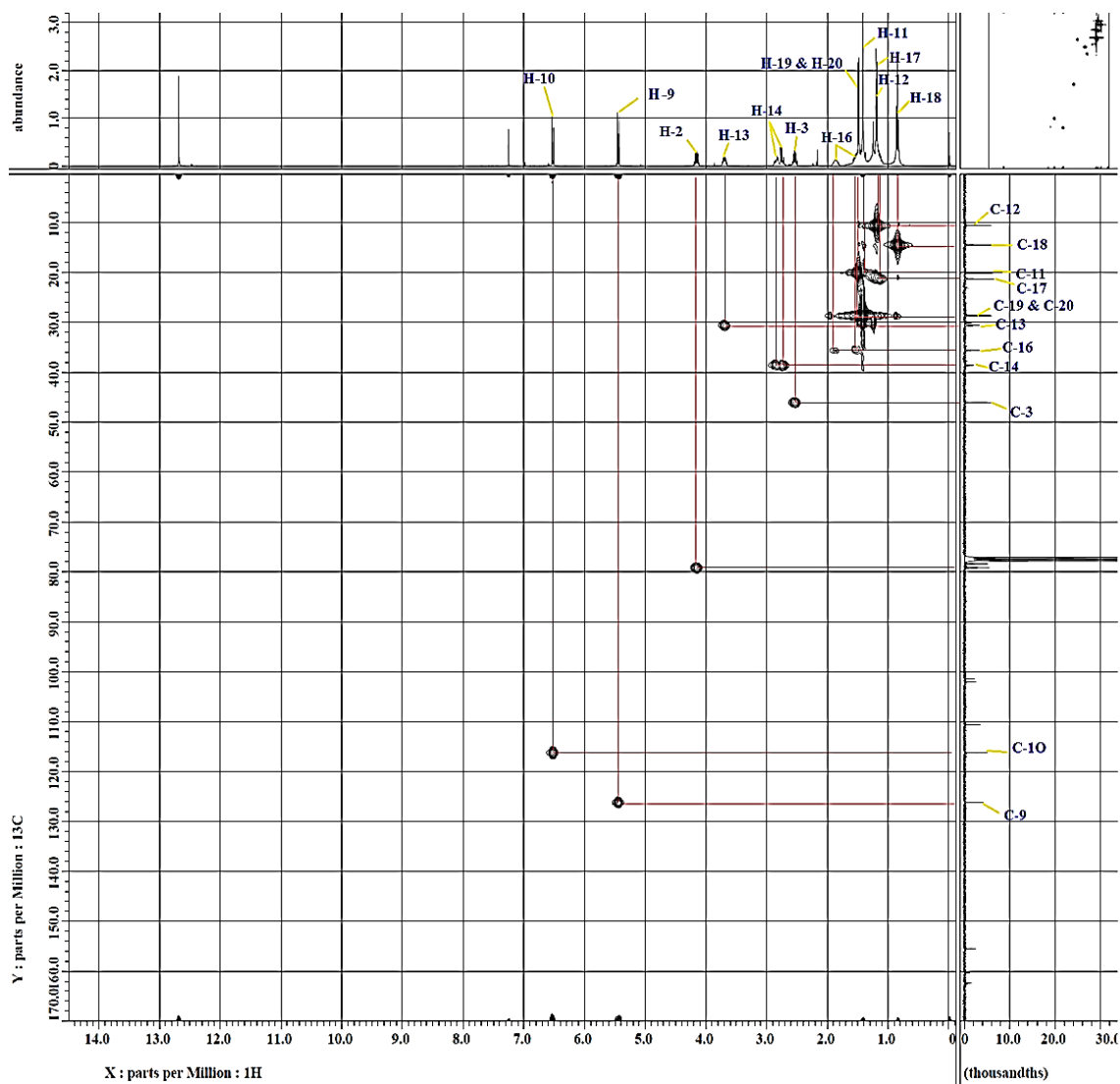
Figure 4.23: HMQC spectrum of calolongic acid (73)
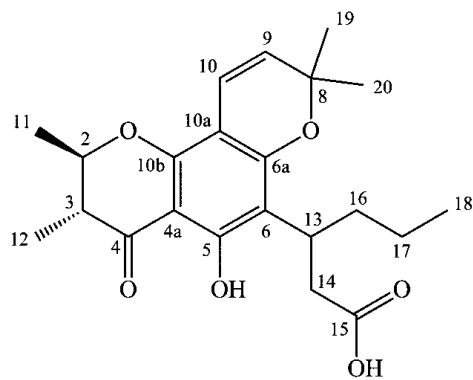
(**73**)
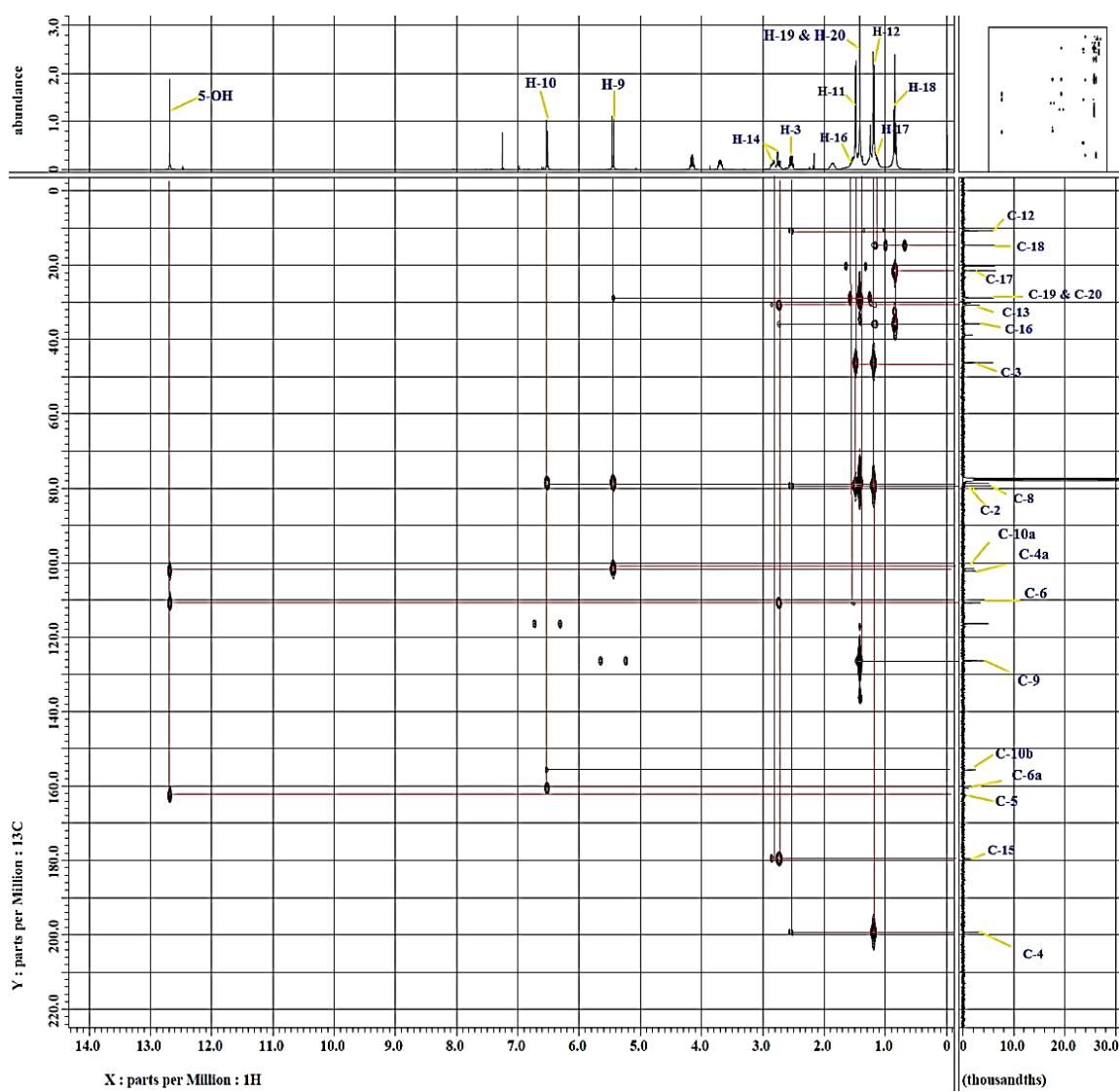
Figure 4.24: HMBC spectrum of calolongic acid (73)

4.1.4 Characterization of Stigmasterol (74)
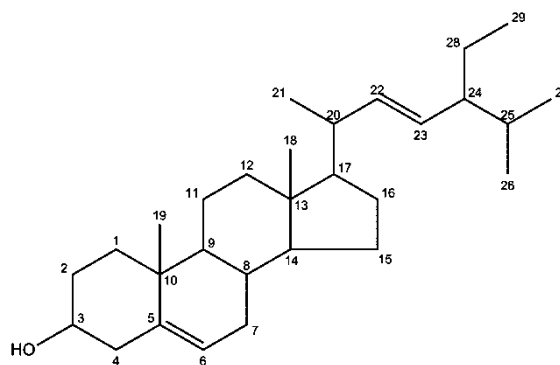
(**74**)

Compound **74** was isolated as white needle-like crystals, mp of 139-141 °C (Lit. 138-140 °C, Ahmed et al., 2013). The optical rotation of the compound was observed at $[\alpha]_D = -14.0°$, which is close to the reported literature value of -16.6^o (Mawa and Said, 2012). Compound **74** gave no visible spot when visualized under UV light at wavelength of 254 nm. It gave brown spot when treated with iodine vapor. Besides, this compound showed negative result in the $FeCl_3$ test, indicating the absence of phenolic moiety in this compound. TLC analysis revealed compound **74** to have R_f value of 0.56 when eluted with a solvent mixture of 60% dichloromethane and 40% hexane.

The molecular ion peak observed at *m/z* 412 in the EIMS spectrum (Figure 4.25) was in correspondence to the molecular formula of $C_{29}H_{48}O$. The IR spectrum (Figure 4.26) revealed absorption bands at 3398 (O-H stretch), 2919 (C-H stretch), 1419 (C-H bend) and 1058 (C-O stretch) cm^{-1}.

81

The ^{1}H NMR spectra (Figures 4.27 and 4.28) exhibited signals for six methyl groups at δ_H 1.01 (3H, d, J = 8.0 Hz), 1.00 (3H, s), 0.83 (3H, t, J = 6.7 Hz), 0.80 (3H, d, J = 7.9 Hz), 0.78 (3H, d, J = 6.7 Hz) and 0.69 (3H, s) assignable to methyl protons H-21, H-18, H-29, H-27, H-26 and H-19, respectively. The three relatively more deshielded proton signals at δ_H 5.34 (1H, d, J = 4.9 Hz), 5.14 (1H, dd, J = 15.2, 8.6 Hz) and 5.00 (1H, dd, J = 15.2, 8.6 Hz) were respectively ascribed to the olefinic protons H-6, H-23 and H-22. Meanwhile, the hydroxymethine proton, H-3 gave a multiplet signal at δ_H 3.51.

In ^{13}C NMR spectrum (Figure 4.29), the presence of two pairs of olefinic carbons and oxymethine carbon was revealed by the relatively downfield signals at δ_C 140.8 (C-5), 138.4 (C-22), 129.3 (C-23), 121.8 (C-6) and 71.9 (C-3). Compound **74** was deduced to be stigmasterol based on the ^{1}H and ^{13}C NMR spectral evidence and by comparison of spectral data with literature values (Pierre and Moses, 2015), and are summarized in Table 4.5.
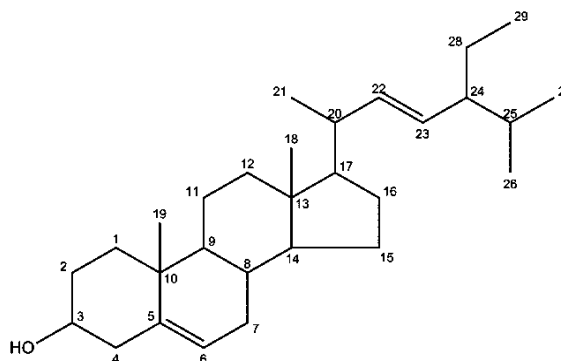
(**74**)

Table 4.5: Summary of NMR data and assignment of stigmasterol (74)

Position	δ$_H$ (ppm)	δ$_C$ (ppm)	*δ$_C$ (ppm)
1	-	37.3	37.2
2	-	32.0	31.6
3	3.51 (1H, m)	71.9	71.7
4	-	42.4	42.2
5	-	140.8	140.8
6	5.34 (1H, d, J = 4.9 Hz)	121.8	121.6
7	-	32.0	31.6
8	-	31.7	31.8
9	-	50.2	50.0
10	-	36.6	36.2
11	-	21.2	21.1
12	-	39.8	39.6
13	-	42.3	42.1
14	-	57.0	56.8
15	-	24.4	24.3
16	-	29.0	28.8
17	-	56.0	55.8
18	1.00 (3H, s)	12.1	12.2
19	0.69 (3H, s)	19.5	19.9
20	-	40.6	40.5
21	1.01 (3H, d, J =8.0 Hz)	21.2	21.0
22	5.00 (1H, dd, J = 15.2, 8.6 Hz)	138.4	138.4
23	5.14 (1H, dd, J = 15.2, 8.6 Hz)	129.3	129.4
24	-	51.3	51.2
25	-	32.0	31.9
26	0.78 (3H, d, J= 6.7 Hz)	21.3	21.2
27	0.80 (3H, d, J= 7.9 Hz)	19.1	19.0
28	-	25.5	25.5
29	0.83 (3H, t, J= 6.7 Hz)	12.3	12.3

*Pierre and Moses, 2015
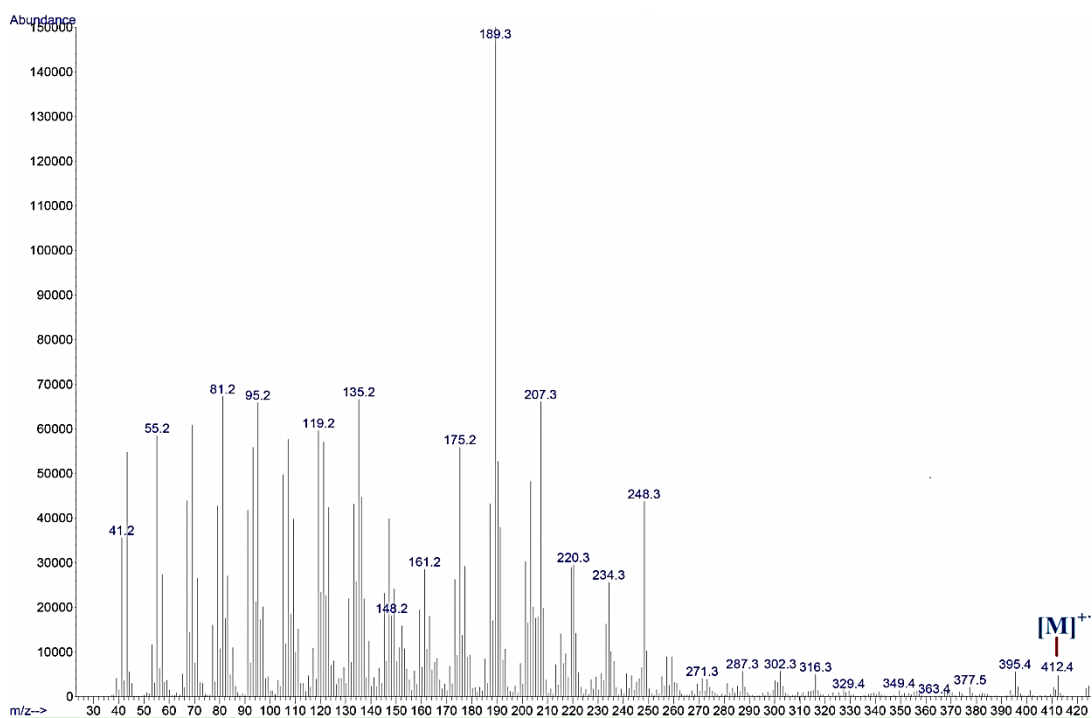
Figure 4.25: EIMS spectrum of stigmasterol (74)
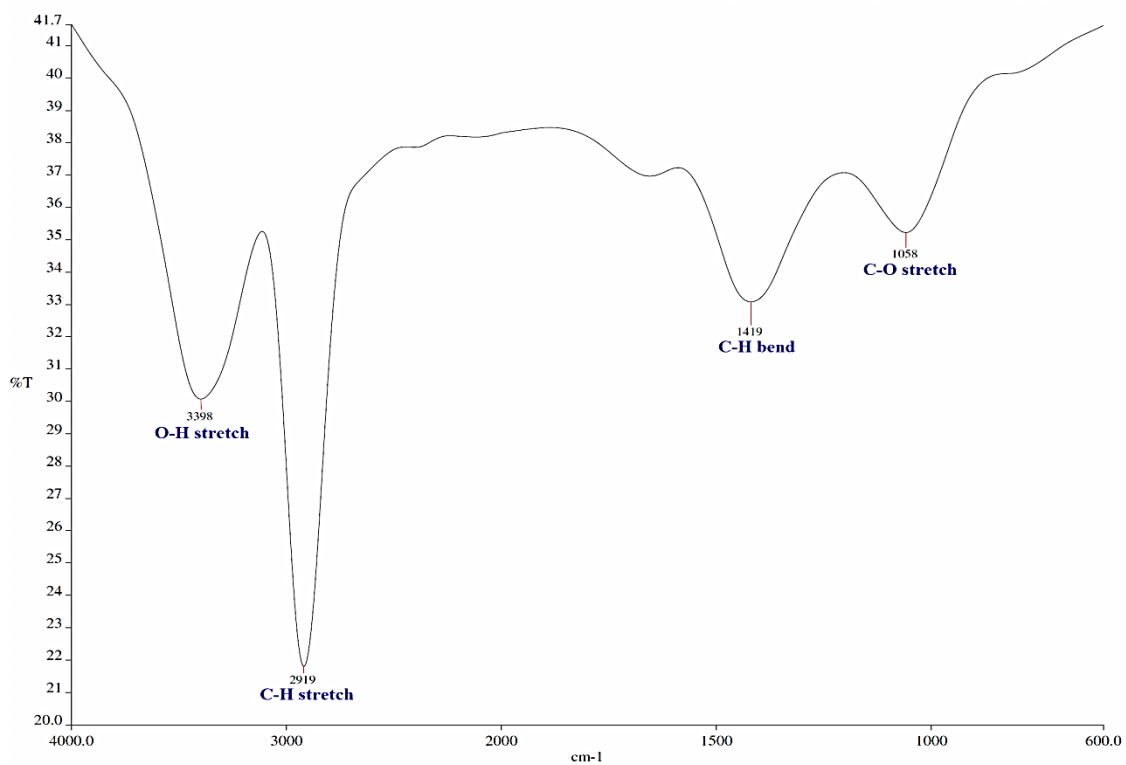
Figure 4.26: IR spectrum of stigmasterol (74)
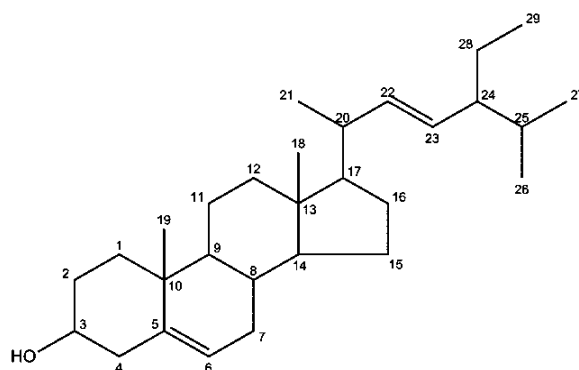
(**74**)
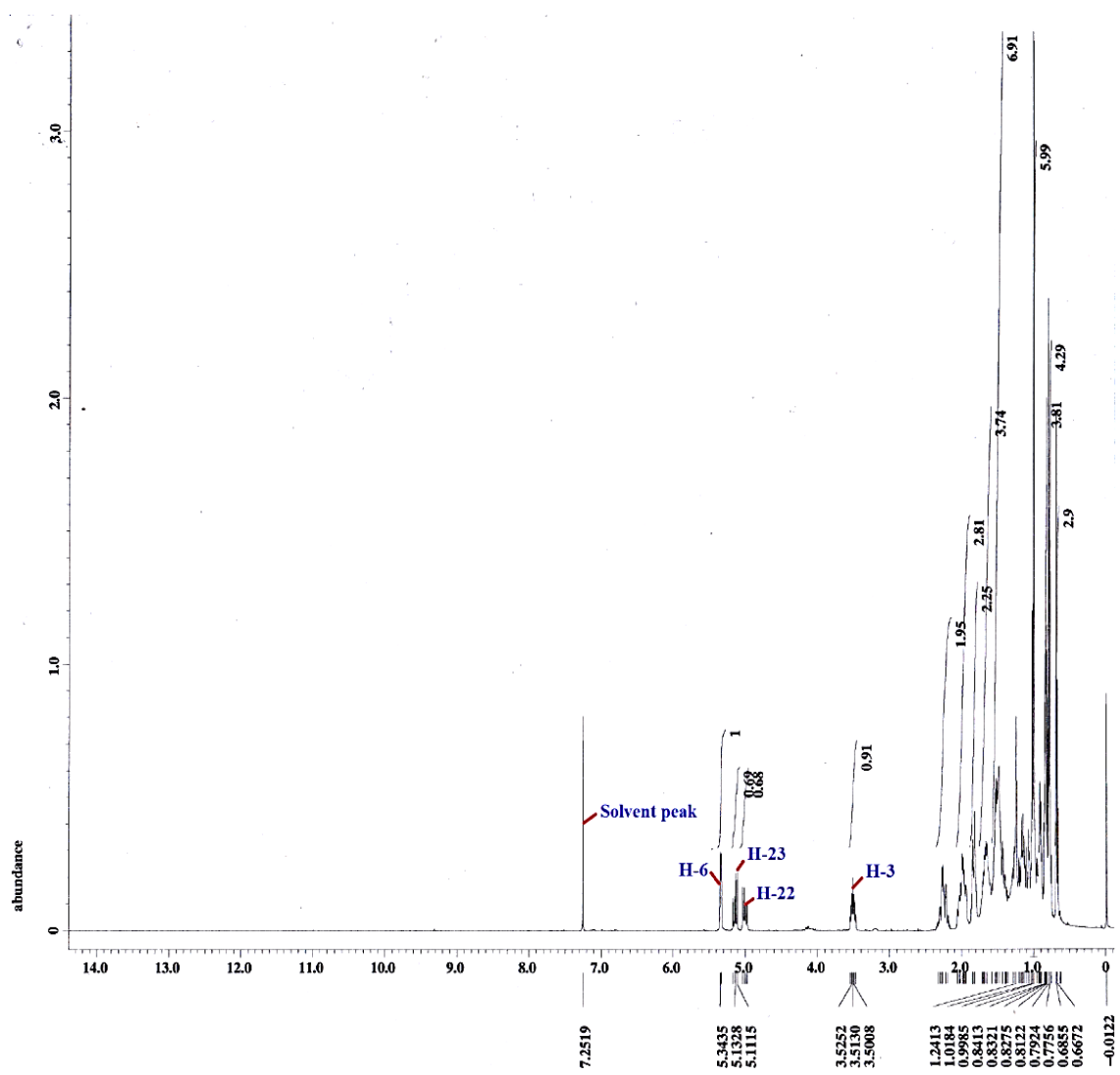
Figure 4.27: ^{1}H NMR spectrum of stigmasterol (**74**) (400 MHz, CDCl$_3$)
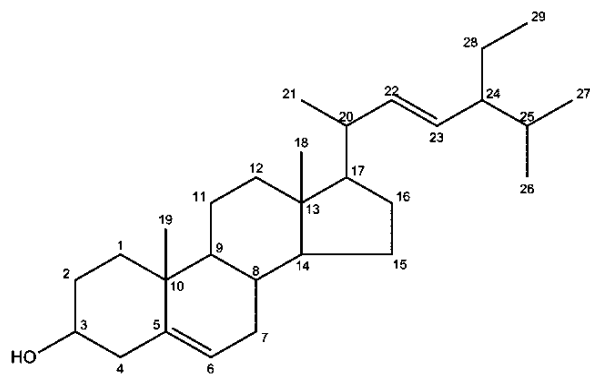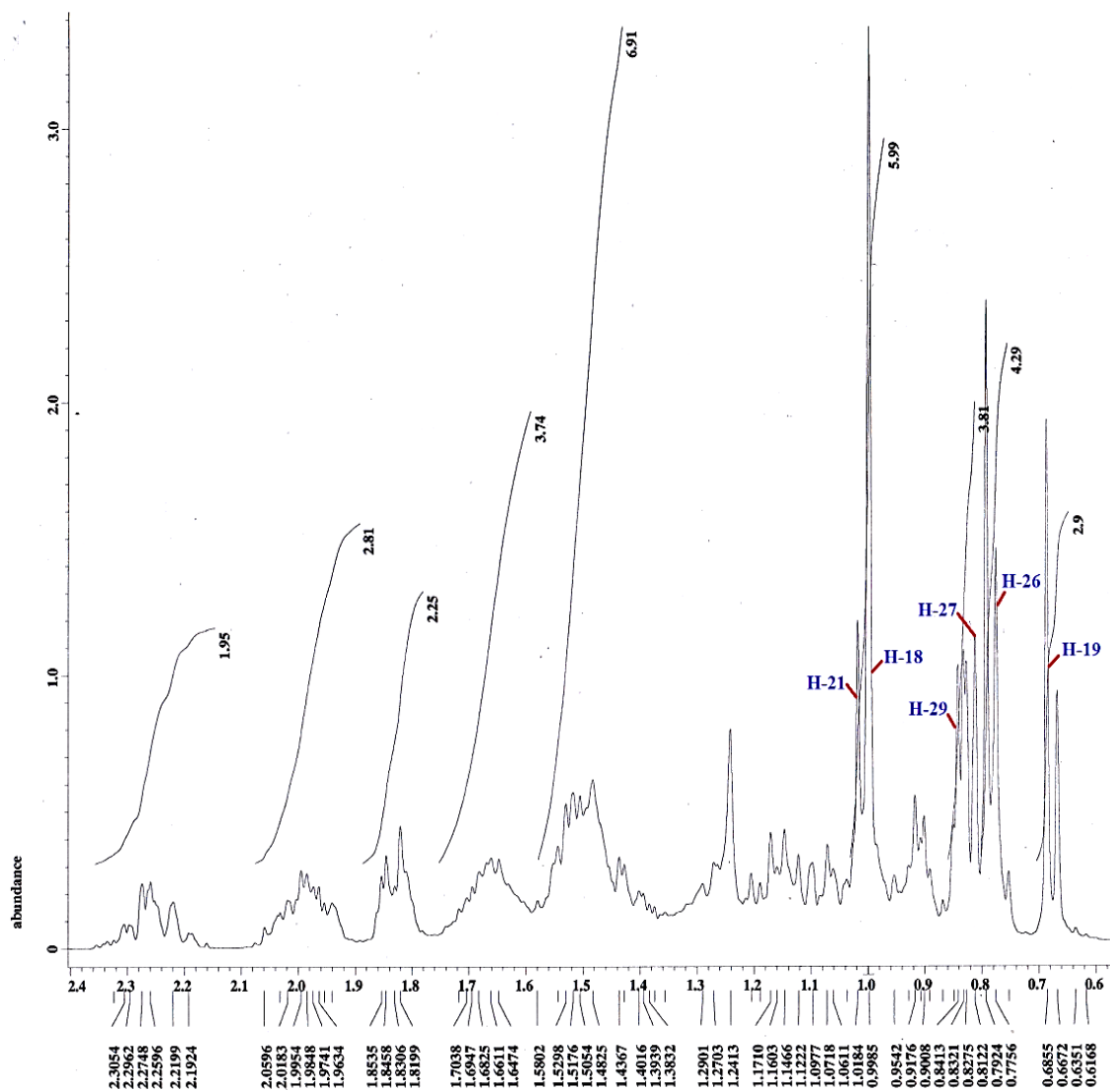
Figure 4.28: Expanded ¹H NMR spectrum (upfield region) of stigmasterol (74) (400 MHz, CDCl₃)
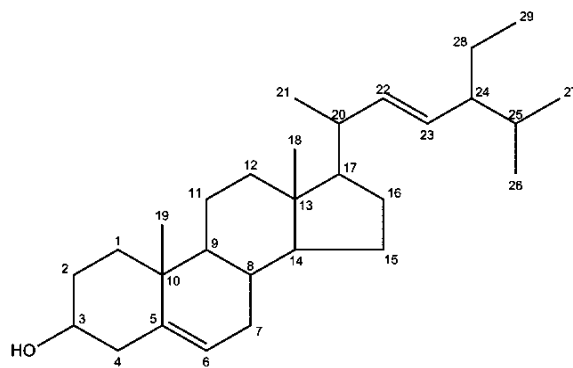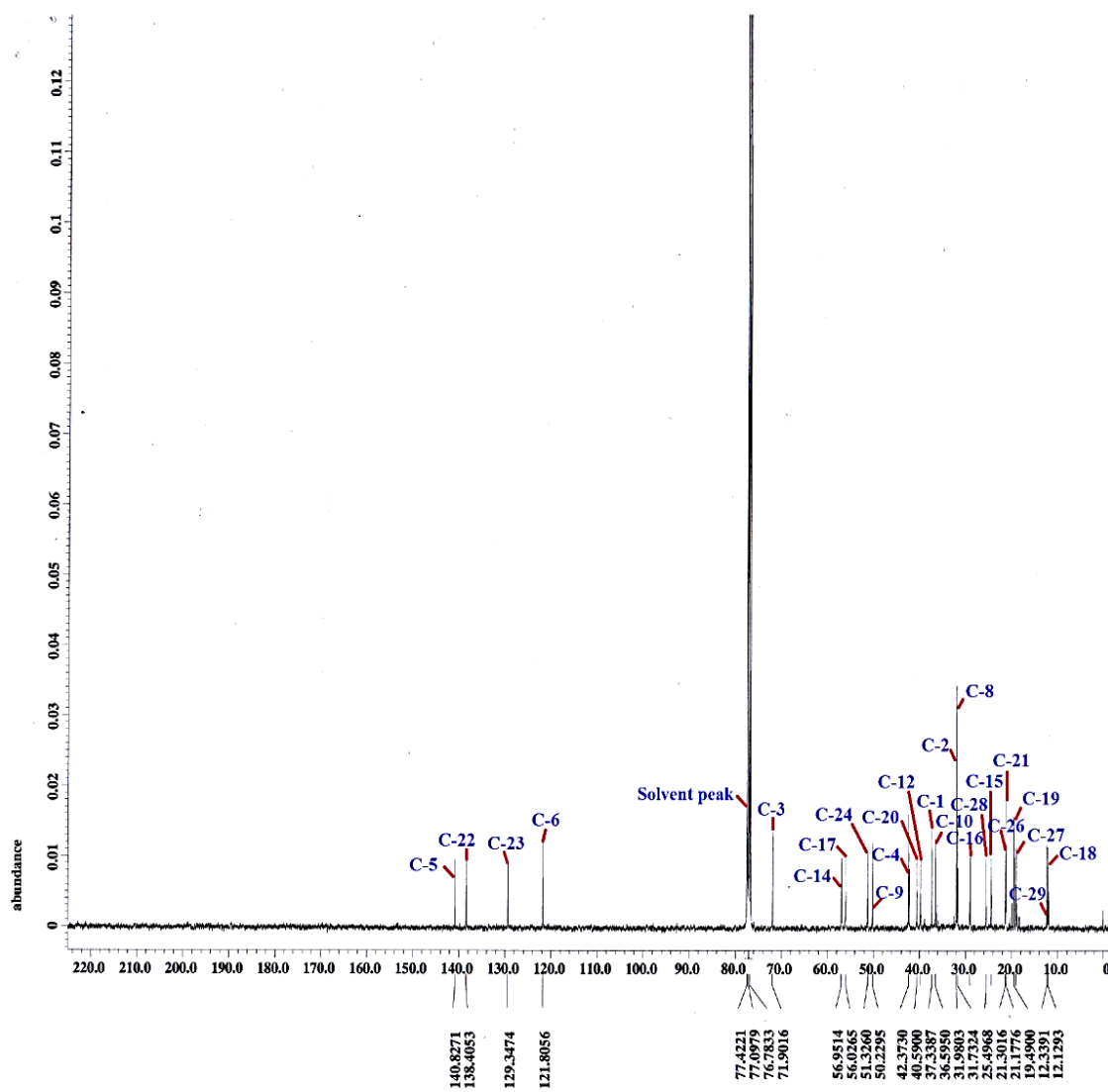
Figure 4.29: ^{13}C NMR spectrum of stigmasterol (**74**) (100 MHz, CDCl$_3$)

87

4.2 Extraction and Isolation of Chemical Constituents from *Calophyllum andersonii*

Solvent extractions of the dried and ground stem bark of *Calophyllum andersonii* (1.0 kg) afforded dichloromethane, ethyl acetate and methanol crude extracts, weighing 24.0, 16.7 and 57.8 g, respectively. The summary of the weight and percentage of yield of crude extracts are shown in Table 4.6.

Table 4.6: Extract yields of *Calophyllum andersonii*

Crude Extract	Weight (g)	Percentage of yield (%)*
Dichloromethane	24.0	2.4
Ethyl Acetate	16.7	1.7
Methanol	57.8	5.8

* Percentage of yield was calculated based on the weight of the dried extract against dry weight of ground stem bark of *Calophyllum andersonii* (1.0 kg) multiplied by 100%.

About 20 g of dichloromethane extract was subjected to Si gel CC (40-63 μm, 8.5 x 50 cm, 600 g) packed in *n*-hexane and eluted with *n*-hexane-dichloromethane mixtures of increasing polarity (90:10, 80:20, 70:30, 60:40, 50:50, 40:60, 30:70, 20:80, 10:90, 0:100), followed by increasing concentration of EtOAc in dichloromethane (10:90, 20:80, 30:70, 40:60, 50:50, 60:40, 70:30, 80:20, 90:10, 100:0) to give 25 fractions (HEBA1-25). Fractions HEBA6-7 and HEBA10 were separately recrystallized from methanol to afford friedelin (**75**, 1069 mg) and friedelinol (**76**, 38 mg). Meanwhile, about 15 g of ethyl acetate extract was subjected to Si gel CC (40-63 μm, 8.5 x 50 cm, 600 g) packed in *n*-hexane and eluted with *n*-hexane-dichloromethane mixtures of increasing polarity (90:10, 80:20, 70:30, 60:40,

50:50, 40:60, 30:70, 20:80, 10:90, 0:100), followed by increasing concentration of EtOAc in dichloromethane (10:90, 20:80, 30:70, 40:60, 50:50, 60:40, 70:30, 80:20, 90:10, 100:0) to give protocatechuic acid (**77**, 904 mg). However, there was no pure compound isolated from the purification of methanol extract via column chromatography. The isolation of compounds is outlined in Figure 4.30.
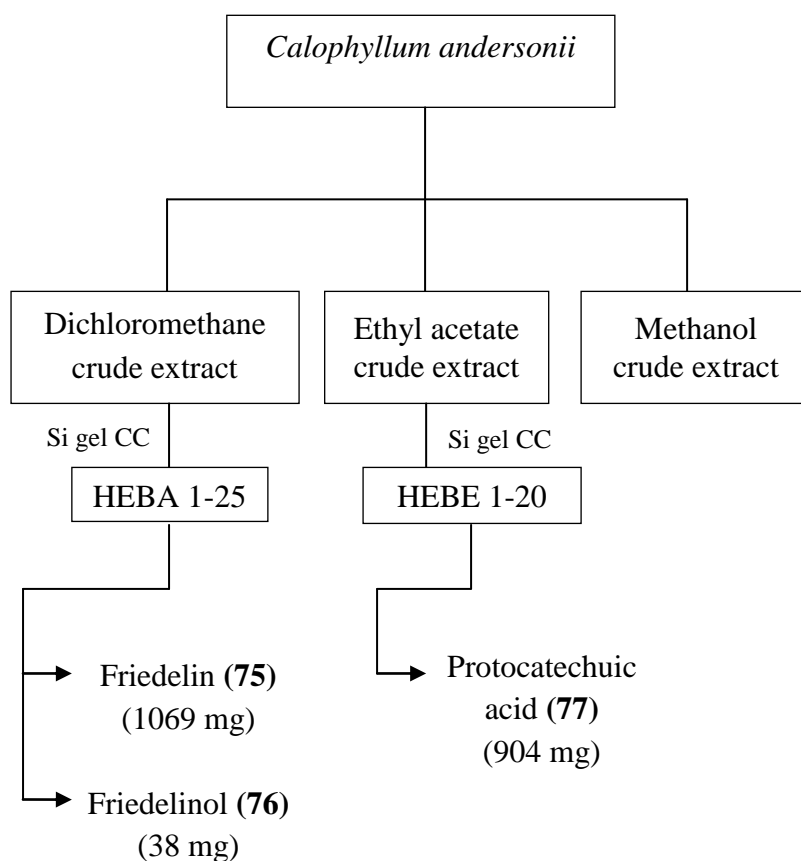
Figure 4.30: Isolation of compounds from the stem bark extracts of
Calophyllum andersonii

4.2.1 Characterization of Friedelin (75)
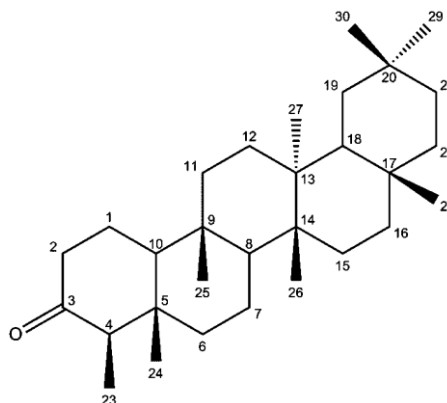
(**75**)

Compound **75** was isolated as white needle-like crystals, with mp 258-259 °C (Lit. 258-259 °C, Annan et al., 2009). Compound **75** gave no visible spot when visualized under UV light (254 nm). This compound showed a positive result in the iodine vapour test. A negative $FeCl_3$ test revealed the absence of phenolic moiety in the compound. Compound **75** gave retention factor, R_f value of 0.29 when eluted with a mobile phase of 90% dichloromethane and 10% ethyl acetate.

Compound **75** has a molecular formula of $C_{30}H_{50}O$ corresponding to the molecular ion peak observed at m/z 426 (Figure 4.31). The IR spectra (Figure 4.32) revealed absorption bands at 2927 (C-H stretch), 1713 (C=O stretch), 1457 (C-H bend) and 1383 (C-H bend) cm^{-1}. The IR signals are comparable with literature data as reported by Ogunnusi et al. (2010).

The ^{1}H NMR spectra (Figures 4.33 and 4.34) showed signals for a typical friedelane triterpenoid. The eight characteristic methyl groups in the friedelane skeleton gave seven strong singlet signals at δ_H 1.16 (H-28), 1.03 (H-27), 0.99 (H-29), 0.98 (H-30), 0.93 (H-26), 0.85 (H-25), 0.70 (H-24) and a doublet signal at δ_H 0.86 (H-23). Apart from that, the methylene protons Ha-2 & Hb-2 and methine proton, H-4 which were in *ortho* position relatively to the carbonyl group gave relatively downfield signals at δ_H 2.37 (dd, *J* = 11.3, 5.4 Hz), 2.26 (m) and 2.24 (m), respectively due to the anisotropic effect.

The ^{13}C NMR spectra (Figures 4.35 and 4.36) displayed a total of 30 carbon signals corresponding to the presence of 7 quaternary carbons, 4 methine, 11 methylene and 8 methyl carbons in the assigned structure. Compound **75** was identified as friedelin based on the spectral evidence and by comparison of ^{1}H and ^{13}C NMR data with literature values (Abbas et al., 2007). The assignment of NMR spectral data for compound **75** is summarized in Table 4.7.
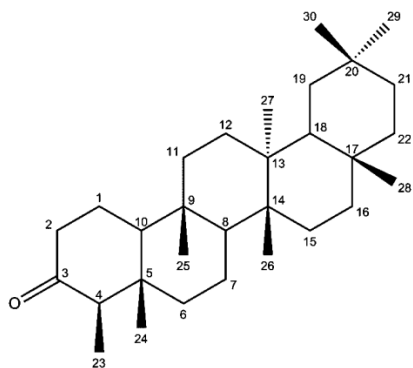
Table 4.7: Summary of NMR data and assignment of friedelin (75)

Position	δ_H (ppm)	$*\delta_H$ (ppm)	δ_C (ppm)	$*\delta_C$ (ppm)
1	1.95 (H$_a$, m)	1.71 (H$_a$, m)	22.4	22.3
	1.72 (H$_b$, m)	1.97 (H$_b$, m)		
2	2.37 (H$_a$, dd, J = 11.3, 5.4 Hz)	2.41 (H$_a$, dd, J =13.0, 3.5 Hz)	41.6	41.5
	2.26 (H$_b$, m)	2.31 (H$_b$, m)		
3	-	-	213.4	213.2
4	2.24 (1H, m)	2.28 (1H, m)	58.3	58.2
5	-	-	42.2	42.2
6	-	-	41.4	41.3
7	-	-	18.3	18.2
8	-	-	53.2	53.1
9	-	-	37.5	37.4
10	-	-	59.5	59.5
11	-	-	35.7	35.6
12	-	-	30.6	30.5
13	-	-	39.8	39.7
14	-	-	38.4	38.3
15	-	-	32.8	32.4
16	-	-	36.1	36.0
17	-	-	30.1	30.0
18	-	-	42.8	42.8
19	-	-	35.4	35.3
20	-	-	28.3	28.2
21	-	-	32.5	32.8
22	-	-	39.3	39.3
23	0.86 (3H, d, J = 6.1 Hz)	0.92 (3H, d, J = 7.0 Hz)	6.9	6.8
24	0.70 (3H,s)	0.75 (3H,s)	14.7	14.7
25	0.85 (3H,s)	0.90 (3H,s)	18.0	18.0
26	0.93 (3H,s)	1.03 (3H,s)	20.3	20.3
27	1.03 (3H,s)	1.07 (3H,s)	18.8	18.7
28	1.16 (3H,s)	1.20 (3H,s)	32.1	32.1
29	0.99 (3H,s)	0.98 (3H,s)	35.1	35.0
30	0.98 (3H,s)	1.02 (3H,s)	31.9	31.8

*Abbas et al., 2007
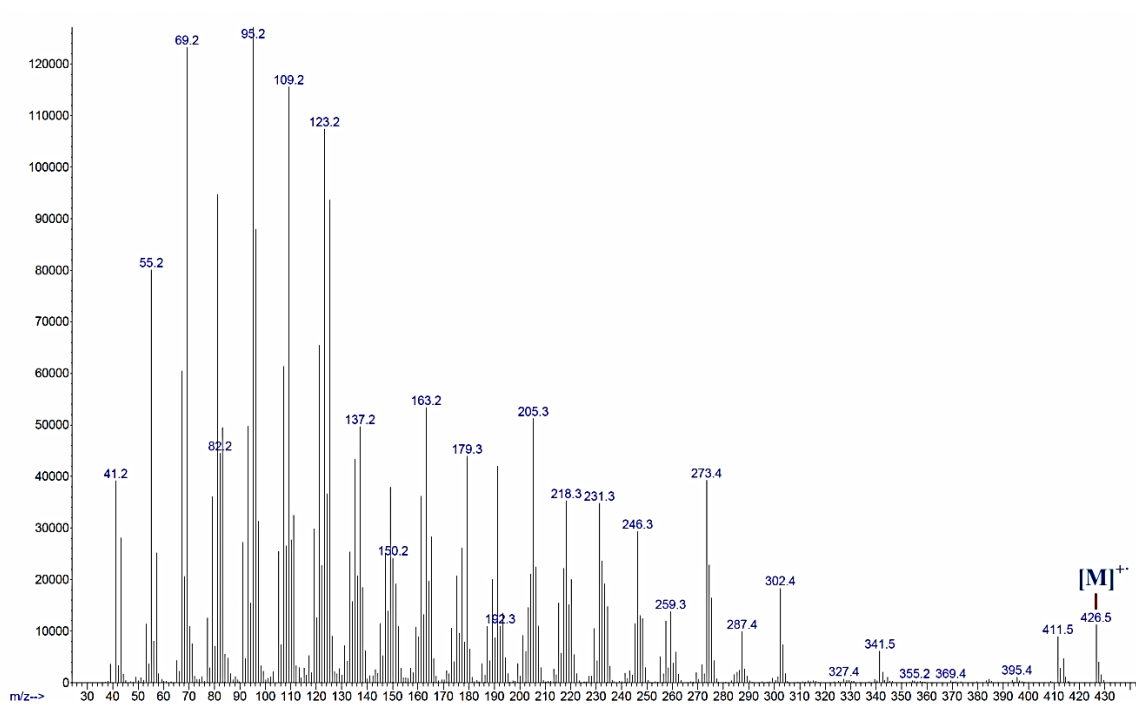
Figure 4.31: EIMS spectrum of friedelin (75)
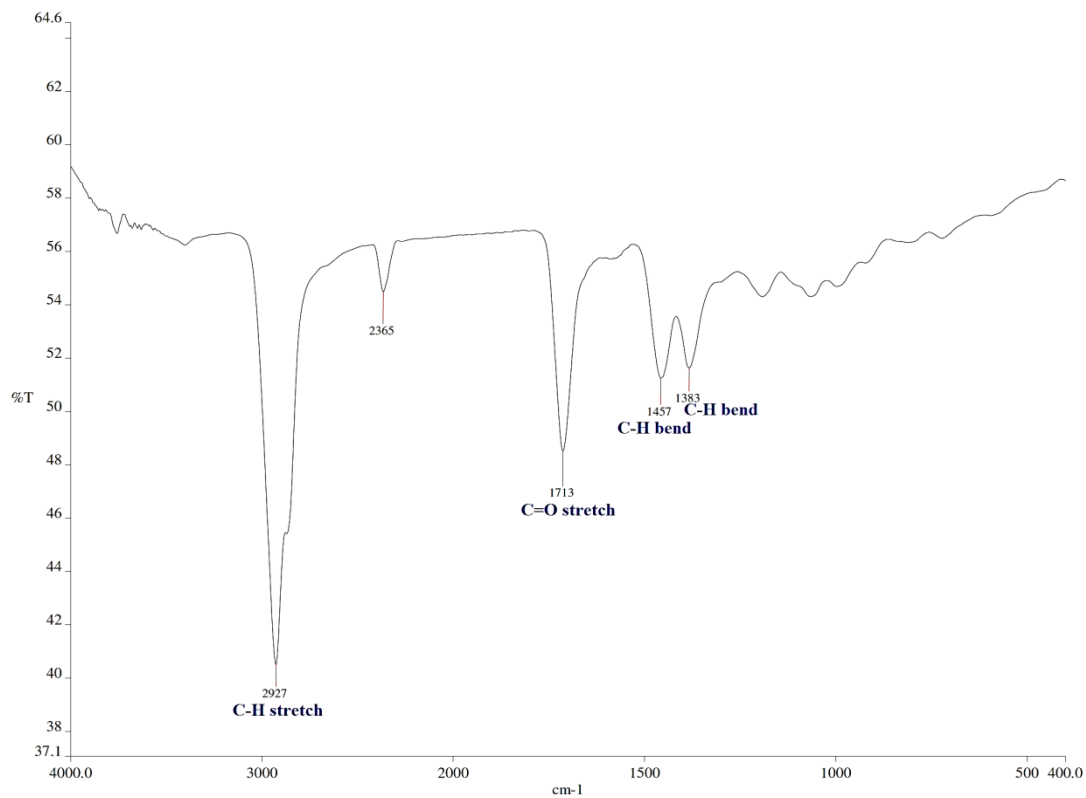
Figure 4.32: IR spectrum of friedelin (75)
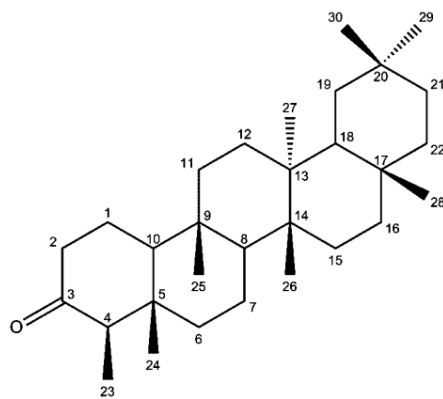
(75)
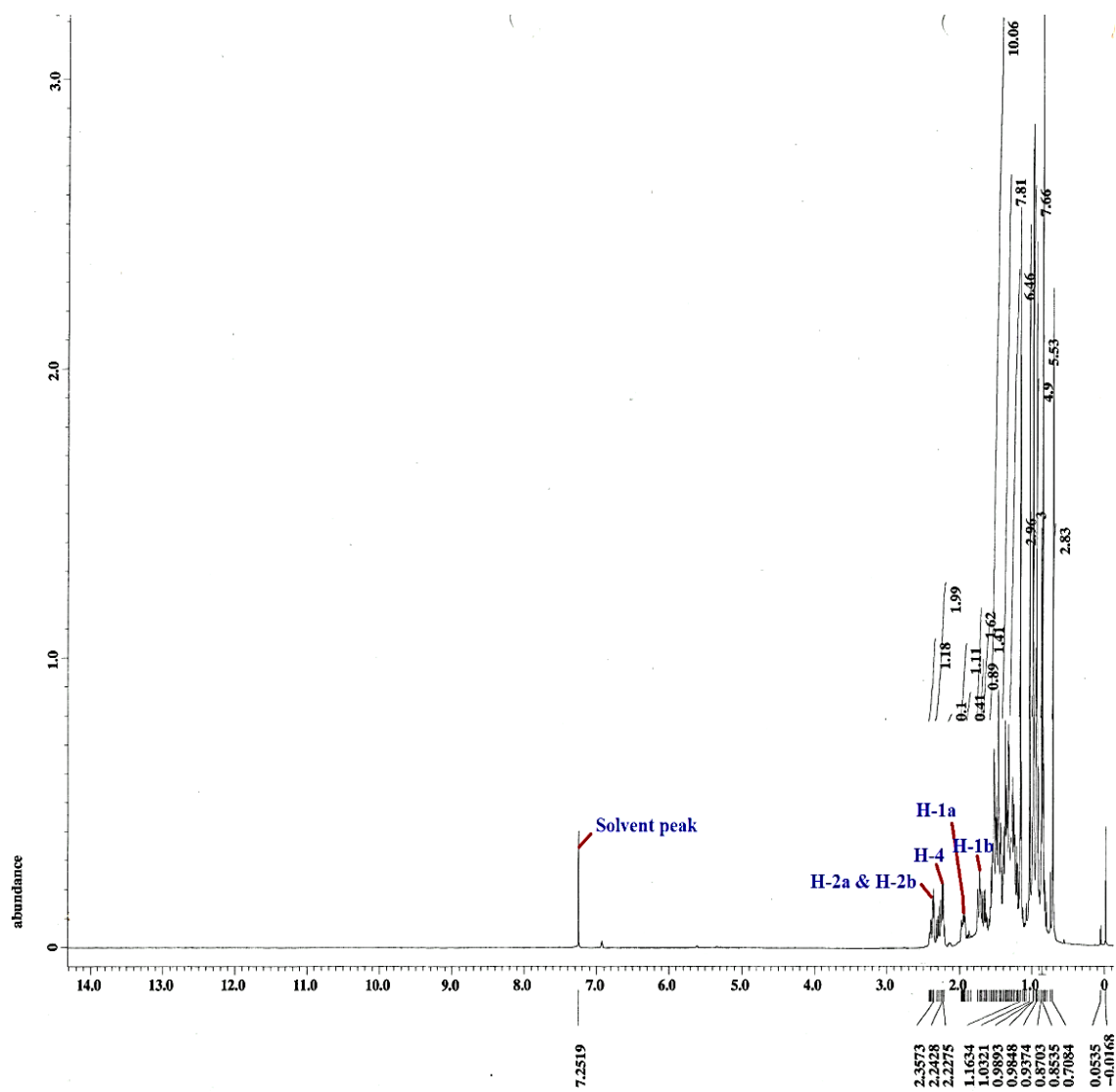
Figure 4.33: ¹H NMR spectrum of friedelin (75) (400 MHz, CDCl₃)
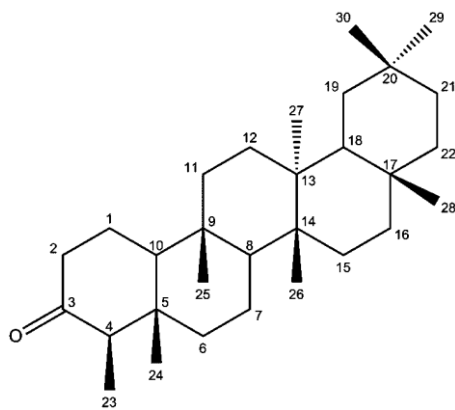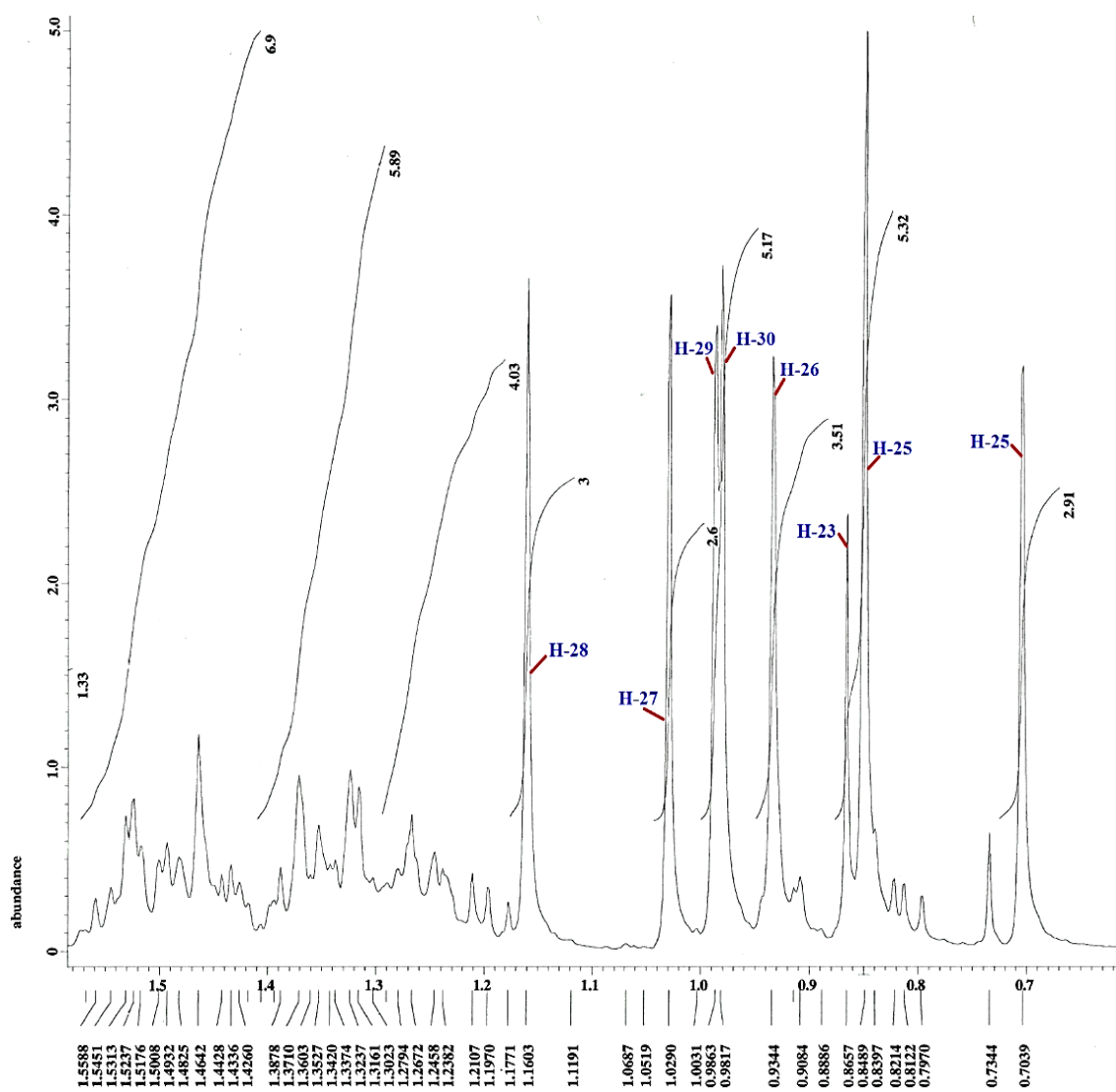
Figure 4.34: Expanded ^{1}H NMR spectrum (upfield region) of friedelin (75) (400 MHz, CDCl$_3$)
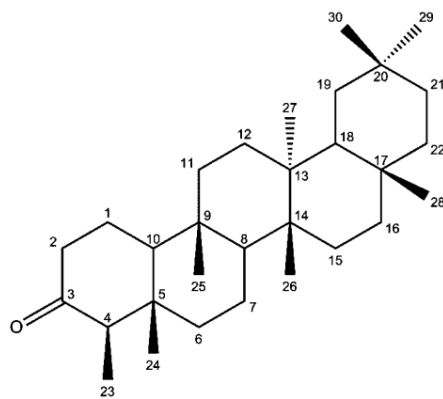
(**75**)
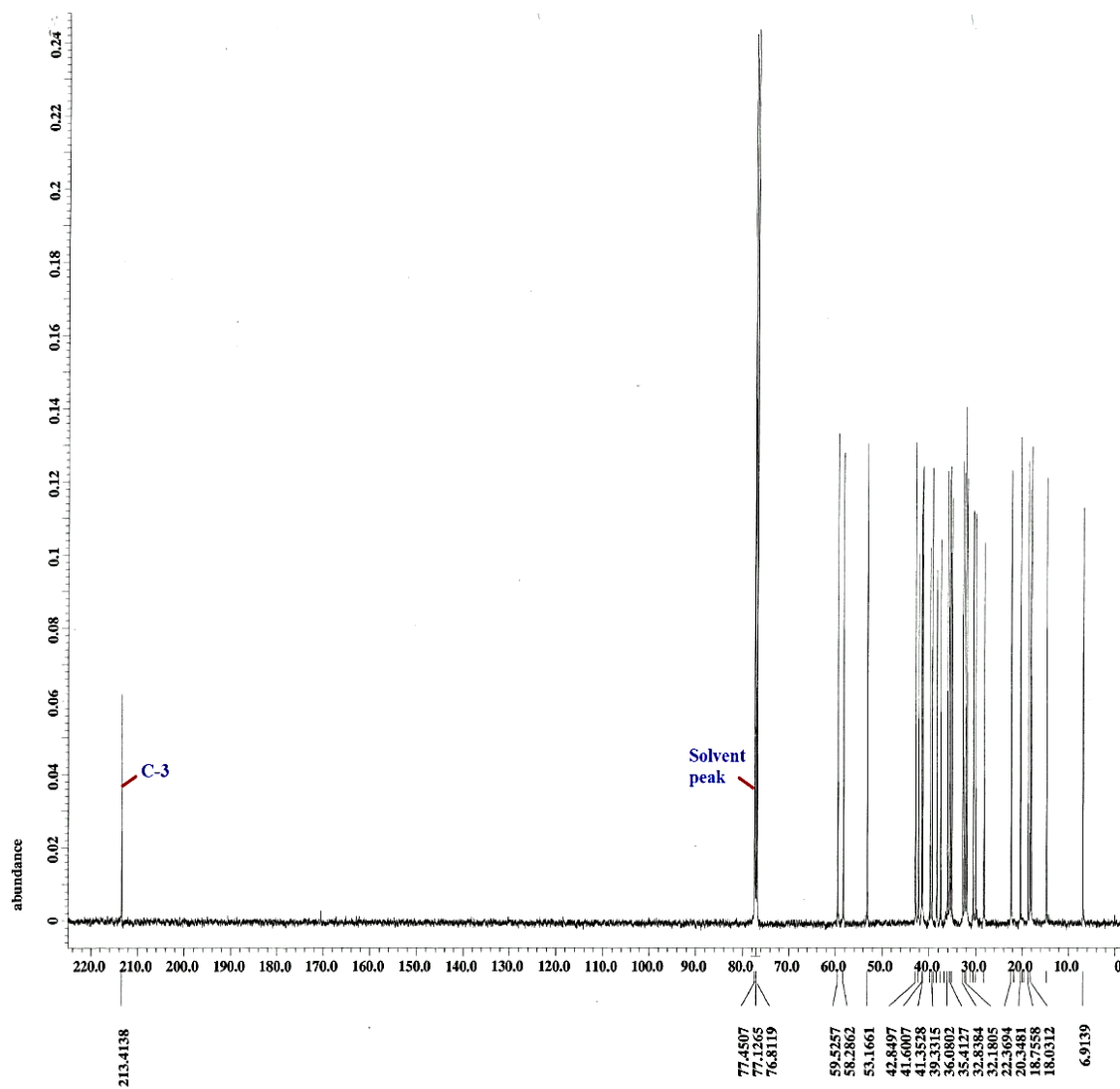
Figure 4.35: ^{13}C NMR spectrum of friedelin (75) (100 MHz, CDCl$_3$)

96
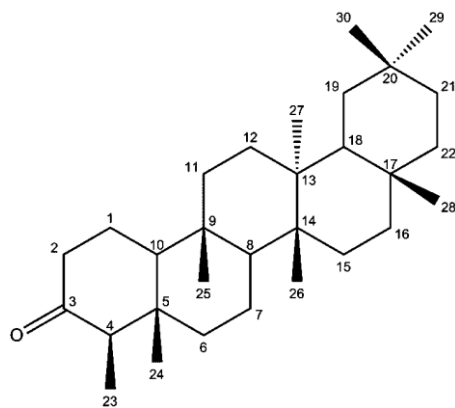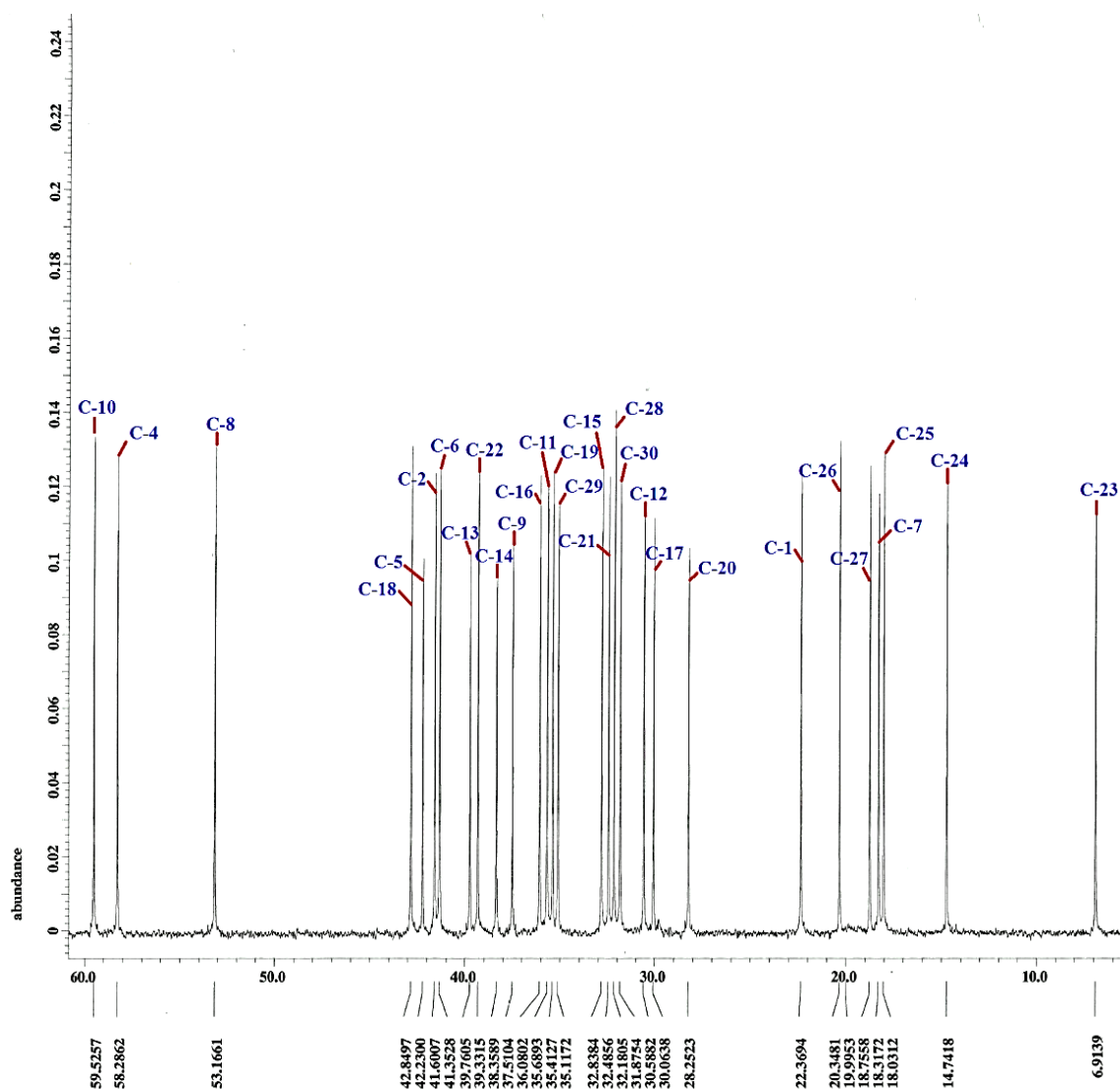
Figure 4.36: Expanded ^{13}C NMR spectrum of friedelin (75) (100 MHz, CDCl$_3$)

4.2.2 Characterization of Friedelinol (76)
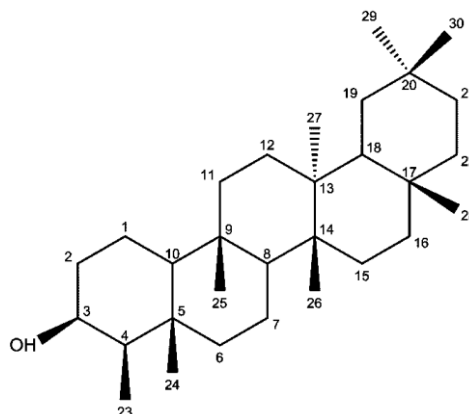
(**76**)

Compound **76** was isolated as white needles, mp of 139-141 °C (Lit. 138-140 °C, Ahmed et al. 2013). This compound gave no visible spot under UV light (254 nm), and a negative result for $FeCl_3$ test indicating the compound to be non-phenolic. In addition, compound **76** gave a single brown spot on developed TLC plate when staining with iodine vapour. This compound showed retention factor, R_f value of 0.52 via a mobile phase of 90% dichloromethane and 10% ethyl acetate.

Compound **76** was deduced to have the molecular formula of $C_{30}H_{52}O$ on the basis of molecular ion peak observed at m/z 428 in the mass spectrum (Figure 4.37). The IR spectrum (Figure 4.38) indicated absorption bands for O-H (3414 cm^{-1}) and C-H stretch (2921 cm^{-1}) and C-H bend (1413 cm^{-1}) functionalities.

The ^{1}H and ^{13}C NMR spectra (Figures 4.39 to 4.42) of compound **76** were closely resembled to that of compound **75** suggesting compound **76** to have a friedelane skeleton. The presence of oxymethine proton signal at δ_H 3.73 (1H, s) in the ^{1}H NMR spectrum (Figure 4.39) and the broad absorption band at 3414 cm^{-1} in the IR spectrum (Figure 4.38) revealed the existence of OH group which is generally found to be linked to carbon C-3 in the friedelane structure. The presence of hydroxyl linked methine carbon C-3 in compound **76** was further confirmed by the downfield signal observed at δ_C 72.8 in the ^{13}C NMR spectrum (Figure 4.41) in place of carbonyl carbon C-3 present in compound **75** which was revealed by the signal at δ_C 213.4 in the ^{13}C NMR spectrum (Figure 4.35).

Compound **76** was established to be friedelinol based on the spectral data and by comparison of ^{1}H and ^{13}C NMR data with literature values (Salazar et al., 2000). The NMR spectral data and assignment of compound **76** are summarized in Table 4.8.
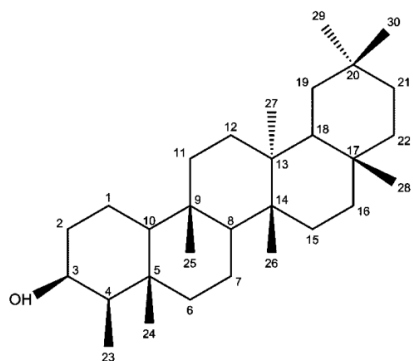
Table 4.8: Summary of NMR data and assignment of friedelinol (76)

Position	δ_H (ppm)	*δ_H (ppm)	δ_C (ppm)	*δ_C (ppm)
1	-	-	15.9	15.8
2	1.88 (H_a, dt, J = 9.2, 2.1 Hz) 1.56 (H_b, s)	1.99 (H_a, qd, J = 13.0, 3.0 Hz) 1.56 (H_b)	35.4	36.1
3	3.73 (1H, s)	3.81 (q)	72.8	71.59
4	-	-	49.2	49.6
5	-	-	37.2	38.1
6	1.73 (1H, m)	1.76 (H_a, dt, J = 12.0, 3.0 Hz) 0.99 (H_b)	41.8	41.9
7	-	-	17.6	17.7
8	-	-	53.3	53.2
9	-	-	37.9	37.2
10	-	-	61.4	61.7
11	-	-	35.3	35.7
12	-	-	30.7	30.7
13	-	-	38.4	38.4
14	-	-	39.4	39.7
15	-	-	32.9	32.3
16	-	-	36.2	35.9
17	-	-	30.1	30.0
18	-	-	42.9	42.9
19	-	-	35.6	35.4
20	-	-	28.3	28.2
21	-	-	32.2	32.9
22	-	-	39.8	39.3
23	0.94 (3H, d, J = 6.7 Hz)	1.02 (d, J = 7.0 Hz)	11.7	12.1
24	0.92 (3H, s)	1.10 (d, J = 7.0 Hz)	16.5	16.6
25	0.85 (3H, s)	0.89 (s)	18.3	18.4
26	0.99 (3H, s)	0.99 (s)	18.7	18.6
27	0.98 (3H, s)	1.02 (s)	20.2	18.7
28	1.16 (3H, s)	1.18 (s)	32.4	32.1
29	1.00 (3H, s)	0.97 (s)	35.1	35.0
30	0.95 (3H, s)	1.02 (s)	31.9	31.9

*Salazar et al., 2013
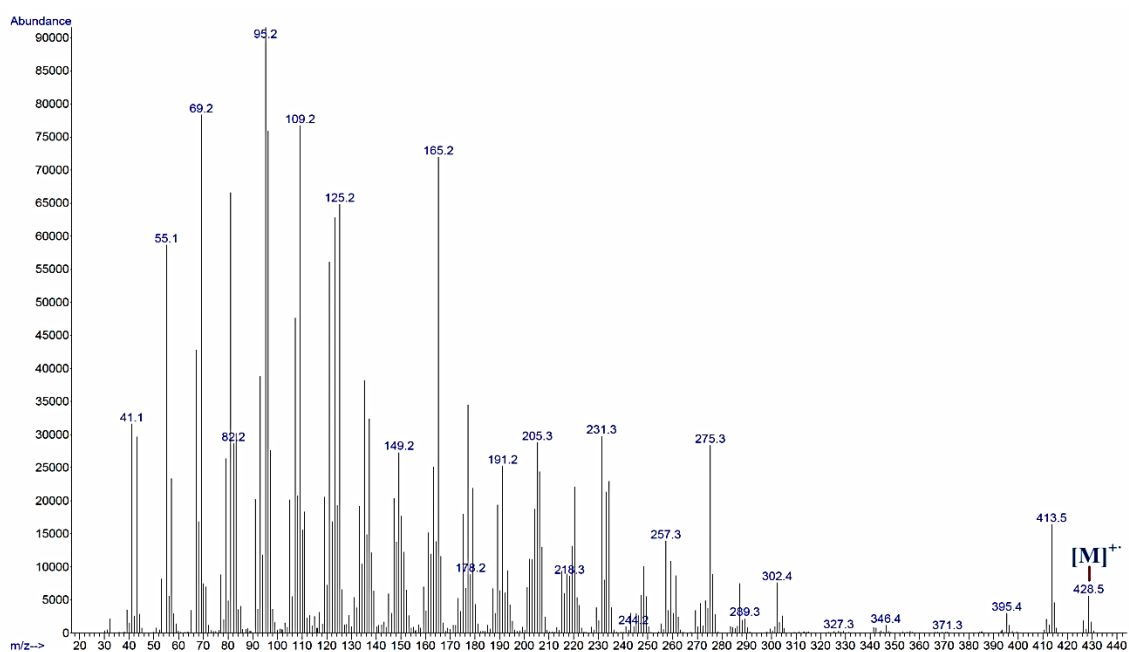
Figure 4.37: EIMS spectrum of friedelinol (76)
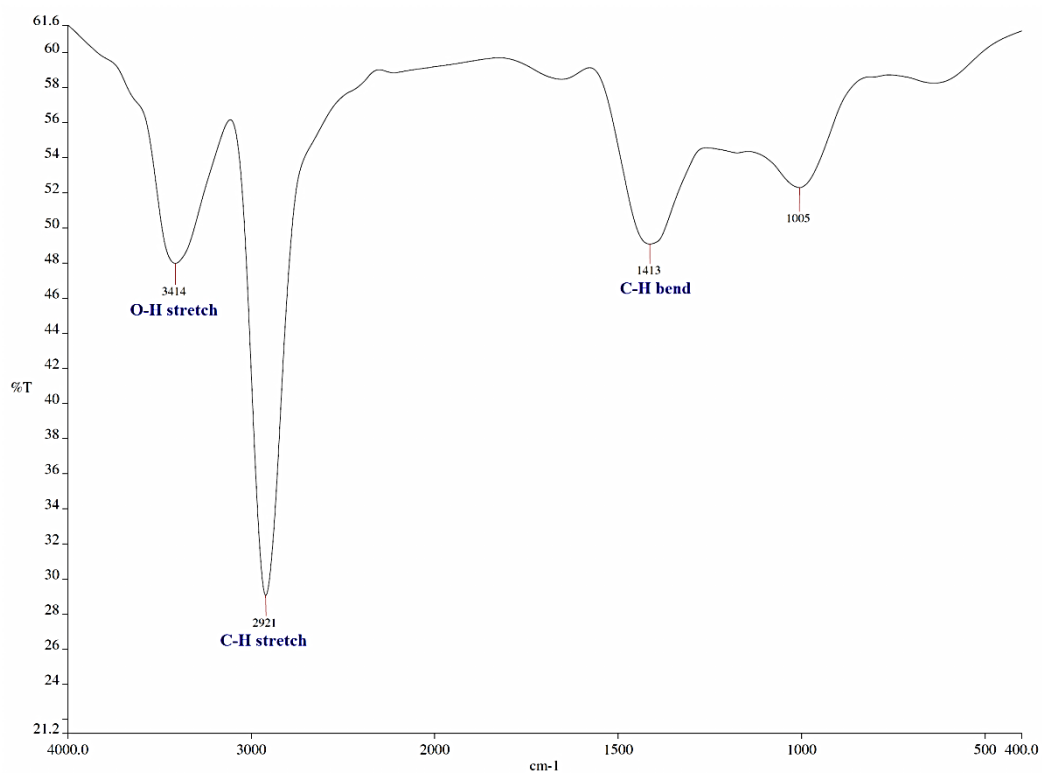
Figure 4.38: IR spectrum of friedelinol (76)
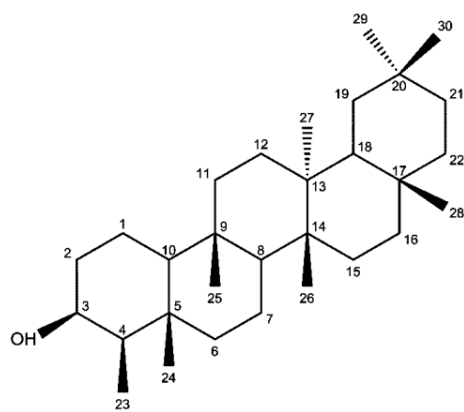
(**76**)
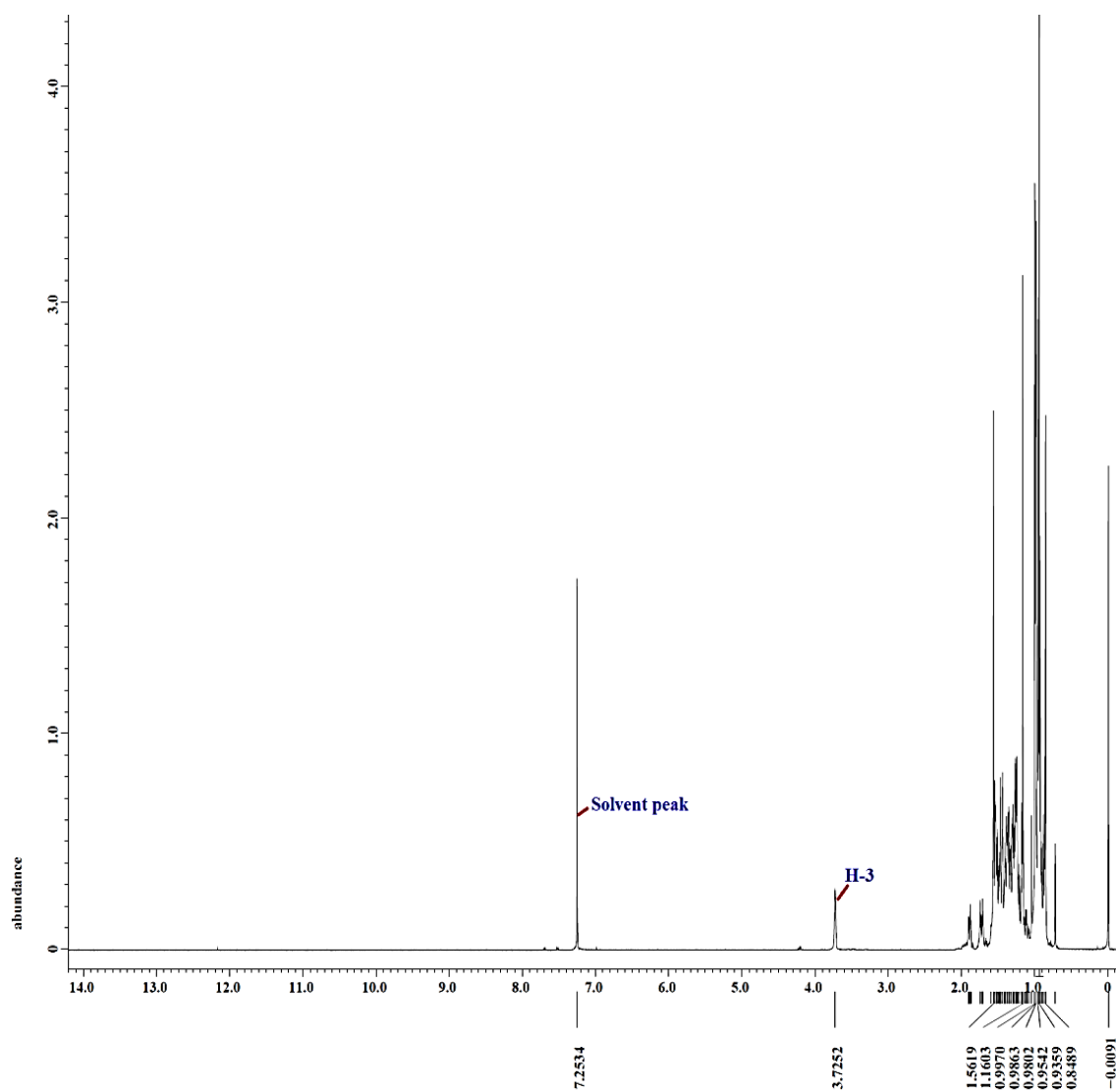
Figure 4.39: ^{1}H NMR spectrum of friedelinol (76) (400 MHz, CDCl$_3$)
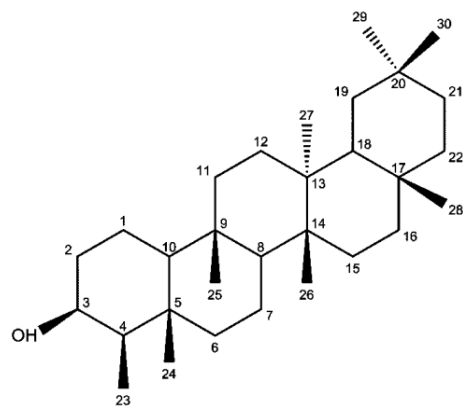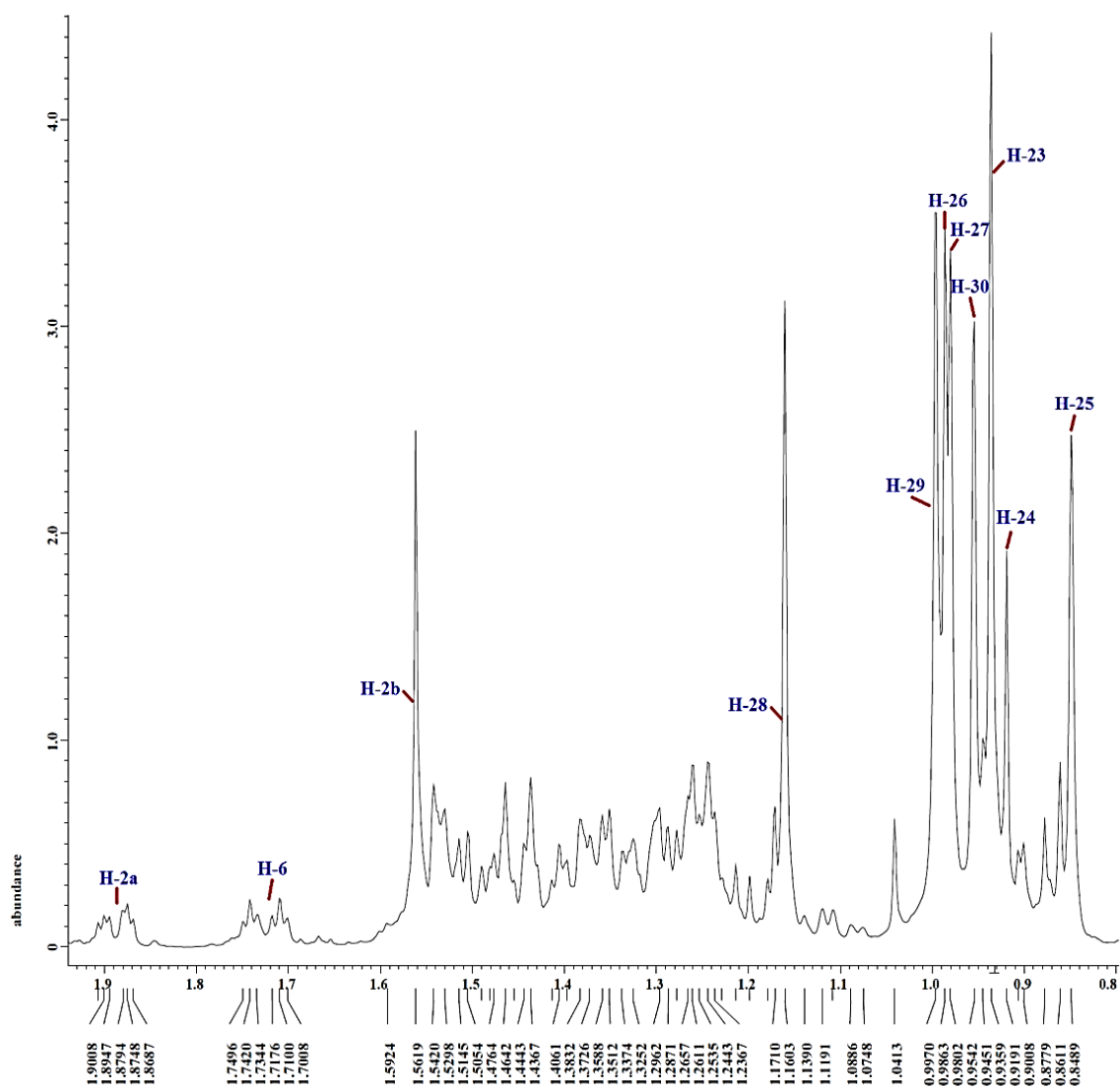
Figure 4.40: Expanded ^{1}H NMR spectrum of friedelinol (76) (400 MHz, CDCl$_3$)
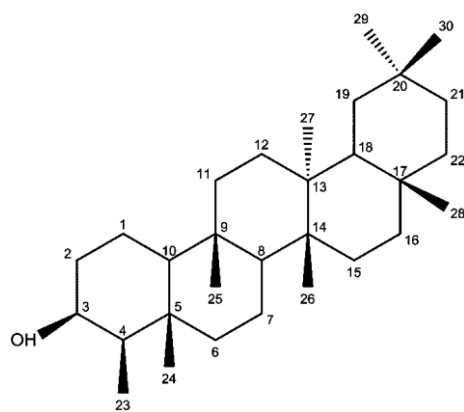
(**76**)
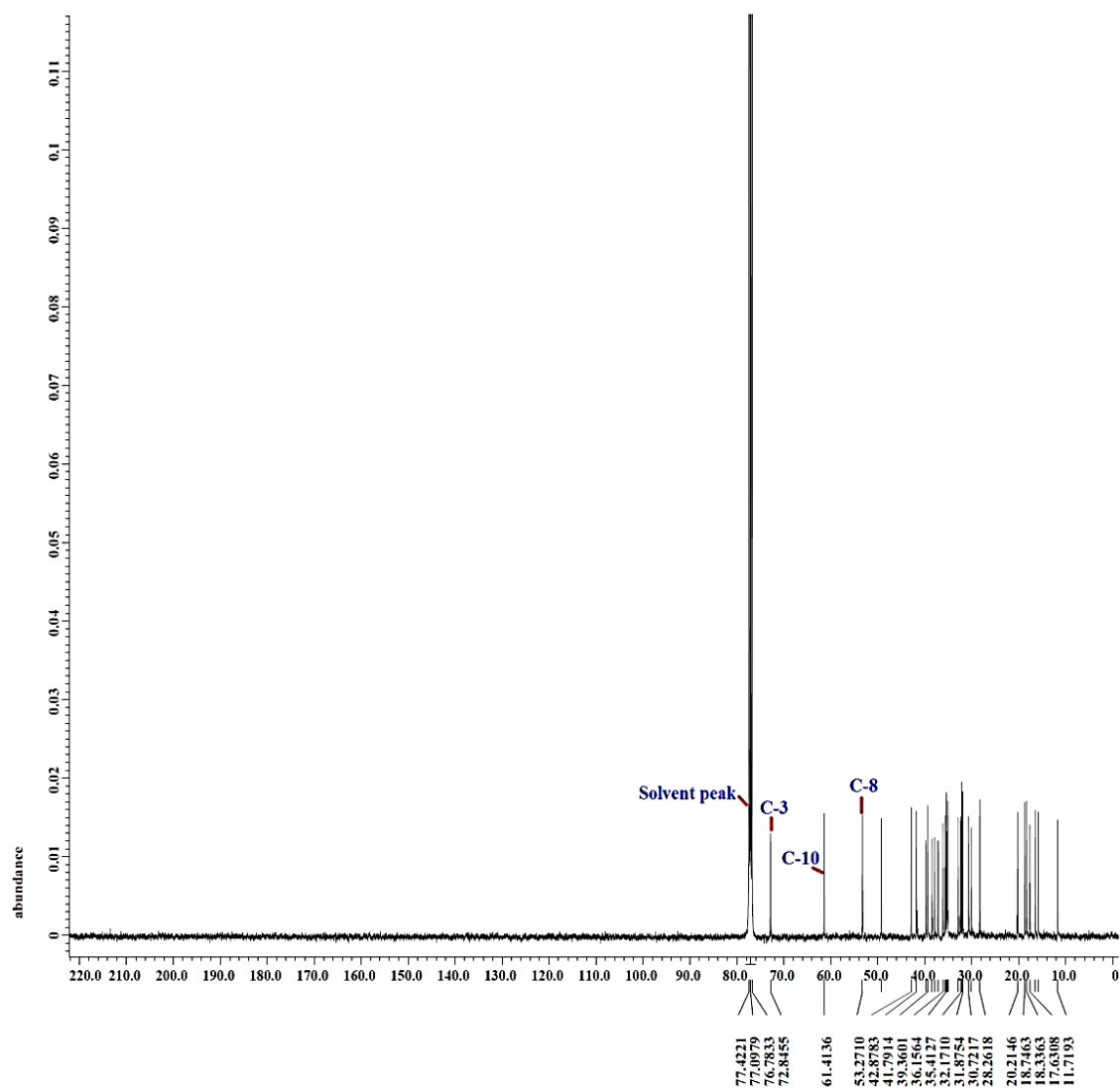
Figure 4.41: ^{13}C NMR spectrum of friedelinol (**76**) (100 MHz, CDCl$_3$)
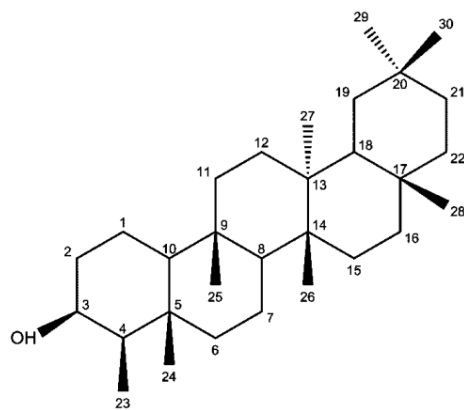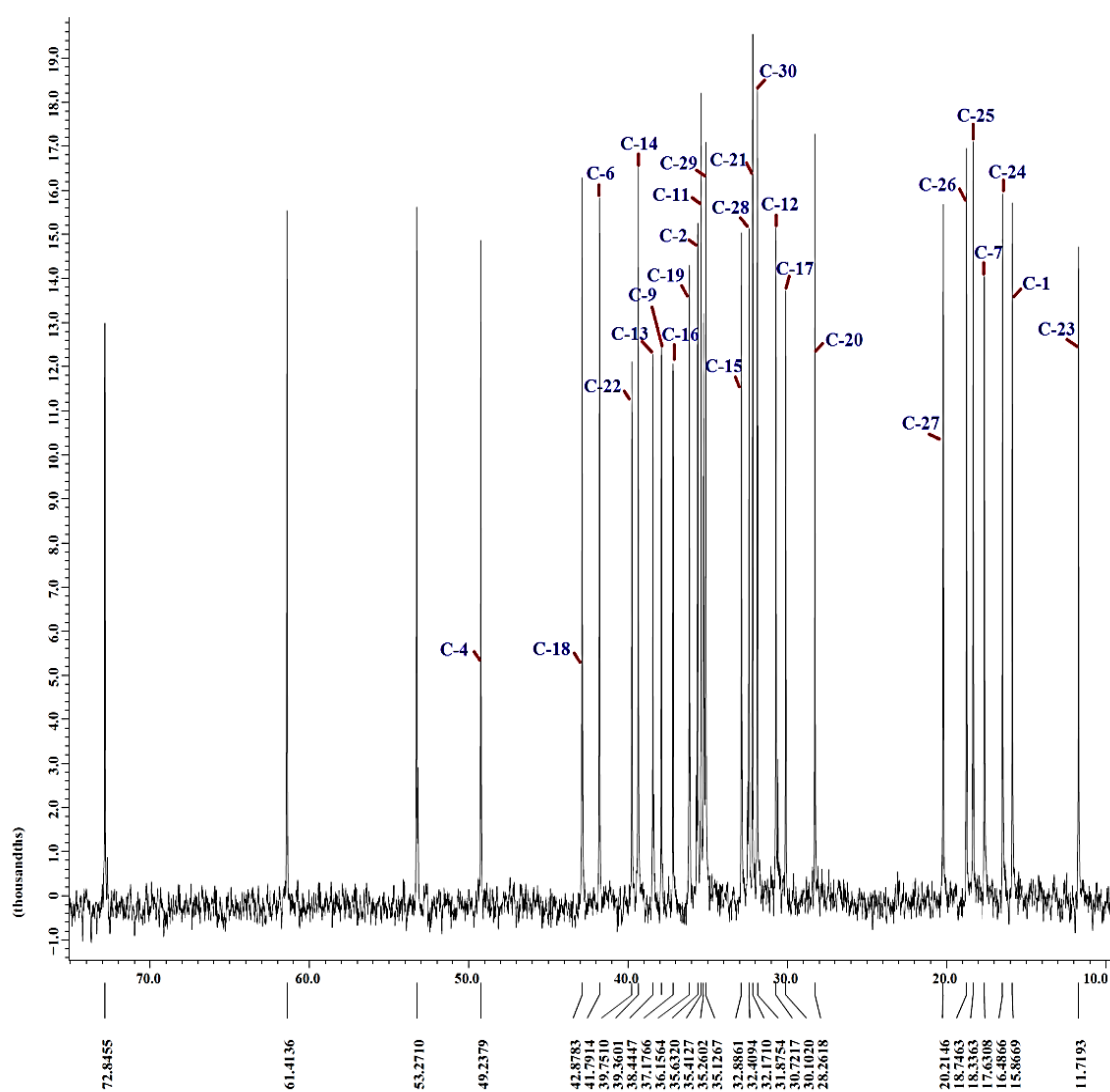
Figure 4.42: Expanded ^{13}C NMR spectrum of friedelinol (76) (100 MHz, CDCl$_3$)

4.2.3 Characterization of Protocatechuic Acid (77)
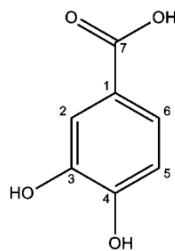
(**77**)

Compound **77** was isolated as brown solids, mp 194-196 °C (Lit. 195-197 °C, Kang et al., 2003). This compound gave a dark red spot under UV light at wavelength of 254 nm and showed a positive result in the iodine vapour test. The phenolic nature exhibited by this compound was indicated by the positive $FeCl_3$ test. Compound **77** showed retention factor, R_f value of 0.51 when eluted with a mobile phase of 40% acetone, 30% dichloromethane and 30% ethyl acetate.

The molecular formula $C_7H_6O_4$ of compound **77** was deduced from the molecular ion peak observed at m/z 154 in the mass spectrum (Figure 4.43). The UV absorption maxima observed at 216.6 and 258.9 nm, (Figure 4.44) revealed compound **77** to be a conjugated compound. The IR spectrum (Figure 4.45) exhibited absorption bands at 3206, 1628 and 1276 cm^{-1} indicating the presence of O-H, aromatic C=C, and C-O functionalities in this compound.

The molecular formula $C_7H_6O_4$ showed a high index of hydrogen deficiency of five for compound **77** indicating the presence of a benzene ring in the assigned structure. In the ^{13}C NMR spectrum (Figure 4.47), three relatively downfield signals observed at δ_C 167.0, 150.0 and 144.8 revealed the presence of a carbonyl carbon and two oxygenated aromatic carbons confirming the benzene ring to be attached with a carboxyl and two hydroxyl groups. A relatively lower ppm value observed for the two oxygenated aromatic carbons at δ_C 150.0 and 144.8 indicated the two hydroxyl groups were vicinally placed in the benzene ring.

In the HMBC spectrum (Figure 4.49), key correlations observed from H-2 to C-4 (δ_C 150.0), C-6 (δ_C 122.8) & C-7 (δ_C 167.0), and H-6 to C-2 (δ_C 116.6), C-4 (δ_C 150.0) & C-7 (δ_C 167.0) indicated the carboxyl group was attached to carbon position C-1. The benzene ring of compound **77** was found to be 1,3,4-trisubstituted as revealed by the multiplicity of proton signals at δ_H 7.50 (1H, d, J = 1.8 Hz), 6.87 (1H, d, J = 7.9 Hz) and 7.45 (1H, dd, J = 7.9, 1.8 Hz).

Based on the spectral evidence, compound **77** was identified as protocatechuic acid and the assigned structure was further confirmed by comparison of ^1H and ^{13}C NMR spectral data of compound **77** with literature values (Syafni et al., 2012).
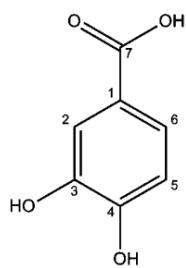
(**77**)

Table 4.9: Summary of NMR data and assignment of protocatechuic acid (77)

Position	δ_H (ppm)	δ_C (ppm)	HMBC
1	-	122.2	-
2	7.50 (1H, d, *J* = 1.8 Hz)	116.6	C-4, 6 & 7
3	-	144.8	-
4	-	150.0	-
5	6.87 (1H, d, *J* = 7.9 Hz)	114.9	C-1 & 3
6	7.45 (1H, dd, *J* = 7.9, 1.8 Hz)	122.8	C-2, 4 & 7
7	-	167.0	-
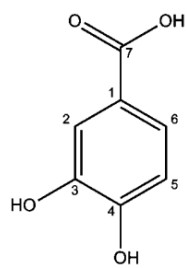
(**77**)
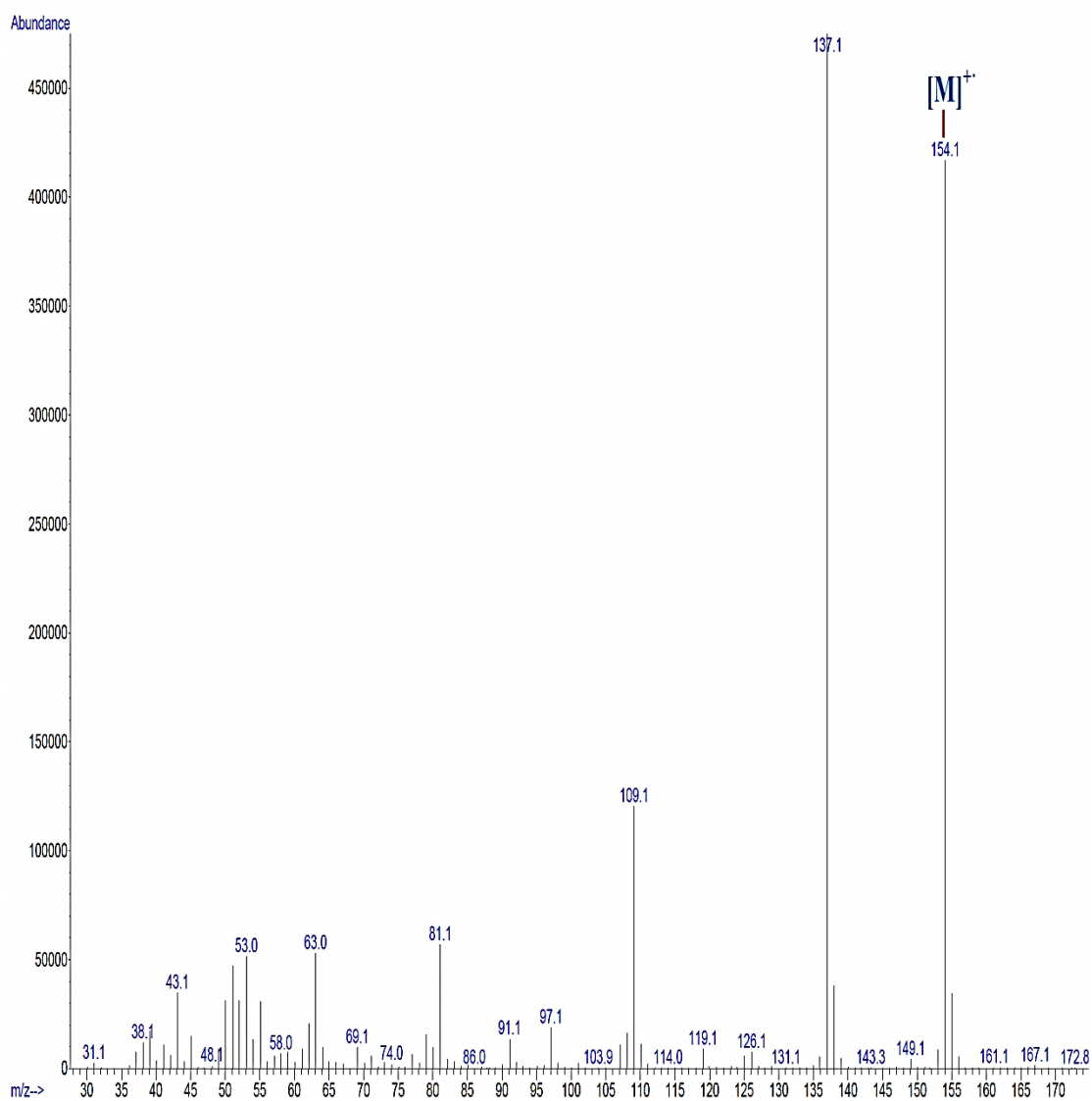
Figure 4.43: EIMS spectrum of protocatechuic acid (77)
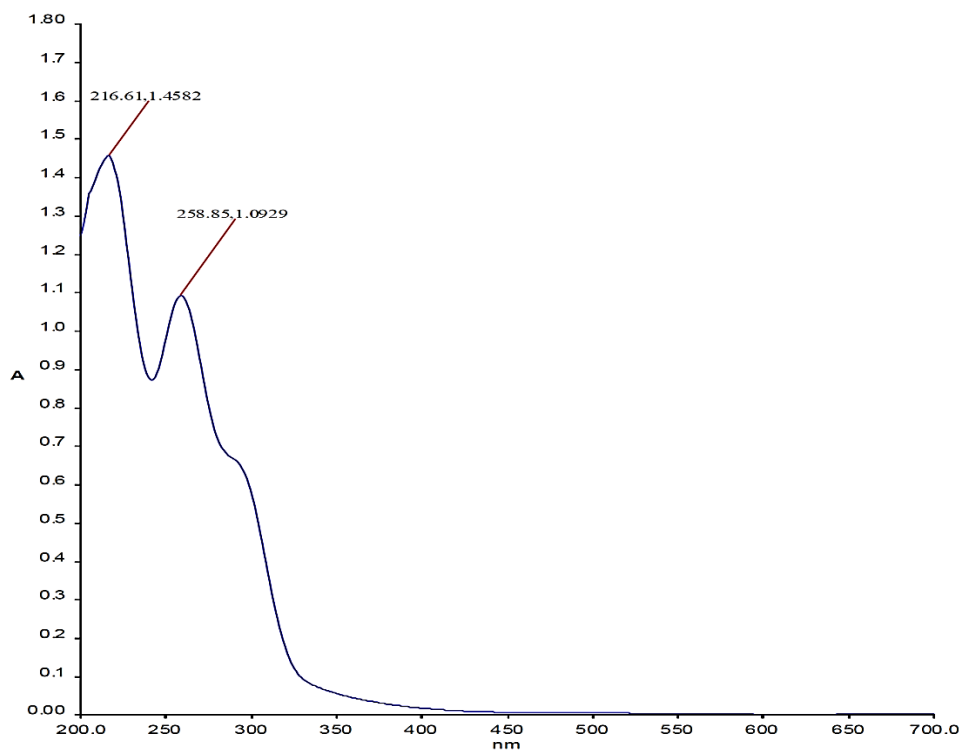
Figure 4.44: UV-Vis spectrum of protocatechuic acid (77)
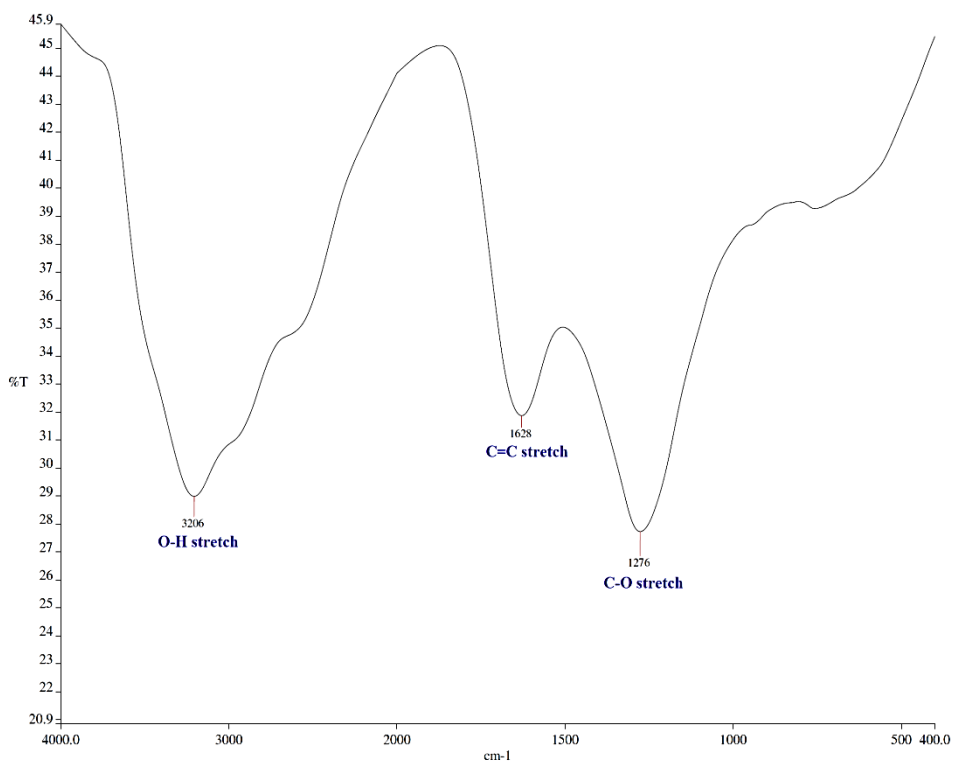
Figure 4.45: IR spectrum of protocatechuic acid (77)

110
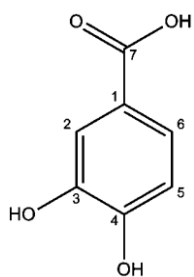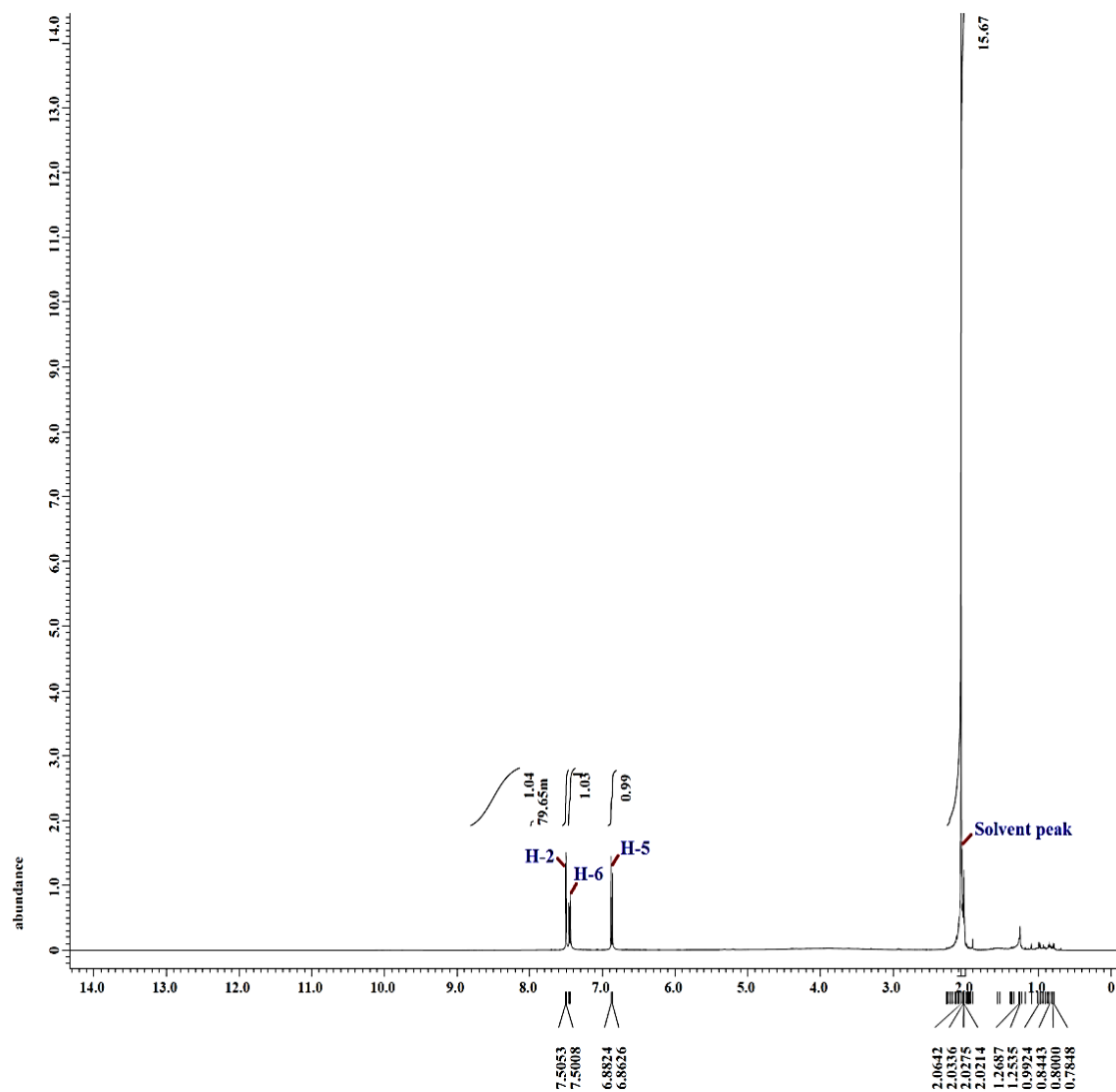
Figure 4.46: ^{1}H NMR spectrum of protocatechuic acid (77) (400 MHz, acetone-d_6)

111
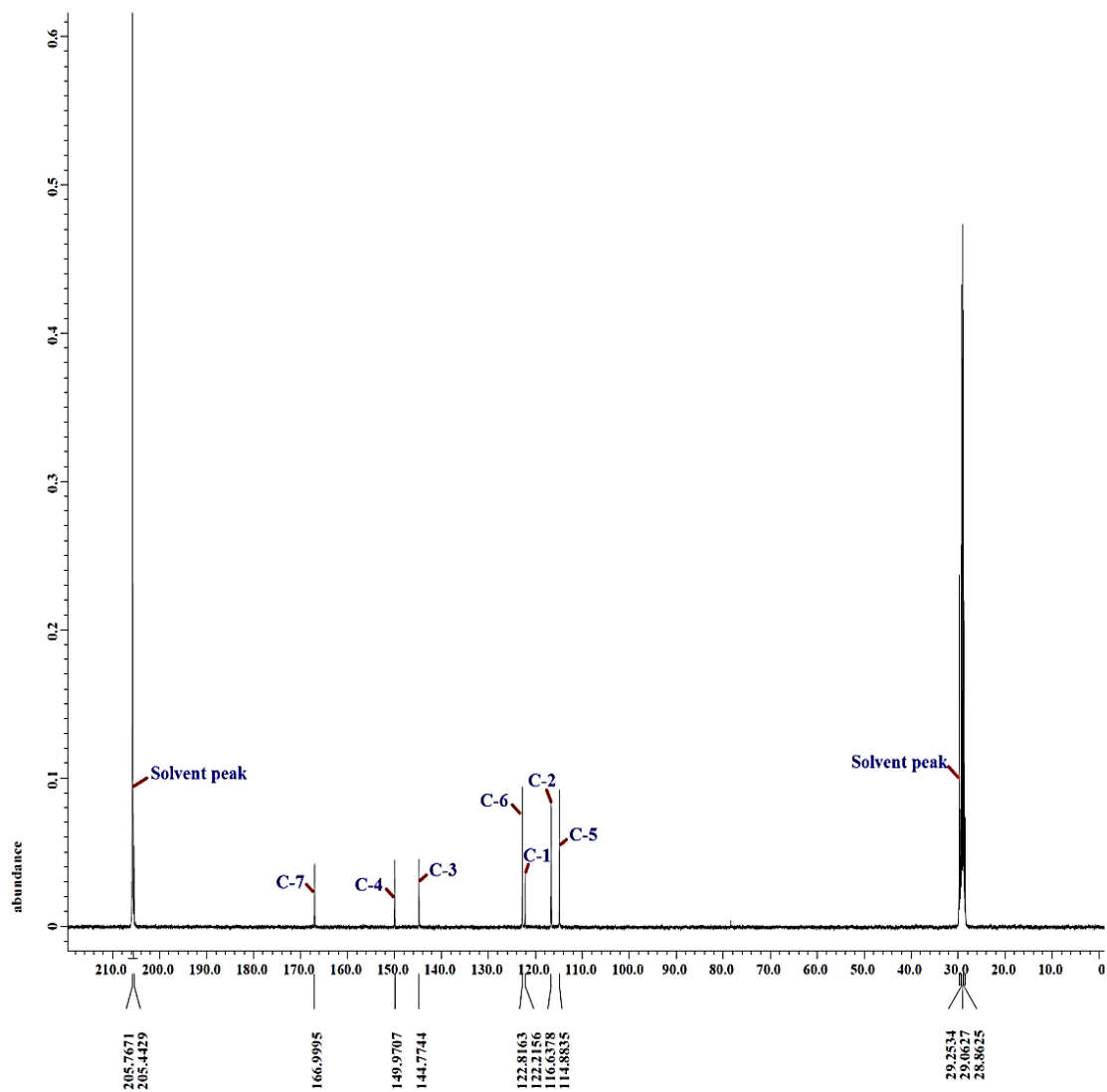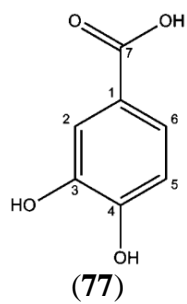
Figure 4.47: ^{13}C NMR spectrum of protocatechuic acid (77) (100 MHz, acetone-d_6)
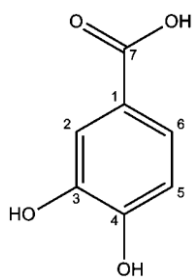
(**77**)
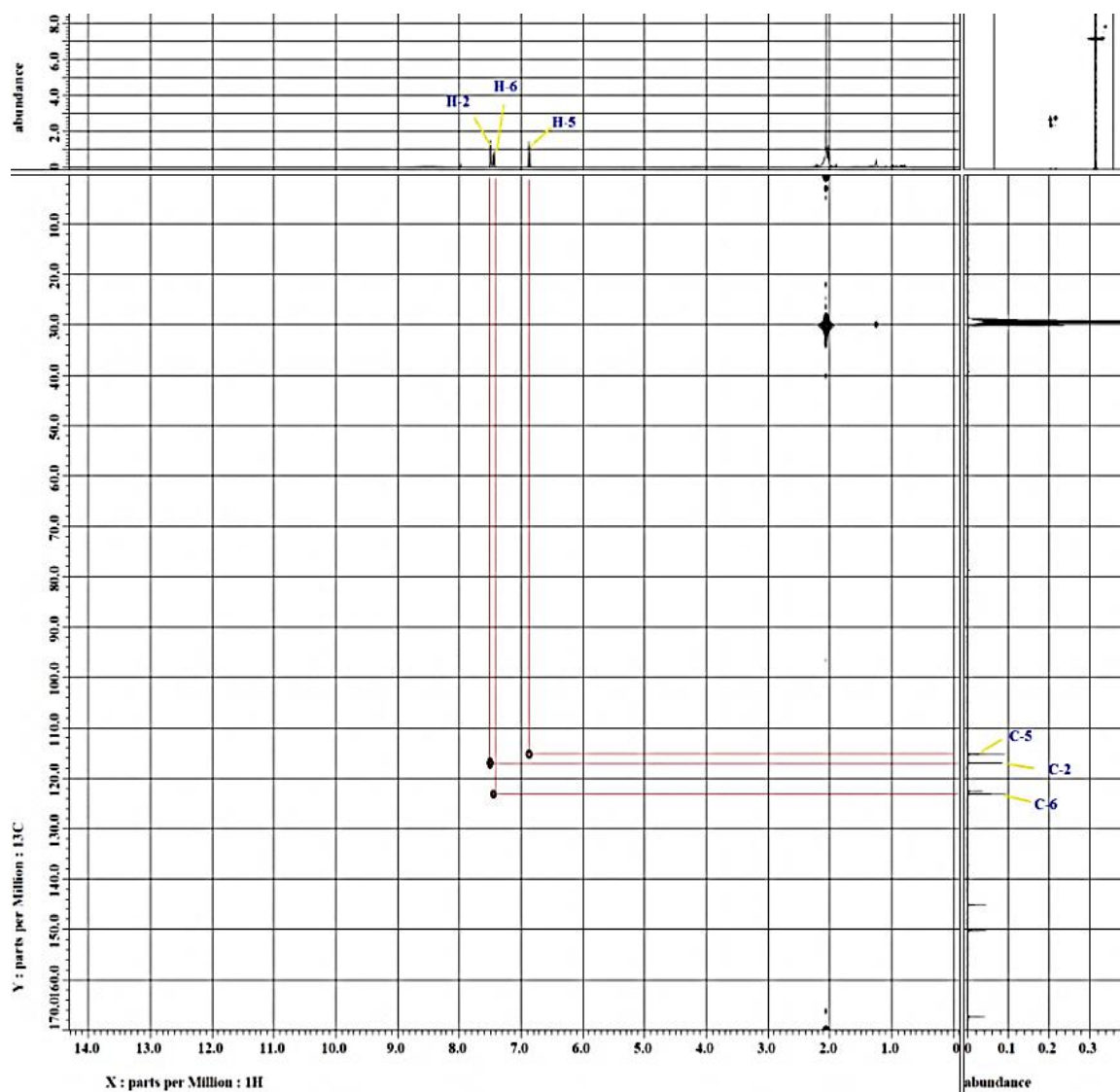
Figure 4.48: HMQC spectrum of protocatechuic acid (77)
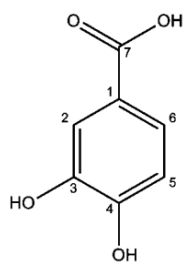
(**77**)
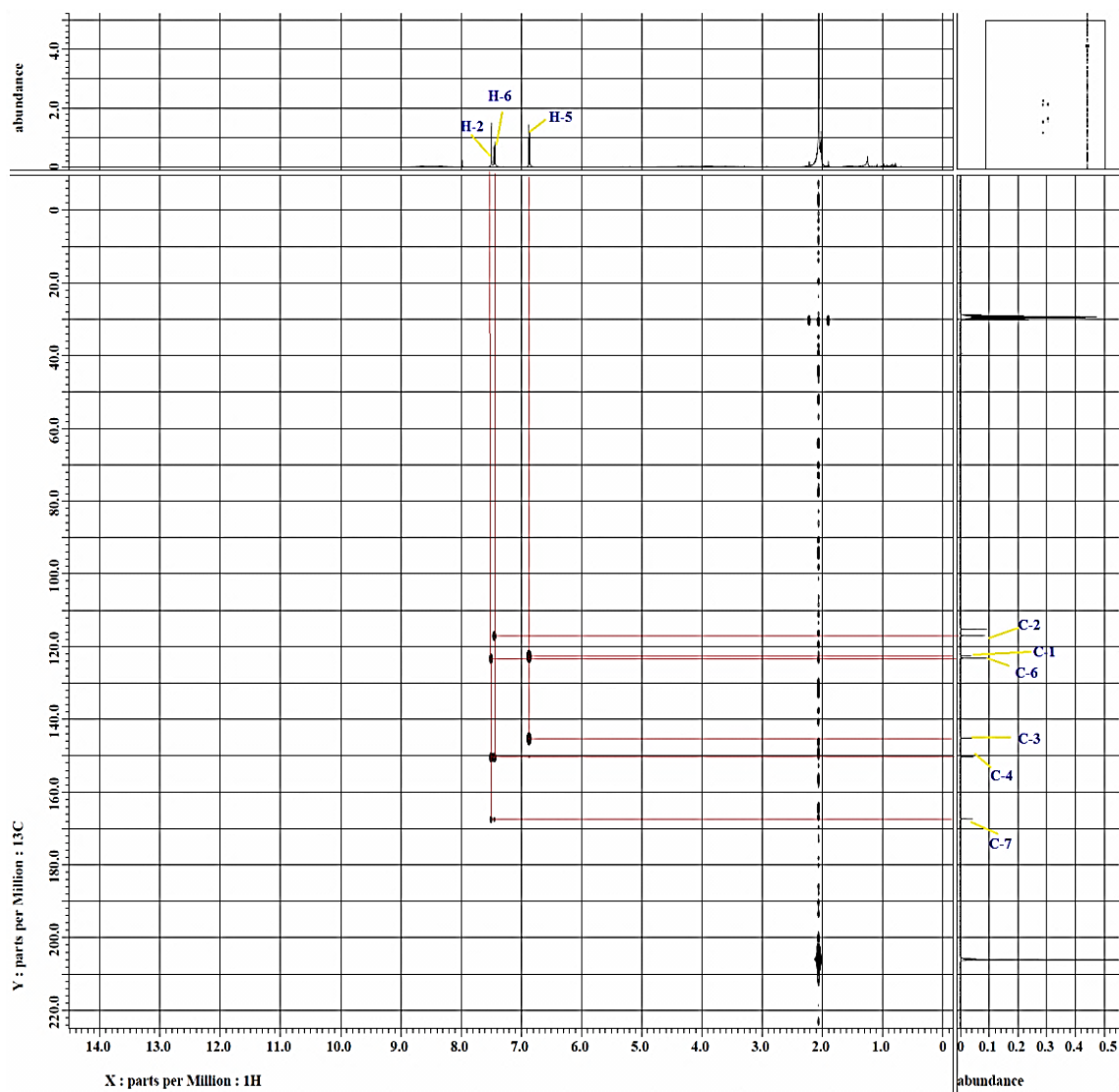
Figure 4.49: HMBC spectrum of protocatechuic acid (77)

114

4.3 Extraction and Isolation of Chemical Constituents from *Calophyllum soulattri*

Solvent extractions on the stem bark of *Calophyllum soulattri* (1.5 kg) afforded 24.8, 18.3 and 173.2 g of dichloromethane, ethyl acetate and methanol extracts, respectively. The summary of the weight and percentage of yield of crude extracts are shown in Table 4.10.

Table 4.10: Extract yields of *Calophyllum soulattri*

Crude Extract	Weight (g)	Percentage of yield (%)*
Dichloromethane	24.8	1.7
Ethyl acetate	18.3	1.2
Methanol	173.2	11.5

* Percentage of yield was calculated based on the weight of the dried extract against dry weight of ground stem bark of *Calophyllum soulattri* (1.5 kg) multiplied by 100%.

About 20 g of dichloromethane extract was subjected to Si gel CC (40-63 μm, 8.5 x 50 cm, 600 g) packed in *n*-hexane and eluted with *n*-hexane-dichloromethane mixtures of increasing polarity (90:10, 80:20, 70:30, 60:40, 50:50, 40:60, 30:70, 20:80, 10:90, 0:100), followed by increasing concentration of EtOAc in dichloromethane (10:90, 20:80, 30:70, 40:60, 50:50, 60:40, 70:30, 80:20, 90:10, 100:0) to give 21 fractions (HECA1-21). Fraction HECA3 (4.8 g) was purified via Si gel CC (40-63 μm, 3.5 x 50 cm, 150 g) packed in *n*-hexane and eluted with *n*-hexane-dichloromethane mixtures of increasing polarity (90:10, 80:20, 70:30, 60:40, 50:50, 40:60, 30:70, 20:80, 10:90, 0:100), followed by increasing concentration of EtOAc in dichloromethane (10:90, 20:80, 30:70, 40:60, 50:50, 60:40, 70:30, 80:20,

90:10, 100:0) giving rise to 10 fractions (HECC1-10). Subfractions HECC3-4 (1.8 g) were combined and purified further via Sephadex LH-20 packed column eluted with a mobile phase of 90% methanol and 10% dichloromethane to yield 10 subfractions (HECN1-10). Subfraction HECN4 (0.3 g) was selected and further subjected to Sephadex LH-20 column chromatography eluted with 90% methanol : 10% dichloromethane to give 26 subfractions (HECP1-26). Subfractions HECP24-26 yielded calosubellinone (**78**) as yellow gum (75 mg). Fraction HECA9 (2.1 g) was fractionated via Si CC (40-63 μm, 3.5 x 50 cm, 150 g) packed in *n*-hexane and eluted with *n*-hexane-dichloromethane mixtures of increasing polarity (90:10, 80:20, 70:30, 60:40, 50:50, 40:60, 30:70, 20:80, 10:90, 0:100), followed by increasing concentration of EtOAc in dichloromethane (10:90, 20:80, 30:70, 40:60, 50:50, 60:40, 70:30, 80:20, 90:10, 100:0) to give 19 subfractions (HECE1-19). Subfraction HECE9 afforded garsubellin B (**79**) as yellow gum (257 mg). Meanwhile, fraction HECA5 (1.8 g) was fractionated via Si CC (40-63 μm, 3.5 x 50 cm, 150 g) packed in *n*-hexane and eluted with same solvent system as above to give 13 subfractions (HECH1-13), in which subfractions HECH4-8 (0.75 g) were purified by using Sephadex LH-20 column eluted with 90% methanol : 10% dichloromethane to give 33 subfractions (HECQ1-33). Subfractions HECQ23-28 afforded soulattrone A (**80**) as white needles (17 mg).

However, no pure compounds were successfully isolated from the purification of ethyl acetate and methanol extracts via column chromatography. The isolation of compounds is outlined in Figure 4.50.

116

```
                    ┌──────────────────────────┐
                    │  Calophyllum soulattri    │
                    └──────────────────────────┘
                                │
          ┌─────────────────────┼─────────────────────┐
 ┌──────────────────┐  ┌──────────────────┐  ┌──────────────────┐
 │  Dichloromethane │  │   Ethyl acetate  │  │    Methanol      │
 │   crude extract  │  │   crude extract  │  │  crude extract   │
 └──────────────────┘  └──────────────────┘  └──────────────────┘
        │ Si gel
        │ CC
 ┌──────────────┐
 │  HECA 1-21   │
 └──────────────┘
        │
   ┌────────────────────────┼────────────────────────┐
┌──────────┐          ┌──────────┐          ┌──────────┐
│ HECA 3   │          │ HECA 5   │          │ HECA 9   │
└──────────┘          └──────────┘          └──────────┘
   │ Si gel              │ Si gel              │ Si gel
   │ CC                  │ CC                  │ CC
┌──────────────┐     ┌──────────────┐     ┌──────────────┐
│ HECC 1-10    │     │ HECH 1-13    │     │ HECE 1-19    │
└──────────────┘     └──────────────┘     └──────────────┘
   │                    │                    │
┌──────────────┐     ┌──────────────┐      └──► Garsubellin
│ HECC 3-4     │     │ HECH 4-8     │            B (79)
└──────────────┘     └──────────────┘          (257 mg)
   │ Sephadex LH-20 CC  │ Sephadex LH-20 CC
┌──────────────┐     ┌──────────────┐
│ HECN 1-10    │     │ HECQ 1-33    │
└──────────────┘     └──────────────┘
   │                    │
┌──────────────┐      └──► Soulattrone A
│ HECN 4       │              (80)
└──────────────┘            (17 mg)
   │ Sephadex LH-20 CC
┌──────────────┐
│ HECP 1-26    │
└──────────────┘
   │
   └──► Calosubellinone
           (78)
         (75 mg)
```

Figure 4.50: Isolation of compounds from the stem bark extracts of
Calophyllum soulattri

4.3.1 Characterization of Calosubellinone (78)

(**78**)
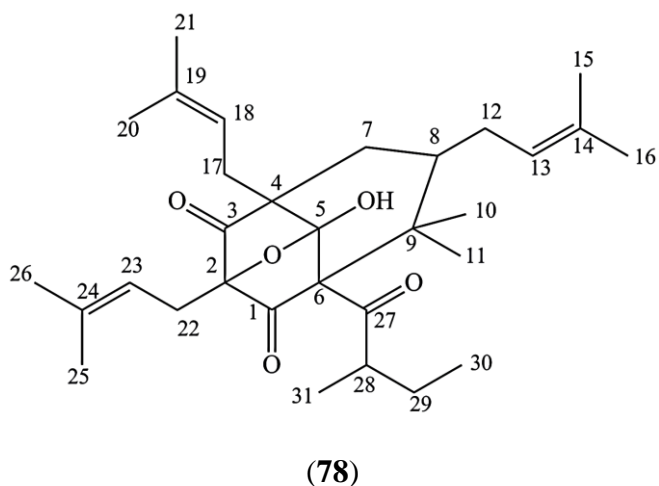
Compound **78** was isolated as yellow gum, giving a specific rotation, $[\alpha]_D$ of +15.6° (EtOH, c 0.60). It appeared as a dark reddish-pink spot on the developed TLC, under UV light at wavelength of 254 nm, and gave a brown spot when treated with iodine vapour. This compound showed negative $FeCl_3$ test indicating compound **78** to be non-phenolic. Compound **78** showed retention factor, R_f value of 0.62 via a mobile phase of 80% n-hexane, 10% dichloromethane and 10% ethyl acetate.

The molecular formula of compound **78** was deduced as $C_{31}H_{46}O_5$ from the HR-EIMS ([M]$^{+\cdot}$ at m/z 498.33612) (Figure 4.51) and EIMS ([M]$^{+\cdot}$ at m/z 498) (Figure 4.52). The UV spectrum (Figure 4.53) showed absorption maxima at 247.6 nm, while the IR spectrum (Figure 4.54) revealed absorption bands at 3440, 2954, 1727 and 1149 indicating the presence of O-H (stretch), C-H (stretch), C=O (stretch) and C-O (stretch) functionalities in the assigned compound.

The ^{1}H and ^{13}C NMR spectra of **78** (Figure 4.55 to 4.58) revealed the presence of three isoprenyl groups [δ_H 4.90 (1H, t, J = 7.3 Hz, H-13), 2.06 (1H, m, H-12), 1.67 (3H, s, H-16) and 1.53 (3H, s, H-15); δ_C 133.4 (C-14), 122.2 (C-13), 27.8 (C-12), 25.9 (C-16) and 18.0 (C-15)], [δ_H 5.26 (1H, t, J = 7.3 Hz, H-18), 2.40 (2H, m, H-17), 1.67 (3H, s, H-21) and 1.54 (3H, s, H-20); δ_C 133.8 (C-19), 119.0 (C-18), 31.0 (C-17), 25.9 (C-21) and 17.8 (C-20)], [δ_H 5.00 (1H, t, J = 7.3 Hz, H-23), 2.74 (Ha-22, dd, J = 15.9, 7.3 Hz), 2.47 (Hb-22, dd, J = 15.3, 7.3 Hz), 1.63 (3H, s, H-26) and 1.62 (3H, s, H-25); δ_C 135.8 (C-24), 116.0 (C-23), 23.8 (C-22), 26.1 (C-26) and 18.0 (C-25)] and a 2-methyl-butanoyl group [δ_H 2.94 (1H, sext, J = 6.7 Hz, H-28), 1.50 (2H, m, H-29), 0.91 (3H, t, J = 7.3 Hz, H-30) and 0.87 (3H, d, J = 6.7 Hz, H-31); δ_C 217.5 (C-27), 45.8 (C-28), 24.7 (C-29), 16.1 (C-31) and 11.7 (C-30)]. Meanwhile, the presence of 10-oxatricyclo[3.3.1.1]decane-2,4-dione nucleus gave carbon resonances at δ_C 209.2 (C-3), 206.9 (C-1), 108.0 (C-5), 97.3 (C-2), 70.4 (C-6), 54.9 (C-4), 44.1 (C-9), 41.1 (C-8) and 33.2 (C-7).

In the HMBC spectrum (Figure 4.60), key correlations from methylene protons H-17 to C-4 (δ_C 54.9), and H-22 to C-1 (δ_C 206.9), C2 (δ_C 97.3) & C-3 (δ_C 209.2) suggested two isoprenyl groups were separately attached to the ring structure at carbon positions C-4 and C-2. Meanwhile, the HMBC correlations from OH to C-4 (δ_C 54.9), C-5 (δ_C 108.0) and C-6 (δ_C 70.4) suggested the OH group to be attached to the acetal-type quaternary carbon C-5. Moreover, both the geminal dimethyl groups, H-10 and H-11 showed correlations with carbons C-6 (δ_C 70.4), C-8 (δ_C 41.1) and C-9 (δ_C 44.1) indicating the two methyl groups to be linked to quaternary carbon C-9. Apart from that, the

presence of a 2-methylbutanoyl group was evidenced to be attached to the relatively deshielded methine carbon C-6 (δ_C 70.4) due to the anisotropic effect of adjacent keto carbonyl of 2-methylbutanoyl group and the ring keto carbonyl group linked to it. Lastly, the third isoprenyl group was found to be attached to the remaining methine carbon C-8 in the ring.

Compound **78** was therefore established to be calosubellinone which is a new compound with the spectral data summarized in Table 4.11. Calosubellinone (**78**) was found to show close resemblance to that of subellinone, a phloroglucinol derivative as reported by Fukuyama et al. (1993) except for the 2-methylbutanoyl group linked to carbon C-6 was replaced by a 2-methylpropanoyl group in subellinone. The assignment of compound **78** was further confirmed by comparison of spectral data with literature values (Fukuyama et al., 1993).
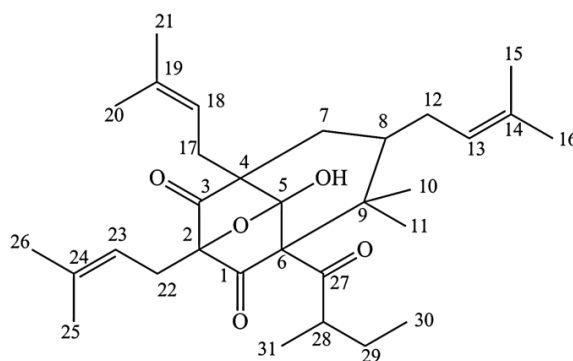
Table 4.11 Summary of NMR data and assignment of calosubellinone (78)

Position	δ_H (ppm)	δ_C (ppm)	HMBC
1	-	206.9	-
2	-	97.3	-
3	-	209.2	-
4	-	54.9	-
5	-	108.0	-
6	-	70.4	-
7	1.87 (H_a, dd, J = 14.0, 3.6 Hz)	33.2	C-3, 5 & 9
	1.21 (H_b, m)		
8	0.93 (1H, m)	41.1	-
9	-	44.1	-
10	0.92 (3H, s)	17.7	C-6, 8, 9 & 11
11	1.22 (3H, s)	23.0	C-6, 8, 9 & 10
12	2.06 (1H, m)	27.8	-
13	4.90 (1H, t, J = 7.3 Hz)	122.2	C-15 & 16
14	-	133.4	-
15	1.53 (3H, s)	18.0	C-13, 14 & 16
16	1.67 (3H, s)	25.9	C-13, 14 & 15
17	2.40 (2H, m)	31.0	C- 4, 18 & 19
18	5.26 (1H, t, J = 7.3 Hz)	119.0	C-20 & 21
19	-	133.8	-
20	1.54 (3H, s)	17.8	C-18, 19 & 21
21	1.67 (3H, s)	25.9	C-18, 19 & 20
22	2.74 (H_a, dd, J = 15.9, 7.3 Hz)	23.8	C-1, 2, 3, 22 & 24
	2.47 (H_b, dd, J = 15.3, 7.3 Hz)		
23	5.00 (1H, t, J = 7.3 Hz)	116.0	C-25 & 26
24	-	135.8	-
25	1.62 (3H, s)	18.0	C-23, 24 & 26
26	1.63 (3H, s)	26.1	C-23 & 24
27	-	217.5	-
28	2.94 (1H, sext, J = 6.7 Hz)	45.8	-
29	1.50 (2H, m)	24.7	-
30	0.91 (3H, t, J = 7.3 Hz)	11.7	-
31	0.87 (3H, d, J = 6.7 Hz)	16.1	C-27, 28 & 29
5-OH	8.11 (OH, s)	-	C-4, 5 & 6
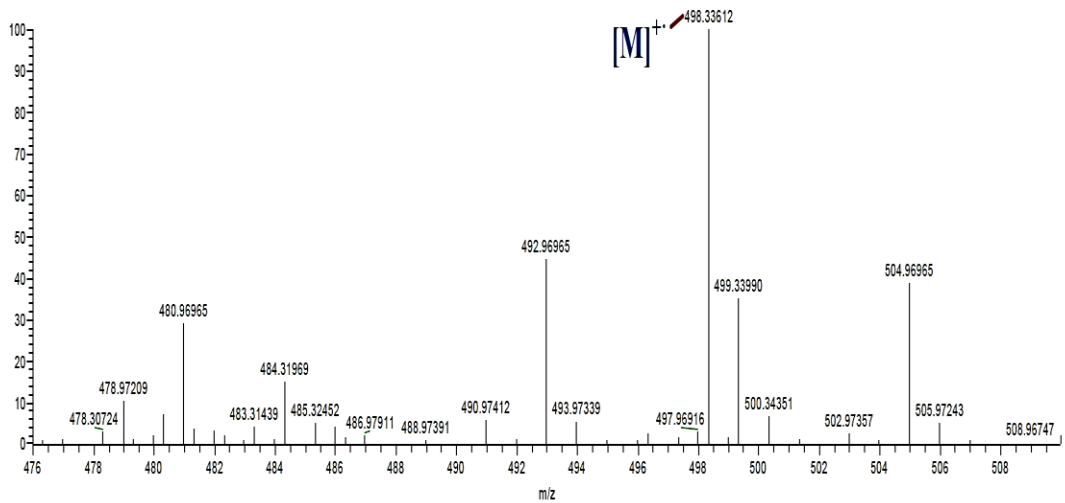
Figure 4.51: HREIMS spectrum of calosubellinone (78)
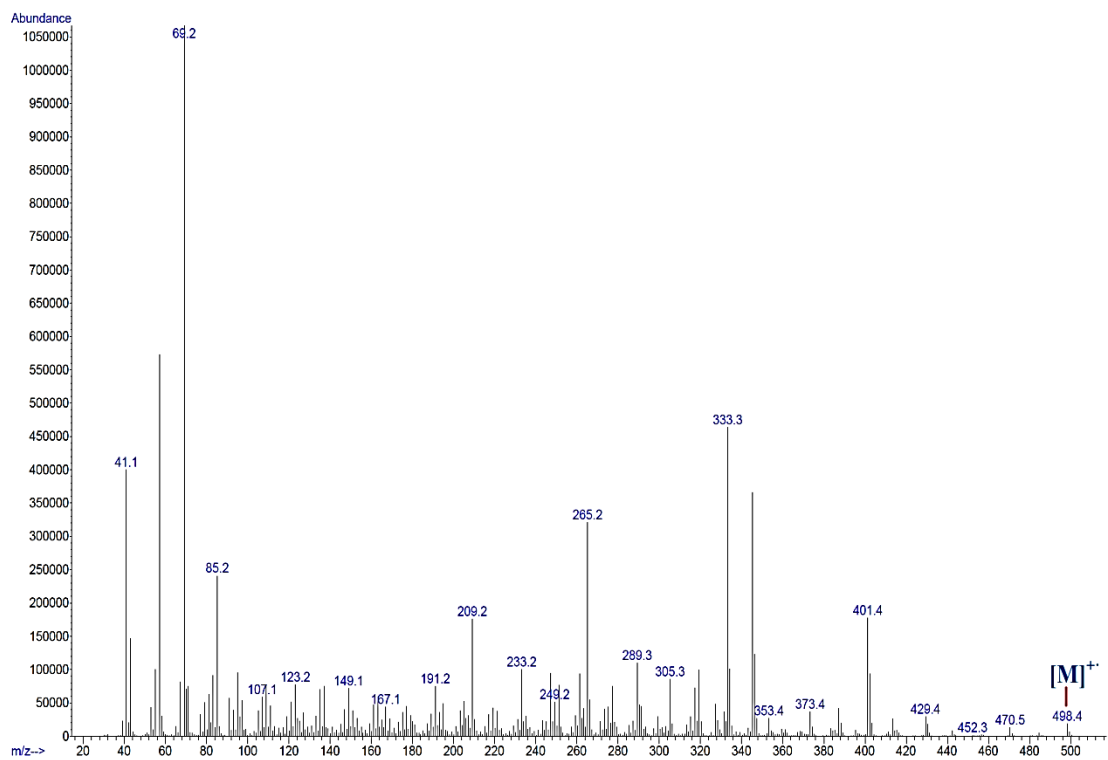
Figure 4.52: EIMS spectrum of calosubellinone (78)
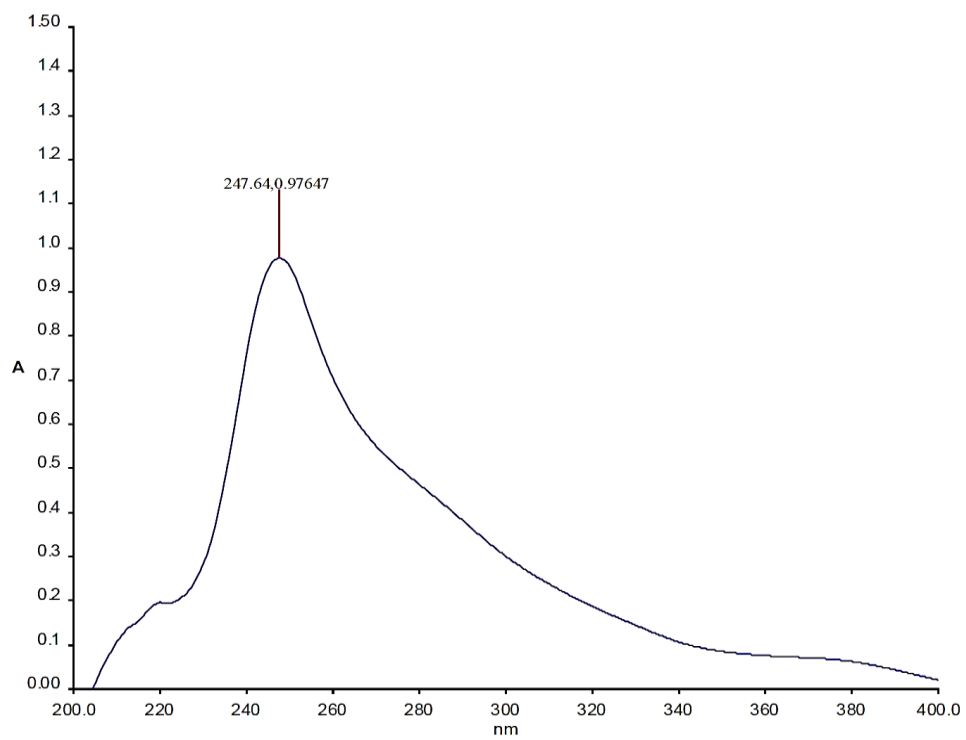
Figure 4.53: UV-Vis spectrum of calosubellinone (78)
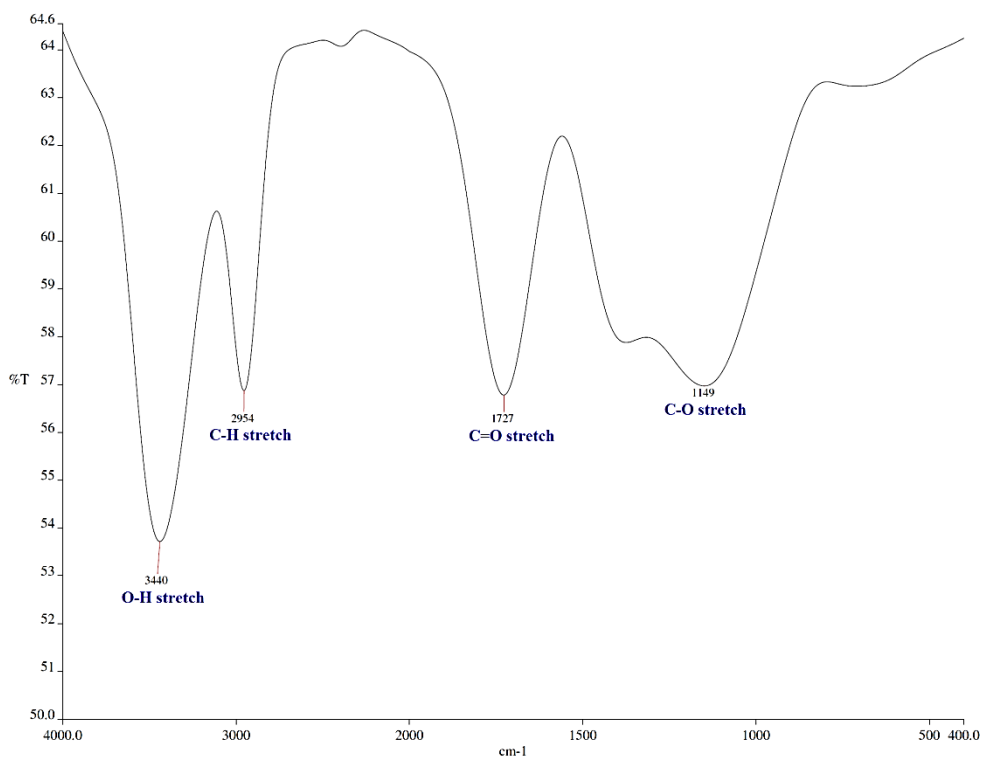
Figure 4.54: IR spectrum of calosubellinone (78)
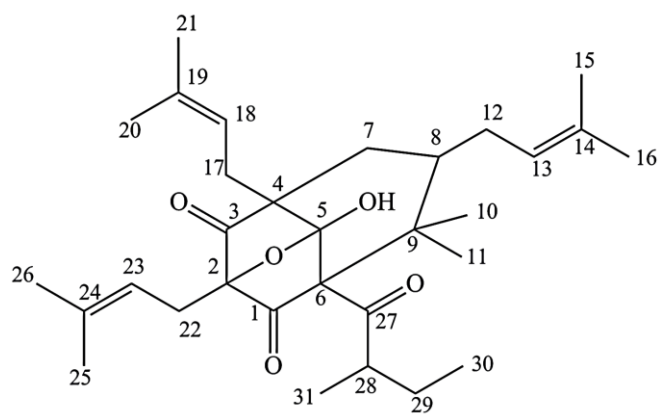
(**78**)
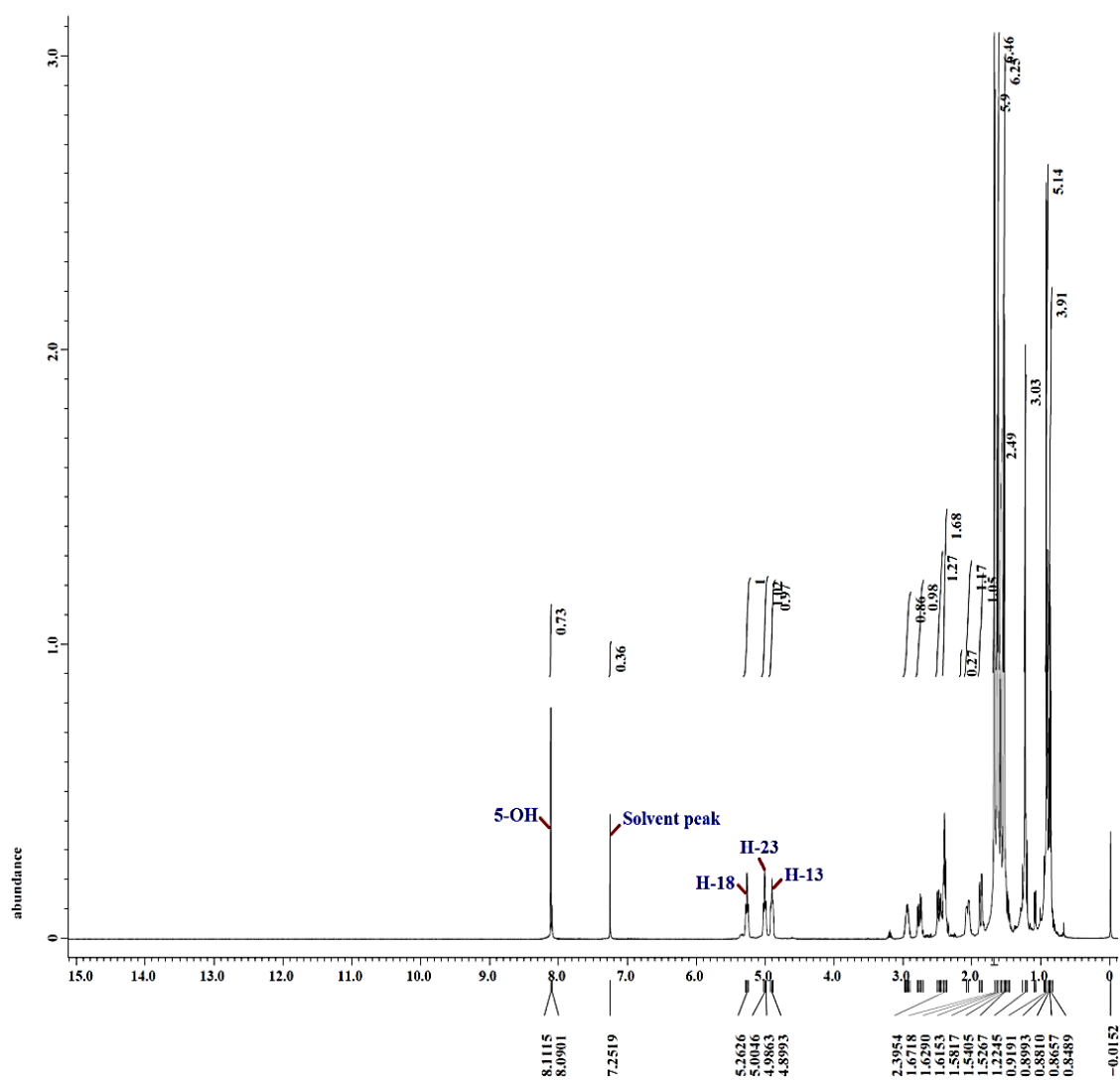
Figure 4.55: ^{1}H NMR spectrum of calosubellinone (**78**) (400 MHz, CDCl$_3$)
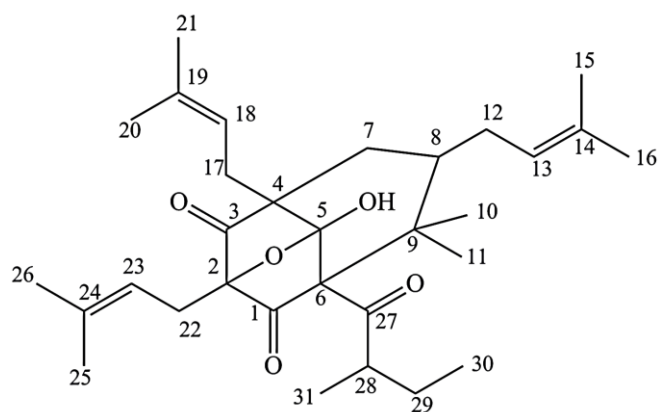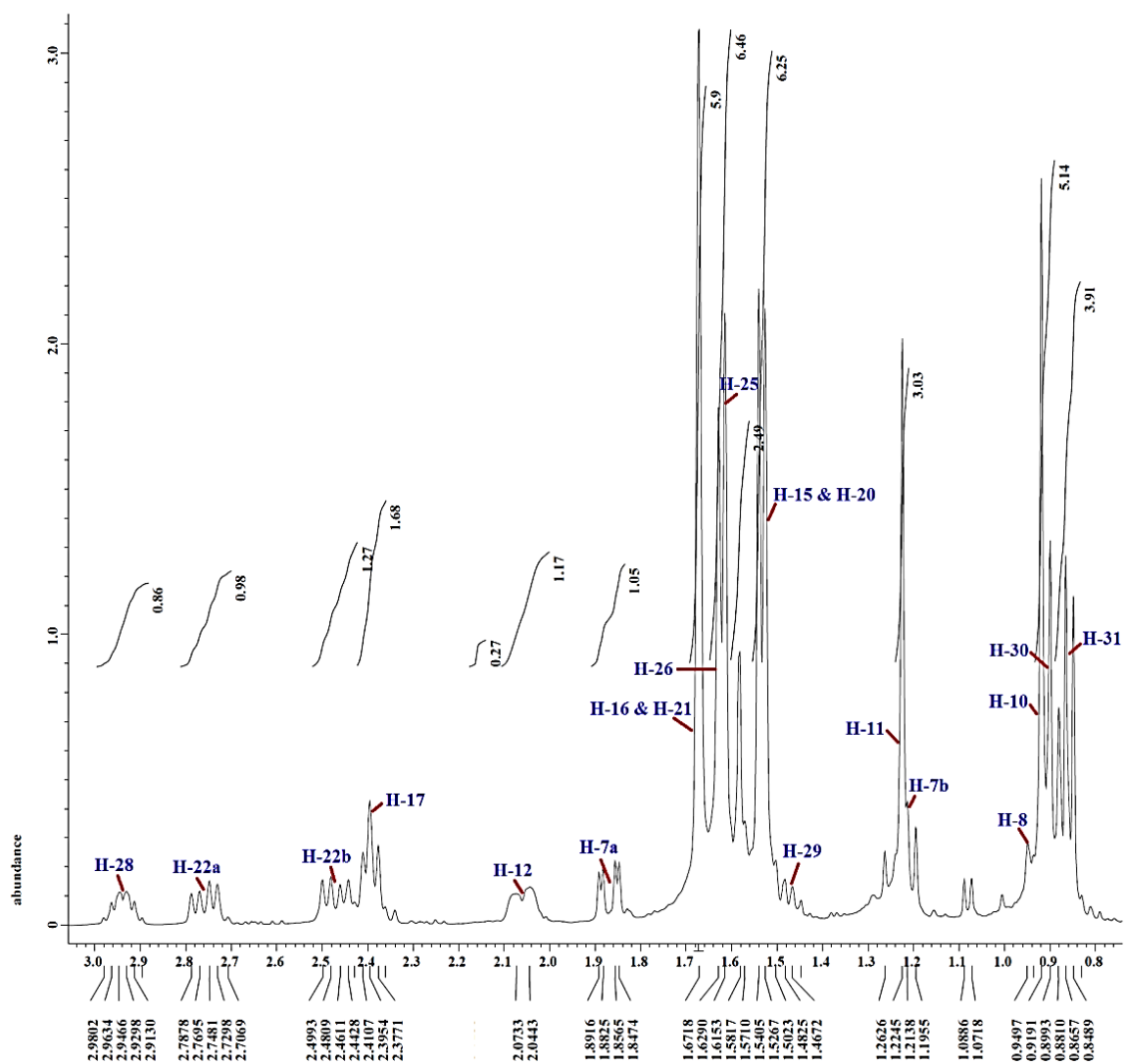
Figure 4.56: Expanded ¹H NMR spectrum of calosubellinone (78) (400 MHz, CDCl₃)
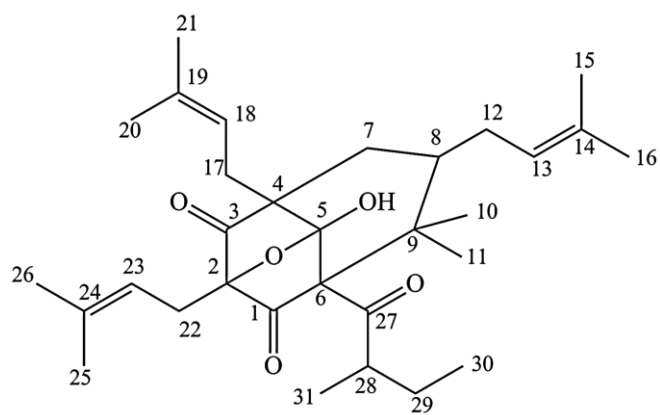
(**78**)
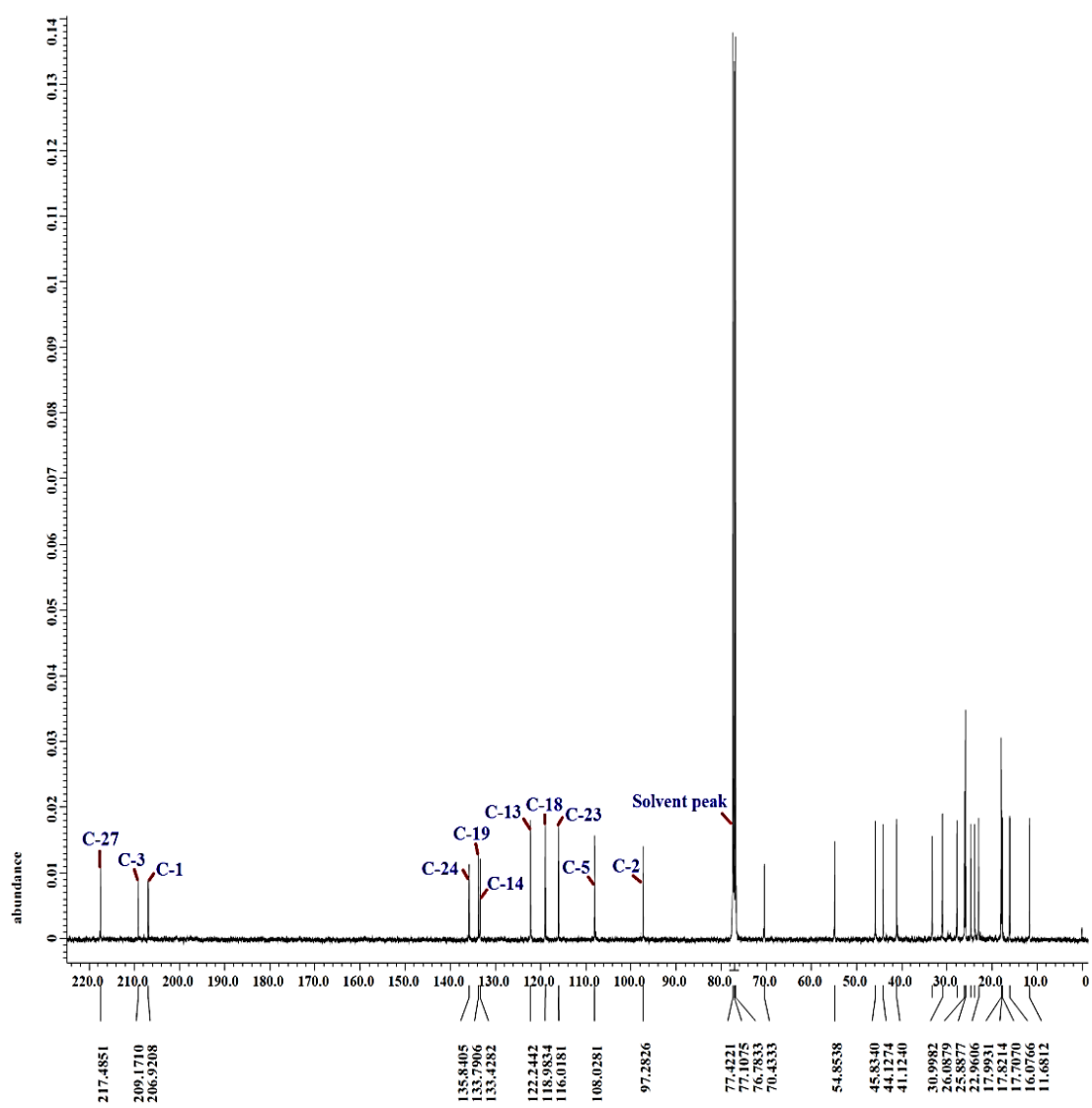
Figure 4.57: ^{13}**C NMR spectrum of calosubellinone (78) (100 MHz, CDCl$_3$)**
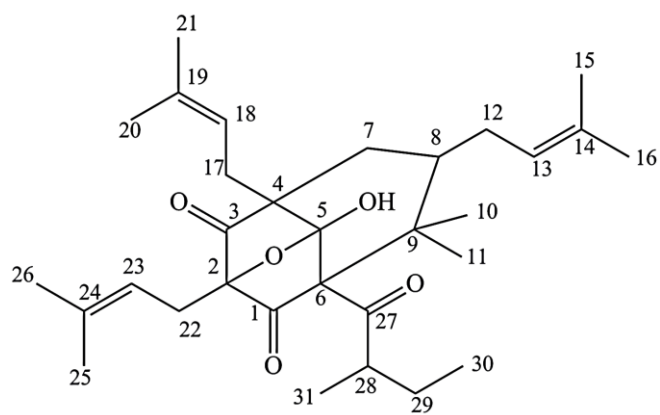
(**78**)
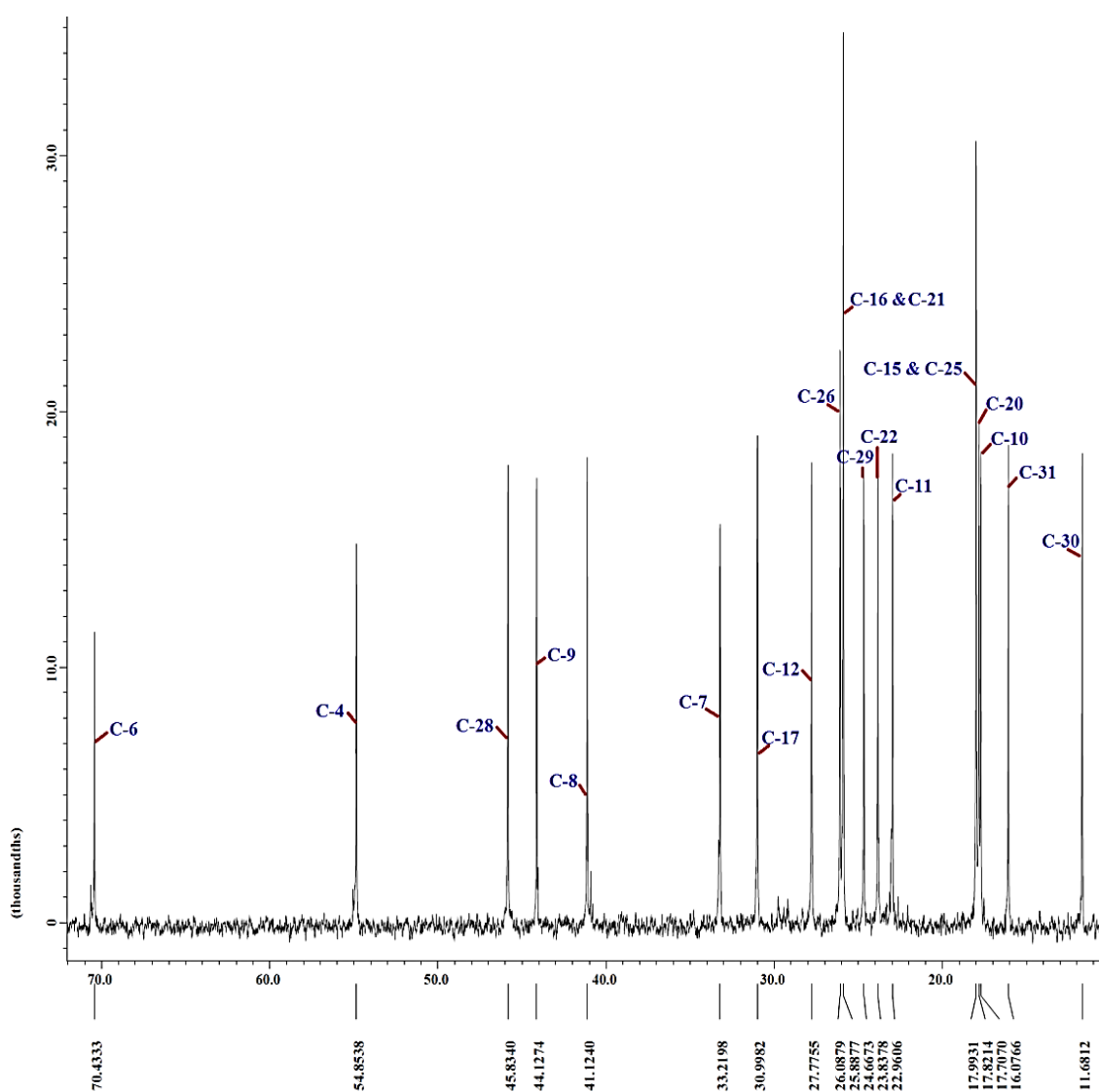
Figure 4.58: Expanded ^{13}C NMR spectrum of calosubellinone (78) (100 MHz, CDCl$_3$)

(**78**)
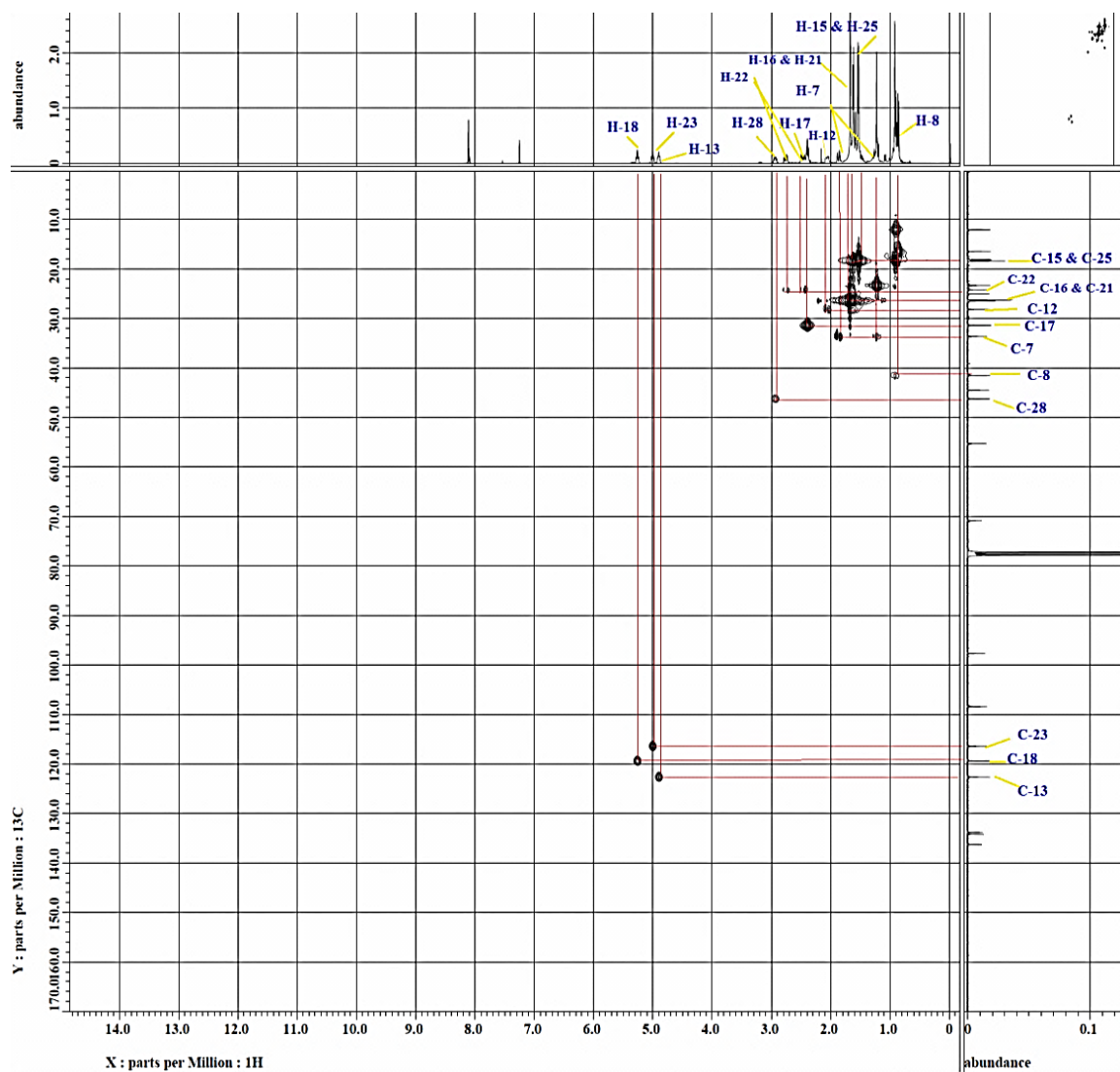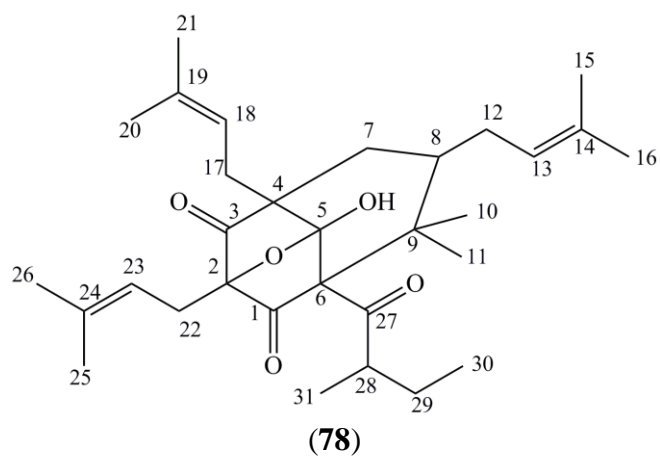
Figure 4.59: HMQC spectrum of calosubellinone (78)
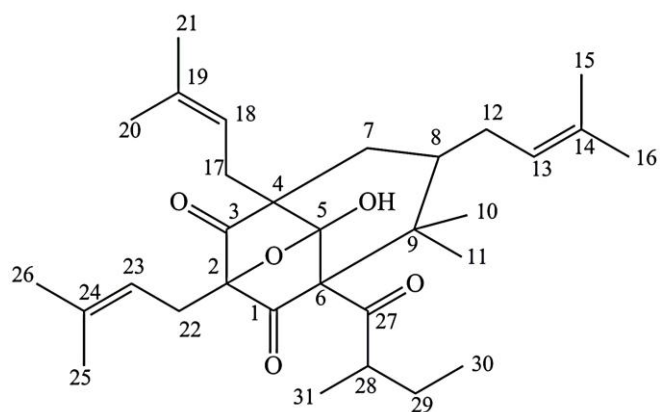
(**78**)
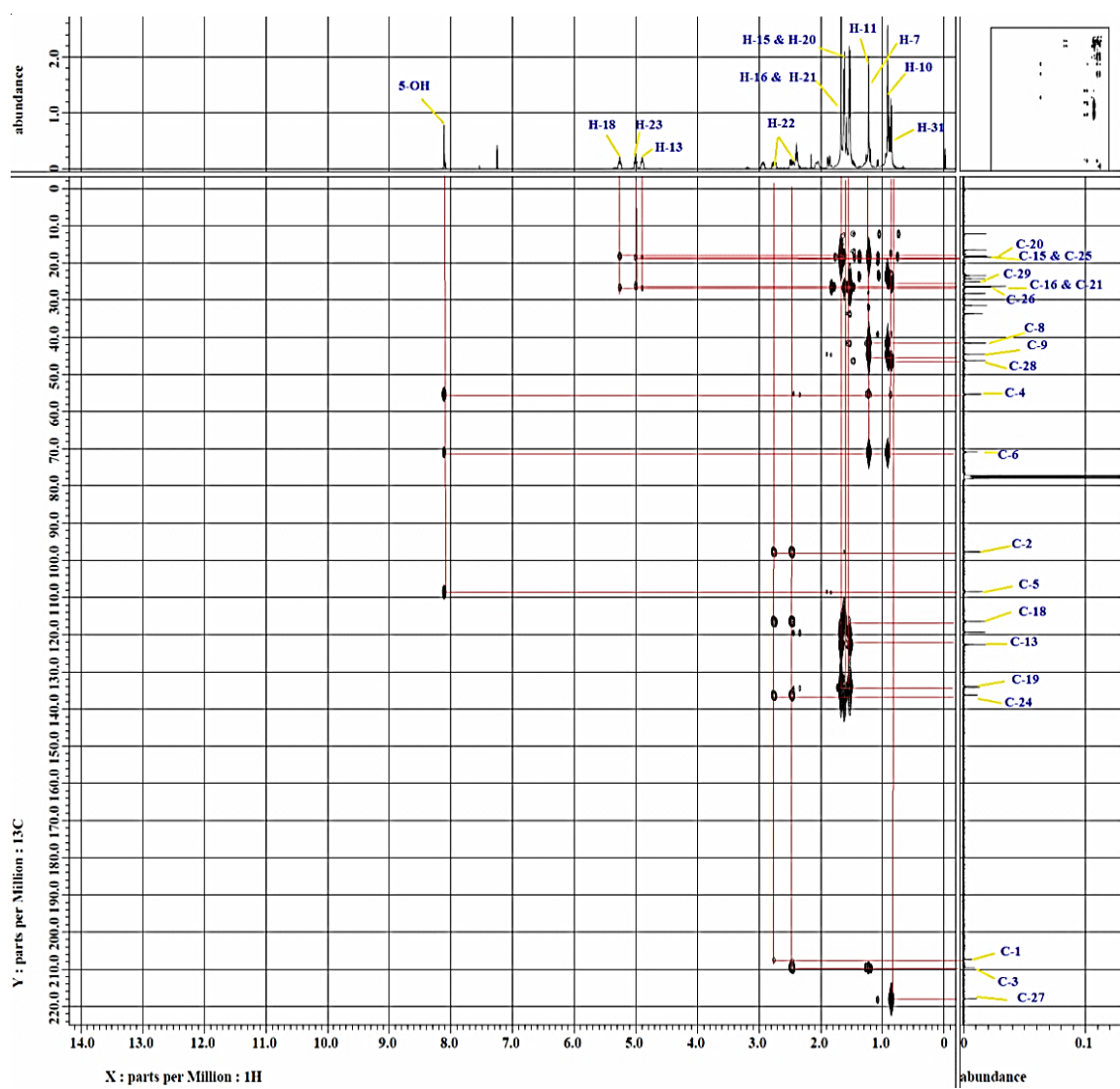
Figure 4.60: HMBC spectrum of calosubellinone (78)

129

4.3.2 Characterization of Garsubellin B (79)
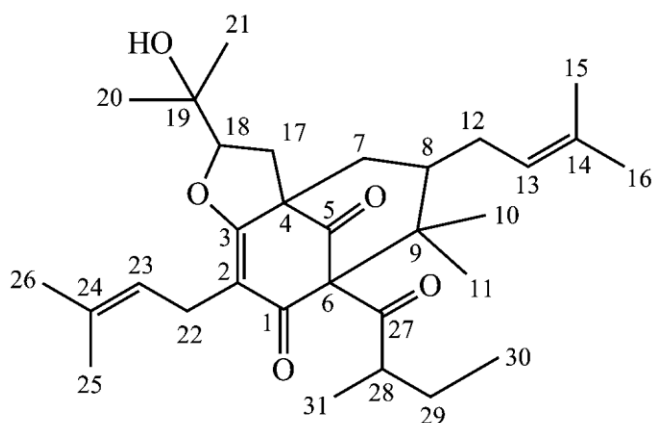
(**79**)

Compound **79** was isolated as yellow gum and showed specific optical rotation, $[\alpha]_D$ of $-36°$ (EtOH, c 0.60) (Lit. $-36°$, Fukuyama et al., 1998). The developed TLC gave a single brown spot under UV light at wavelength of 254 nm, and was stained brown when treated with iodine vapour. However, this compound showed a negative result in the $FeCl_3$ test revealing it to be non-phenolic. This compound gave a retention factor, R_f value of 0.69 via a mobile phase of 40% hexane, 40% dichloromethane and 20% ethyl acetate.

Compound **79** was established to have a molecular formula of $C_{31}H_{46}O_5$ which was deduced from the EIMS ($[M]^{+\cdot}$ at m/z 498) (Figure 4.61). In addition, the UV spectrum (Figure 4.62) revealed absorption maxima at 218.0 and 268.7 nm, and the IR spectrum (Figure 4.63) showed absorption bands at 3448, 2956 and 1633 cm^{-1}, indicating the presence of O-H, C-H and C=C functionalities, respectively.

The ^{1}H and ^{13}C NMR spectra (Figures 4.64 to 4.67) of compound **79** showed the presence of a bicyclo[3.3.1]non-3-ene-2,9-dione framework [δ_H 1.98 (1H, m, H$_a$-7) and 1.43 (2H, m, H$_b$-7 and H-8); δ_C 204.6 (C-5), 193.0 (C-1), 173.1 (C-3), 116.5 (C-2), 82.2 (C-6), 59.6 (C-4), 46.5 (C-9), 42.4 (C-8) and 38.5 (C-7)], a 2-methylbutanoyl group [δ_H 1.67 (1H, m, H-28), 1.60 (1H, m, H$_a$-29), 1.35 (1H, m, H$_b$-29), 1.02 (3H, d, J = 6.1 Hz, H-31) and 0.70 (3H, t, J = 7.3 Hz, H-30); δ_C 208.7 (C-27), 48.8 (C-28), 27.5 (C-29), 16.6 (C-31) and 11.5 (C-30)], and two 3-methyl-2-butenoyl groups [δ_H 4.88 (1H, t, J = 7.4 Hz, H-13), 2.09 (1H, m, H$_a$-12), 1.55 (1H, m, H$_b$-12), 1.63 (3H, s, H-16) and 1.50 (3H, s, H-15); δ_C 133.5 (C-14), 122.3 (C-13), 26.6 (C-12), 25.9 (C-16) and 17.9 (C-15)] and [δ_H 5.00 (1H, t, J = 7.3 Hz, H-23), 3.10 (1H, dd, J = 14.3, 7.0 Hz, H$_a$-22), 2.96 (1H, dd, J = 13.4, 7.6 Hz, H$_b$-22), 1.64 (3H, s, H-25) and 1.58 (3H, s, H-26); δ_C 132.4 (C-24), 121.2 (C-23), 25.7 (C-26), 22.2 (C-22) and 17.9 (C-25). Apart from that, carbon resonances at δ_C 90.2 (C-18), 70.9 (C-19), 30.3 (C-17), 26.8 (C-20) and 24.3 (C-21) indicated the presence of 2-(2-hydroxypropan-2-yl)tetrahydrofuran ring moiety.

In the HMBC spectrum (Figure 4.69), cross-peaks from proton H-17 to C-3 (δ_C 173.1), C-4 (δ_C 59.6), C-5 (δ_C 204.6) and C-7 (δ_C 38.5) indicated that the 2-(2-hydroxypropan-2-yl)tetrahydrofuran ring was fused to the bicyclo[3.3.1] non-3-ene-2,9-dione core at carbons C-3 and C-4. The HMBC correlations from proton H-10 to carbons C-6 (δ_C 82.2), C-8 (δ_C 42.4), C-9 (δ_C 46.5) and C-11 (δ_C 22.8), and from proton H-11 to carbons C-6 (δ_C 82.2), C-8 (δ_C 42.4), C-9 (δ_C 46.5) and C-10 (δ_C 16.1) confirmed that the *gem*-dimethyl group was attached to carbon C-9. The NMR data of compound **79** (Table 4.12) were

131

consistent with the literature data reported by Fukuyama et al. (1998). Hence, compound **79** was established to be garsubellin B which was previously reported for its isolation from *Garcinia subelliptica*.
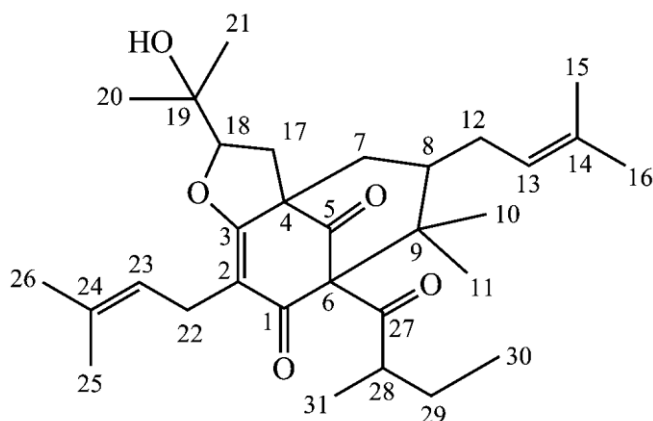
Table 4.12: Summary of NMR data and assignment of garsubellin B (79)

Position	δ_H (ppm)	δ_C (ppm)	HMBC
1	-	193.0	-
2	-	116.5	-
3	-	173.1	-
4	-	59.6	-
5	-	204.6	-
6	-	82.2	-
7	1.98 (H_a, m); 1.43 (H_b, m)	38.5	C-3, 4, 5, 8 & 9
8	1.43 (1H, m)	42.4	C-10
9	-	46.5	-
10	0.99 (3H, s)	16.1	C-6, 8, 9 & 11
11	1.21 (3H, s)	22.8	C-6, 8, 9 & 10
12	2.09 (H_a, m); 1.55 (H_b. m)	26.6	C-13 & 14
13	4.88 (1H, t, $J = 7.4$ Hz)	122.3	C-15 & 16
14	-	133.5	-
15	1.50 (3H, s)	17.9	C-13, 14 & 16
16	1.63 (3H, s)	25.9	C-13, 14 & 15
17	2.61 (H_a, dd, $J = 12.8, 11.0$ Hz) 1.73 (H_b, m)	30.3	C-3, 4, 5, 7, 18 &19
18	4.51 (1H, dd, $J = 10.7, 5.8$ Hz)	90.2	-
19	-	70.9	-
20	1.32 (3H, s)	26.8	C-18, 19 & 21
21	1.17 (3H, s)	24.3	C-18, 19 & 20
22	3.10 (H_a, dd, $J = 14.3, 7.0$ Hz) 2.96 (H_b, dd, $J = 14.3, 7.6$ Hz)	22.2	C-1, 2, 3, 23 & 24
23	5.00 (1H, t, $J = 7.3$ Hz)	121.2	C-22, 25 & 26
24	-	132.4	-
25	1.64 (3H, s)	17.9	C-23, 24 & 26
26	1.58 (3H, s)	25.7	C-23, 24 & 25
27	-	208.7	-
28	1.67 (1H, m)	48.8	-
29	1.60 (H_a, m); 1.35 (H_b, s)	27.5	-
30	0.70 (3H, t, $J = 7.3$ Hz)	11.5	C-28 & 29
31	1.02 (3H, d, $J = 6.1$ Hz)	16.6	C-27, 28 & 29
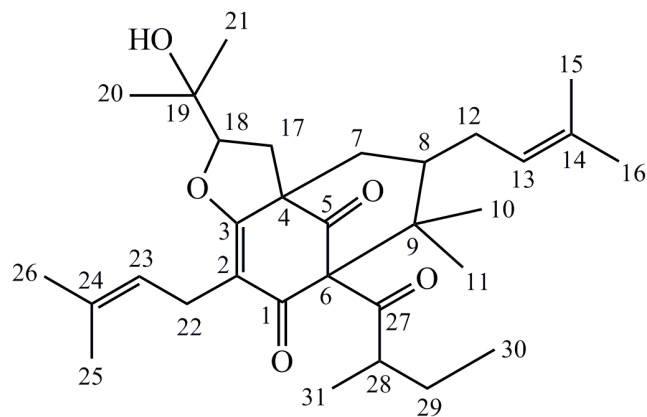
(**79**)
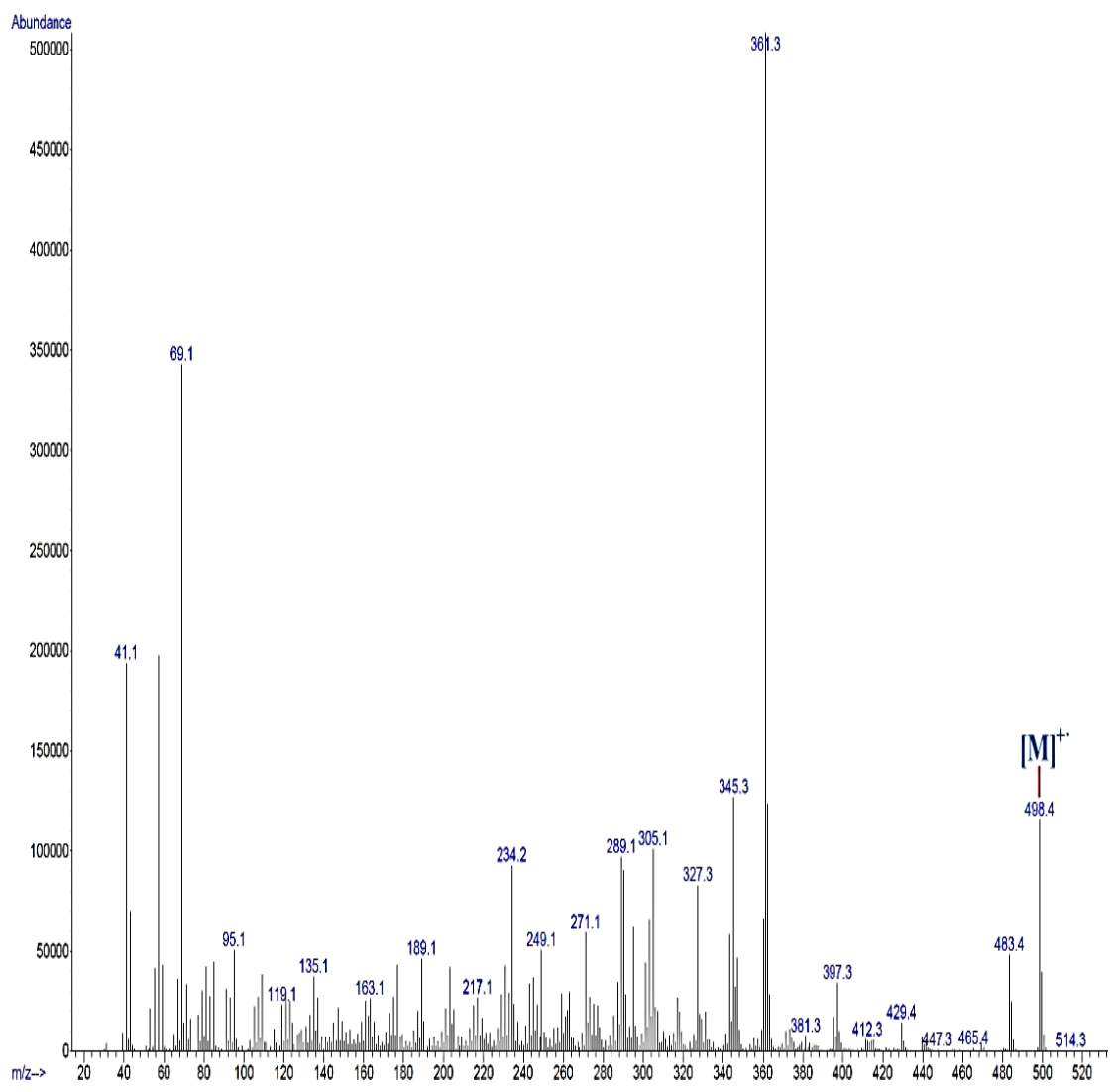
Figure 4.61: EIMS spectrum of garsubellin B (79)
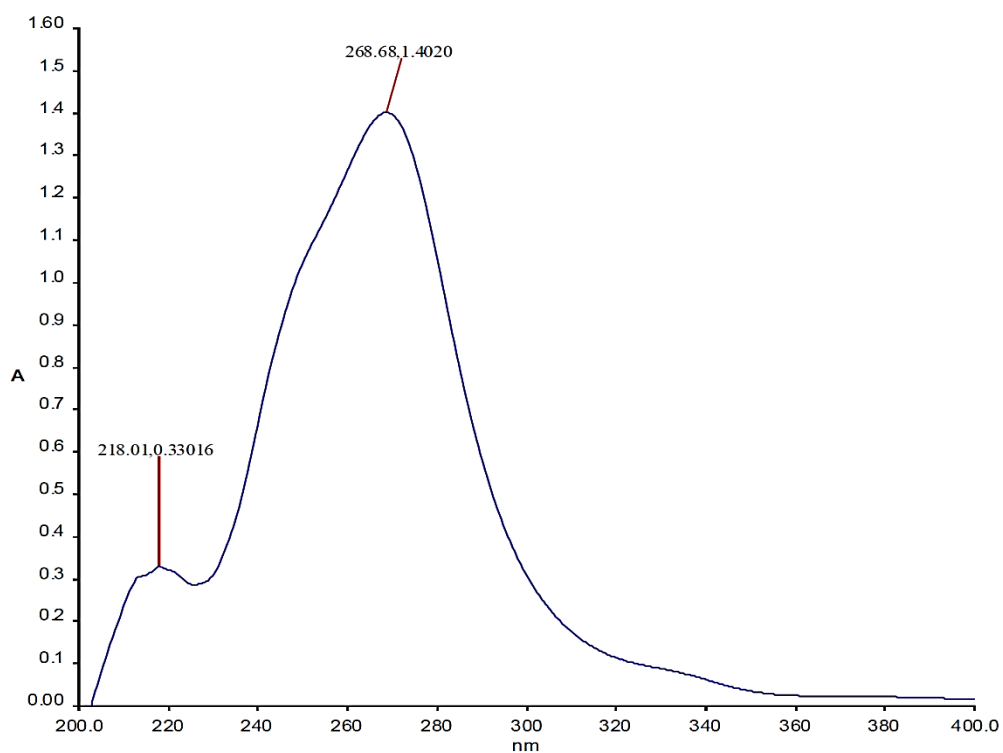
Figure 4.62: UV-Vis spectrum of garsubellin B (79)
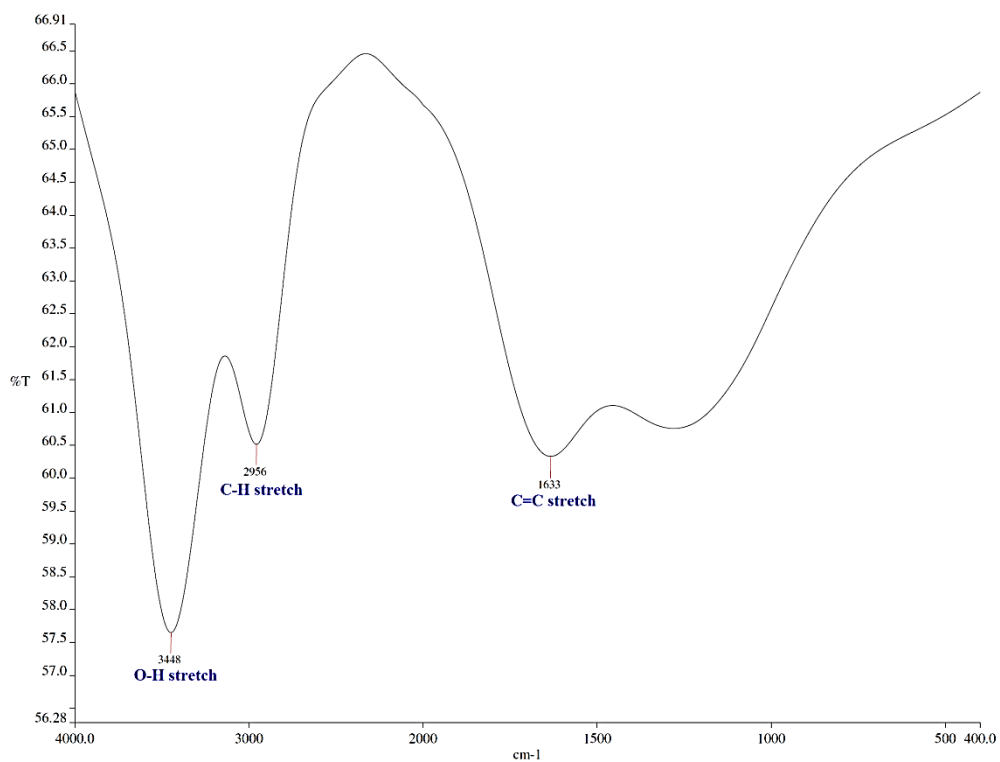
Figure 4.63: IR spectrum of garsubellin B (79)
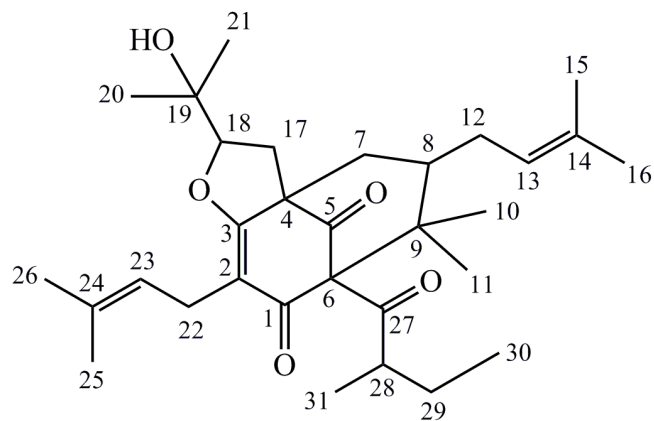
(**79**)
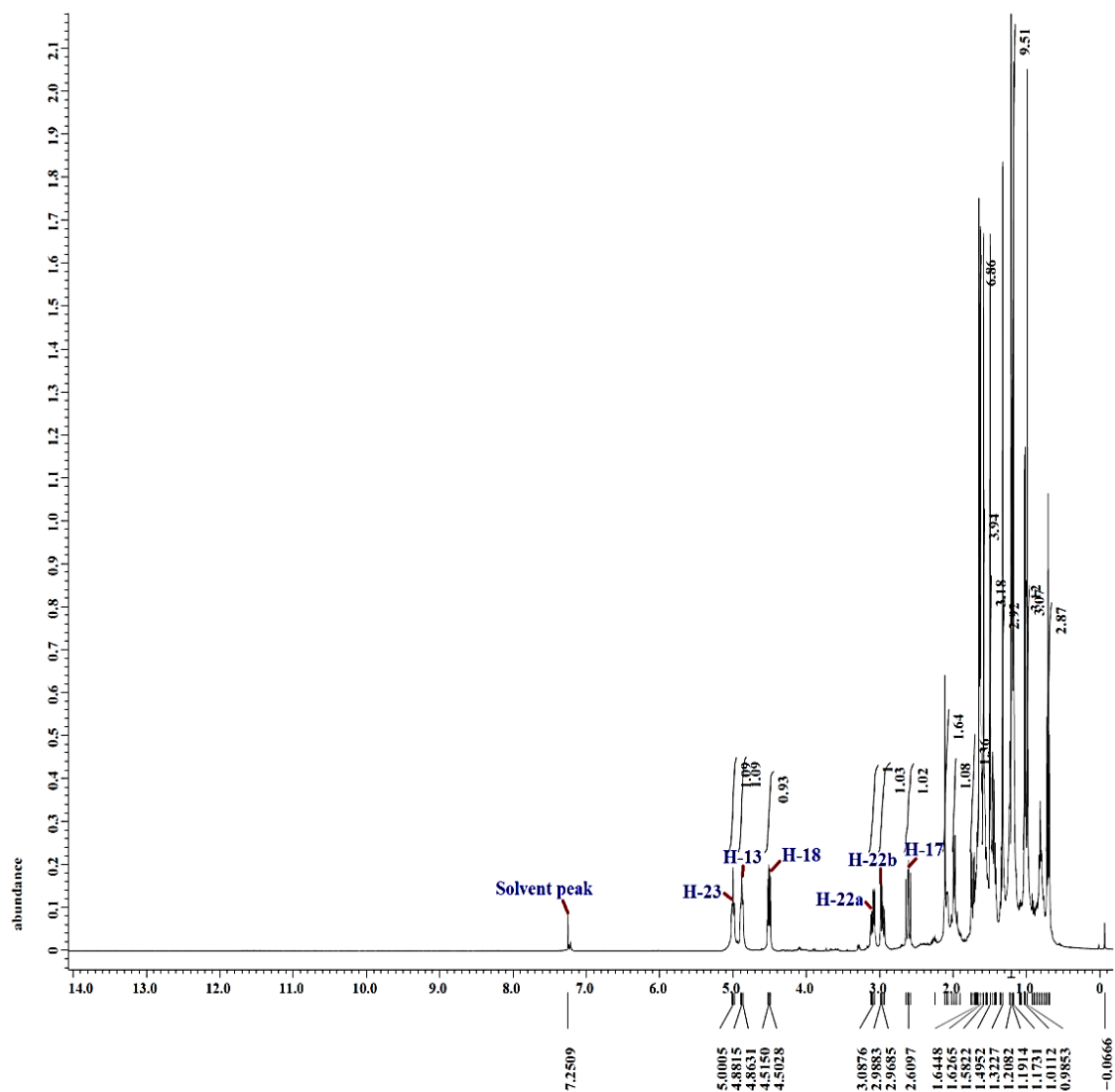
Figure 4.64: ^{1}H NMR spectrum of garsubellin B (79) (400 MHz, CDCl$_3$)
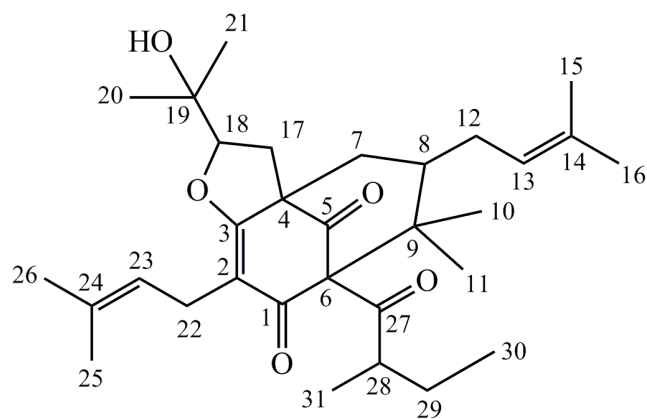
(**79**)
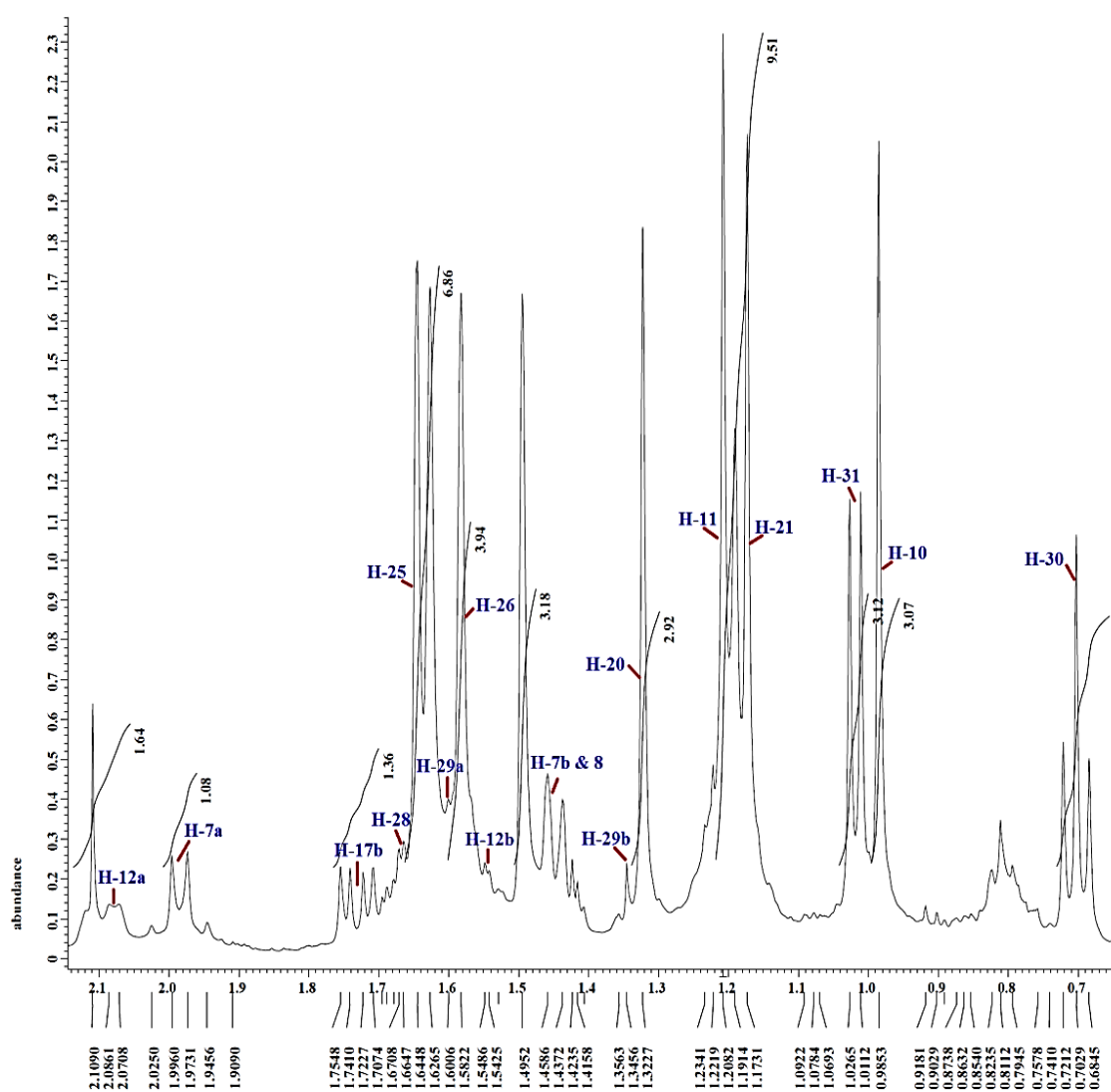
Figure 4.65: Expanded ^{1}H NMR spectrum of garsubellin B (79) (400 MHz, CDCl₃)
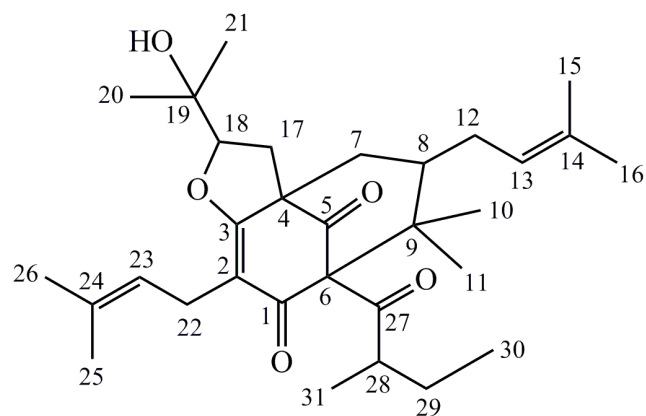
(**79**)
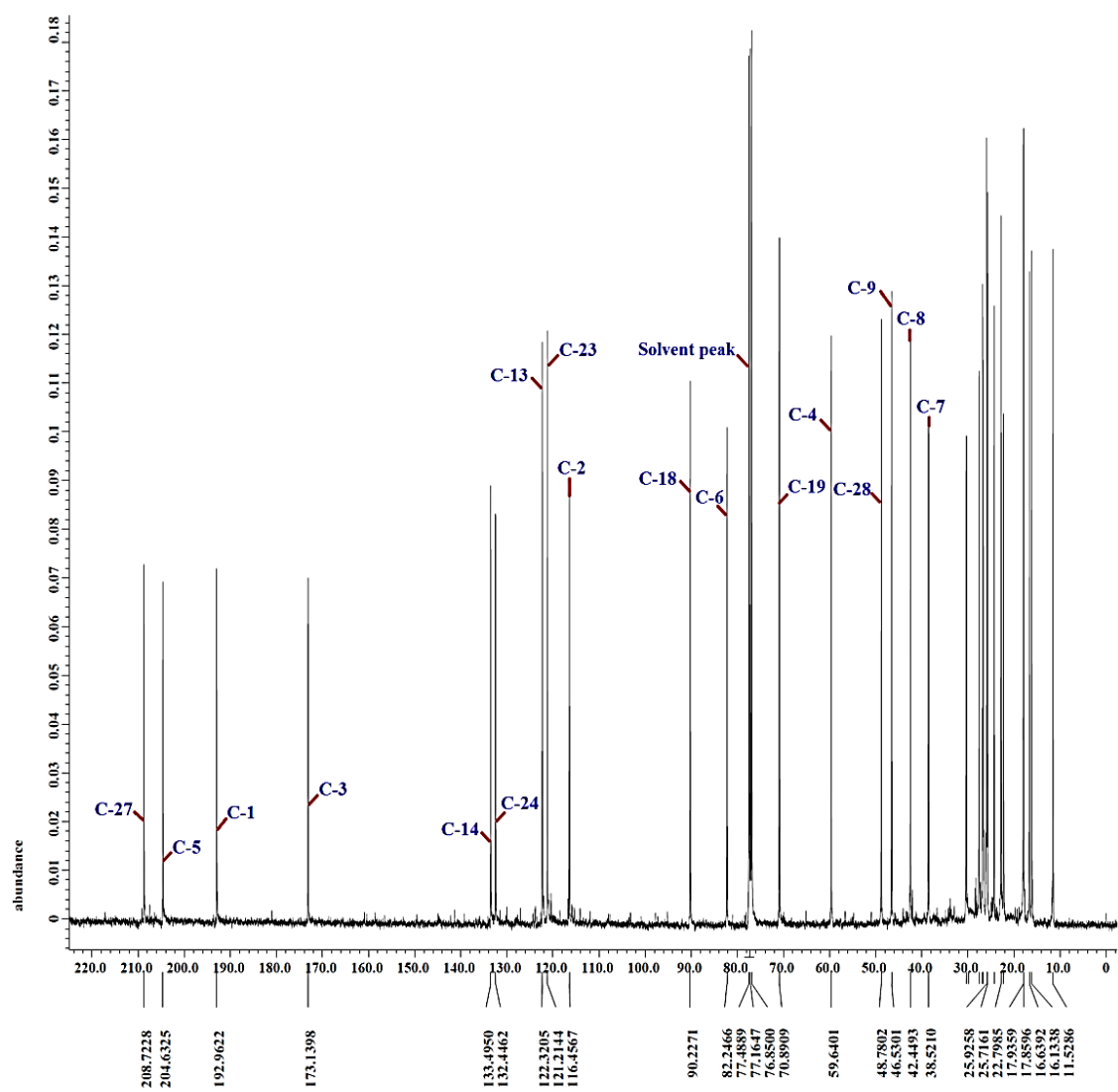
Figure 4.66: ^{13}C NMR spectrum of garsubellin B (**79**) (100 MHz, CDCl$_3$)

138
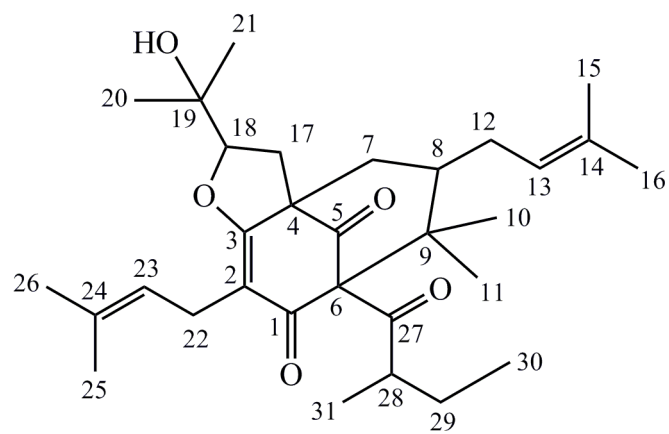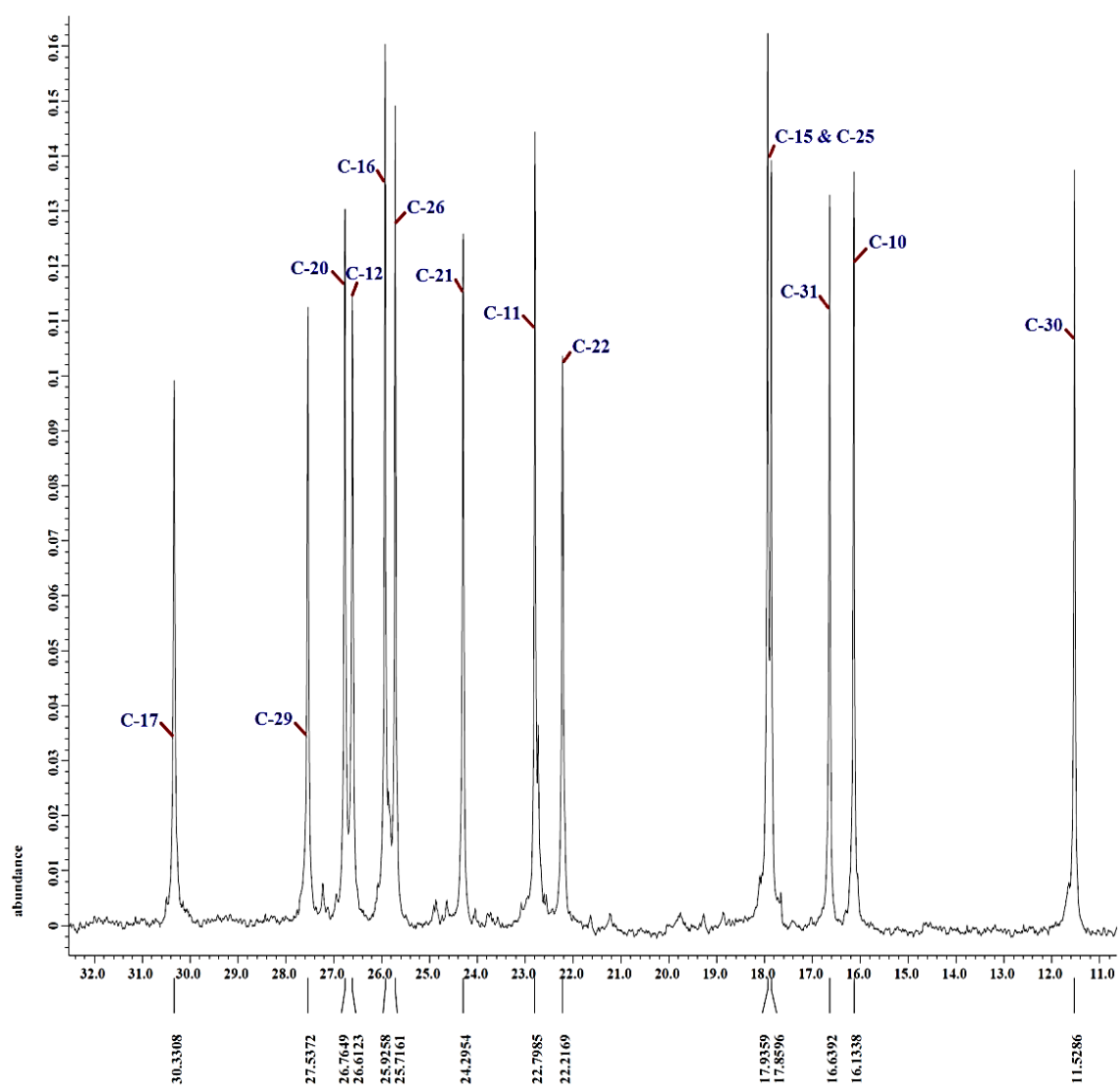
Figure 4.67: Expanded ^{13}C NMR spectrum of garsubellin B (79) (100 MHz, CDCl$_3$)

(**79**)
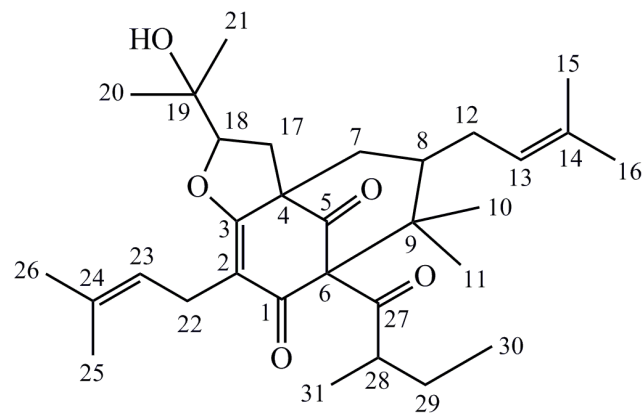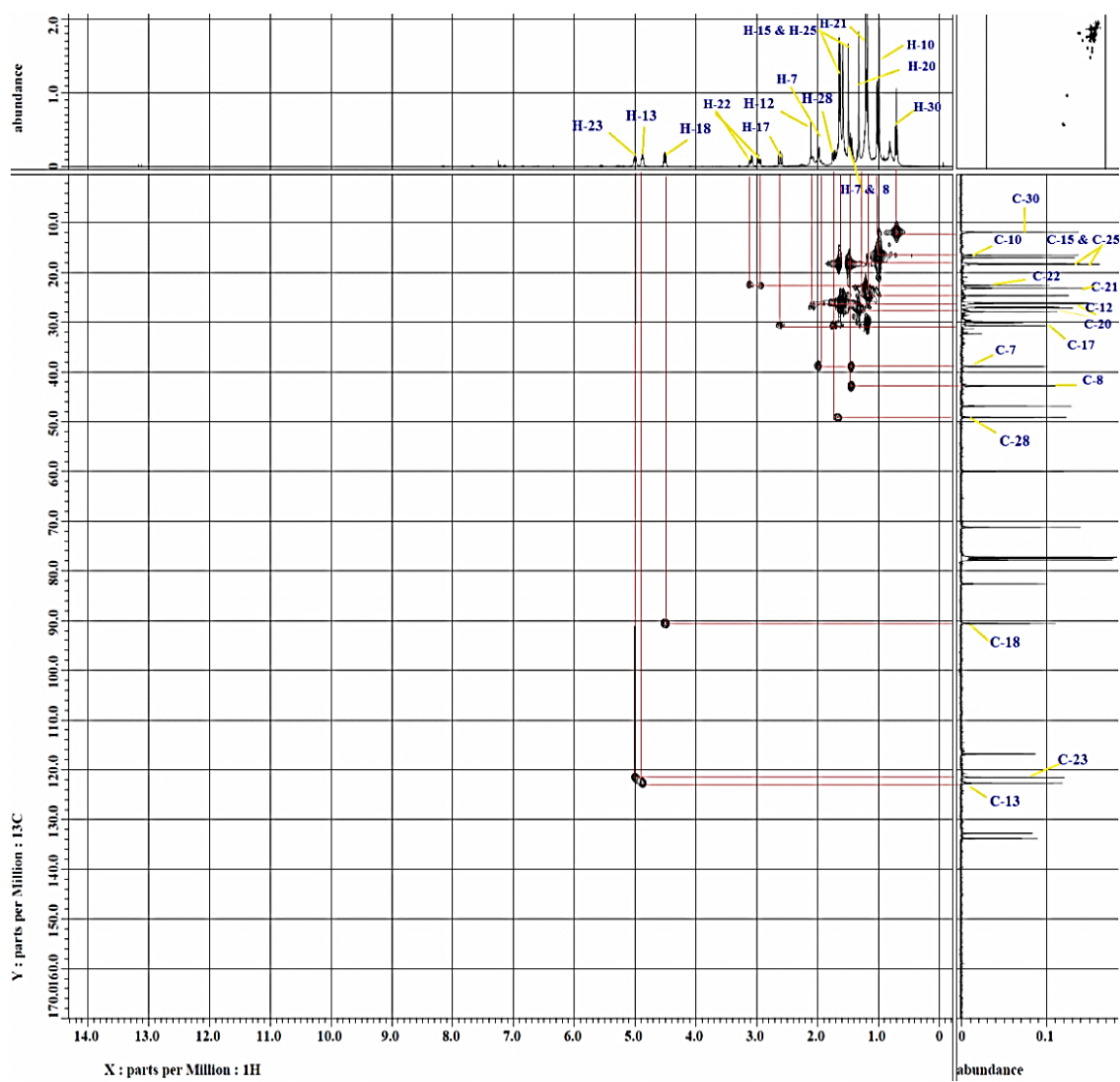
Figure 4.68: HMQC spectrum of garsubellin B (79)
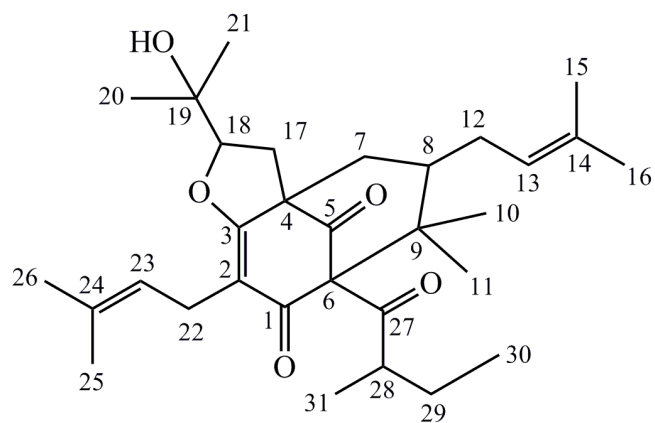
(**79**)
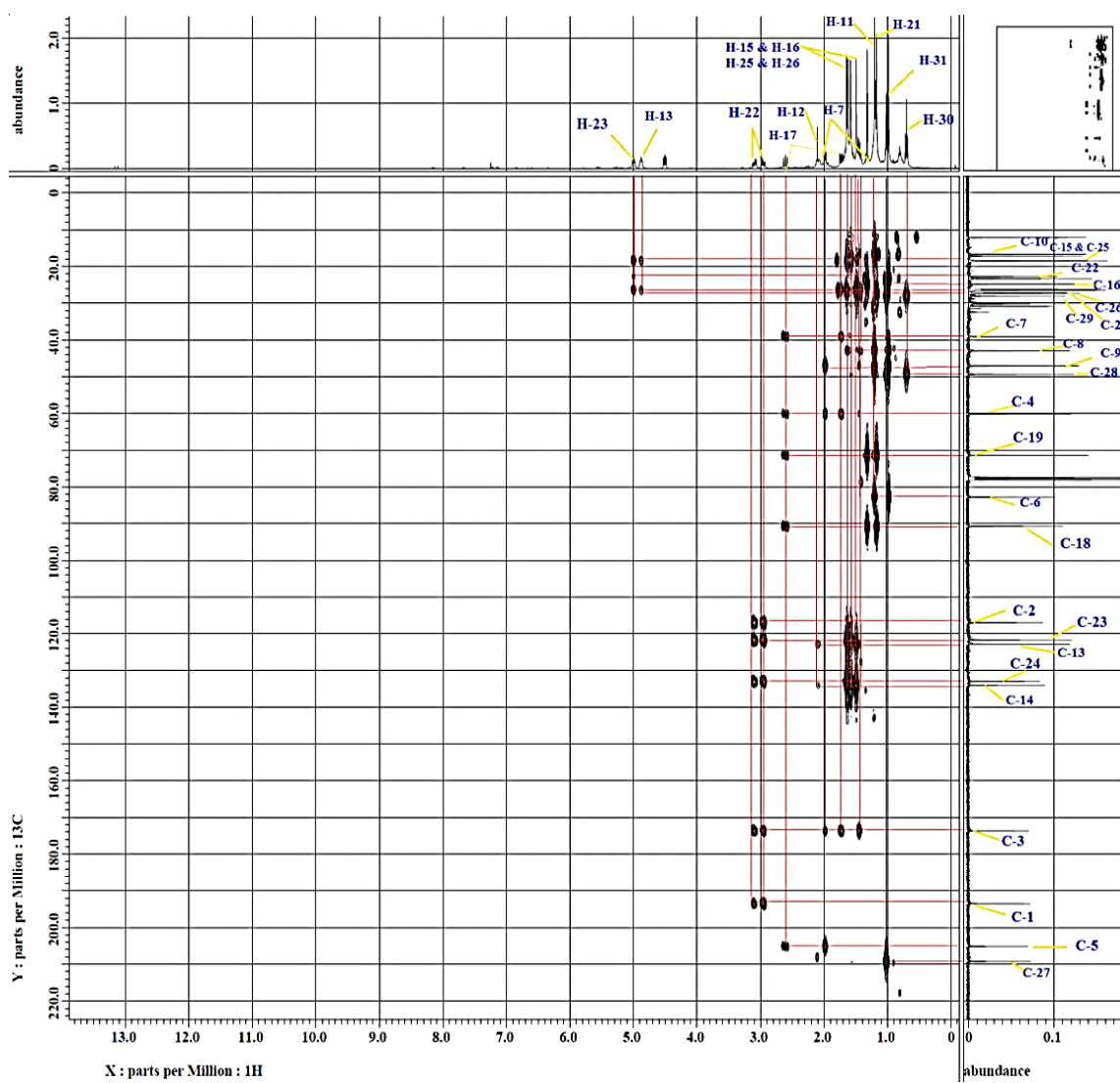
Figure 4.69: HMBC spectrum of garsubellin B (79)

4.3.3 Characterization of Soulattrone A (80)
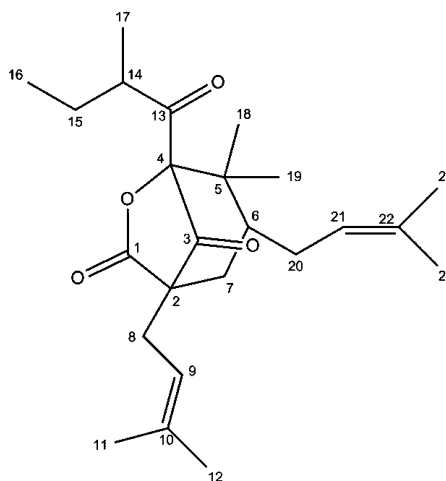
(**80**)

Compound **80** was obtained as white needles with mp 104-106 °C (Lit. 113-114 °C, Nigam et al., 1988). It has a specific rotation, $[\alpha]_D$ of $-155.6°$ (EtOH, c 0.60) which is close to the reported literature value of $-157.3°$ (Nigam et al., 1988). Compound **80** gave no visible spot when visualized under UV light at wavelength of 254 nm, and gave brown spot when treated with iodine vapour. Moreover, the negative $FeCl_3$ test revealed the absence of phenolic moiety in this compound. This compound showed retention factor, R_f value of 0.74 when eluted with a mobile phase of 60% hexane, 20% dichloromethane and 20% ethyl acetate.

Compound **80** has a molecular formula of $C_{24}H_{36}O_4$ corresponding to the molecular ion peak observed at m/z 388 (Figure 4.70), whereas the IR

spectrum (Figure 4.71) showed absorption bands at 2923 (C-H stretch), 1708 (C=O stretch) and 1410 (C-H bend) cm^{-1}.

The ^{1}H and ^{13}C NMR spectra (Figures 4.72 to 4.74) of compound **80** revealed the presence of a 6-oxabicyclo [3.2.1] octane-7,8-dione core [δ_H 2.13 (1H, dd, J = 13.1, 4.0 Hz, H$_b$-7), 1.51 (1H, m, H$_a$-7) and 1.67 (1H, m, H-6); δ_C 201.6 (C-3), 172.1 (C-1), 96.9 (C-4), 57.0 (C-2), 49.6 (C-5), 41.9 (C-6) and 41.1 (C-7)], a 2-methylbutanoyl group [δ_H 2.82 (1H, m, H-14), 1.71 (1H, m, H$_b$-15), 1.28 (1H, m, H$_a$-15), 0.86 (3H, t, J = 7.3 Hz, H-16) and 0.83 (3H, d, J = 6.7 Hz, H-17); δ_C 205.0 (C-13), 44.8 (C-14), 24.6 (C-15), 16.0 (C-17) and 11.9 (C-16)] and two 3-methyl-2-butenyl groups at [δ_H 4.97 (1H, brs, H-21), 2.00 (1H, m, H$_b$-20), 1.67 (1H, m, H$_a$-20), 1.67 (3H, s, H-23) and 1.54 (3H, s, H-24); δ_C 134.2 (C-22), 121.6 (C-21), 27.4 (C-20), 25.9 (C-23) and 18.0 (C-24)] and [δ_H 5.03 (1H, t, J = 7.3 Hz, H-9), 2.39 (2H, m, H-8), 1.66 (3H, s, H-12) and 1.62 (3H, s, H-11); δ_C 136.7 (C-10), 117.0 (C-9), 26.3 (C-8), 25.8 (C-11) and 18.1 (C-12)].

In the HMBC spectrum (Figure 4.76), cross peaks from proton H-8 to C-1 (δ_C 172.1), C-2 (δ_C 57.0), C-3 (δ_C 201.6), C-9 (δ_C 117.0) and C-10 (δ_C 136.7) indicated that a 3-methyl-2-butenyl group was linked to the position C-2 of the 6-oxabicyclo[3.2.1]octane-7,8-dione core. Moreover, the HMBC correlations from protons H-18 and H-19 to carbons C-4 (δ_C 96.9), C-5 (δ_C 49.6) and C-6 (δ_C 41.9) deduced that the *gem*-dimethyl group was attached to carbon position C-5 of the bicyclic ring. The NMR data and assignment of compound **80** are summarized in Table 4.13. The spectral data of compound **80** were in

agreement with the literature data reported by Nigam et al. (1998). Hence, compound **80** was assigned as soulattrone A which was previously reported for its isolation from *Calophyllum soulattri*.
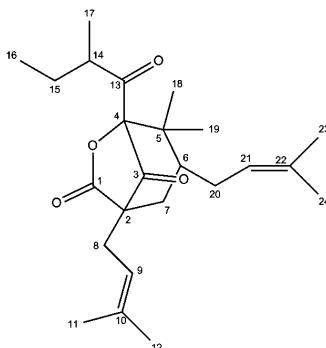
Table 4.13 Summary of NMR data and assignment of soulattrone A (80)

Position	δ_H (ppm)	δ_C (ppm)	HMBC
1	-	172.1	-
2	-	57.0	-
3	-	201.6	-
4	-	96.9	-
5	-	49.6	-
6	1.67 (1H, m)	41.9	
7	1.54 (H_a, m)	41.1	C-1, 3, 5 & 6
	2.13 (H_b, dd, J = 13.1, 4.0 Hz)		
8	2.38 (2H, m)	26.3	C-1, 2, 3, 9 & 10
9	5.03 (1H, t, J = 7.3 Hz)	117.0	C-8, 11 & 12
10	-	136.7	-
11	1.62 (3H, s)	25.8	C-9, 10 & 12
12	1.66 (3H, s)	18.1	C-9, 10 & 11
13	-	205.0	-
14	2.83 (1H, m)	44.8	C-13, 15 & 17
15	1.28 (H_a, m)	24.6	C-13, 14, 16 & 17
	1.71 (H_b, m)		
16	0.86 (3H, t, J = 7.3 Hz)	11.9	C-14 & 15
17	0.84 (3H, d, J = 6.7 Hz)	16.0	C-13, 14 & 15
18	1.14 (3H,s)	16.2	C-4, 5 & 6
19	1.08 (3H, s)	22.4	C-4, 5 & 6
20	1.67 (H_a, m)	27.4	C-7
	2.00 (H_b, m)		
21	4.97 (1H, brs)	121.6	C-23 & 24
22	-	134.2	-
23	1.67 (3H, s)	25.9	C-21, 22 & 24
24	1.54 (3H, s)	18.0	C-21, 22 & 23
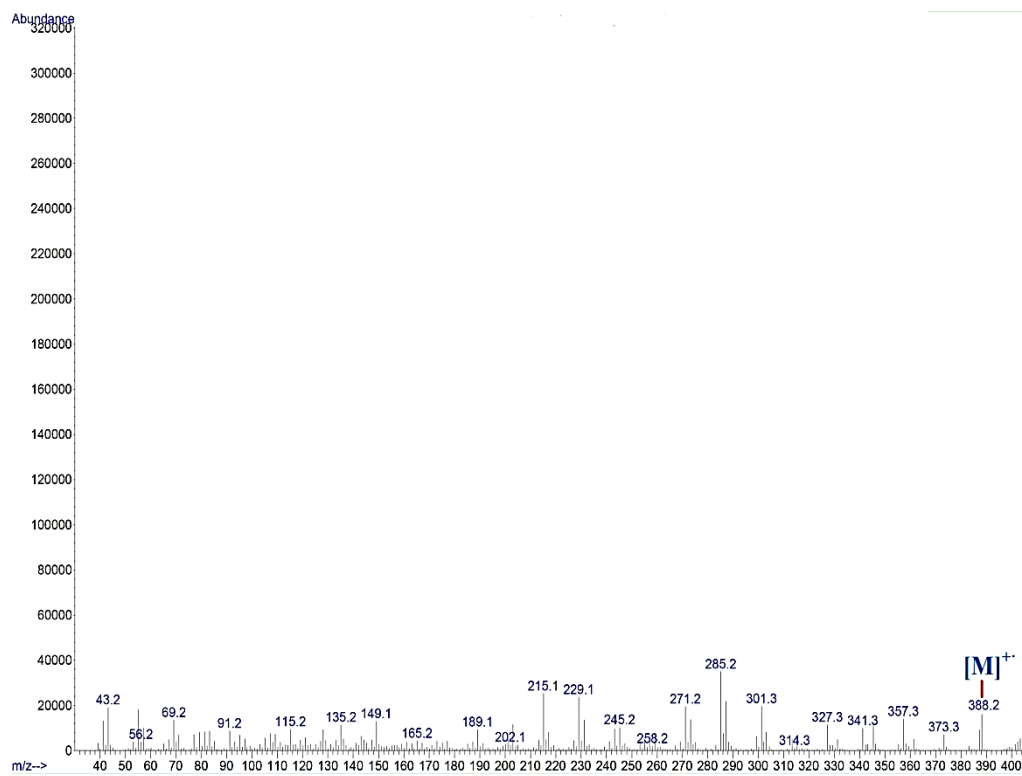
Figure 4.70: EIMS spectrum of soulattrone A (80)
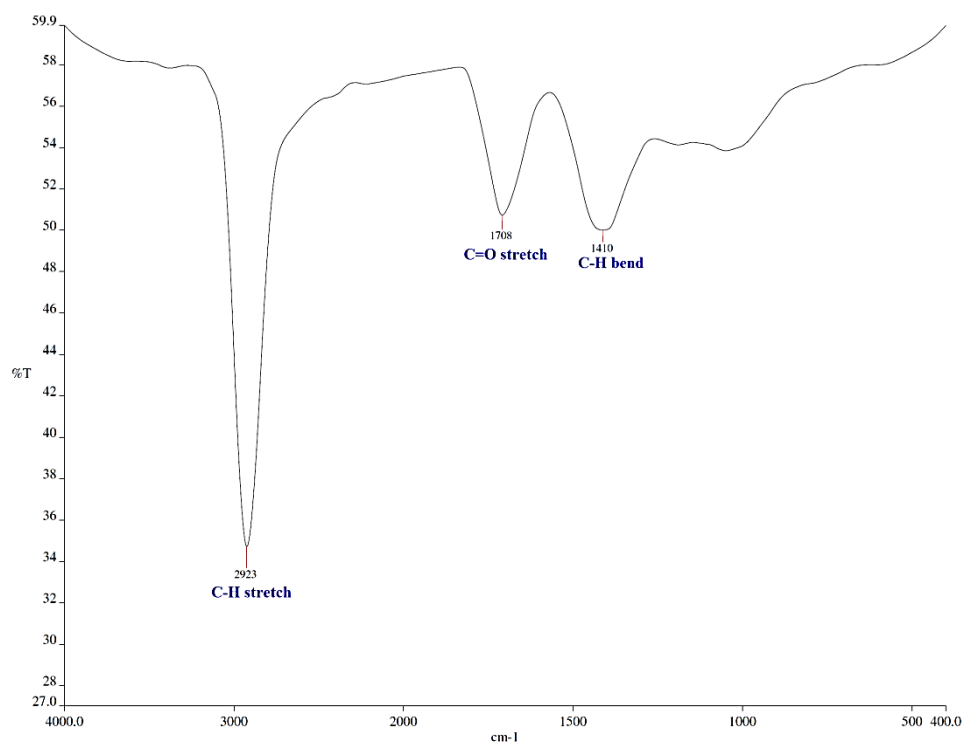
Figure 4.71: IR spectrum of soulattrone A (80)

145
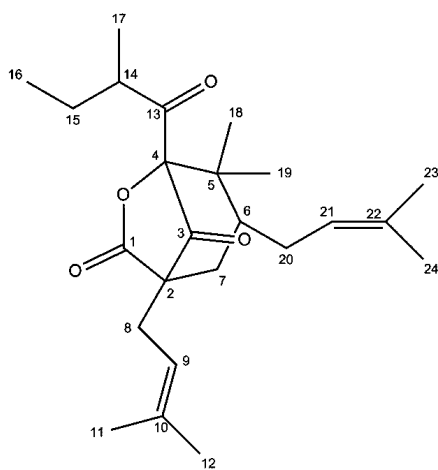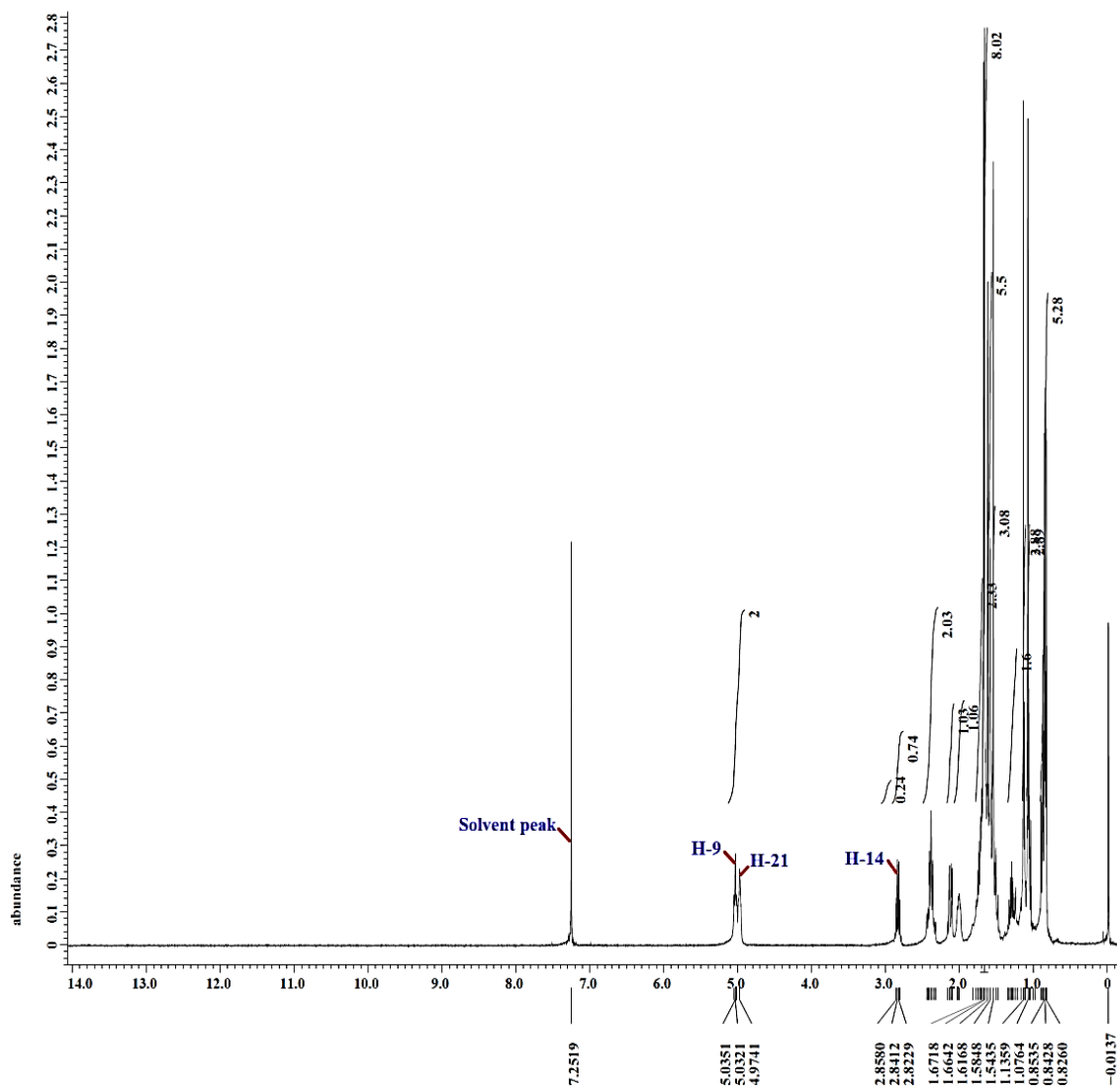
Figure 4.72: ^{1}H NMR spectrum of soulattrone A (**80**) (400 MHz, CDCl$_3$)

146
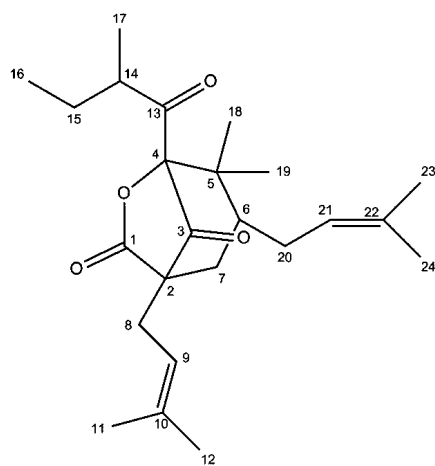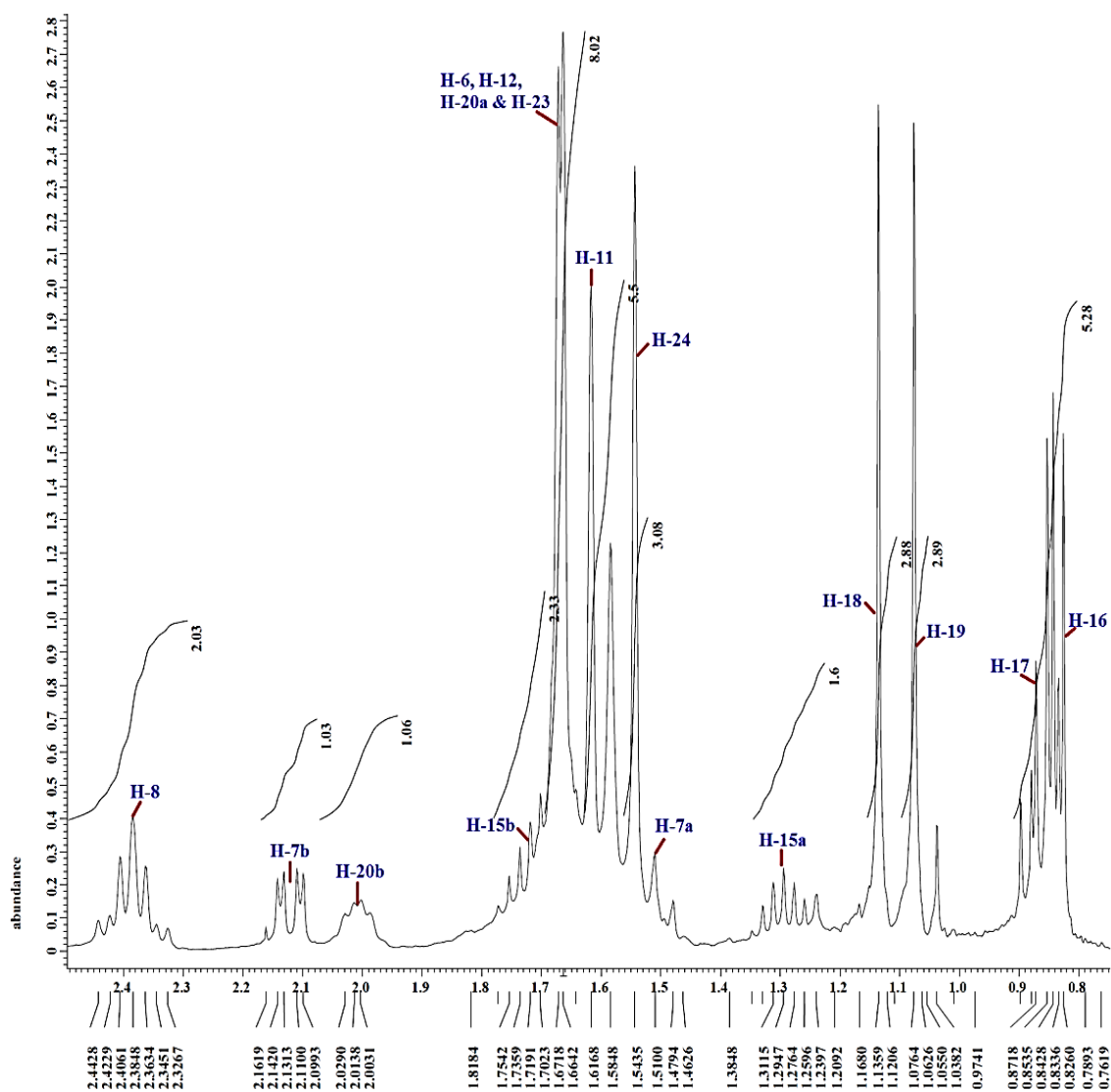
Figure 4.73: Expanded ^{1}H NMR spectrum of soulattrone A (80) (400 MHz, CDCl$_3$)
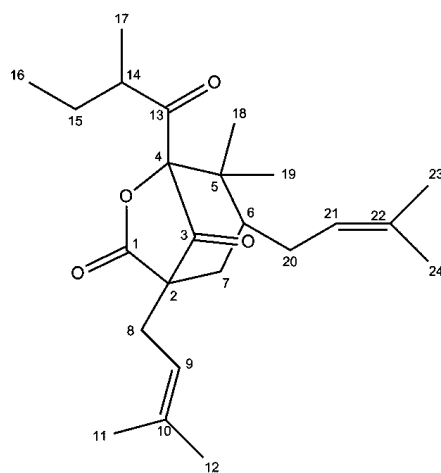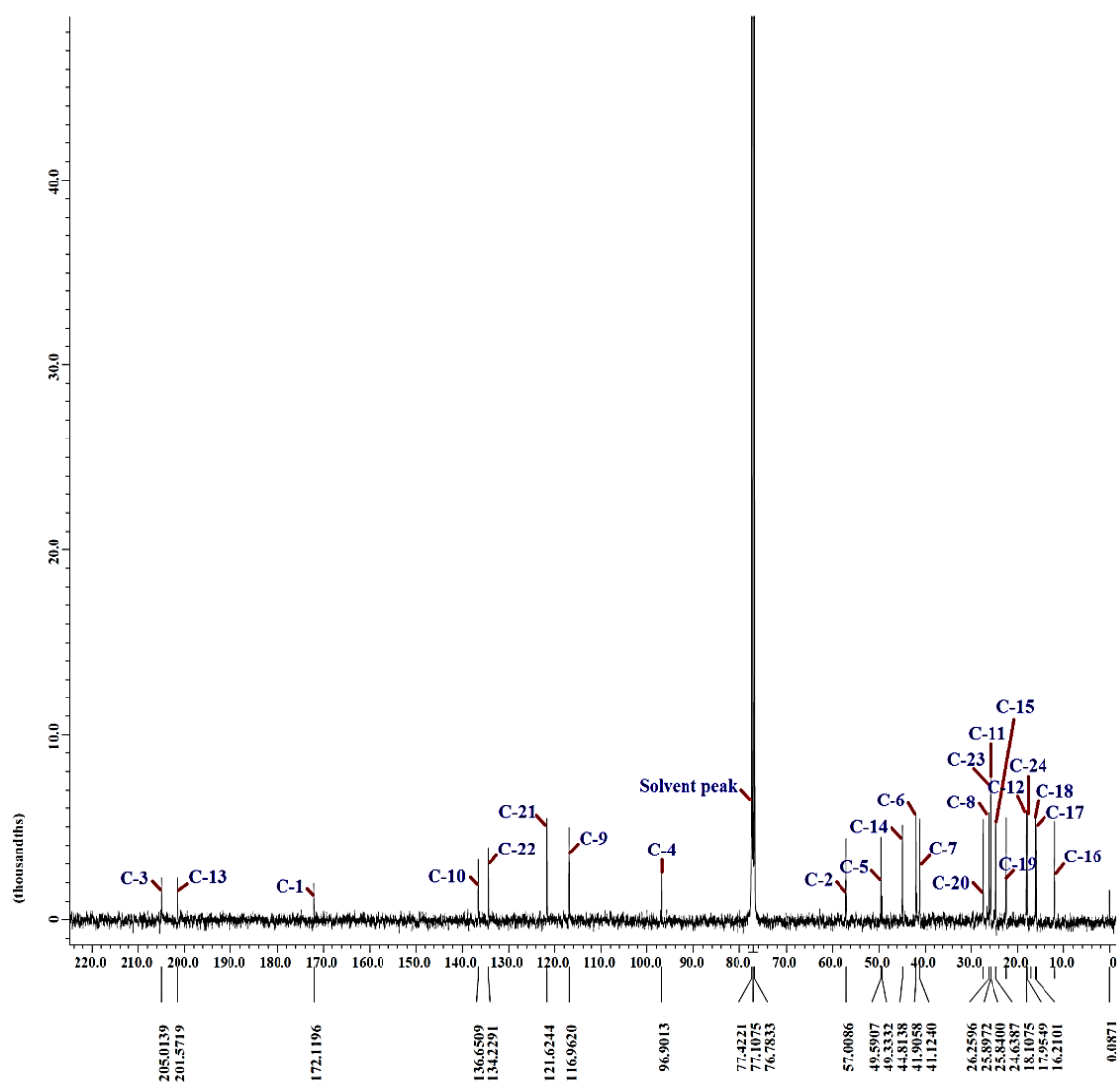
Figure 4.74: ^{13}C NMR spectrum of soulattrone A (80) (100 MHz, CDCl$_3$)
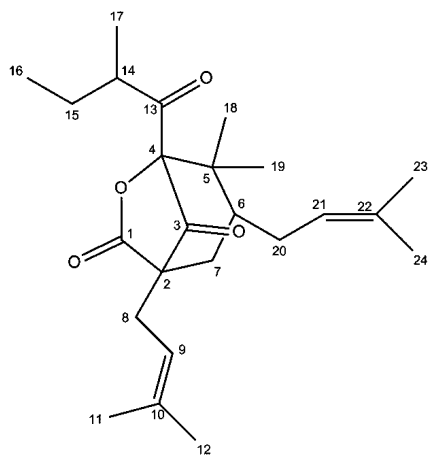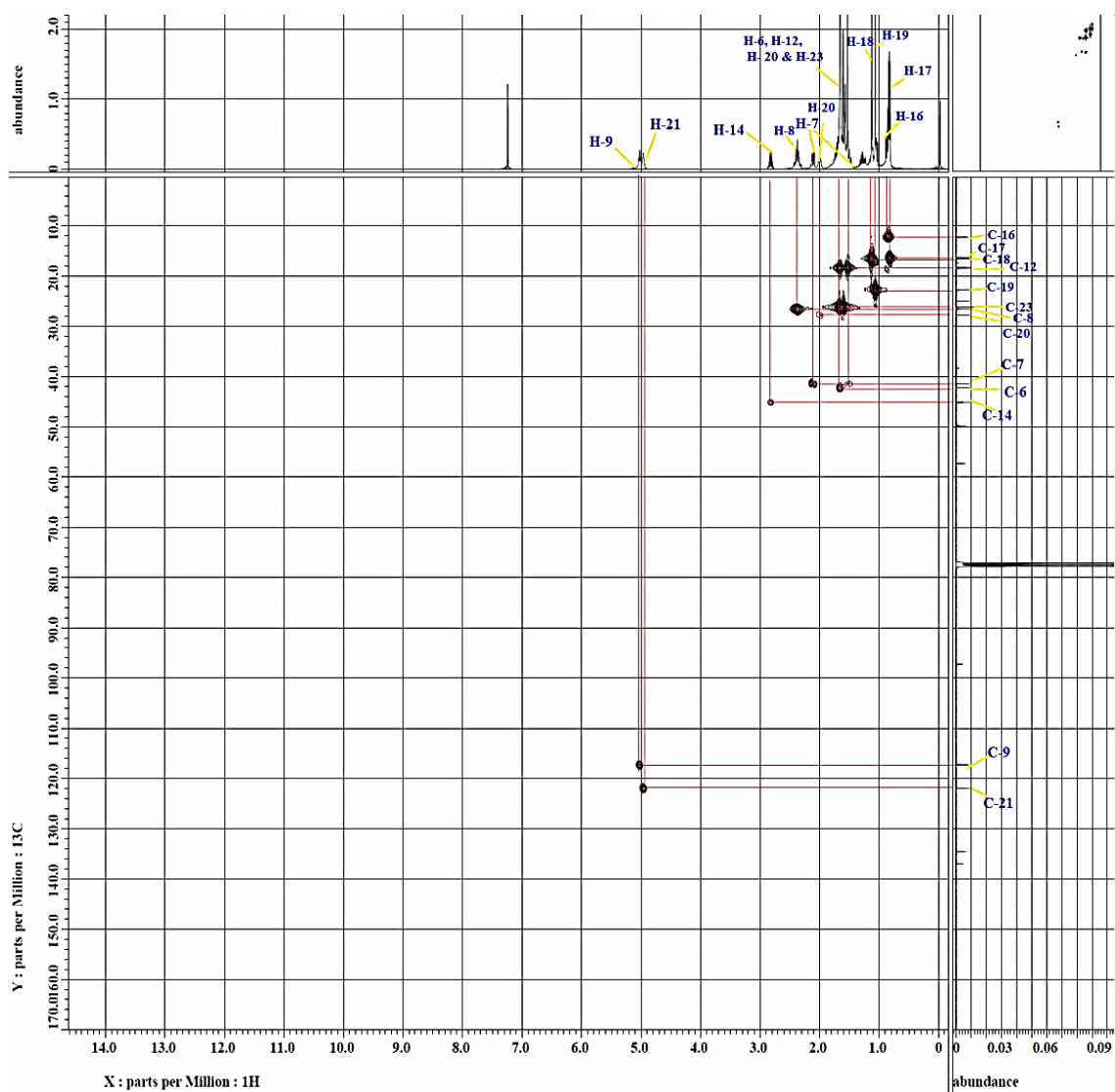
Figure 4.75: HMQC spectrum of soulattrone A (80)
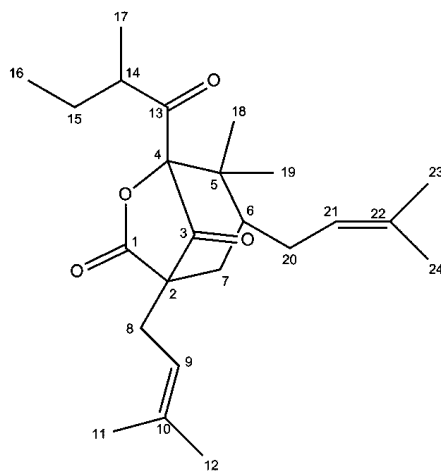
(**80**)
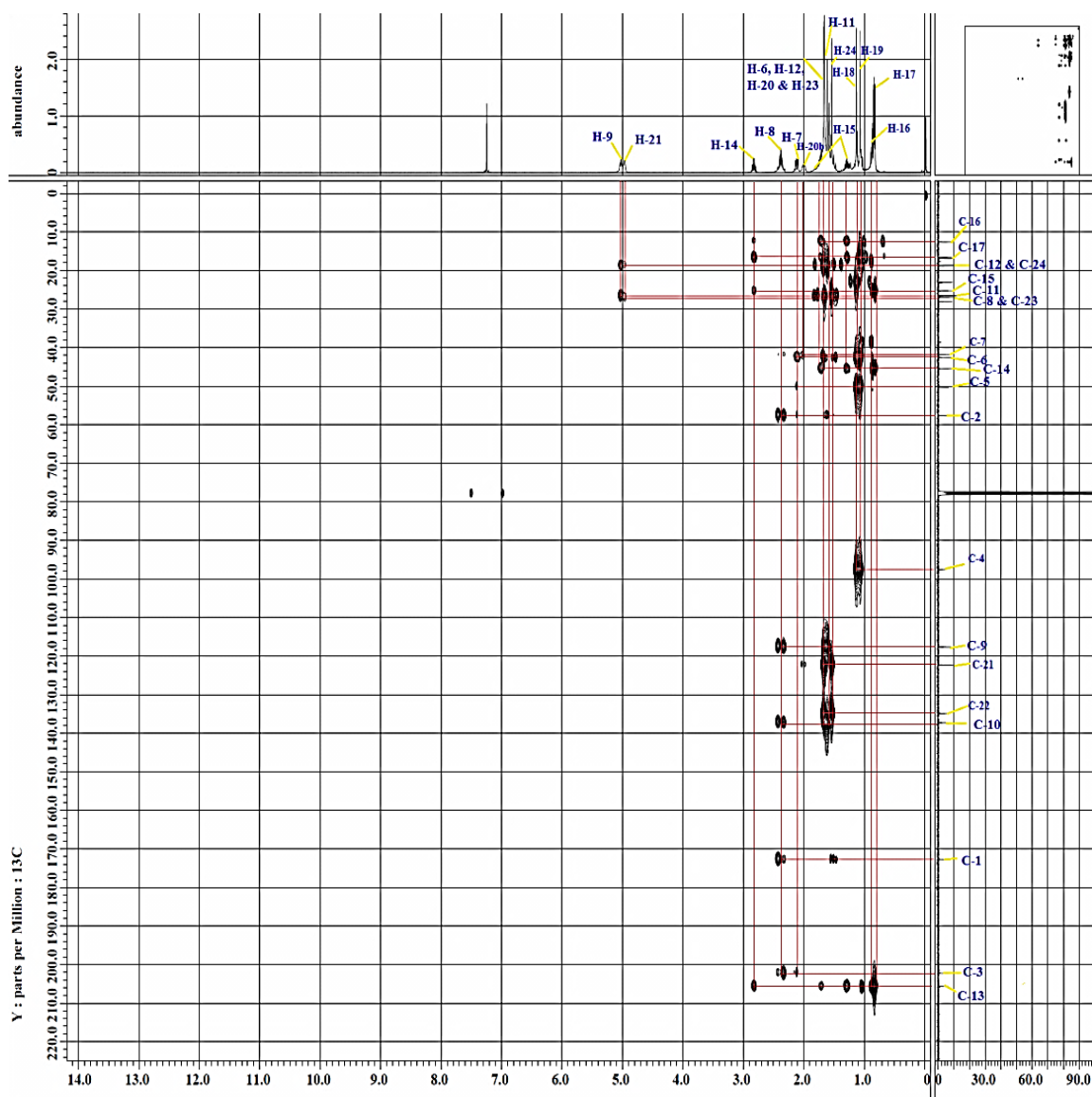
Figure 4.76: HMBC spectrum of soulattrone A (80)

4.4 Bioassay Result

4.4.1 Cytotoxic Activity

All the crude extracts and pure compounds obtained from *C. teysmannii*, *C. andersonii* and *C. soulattri* were screened for their cytotoxic activities against the four cancer cell lines, HeLa (cervical carcinoma), MDA-MB-231 (breast adenocarcinoma), LS174T (colorectal carcinoma), T98G (ganglioblastoma) and a normal human cell line, HEK293 (human embryonic kidney cells). The results of assay for crude extracts and pure compounds are displayed in Tables 4.14 and 4.15, respectively.

According to National Cancer Institute (NCI), crude extracts are considered to be cytotoxic if the IC_{50} value obtained is below 30 μg/mL (Suffness and Pezzuto, 1990). In this assay, only the dichloromethane and ethyl acetate crude extracts of *C. teysmannii* showed significant cytotoxicity against HeLa cancer cell line, with IC_{50} values of less than 30 μg/mL. Although the dichloromethane crude extract of *C. teysmannii* was found to be cytotoxic towards HeLa cancer cells, it exhibited poor cancer-specific cytotoxicity when tested with normal human HEK293 cells. On the other hand, the ethyl acetate crude extract of *C. teysmannii* showed a relatively better cancer-specific cytotoxicity with IC_{50} value against normal human HEK293 cells which was about 2-fold higher than that of HeLa cancer cells.

Table 4.14: Cytotoxic results of crude extracts against cancer and normal cell lines

Plant and Crude Extracts	IC$_{50}$ (µg/mL)[a]				
	HeLa	MDA-MB-231	LS174T	T98G	HEK293
C. teysmannii					
DCM	24.4±0.4	38.1±0.2	>100	80.3±1.4	16.0±0.1
EA	25.3±0.3	32.4±0.5	>100	>100	64.0±0.4
MeOH	79.4±1.3	70.2±0.2	86.8±1.2	>100	>100
C. andersonii					
DCM	54.7±0.6	>100	90.8±1.2	>100	18.0±0.3
EA	>100	46.7±0.8	>100	>100	>100
MeOH	>100	63.8±1.2	82.7±1.9	60.9±1.4	17.0±0.2
C. soulattri					
DCM	54.7±0.6	43.7±0.7	77.9±0.8	39.6±1.3	41.0±0.2
EA	>100	32.1±0.3	>100	>100	>100
MeOH	>100	34.6±1.0	74.0±0.7	30.4±0.3	>100
Positive Controls					
Cisplatin	4.9±0.4	-	9.3±1.5	11.8±0.6	-
Doxorubicin	-	2.3±0.2	-	-	-

[a]Data are reported as mean ± SD for minimum three independent experiments

Table 4.15: Cytotoxic results of pure compounds against cancer and normal cell lines

Compounds	IC$_{50}$ (µg/mL)[a]				
	HeLa	**MDA-MB-231**	**LS174T**	**T98G**	**HEK293**
Caloteysmannic acid (**71**)	7.1±1.1	4.2±0.7	9.9±1.1	11.3±0.6	>100
Isocalolongic acid (**72**)	10.5±0.5	6.3±0.5	11.8±1.3	8.1±0.2	68.0±0.4
Calolongic acid (**73**)	11.3±0.9	7.8±0.3	11.5±0.9	12.7±0.3	80.0±0.1
Stigmasterol (**74**)	11.8±0.7	28.4±0.4	25.0±1.1	8.6±0.6	>100
Friedelin (**75**)	27.2±0.5	47.3±0.5	49.9±1.8	25.7±0.9	>100
Friedelinol (**76**)	53.8±0.7	36.0±0.6	67.3±0.5	15.6±0.3	>100
Protocatechuic acid (**77**)	6.2±0.5	8.4±0.3	13.4±0.4	8.2±0.2	>100
Calosubellinone (**78**)	9.6±0.8	21.8±0.2	31.2±0.2	14.7±0.7	87.0±0.2
Garsubellin B (**79**)	8.2±0.5	8.8±1.2	26.6±0.9	30.0±0.2	>100
Soulattrone A (**80**)	28.3±0.2	28.0±0.9	27.5±1.3	55.3±0.7	>100
Positive Controls					
Cisplatin	4.9±0.4	-	9.3±1.5	11.8±0.6	-
Doxorubicin	-	2.3±0.2	-	-	-

[a]Data are reported as means ± SD for minimum three independent experiments

The cytotoxic results of pure compounds revealed that the growth inhibitory activity against the four cancer cell lines was significantly associated with the chemical classes of test compounds. Basically, the test compounds in this assay can be divided into four major classes which are chromanone acids (compounds **71**, **72** and **73**), simple phenolic compound (compound **77**), phloroglucinol derivatives (compounds **78** and **79**), and terpenoids (**74**, **75**, **76** and **80**). On the basis of assay results, the test compounds can be classified in the following order of decreasing cytotoxicity: chromanone acids > simple phenolic compound > phloroglucinol derivatives > terpenoids, against all the cancer cell lines except for HeLa cell line in which the chromanone acids, simple phenolic compound and phloroglucinol derivatives showed a comparable cytotoxicity which was found to be stronger than terpenoids. These findings indicated that phenolic compounds exhibited a much potent antiproliferative activity towards the four cancer cell lines as compared to non-phenolic compounds in this assay.

The development of cancer is likely to be linked to oxidative stress. The production of reactive oxygen species (ROS) during aerobic metabolism is inevitable. The accumulation of ROS at cellular levels is highly toxic to the body, leading to a condition called oxidative stress (Sies, 1997). This can impose serious injuries to various cellular biomolecules causing damage to tissues and organs, resulting in chronic disease (Bennett et al., 2012) such as cancer. Extensive study in human cell cultures revealed resveratrol, a phenolic compound to suppress angiogenesis and metastasis of cancer cells. The anticarcinogenic effect of resveratrol appears to be closely associated with its

antioxidant activity (Pandey and Rizvi, 2009). It was also reported that the cytotoxic effects of phenolic compounds on cancer inhibition were resemblance to those specific fatty acids such as conjugated linoleic acids and omega fatty acids which are known for their antioxidant activity (Wahle et al., 2010). Hence, this suggested the role of antioxidants in cancer inhibitory activity which was in consistent with the assay findings showing that phenolic compounds which are comparatively a stronger antioxidant than terpenoid compounds, were found to exhibit a greater cytotoxic effect on the cancer cell line tested.

Chromanone acids **71**, **72** and **73** showed comparable and promising cytotoxic effects on HeLa, MDA-MB-231, LS174T and T98G cancer cell lines with IC_{50} values in the range of 4.2 to 11.8 μg/mL. This could be accounted to the presence of 2,3-dimethylchromanone nucleus and side chain moieties such as hydroxyl and carboxyl groups in the structures. According to Anantharaju et al. (2016), the key functional groups required for eliciting potent anticancer activities are the involvement of aromatic ring, number and position of hydroxyl groups, and the presence of an unsaturated short fatty acid side chain which were found to be in agreement with the structural requirement for compounds **71**, **72** and **73**. Apart from that, both diastereomers **72** and **73** were reported to show comparable inhibitory activities in the assay suggesting that a variation in the stereochemical structure of chromanone nucleus does not affect much of the cytotoxic effect on the cancer cell lines tested. On top of that, all the chromanone acids **71**, **72** and **73** were found to exhibit good cancer-specific cytotoxicity with IC_{50} value against normal human HEK293

cells which was at least 5-fold higher than that of cancer cells. Compounds **71**, **72** and **73** also showed comparable growth inhibitory activities with the positive control, cisplatin towards LS174T and T98G cancer cells.

Protocatechuic acid (**77**) which is a simple phenolic compound, displayed good cytotoxic effects on all the four cancer cell lines tested with IC_{50} values ranging from 6.2 to 13.4 μg/mL. Among these cancer cell lines, T98G cancer cells was found to be highly susceptible to compound **77** with IC_{50} value of 8.2 μg/mL showing a better growth inhibitory activity than the standard, cisplatin with IC_{50} value of 11.8 μg/mL. Interestingly, this finding was in agreement with literature, in which gallic acid, a simple phenolic compound, was reported to show strong inhibitory activity towards glioma cell lines in a dose dependent manner (Lu et al., 2010). Hence, these findings would draw interest on the role of protocatechuic acid (**77**) in the treatment of cancers associated with central nervous system. In another study conducted by Yin et al. (2009), it was reported that treatment with compound **77** caused prominent apoptotic effects in human lung, liver, cervix, prostate and breast cancer cells. It was also reported that compound **77** triggered inhibitory activity by increasing DNA fragmentation, decreasing mitochondrial membrane potential, lowering Na^+-K^+-ATPase activity, and elevating caspase-3 and caspase-8 activities in these cells. This compound also suppressed cell adhesion and the production of VEGF, IL-6, IL-8, and ICAM-1 in these five cancer cells.

Meanwhile, among the phloroglucinol derivatives, garsubellin B (**79**) showed greater cytotoxic activities than calosubellinone (**78**), against all the cancer

cell lines tested except for T98G cell line. Compound **79** displayed promising antiproliferative activities towards HeLa and MDA-MB-231 cancer cell lines with IC_{50} values of 8.2 and 8.8 µg/mL, respectively. On the other hand, compound **78** showed significant activities against HeLa and T98G cancer cell lines with IC_{50} values of 9.6 and 14.7 µg/mL, respectively. In a previous study by Lu et al. (2012), a phloroglucinol derivative, namely (2,4-bis(4-fluorophenylacetyl) phloroglucinol (BFP) was reported to induce cell death of human glioma cells through apoptotic mechanism. Furthermore, analysis of literature data has highlighted the significant role played by phloroglucinol core on inducing cell killing effect on cancer cells. For instance, a study conducted on the anticancer properties of different myrtucommulones isolated from *Myrtus communis* reported that myrtucommulones with phloroglucinol core showed selective cytotoxic effects against prostate and breast cancer cell lines, whereas those myrtucommulones without phloroglucinol core did not exert any cytotoxic effects (Ogur, 2014).

As for the terpenoids, stigmasterol (**74**) with a steroidal skeleton was found to exhibit a more potent inhibitory activity towards T98G cancer cell line with IC_{50} value of 8.6 µg/mL in comparison with the positive control, cisplatin with IC_{50} value of 11.8 µg/mL. In general, compound **74** displayed relatively higher cytotoxic activities than the friedelane triterpenoids **75** and **76** against all the cancer cell lines tested. According to Ibrahim et al. (2012), the presence of free OH group at C-3 in the sterol skeleton of compound **74** may be crucial for the *in vitro* growth inhibitory activity of this compound towards cancer cells.

4.4.2 Antioxidant Activity

All the crude extracts and pure compounds obtained from the plants studied were screened for their antioxidant activity via DPPH assay. Tables 4.16 and 4.17 summarize the assay results of the crude extracts and pure compounds, respectively.

Based on the assay results, in general, it was observed that the methanol crude extracts of plants studied showed a greater antioxidant potential than the ethyl acetate crude extracts, and the latter in turn showed a higher antioxidant activity than the dichloromethane crude extracts except for methanol and ethyl acetate crude extracts of *C. andersonii* which showed an equal antioxidant potential. According to Do et al. (2013), methanol extracts have been commonly found to contain a high amount of polyphenols such as gallic acid, caffeic acid, catechin and procyanidins B1 and B2, which are strong antioxidants. On the contrary, dichloromethane extracts were mostly comprised of compounds of lower polarity such as terpenoids and fatty acids that possess weak antioxidant activity. Apart from that, it was found that the methanol crude extract of *C. teysmannii*, and methanol and ethyl acetate crude extracts of *C. andersonii* were reported to show comparable activities with the positive control, vitamin C (IC_{50}=4.0 μg/mL) with their IC_{50} values of 4.5 μg/mL.

Table 4.16: Antioxidant results of crude extracts

Plant Species	Extracts	IC$_{50}$ (µg/mL)[a]
C. teysmannii	DCM	>240
	EA	40.0±0.1
	MeOH	4.5±0.1
C. andersonii	DCM	185.0±0.2
	EA	4.5±0.3
	MeOH	4.5±0.2
C. soulattri	DCM	12.5±0.1
	EA	10.0±0.1
	MeOH	9.5±0.1
Positive Controls		
Vitamin C		4.0±0.1
Kaempferol		8.0±1.0

[a]Data are reported as means ± standard deviation for minimum three independent experiments

Table 4.17: Antioxidant results of pure compounds

Compounds	IC$_{50}$ (µg/mL)[a]
Caloteysmannic acid (**71**)	>240
Isocalolongic acid (**72**)	>240
Calolongic acid (**73**)	>240
Stigmasterol (**74**)	>240
Friedelin (**75**)	>240
Friedelinol (**76**)	>240
Protocatechuic acid (**77**)	4.0±0.1
Calosubellinone (**78**)	8.5±1.0
Garsubellin B (**79**)	24.0±0.2
Soulattrone A (**80**)	20.0±0.1
Positive Controls	
Vitamin C	4.0±0.1
Kaempferol	8.0±1.0

[a]Data are reported as means ± standard deviation for minimum three independent experiments

The antioxidant results revealed that the pure compounds exerted antioxidant activity according to their chemical classes in the following decreasing order of radical scavenging activity: simple phenolic compound > phloroglucinol derivatives > terpenoids > chromanone acids. Protocatechuic acid (**77**) showed the highest antioxidant activity which was comparable with the standard, vitamin C, as both exhibited the same IC_{50} value of 4.0 μg/mL. This promising result was supported by literature reported by Li et al. (2011) which highlighted that compound **77** displayed a much more effective *in vitro* antioxidant activity in both lipid and aqueous media as compared to Trolox. This is due to the fact that phenolic compounds generally showed good antioxidant activity, attributed to the presence of hydroxyl groups that are prone to donate a hydrogen atom or an electron to the free radicals (Dai and Mumper, 2010).

Meanwhile, phloroglucinol derivatives **78** and **79** showed significant antioxidant activity with IC_{50} values of below 25 μg/mL. Calosubellinone (**78**) was found to exhibit almost three-fold much higher antioxidant activity than garsubellin B (**79**), and a comparable activity with the positive control, kaempferol (IC_{50} = 8.0 μg/mL). On the contrary, poor antioxidant activity was observed for chromanone acids **71**, **72** and **73**, and terpenoids **74**, **75** and **76**. According to Balasundram et al. (2006), the number and positions of hydroxyl groups along with the nature of substitutions on aromatic rings are the key determinants for radical scavenging activity. In this assay, albeit the presence of phenolic moiety in compounds **71**, **72** and **73**, they failed to exhibit

significant antioxidant activity. This was mainly attributed to the chelation between the phenolic hydroxyl group, 5-OH and the carbonyl group at *peri*-position in compounds **71**, **72** and **73** which was found to markedly reduce the antioxidant potency of these compounds. Meanwhile, the lack of phenolic nature in terpenoids **74**, **75** and **76** explains their poor antioxidant activity.

CHAPTER 5

CONCLUSION

5.1 Conclusion

Phytochemical study on the stem bark extracts of *Calophyllum teysmannii* afforded a new and two known chromanone acids, namely caloteysmannic acid (**71**), isocalolongic acid (**72**), calolongic acid (**73**) and a sterol, stigmasterol (**74**), whereas the stem bark extracts of *Calophyllum andersonii* gave two triterpenoids, friedelin (**75**) and friedelinol (**76**), and a simple phenolic compound, protocatechuic acid (**77**). Meanwhile, study on *Calophyllum soulattri* yielded a new and a known phloroglucinol derivatives, namely calosubellinone (**78**) and garsubellin B (**79**), and a terpenoid, soulattrone A (**80**).

All the crude extracts and isolated compounds were screened for their cytotoxic activities against a panel of cancer cell lines including HeLa, MDA-MB-231, LS174T and T98G, and a normal human cell line, HEK293. Under our assay conditions, only the dichloromethane and ethyl acetate crude extracts of *C. teysmannii* showed significant cytotoxicity against HeLa cancer cell line, with IC_{50} values of less than 30 μg/mL. Meanwhile, the growth inhibitory activity of test compounds was found to show close relationship to their chemical classes whereby test compounds were reported to show

decreasing cytotoxic effect according to their chemical classes in the following order: chromanone acids **71**, **72** & **73** > simple phenolic compound **77** > phloroglucinol derivatives **77** & **78** > terpenoids **74**, **75**, **76** & **80**.

Chromanone acids **71**, **72** and **73** showed promising cytotoxic activities towards HeLa, MDA-MB-231, LS174T and T98G cancer cell lines with IC_{50} values in the range of 4.2 to 11.8 μg/mL. Moreover, these compounds were found to exhibit good cancer-specific cytotoxicity with IC_{50} value against normal human HEK293 cells which was at least 5-fold higher than that of cancer cells. On top of that, compounds **71**, **72** and **73** also showed comparable growth inhibitory activities with the positive control, cisplatin towards LS174T and T98G cancer cells. The findings have highlighted the therapeutic potential of chromanone acid derivatives in the treatments of cancers.

Besides, protocatechuic acid (**77**) which is a simple phenolic compound, exhibited good cytotoxic effects on all the four cancer cell lines tested with IC_{50} values ranging from 6.2 to 13.4 μg/mL. Among these cancer cell lines, T98G cancer cells was found to be highly susceptible to compound **77** with IC_{50} value of 8.2 μg/mL showing a better growth inhibitory activity than the standard, cisplatin with IC_{50} value of 11.8 μg/mL. Meanwhile, other compounds **74**, **75**, **76**, **78**, **79** and **80** displayed moderate to weak activities against the tested cancer cell lines.

In the DPPH assay, the crude extracts of plants studied showed decreasing antioxidant potential in the following order: methanol crude extracts > ethyl acetate crude extracts > dichloromethane crude extracts. Protocatechuic acid (**77**) showed the highest antioxidant activity with IC_{50} value of 4.0 µg/mL which was identical to that of positive control, vitamin C. Besides, calosubellinone (**78**) also showed strong radical scavenging activity (IC_{50} = 8.5 µg/mL) comparable to the positive control, kaempferol (IC_{50} = 8.0 µg/mL). On the contrary, poor antioxidant activity was observed for chromanone acids **71**, **72** and **73**, and terpenoids **74**, **75** and **76** with IC_{50} values above 240.0 µg/mL.

5.2 Future Study

This research has successfully yielded two new compounds with some promising biological findings which may serve as valuable information for further investigation into the chemical analogues of active compounds via synthetic approach to study the structural requirements for optimal growth inhibitory activities towards HeLa, MDA-MB-231, LS174T and T98G cancer cell lines. Besides, potential compounds discovered from this study should be further studied for their mechanism of action in future.

REFERENCES

Abbas, J., Kardono, L., Hanafi, M., Kosela, S. and Qin, G. W., 2007. Canophyllol and calaustralin from two Indonesian species of *Calophyllum. Research Center for Chemistry LIPI*, pp. 28-39.

Ahmed, J. et al., 2013. Isolation of steroids from *n*-hexane extract of the leaves of *Saurauia roxburghii. International Food Research Journal,* 20 (5), pp. 2939-2943.

American Cancer Society. 2016. Cancer facts and figures.Atlanta: American Cancer Society; 2016 [Online]. Available at: https://www.cancer.org/research/cancer-facts-statistics/all-cancerfacts-figures/cancer-facts-figures-2016.html [Accessed 3 January 2017].

Ampofo, S.A. and Waterman, P.G., 1986. Xanthones and neoflavonoids from two Asian species of *Calophyllum. Phytochemistry*, 25 (11), pp. 2617-2620.

Anantharaju, P.G., Gowda, P.C., Vimalambike, M.G. and Madhunapantula, S.V., 2016. An overview on the role of dietary phenolics for the treatment of cancers. *Nutrition Journal*, 15 (1), pp. 99.

Annan, F., Adu, F. and Gbedema, S.Y., 2009. Friedelin: A bacterial resistance modulator from *Paullinia Pinnata* L, *Journal of Science and Technology*, 29 (1), pp. 152-159.

Antonio, A.B., Berber, L.P.A. and Sosa, F.C., 2014. Biological importance of phytochemicals from *Calophyllum brasiliense* Cambess. *Annual Research and Review in Biology*, 4 (10), pp. 1502-1517.

Balasundram, N., Sundram, K. and Samman, S., 2006. Phenolic compounds in plants and agri-industrial by-products: Antioxidant activity occurrence, and potential uses. *Food chemistry*, 99, pp. 191-203.

Banerji, A., Deshpande, A. D., Prabhu, B. R. and Pradhan, P., 1994. Tomentotone, a new xanthonoid from the stem bark of *Calophyllum tomentosum. Journal of Natural Products*, 57 (3), pp. 396-399.

Bennett, L.L., Rojas, S. and Seefeldt, T., 2012. Role of antioxidants in the prevention of cancer. *Journal of Experimental and Clinical Medicine*, 4 (4), pp. 215-222.

Breck, G.D. and Stout, G.H., 1969. *Calophyllum* products: A new 4-phenylcoumarin from *C. australianum. Journal of Organic Chemistry*, 34, pp. 4203–4204.

Bruneton, J., 1993. *Pharmacognosie-Phytochimie: Plantes Medicinales*. Paris: Technique & Documents Lavoisier.

Calixto J.B., 2000. Efficacy, safety, quality control, marketing and regulatory guidelines for herbal medicines (phytotherapeutic agents). *Brazilian Journal of Medicine and Biological Research*, 33 (2) pp. 179–189.

Cao, S.G., Sim, K.Y. and Goh, S.H., 1997. Biflavonoids of *Calophyllum venulosum. Journal of Natural Products,* 60 (12), pp. 1245-1250.

Carpenter, I., Locksley, H.D. and Scheinmann, F., 1969. Extractives from Guttiferae. Part X. The isolation and structure of four xanthones from *Calophyllum canum. Journal of Chemical Society (C),* pp. 486-488.

Chao, S.G., Sim, K.Y. and Goh, S.H., 1997. Biflavonoids of *Calophyllum venulosum. Journal of Natural Products*, 60, pp. 1245-1250.

Chintalapally, S. and Rao, M., 2016. Origin, evolution and milestones in the field of natural product research. *International Journal of Current Microbiology and Applied Sciences,* 5 (8), pp. 89-92.

Dahanayake, M., Kitagawa, I., Somanathan, R. and Sultanbawa, M.V.S., 1974. Chemical investigation of ceylonese plants.Part VII. Extractives *of Calophyllum thwaitesii* Planch and Triana and *Calophyllum walker* Wight (Guttiferae). *Journal of Chemical Society, Perkin Trans. 1*, pp. 2510-2514.

Dai, H.F. et al., 2010. Caloxanthones O and P: Two new prenylated xanthones from *Calophyllum inophyllum. Molecules,* 15, pp. 606-612.

Dai, J. and Mumper, R.J., 2010. Plant phenolics: extraction, analysis and their antioxidant and anticancer properties. *Molecules*, 15, pp. 7313-7352.

Dharmaratne, H.R.W., Sotheeswaran, S. and Balasubramaniam, S, 1984. Triterpenes and neoflavonoids of *Calophyllum lankaensis* and *Calophyllum thwaitesii*. *Phytochemistry*, 23 (11), pp. 2601-2603.

Dharmaratne, H.R.W., Perera, D.S.C., Marasinghe, G.P.K. and Jamie, J., 1999. A chromene acid from *Calophyllum cordato-oblongum. Phytochemistry*, 51 (1), pp. 111-113.

Do, Q.D. et al., 2013. Effect of extraction solvent on total phenol content, total flavonoids content, and antioxidant activity of *Limnophila aromatic*. *Journal of Food and Drug Analysis,* 22 (3), pp. 296-302.

Dweck, A.C. and Meadows, T., 2002. Tamanu (*Calophyllum inophyllum*) - the African, Asian, Polynesian and Pacific Panacea. *International Journal of Cosmetic Science*, 24 (6), pp. 341-348.

Ee, G.C.L. et al., 2011. Soulamarin, a new coumarin from stem bark of *Calophyllum soulattri*. *Molecules*, 16, pp. 9721-9727.

Ferchichi, L. et al., 2012. Bioguided fractionation and isolation of natural inhibitors of advanced glycation end-products (AGEs) from *Calophyllum flavoramulum. Phytochemistry,* 78, pp. 98-106.

Filho, V.C., Silva, C.M. and Niero, R., 2009. Chemical and pharmacological aspects of the genus *Calophyllum. Chemistry and Biodiversity*, 6 (3) pp. 313-327.

Fukuyama, Y., Kanashi, A., Tana, N. and Kuwagama, A., 1993. Subellinone, a polyisoprenylated phloroglucinol derivatives from *Garcinia subelliptica. Phytochemistry*, 33 (2), pp. 483-485.

Fukuyama, Y., Minami, H. and Kuwagama, A., 1998. Garsubellins, polyisoprenylated phloroglucinol derivatives from *Garcinia subelliptica. Phytochemistry*, 49 (3), pp. 853-857.

Govindachari, T., Prakash, D. and Viswanathan, N., 1967. Chemical constituents of *Calophyllum apetalum* Willd. *Tetrahedron Letters*, 42, pp. 4177-4181.

Guerreiro, E., Kunesch, G. and Polonsky, J., 1971. Les constituants des graines de *Calophyllum chapelieri* (Guttiferae). *Phytochemistry,* 10 (9), pp. 2139-2145.

Guerreiro, E., Kunesch, G. and Polonsky., 1973. Chromanones de l'e´corce de *Calophyllum recedens*. *Phytochemistry*, 12 (1), pp. 185–189.

Guilet, D. et al., 2001. Novel cytotoxic 4-phenylfuranocoumarins from *Calophyllum dispar*. *Journal of Natural Products*, 64 (5), pp. 563-568.

Gunalatika, A.A.L., Silva, A.M.Y.J.D., Sotheeswaran, S., Balasubramaniam, S. and Wazeer, M.I.M., 1984. Terpenoid and biflavonoid constituents of *Calophyllum alaba* and *Garcinia spicata* from Sri Lanka. *Phytochemistry*, 23 (2), pp. 323-328.

Ha, L.D., Hansen, P.E., Duus, F., Pham, H.D. and Nguyen, L.D., 2012. A new chromanone acid from the bark of *Calophyllum dryobalanoides. Phytochemistry Letters,* 5, pp. 287-291.

Hay, A.E. et al., 2003. Antifungal chromans inhibiting the mitochondrial respiratory chain of pea seeds and new xanthones from *Calophyllum caledonicum. Planta Medica*, 69, pp. 1130–1135.

Hay, A.E. et al., 2004. Antimalarial xanthones from *Calophyllum caledonicum* and *Garcinia vieillardii. Life Sciences*, 75 (25), pp. 3077-3085.

Huerta-Reyes, M. et al., 2004. HIV-1 inhibitory compounds from *Calophyllum brasiliense* leaves. *Biological and Pharmaceutical Bulletin*, 27 (9), pp. 1471-1475.

Ibrahim, et al., 2012. New ursane-type triterpenes from the root bark of *Calotropis procera. Phytochemistry Letters,* 5, pp. 490-495.

Inuma, M. et al., 1997. Prenylated xanthonoids from *Calophyllum apetalum. Phytochemistry*, 46 (8), pp. 1423-1429.

Ito, C. et al., 1999. A new biflavonoid from *Calophyllum panciflorum* with antitumor-promoting activity. *Journal of Natural Products*, 62 (12), pp. 1668-1671.

Ito, C. et al., 2002. Chemical constituents of *Calophyllum brasiliensis*: structure elucidation of seven new xanthones and their cancer chemopreventive activity. *Journal of Natural Products*, 65 (3), pp. 267-272.

Ito, C. et al., 2003. Chemical constituents of *Calophyllum brasiliense*. 2. Structure of three new coumarins and cancer chemopreventive activity of 4-substituted coumarins. *Journal of Natural Products,* 66 (3), pp. 368-371.

Joint United Nations Programme on HIV/AIDS (UNAIDS), 2003. *AIDS* epidemic update [Online]. Available at: http://data.unaids.org/pub/report/2003/2003_epiupdate_en.pdf [Accessed 19 June 2015].

Kang, W.Y., Li, G.H. and Hao, X.J., 2003. Two new triterpenes from *Neonauclea sessilifolia. Acta Botanica Sinica*, 45 (8), pp. 1003-1007.

Kashman, Y. et al., 1992. The calanolides, a novel HIV Inhibitory class of coumarin derivatives from the tropical rainforest tree, *Calophyllum lanigerum. Journal of Medical Chemistry,* 35, pp. 2735–2743.

Kawazu, K., Ohigashi, H. and Mitsui, T., 1968. The piscicidal constituents of *Calophyllum inophyllum. Tetrahedron Letters*, 19, pp. 2383–2385.

Laure, F. et al., 2005. Structures of new secofriedelane and friedelane acids from *Calophyllum inophyllum* of French Polynesia. *Magnetic Resonance in Chemistry*, 43, pp. 65-68.

Leonti, M., Vibrans, H., Sticher, O. and Heinrich, M., 2001. *Proceedings of the 42nd Annual Meeting of the American Society of Pharmacognosy.* Mexico: Oaxaca.

Li, Y. et al., 2010. Triterpenoids from *Calophyllum inophyllum* and their growth inhibitory effects on human leukemia HL-60 cells. *Fitoterapia*, 81, pp. 586-589.

Li, X., Wang, X., Chen, D. and Chen, S., 2011. Antioxidant activity and mechanism of protocatechuic acid *in vitro. Functional Foods in Health and Disease,* 7, pp. 232-244.

Lu, Y. et al., 2010. Gallic acid suppresses cell viability, proliferation, invasion and angiogenesis in human glioma cells. *European Journal of Pharmacology*, 641 (2-3), pp. 102-107.

Lu, D.Y. et al., 2012. The novel phloroglucinol derivative BFP induces apoptosis of glioma cancer through reactive oxygen species and endoplasmic reticulum stress pathways. Phytomedicine, 19, pp. 1093-1100.

Ma, C.H., Chen, B., Qi, H.Y., Li, B.G. and Zhang, G.L., 2004. Two pyranocoumarins from the seeds of *Calophyllum polyanthum. Journal of Natural Products,* 67 (9), pp. 1598-1600.

Mah, S.H., Ee, G.C.L., Teh, S.S. and Sukari, M.A., 2015. Antiproliferative xanthones derivatives from *Calophyllum inophyllum* and *Calophyllum soulattri. Pakistan Journal of Pharmaceutical Sciences*, 28 (2), pp. 425-429.

Maia, F., Almeida, M.R., Gales, L., Kijjoa, K., Pinto, M.M., Saraiva, M.J. and Damas, A.M., 2005. The binding of xanthone derivatives to transthyretin. *Biochemical Pharmacology,* 70, pp. 1861–1869.

Mawa, S. and Said, I. M., 2012. Chemical constituents of *Garcinia prainiana. Sains Malaysiana*, 41 (5), pp. 585-590.

McKee, T. C. et al., 1996. New pyranocoumarins isolated from *Calophyllum lanigerum* and *Calophyllum teysmannii. Journal of Natural Products*, 59 (1), pp. 754-758.

Melo, M. S. et al., 2014. A systematic review for anti-inflammatory property of Clusiaceae family: A preclinical approach. *Evidence-Based Complementary and Alternative Medicine,* 2014, ID: 960258.

Morel, C. et al., J., 2000. New xanthones from *Calophyllum caledonicum. Journal of Natural Products*, 63 (11), pp. 1471-1474.

Morel, C. et al., 2002. New and antifungal xanthones from *Calophyllum caledonicum. Planta Medica*, 68 (1), pp. 41-44.

Nasir, N. et al., 2013. Xanthones from *Calophyllum gracilipes* and their cytotoxic activity. *Sains Malaysiana*, 42 (9), pp. 1261-1266.

Nguyen, L.T.T. et al., 2012. Polyisoprenylated acylphloroglucinols and a polyisoprenylated tetracyclic xanthone from the bark of *Calophyllum thorelii. Tetrahedron Letters*, 53 (1), pp. 4487-4493.

Nigam, S.K. and Mitra, C.R., 1969. Constituents of *Calophyllum apetalum* and *C. tomentosum* trunk bark. *Phytochemistry*, 8 (1), pp. 323-324.

Nigam, S.K. et al., 1988. Soulattrone, a C24 terpenoid from *Calophyllum soulattri. Phytochemistry*, 27 (2), pp. 527-530.

Ogunnusi, T.A., Oso, B.A. and Dosumu, O.O., 2010. Isolation and antibacterial activity of triterpenes from *Euphorbia kamerunica* Pax. *International Journal of Biological and Chemical Sciences*, 4 (1), pp. 158-167.

Ogur, R., 2014. Studies with *Myrtuscommunis*L: Anticancer properties. Journal of Intercultural Ethnopharmacology, 3 (4), pp. 135-137.

Orwa, C., Mutua, A., Kindt, R., Jamnadass, R. and Simons, A., 2009. Agroforestree database: a tree species reference and selection guide version 4.0. *World Agroforestry Centre ICRAF, Nairobi, KE*.

Pandey, K.B. and Rizvi, S.I., 2009. Plant polyphenols as dietary antioxidants in human health and disease. *Oxidative Medicine and Cellular Longevity*, 2 (5), pp. 270-278.

Pengsuparp, T., Serit, M., Hughes, S.H., Soejarto, D.D. and Pezzuto, J.M., 1996. Specific inhibition of Human Immunodeficiency Virus type 1 reverse transcriptase mediated by soulattrolide, a coumarin isolated from the latex of *Calophyllum teysmannii*. *Journal of Natural Products*, 59 (9), pp. 839-842.

Piccinelli, A.L. et al., 2013. A fast and efficient HPLC-PDA–MS method for detection and identification of pyranochromanone acids in *Calophyllum* species. *Journal of Pharmaceutical and Biomedical Analysis*, 76, pp. 157– 163.

Pierre, L.L. and Moses, M.N., 2015. Isolation and characterization of stigmasterol and β-sitosterol from *Odontonema strictum* (Acanthaceae). *Journal of Innovations in Pharmaceuticals and Biological Sciences*, 2 (1), 88-95.

Plattner, R., Spencer, G., Weisleder, D. and Kleiman, R., 1974. Chromanone acids in *Calophyllum brasiliense* seed oil. *Phytochemistry*, 13 (11), pp. 2597-2602.

Roepke, J. et al., 2010. Vinca drug components accumulate exclusively in leaf exudates of Madagascar periwinkle. *Proceedings of the National Academy of Sciences*, 107 (34), pp. 15287-15292.

Roig, J. T., 1988. *Plantas Medicinales, Aromáticas o Venenosas de Cuba.* Havana: Editorial Cientı́fico-Técnica.

Salazar, G.C.M., Silva, G.D.F., Duarte, L.P., Filho, S.A.V. and Lula, I.S., 2000. Two epimeric friedelane triterpenes isolated from Maytenus truncata Reiss: 1H and 13C chemical shift assignments. *Magnetic Resonance in Chemistry*, 38, pp. 977-980.

Sarker, S.D. and Nahar, L., 2012. *Natural products isolation*, New York: Springer.

Sartori, N., Canepelle, D., de Sousa, P.J. and Martins, D., 1999. Gastroprotective effect from *Calophyllum brasiliense* Camb. bark on experimental gastric lesions in rats and mice. *Journal of Ethnopharmacology*, 67 (2), pp. 149-156.

Shen, Y.C., Wang, L.T., Khalil, A.T., Chiang, L.C. and Cheng, P.W., 2005. Bioactive pyranoxanthones from the roots of *Calophyllum blancoi*. *Chemical & Pharmaceutical Bulletin*, 53 (2), pp. 244-247.

Sies, H., 1997. Physiological society symposium: Impaired endothelial and smooth muscle cell function in oxidative stress. *Experimental Physiology*, 82, pp. 291-295.

Sousa, G.F. et al., 2012. New Triterpenes from *Maytenus robusta*: Structural elucidation based on NMR experimental data and theoretical calculations. Molecules, 17, pp. 13439-13456.

Souza, M.D.C. et al., 2009. *In vitro* and *in vivo* anti-*Helicobacter pylori* activity of *Calophyllum brasiliense* Camb. *Journal of Ethnopharmacology*, 123, pp. 452-458.

Spino, C., Dodier, M. and Sotheeswaran, S., 1998. Anti-HIV coumarins from *Calophyllum* seed oil. *Bioorganic & Medicinal Chemistry Letters*, 8, pp. 3475-3478.

Stevens, P. F., 1980. *Calophyllum castaneum. Journal of the Arnold Arboretum*, 61 (2), pp. 361.

Stout, G.H. and Sears, K.D., 1968. *Calophyllum* products. III. The structure of blancoic acids. *The Journal of Organic Chemistry*, 33 (11), pp. 4185-4190.

Stout, G.H., Hickernell, G.K. and Sears, K.D. 1968. *Calophyllum* products. IV. Papuanic and isopapuanic acids. *The Journal of Organic Chemistry*, 33 (11), pp. 4191-4200.

Suffness, M. and Pezzuto, J.M., 1990. Assays related to cancer drug discovery. *Methods in Plant Biochemistry: Assays for Bioactivity*, 6, pp. 71–133.

Syafni, N., Putra, D.P. and Arbain, D., 2012. 3,4-dihydroxybenzoic acid and 3,4-dihydroxybenzaldehyde from the fern *Trichomaneschinense*L. ; Isolation, antimicrobial and antioxidant properties. *Indonesian Journal of Chemistry*, 12 (3), pp. 273-278.

Taher, M., Idris. M. S., Ahmad, F. and Arbain, D., 2005. A polyisoprenylated ketone from *Calophyllum enervosum. Phytochemistry*, 66, pp. 723-726.

Talapatra, S.K. and Talapatra, B., 2015. *Chemistry of Plant Natural Products*. New York: Springer.

Velioglu, Y.S., Mazza, G., Gao, L. and Oomah, B.D., 1998. Antioxidant activity and total phenolics in selected fruits, vegetables and grain products. *Journal of Agricultural and Food Chemistry*, 46, pp. 4113-4117.

Vo, V.C., 1997. *Dictionary of Medicinal Plants in Vietnam*. Ho Chi Minh City: Medical Publishing House.

Wahle, K.W.J., Rotondo, D., Brown, I. and Heys, S.D., 2010. Plant phenolics in the prevention and treatment of cancer. *Advances in Experimental Medicine and Biology,* 698, pp. 36-51.

World Health Organisation (WHO), 2002. *Traditional medicine strategy* [Online]. Available from: http://apps.who.int/medicinedocs/en/d/Js2297e/. [Accessed 19 June 2015].

World Health Organisation (WHO), 2011. *The world medicines situation* [Online]. Available from: http://www.who.int/topics/infectious_diseases/en/. [Accessed 19 June 2015].

Yin, M.C., Lin, C.C., Wu, H.C., Tsao, S.M. and Hsu, C.K., 2009. Apoptotic effects of protocatechuic acid in human breast, lung, liver, cervix, and prostate cancer cells: Potential mechanisms of action. *Journal of Agricultural and Food Chemistry*, 57, pp. 6468-6473.

Zhang, L. and Demain, A.L., 2005. *Natural Products Drug Discovery and Therapeutic Medicine*. Totowa, New Jersey: Humana Press.
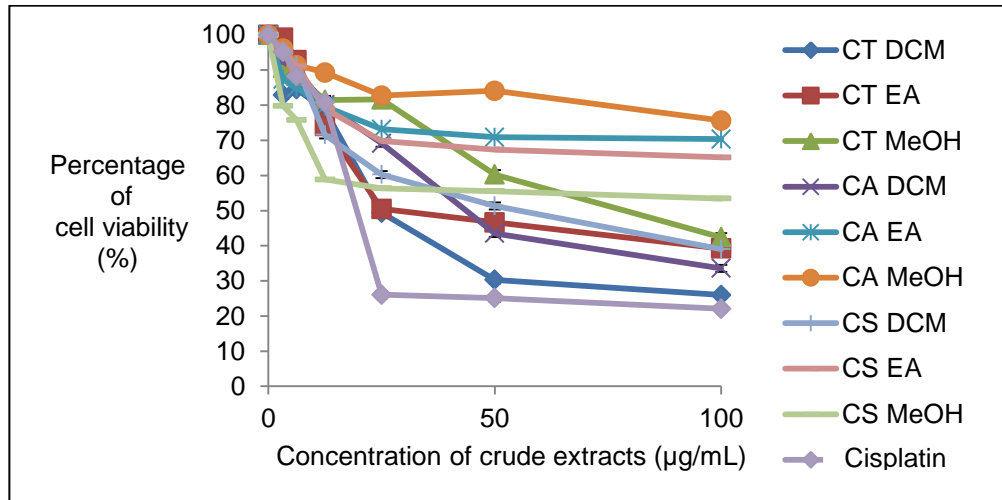
Figure 7.1: Cell killing curve of crude extracts on HeLa cancer cell line. The cytotoxicity was determined via MTT assay after 72 hours incubation.
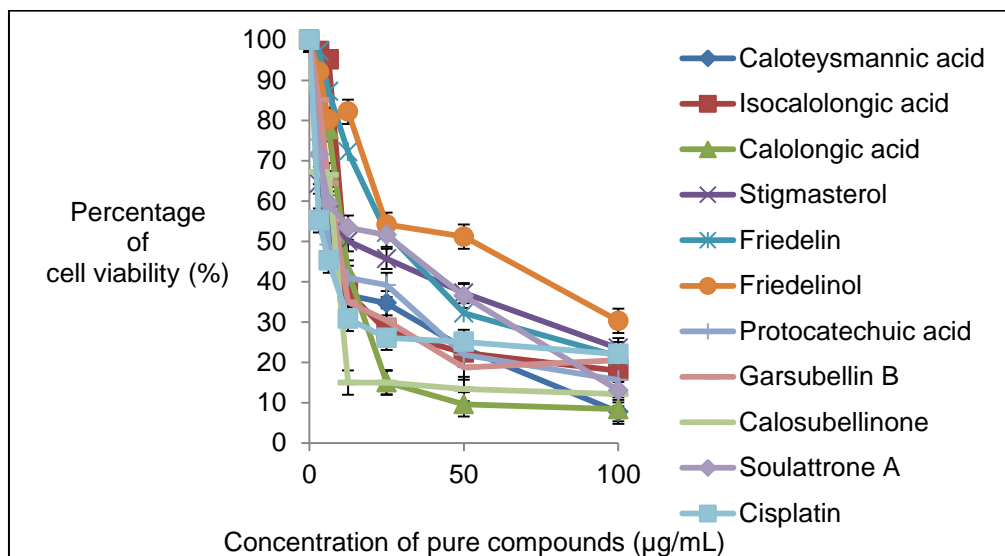
Figure 7.2: Cell killing curve of pure compounds on HeLa cancer cell line. The cytotoxicity was determined via MTT assay after 72 hours incubation.
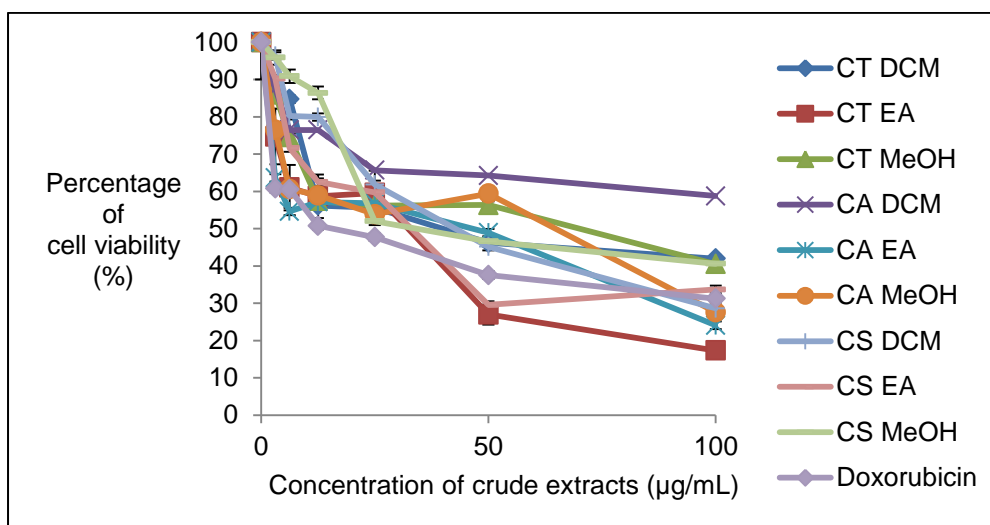
Figure 7.3: Cell killing curve of crude extracts on MDA-MB-231 cancer cell line. The cytotoxicity was determined via MTT assay after 72 hours incubation.
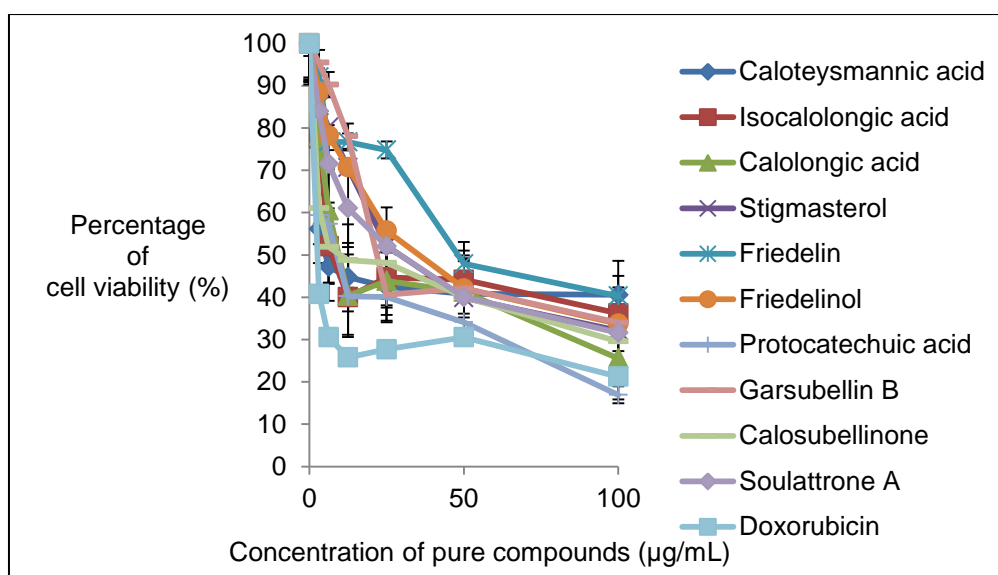
Figure 7.4: Cell killing curve of pure compounds on MDA-MB-231 cancer cell line. The cytotoxicity was determined via MTT assay after 72 hours incubation.
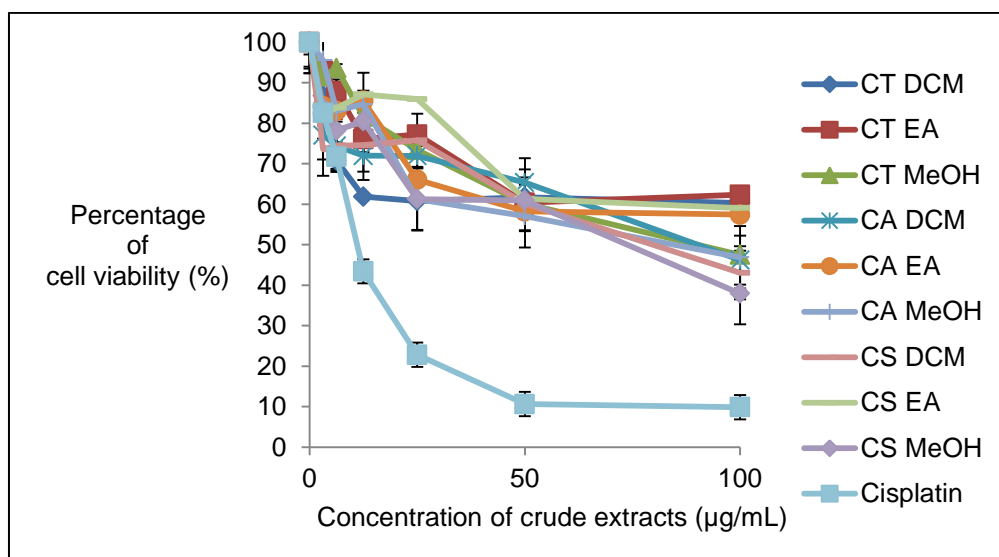
Figure 7.5: Cell killing curve of crude extracts on LS174T cancer cell line. The cytotoxicity was determined via MTT assay after 72 hours incubation.
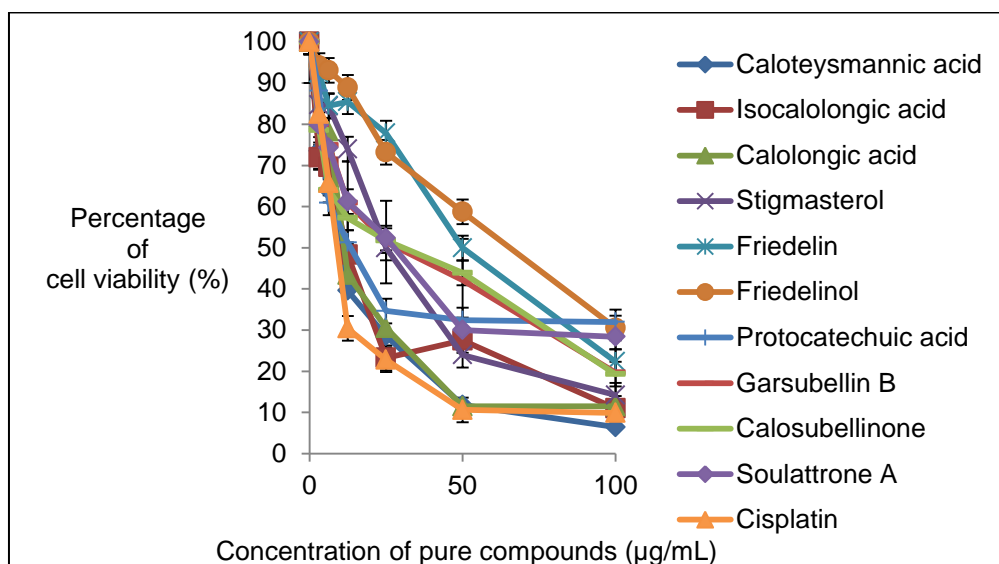
Figure 7.6: Cell killing curve of pure compounds on LS174T cancer cell line. The cytotoxicity was determined via MTT assay after 72 hours incubation.
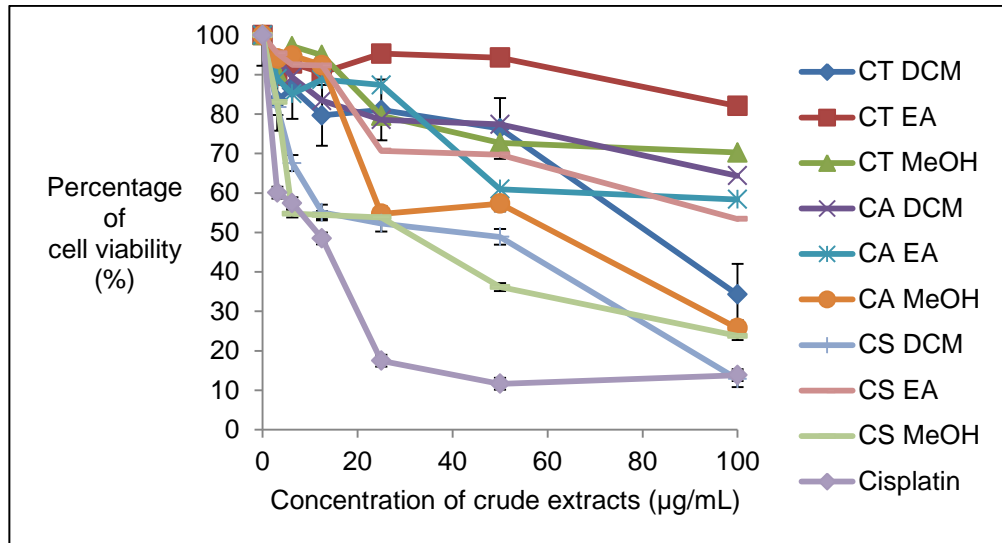
Figure 7.7: Cell killing curve of crude extracts on T98G cancer cell line. The cytotoxicity was determined via MTT assay after 72 hours incubation.
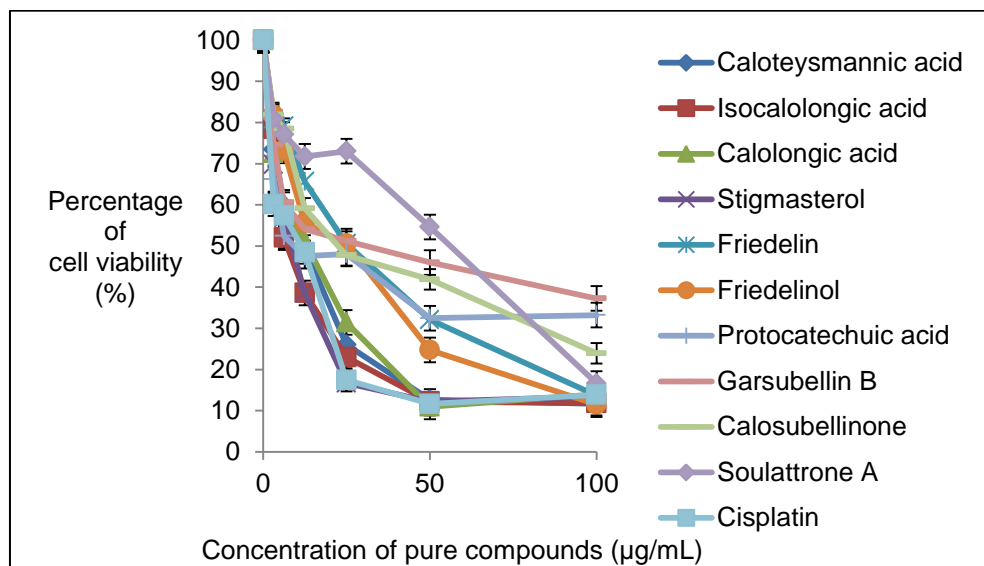
Figure 7.8: Cell killing curve of pure compounds on T98G cancer cell line. The cytotoxicity was determined via MTT assay after 72 hours incubation.
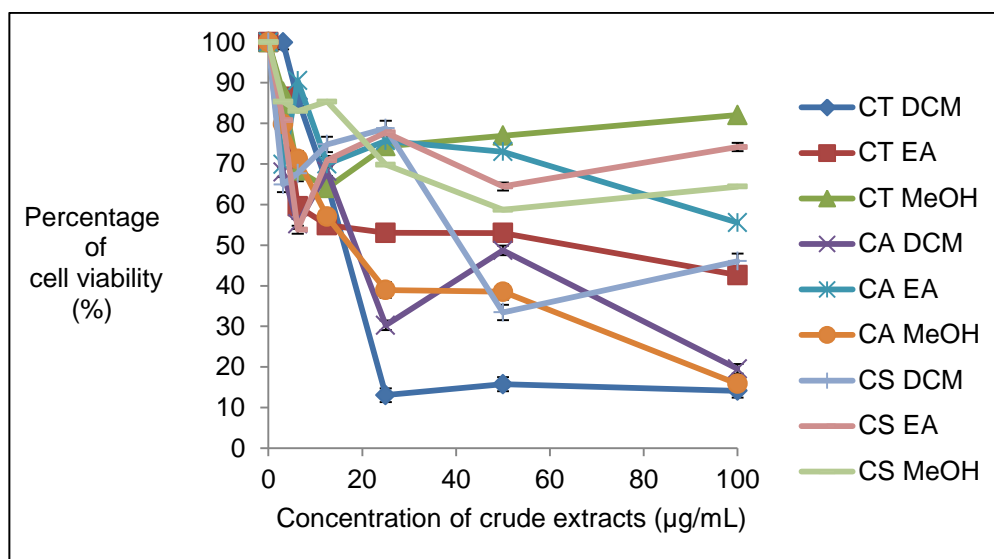
Figure 7.9: Cell killing curve of crude extracts on HEK293 normal cell line. The cytotoxicity was determined via MTT assay after 72 hours incubation.
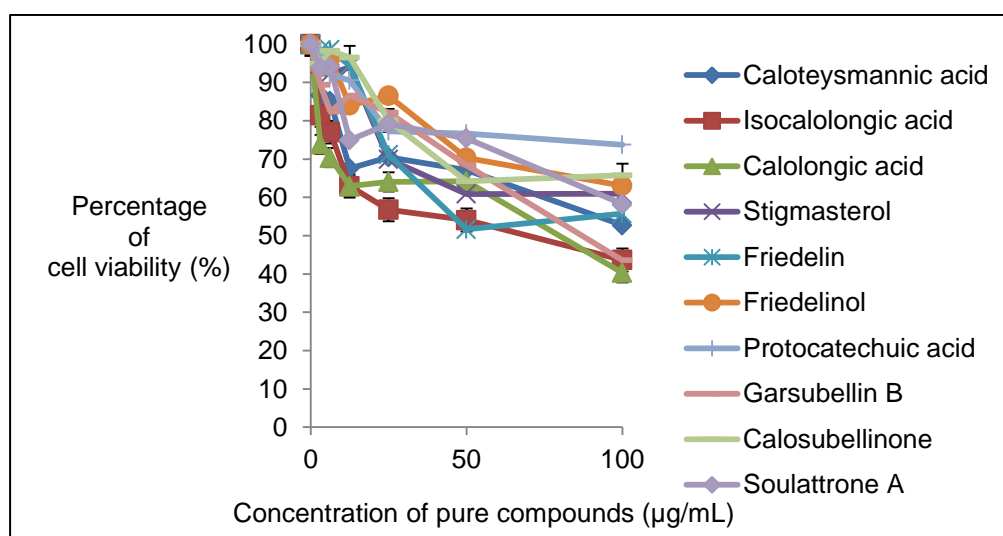
Figure 7.10: Cell killing curve of pure compounds on HEK293 normal cell line. The cytotoxicity was determined via MTT assay after 72 hours incubation.
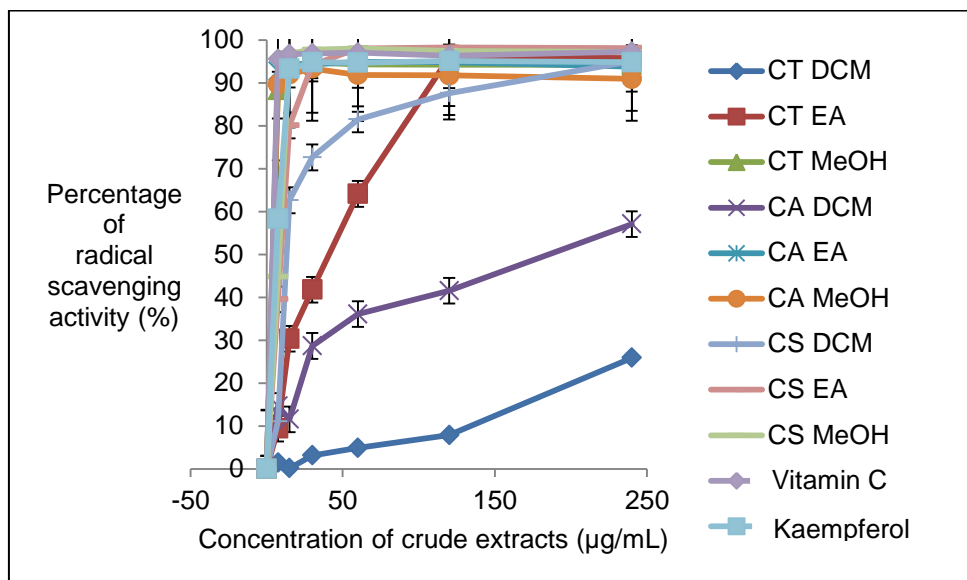
Figure 7.11: Graph of inhibition rate (%) against concentration of crude extracts
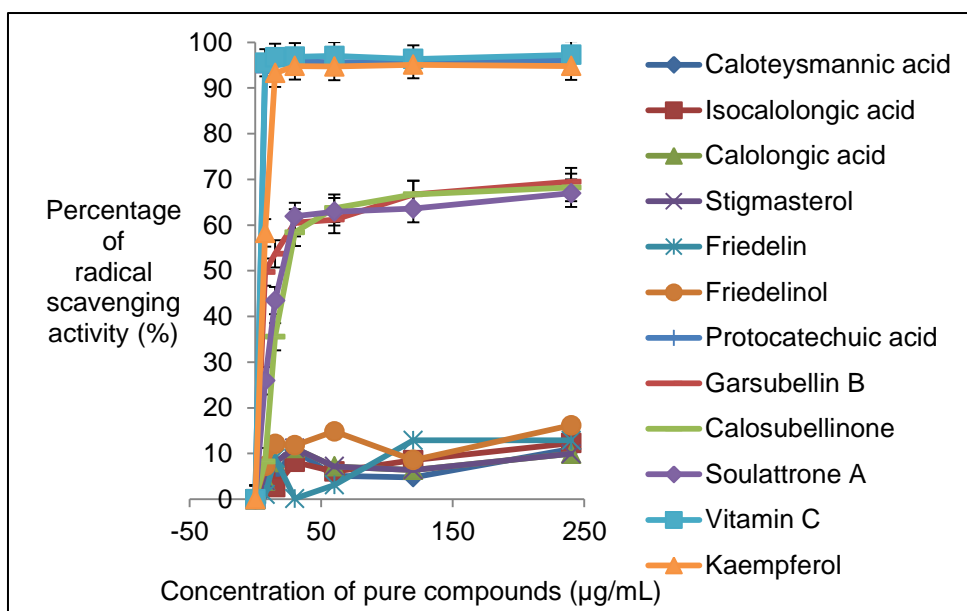
Figure 7.12: Graph of inhibition rate (%) against concentration of pure compounds

LIST OF PUBLICATIONS

1. Lim, C.K., Subramaniam, H., Say, Y.H., Jong, V.Y.M., Khaledi, H. and Chee, C.F., 2015. A new chromanone acid from the stem bark of *Calophyllum teysmannii. Natural Product Research,* 29 (21), pp. 1970-1977.

2. Lim, C.K., 2016. In vitro cytotoxic activity of isolated compounds from Malaysian *Calophyllum* species. *Medicinal Chemistry Research*, 25 (8), pp. 1686-1694.

3. Thiagarajan, S., Yong, F.L., Subramaniam, H., Jong, V.Y.M., Lim, C.K and Say, Y.H., 2017. Anti-obesity effect of phenylcoumarins from two *Calophyllum* spp in 3T3-L1 adipocytes. *Tropical Journal of Pharmaceutical Research*, 16 (3), pp. 563-572.

4. Lim, C.K., Subramaniam, H., Say, Y.H. and Jong, V.Y.M., 2017. Cytotoxic compounds from the stem bark of *Calophyllum soulattri. Natural Product Communications,* 12 (9), pp. 1469-1471.
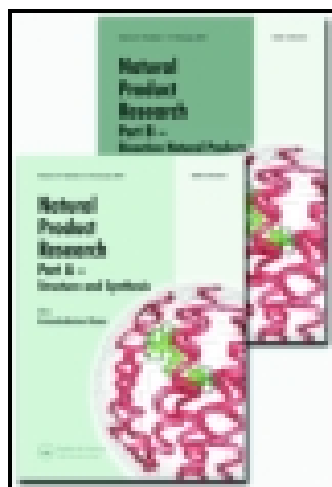
A new chromanone acid from the stem bark of Calophyllum teysmannii

Chan Kiang Lim[a], Hemaroopini Subramaniam[a], Yee How Say[a],
Vivien Yi Mian Jong[b], Hamid Khaledi[c] & Chin Fei Chee[c]

[a] Faculty of Science, Universiti Tunku Abdul Rahman, Jalan
Universiti, Bandar Barat, 31900 Kampar, Perak, Malaysia

[b] Centre for Applied Sciences, Faculty of Applied Sciences,
Universiti Teknologi MARA, Samarahan Campus 2, Jalan Meranek,
94300 Kota Samarahan, Sarawak, Malaysia

[c] Department of Chemistry, University of Malaya, 50603 Kuala
Lumpur, Malaysia
Published online: 26 Feb 2015.

PLEASE SCROLL DOWN FOR ARTICLE

Taylor & Francis
Taylor & Francis Group

A new chromanone acid from the stem bark of *Calophyllum teysmannii*

Chan Kiang Lim[a]*, Hemaroopini Subramaniam[a], Yee How Say[a], Vivien Yi Mian Jong[b], Hamid Khaledi[c1] and Chin Fei Chee[c]

[a]*Faculty of Science, Universiti Tunku Abdul Rahman, Jalan Universiti, Bandar Barat, 31900 Kampar, Perak, Malaysia;* [b]*Centre for Applied Sciences, Faculty of Applied Sciences, Universiti Teknologi MARA, Samarahan Campus 2, Jalan Meranek, 94300 Kota Samarahan, Sarawak, Malaysia;* [c]*Department of Chemistry, University of Malaya, 50603 Kuala Lumpur, Malaysia*
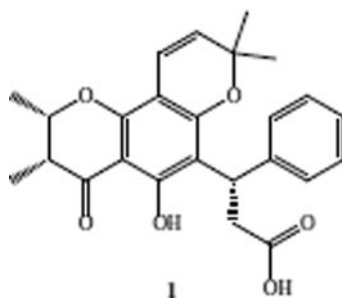
A new chromanone acid, namely caloteysmannic acid (**1**), along with three known compounds, calolongic acid (**2**), isocalolongic acid (**3**) and stigmasterol (**4**) were isolated from the stem bark of *Calophyllum teysmannii*. All these compounds were evaluated for their cytotoxic and antioxidant activities in the MTT and DPPH assays, respectively. The structure of compound **1** was determined by means of spectroscopic methods including 1D and 2D NMR experiments as well as HR-EIMS spectrometry. The stereochemical assignment of compound **1** was done based on the NMR results and X-ray crystallographic analysis. The preliminary assay results revealed that all the test compounds displayed potent inhibitory activity against HeLa cancer cell line, in particular with compound **1** which exhibited the highest cytotoxic activity comparable to the positive control used, cisplatin. However, no significant antioxidant activity was observed for all the test compounds in the DPPH radical scavenging capacity assay.

Keywords: chromanone acid; caloteysmannic acid; *Calophyllum teysmannii*; cytotoxic; NMR spectroscopy; X-ray crystallography

1. Introduction

The genus *Calophyllum* is a huge group of tropical trees consisting of about 180–200 different species (Crane et al. 2005). This genus is well known to be a rich source of bioactive coumarins, xanthones, biflavonoids and chromanones, some of which were reported to exhibit a broad-spectrum of biological activities including antiviral, antitumour-promoting, cytotoxic, antimalarial and antibacterial (Su et al. 2008; Cechinel et al. 2009). Among these compounds,

---

*Corresponding author. Email: cklim@utar.edu.my

chromanone derivatives are found to be structurally unique due to their interesting stereochemical diversity. The chromanone core contains two stereocenters at carbons C-2 and C-3 in addition to the stereocenter found in the attached alkyl side chain which consists of 5–8 carbons in length, and frequently with a bonded carboxyl group, such as blancoic acid, calolongic acid, apetalic acid, papuanic acid and their stereoisomers (Plattner et al. 1974; Piccinelli et al. 2013). Isolation of chromanone derivatives, in particular with the linear and angular pyranochromanones are common from *Calophyllum brasiliense* (Plattner et al. 1974), *Calophyllum inophyllum* (Prasad et al. 2012), *Calophyllum papuanum* (Stout et al. 1968), *Calophyllum blancoi* (Stout and Sears 1968), *Calophyllum pinetorum* (Piccinelli et al. 2013) and *Calophyllum dryobalanoides* (Ha et al. 2012). Biologically, chromanone derivatives were reported to be HIV-1 1N inhibitors (Dziewulska-Kułaczkowska and Bartyzel 2013) and showed potential anticancer (Kanagalakshmi et al. 2010), antibacterial (Cottiglia et al. 2004) and antifungal (Hay et al. 2003) activities. In this article, we describe the NMR elucidation and crystal structure of the new compound, caloteysmannic acid (**1**). To our knowledge, this is the first report about the isolation of chromanone acid from *Calophyllum teysmannii* apart from the previously reported coumarins and xanthones (Su et al. 2008). The cytotoxic and antioxidant activities of isolated compounds from this species are also reported.

2. Results and discussion

2.1. *Phytochemical investigation*

Phytochemical study on the dichloromethane extract yielded three pyranochromanone acids, namely caloteysmannic acid (**1**), calolongic acid (**2**) (Piccinelli et al. 2013), isocalolongic acid (**3**) (Plattner et al. 1974), and a sterol, stigmasterol (**4**) (Ibrahim et al. 2012).

Compound **1** was isolated via column chromatography (CC) and recrystallised from methanol as yellow cubic crystals, m.p. 159–161°C, and the phenolic nature of this compound was indicated by the positive $FeCl_3$ test. The molecular formula $C_{25}H_{26}O_6$ was deduced from EIMS ($[M]^{+\cdot}$ at m/z 422) and HR-EIMS ($[M]^{+\cdot}$ at m/z 422.17299). The UV absorption maxima at 214, 271, 300 and 367 nm suggested the presence of a pyranochromanone moiety that is typical to isocalolongic acid (Guerreiro et al. 1973), apetalic acid (Plattner et al. 1974), chapelieric acid (Gunatilaka et al. 1984), and other chromanone derivatives. The IR spectrum exhibited absorption bands at 3429 (O—H), 3031 (O—H of carboxylic acid), 1706 (C=O of carboxylic acid) and 1621 cm^{-1} (conjugated C=O).

The ^{1}H and ^{13}C NMR spectra of **1** (Supplementary Figures S1 and S3) revealed the presence of a 2,3-dimethylchromanone core [δ_H 4.62 (1H, qd, $J = 6.7$ and 3.1 Hz, H-2), 2.62 (1H, qd, $J = 7.3$ and 3.1 Hz, H-3), 1.34 (3H, d, $J = 6.7$ Hz, H-11) and 1.09 (3H, d, $J = 7.3$ Hz, H-12); δ_C 201.4 (C-4), 76.5 (C-2), 44.0 (C-3), 15.8 (C-11) and 9.0 (C-12)], a chelated hydroxyl group [δ_H 12.96 (s, 5-OH)], and a 2,2-dimethylpyran ring [δ_H 6.49 (1H, d, $J = 10.4$ Hz, H-10), 5.53 (1H, d, $J = 10.4$ Hz, H-9), 1.42 (3H, s, H-16) and 1.18 (3H, s, H-17); δ_C 126.3 (C-9), 115.6 (C-10), 78.3 (C-8), 27.6 (C-16) and 27.3 (C-17)]. Meanwhile, the resonances for a methine [δ_H 5.09 (1H, t, $J = 8.0$ Hz, H-13); δ_C 35.0 (C-13)], a methylene [δ_H 3.34 (1H, dd, $J = 15.9$, 8.5 Hz, H$_a$-14) and 3.12 (1H, dd, $J = 15.9$, 7.3 Hz, H$_b$-14); δ_C 36.4 (C-14)], a carboxylic group (δ_C 173.3, C-15), and a mono-substituted benzene ring [δ_H 7.40 (2H, d, $J = 7.3$ Hz, H-2′ & H-6′), 7.21 (2H, t, $J = 7.3$ Hz, H-3′ & H-5′) and 7.09 (1H, t, $J = 7.3$ Hz, H-4′); δ_C 143.9 (C-1′), 127.9 (C-3′ & C-5′), 127.8 (C-2′ & C-6′) and 125.9 (C-4′)] indicated the presence of 3-phenylpropanoic acid side chain. In the HMBC spectrum, key correlations from a pair of olefinic protons H-9 to C-8 (δ_C 78.3) and C-10a (δ_C 101.6); H-10 to C-6a (δ_C 159.6) and C-8 (δ_C 78.3) suggested the 2,2-dimethylpyran ring was angularly fused to the 2,3-dimethylchromanone nucleus at carbon positions C-6a and C-10a. Moreover, the HMBC correlations from H-13 to C-1′ (δ_C 143.9), C-2′ (δ_C 127.8), C-5 (δ_C 161.6), C-6 (δ_C 111.8), C-6′ (δ_C 127.8), C-14 (δ_C 36.4) and C-15 (δ_C 173.3);

H-14 to C-1′ (δ_C 143.9), C-6 (δ_C 111.8), C-13 (δ_C 35.0) and C-15 (δ_C 173.3) suggested the presence of 3-phenylpropanoic acid unit which was attached to the pyranochromanone core at carbon position C-6. On the basis of the above spectral evidence, caloteysmannic acid was established to have structure **1** (Figure 1) which had not been previously reported.

Compound **1** was found to have three asymmetric centres at carbons C-2, C-3 and C-13 which could lead to a total of eight possible stereoisomers. The stereochemical assignment of this compound was done based on the NMR and X-ray crystallographic analyses. The *cis*-coupling of protons H-2 and H-3 was evidenced from the coupling constant of 3.1 Hz observable in both proton signals of H-2 and H-3 at δ_H 4.62 and 2.62, respectively (Stout et al. 1968). This is consistent with axial-equatorial arrangement for protons H-2 and H-3 meaning that the configuration of 2,3-dimethylchromanone ring could be either 2*S*,3*R* or 2*R*,3*S* (Ha et al. 2012). The crystal structure of **1** (Figure 2) was determined by X-ray diffraction analysis which confirmed the compound to have absolute configuration of 2*S*,3*R* at asymmetric carbons C-2 and C-3. Apart from that, the asymmetric carbon C-13 located at the side chain moiety was deduced to have *S* configuration. Based on the spectral evidence, compound **1** was identified as (*S*)-3-[(2*S*,3*R*)-5-hydroxy-2,3,8,8-tetramethyl-4-oxo-2,3,4,8-tetrahydropyrano[2,3-*f*]chromen-6-yl]-3-phenylpropanoic acid.

Meanwhile, diastereoisomers **2** and **3** (Figure 1) were identified to have structures similar to that of compound **1** except for the hexanoic acid moiety at carbon position C-6 rather than 3-phenylpropanoic acid unit. Compounds **2**–**4** were identified as calolongic acid, isocalolongic acid and stigmasterol by comparing their NMR and MS data with those reported in literature (Guerreiro et al. 1973; Huerta-Reyes et al. 2004; Zhai et al. 2014).
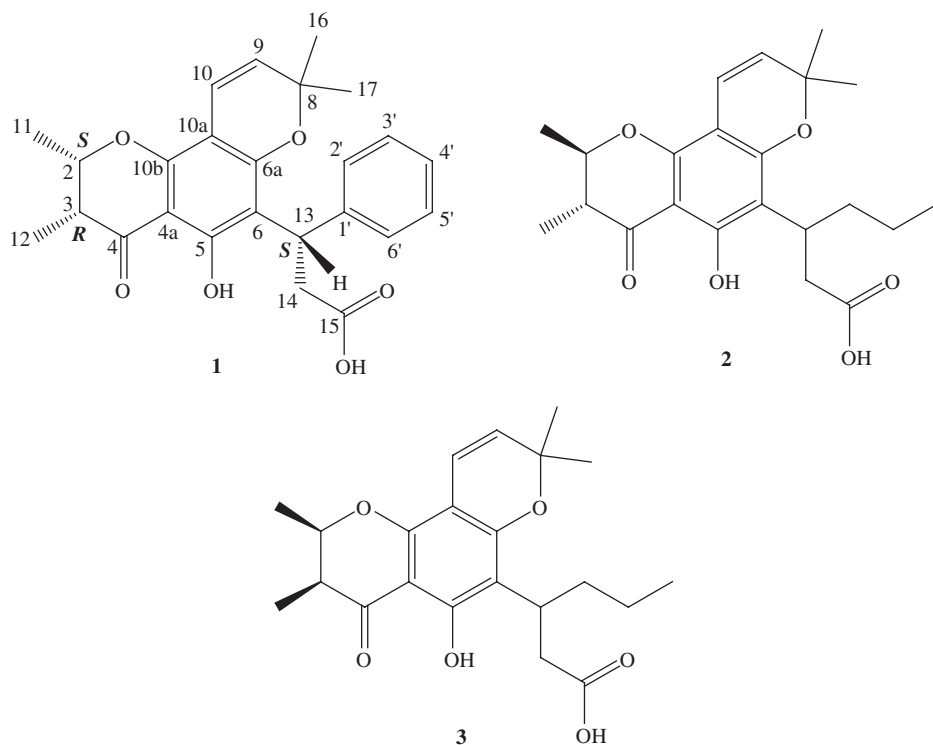
Figure 1. Compounds **1**–**3** isolated from the stem bark of *Calophyllum teysmannii*.
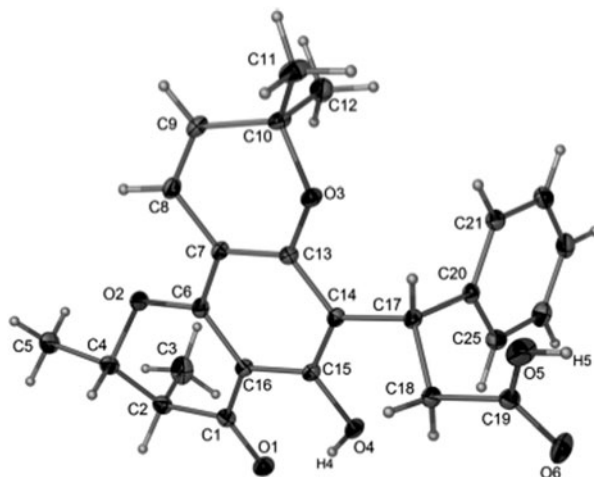
Figure 2. X-ray crystal structure of **1** with thermal ellipsoids drawn at the 50% probability level.

2.2. *Cytotoxic and DPPH activities*

The cytotoxic activity of isolated compounds **1**–**4** against HeLa cancer cell line was evaluated and the results are shown in Table 1. All the test compounds were found to exhibit strong inhibitory activity comparable to the positive control used, cisplatin. On the other hand, all the test compounds gave no significant antioxidant activity by showing IC_{50} values of more than 240 µg/mL in the DPPH assay.

3. Experimental

3.1. *General experimental procedures*

Melting points were determined on a Stuart SMP10 melting point apparatus (Barloworld Scientific Limited, Staffordshire, UK) and are uncorrected. Optical rotations were performed on a JASCO P-1020 polarimeter (JASCO, Tokyo, Japan). UV spectra were recorded in EtOH or CHCl$_3$ on a Perkin–Elmer Lambda 35 UV/VIS spectrophotometer (Perkin-Elmer, Waltham, MA, US), and IR spectra were obtained in KBr using a Perkin–Elmer Spectrum RXI FTIR spectrophotometer (Perkin-Elmer, Waltham, MA, US), respectively. NMR spectra were measured on a JEOL JNM-ECX 400 MHz FTNMR spectrometer (JEOL, Tokyo, Japan) in CDCl$_3$ or acetone-d_6 with TMS as the internal standard. Chemical shifts (δ) are reported in ppm and coupling constants (J) are expressed in Hertz. EIMS and HR-EIMS were acquired on an Agilent 5975C MSD (Agilent Technologies, Santa Clara, CA, US) and Thermo Finnigan MAT95XL (Thermo Fisher, Bremen, Germany) mass spectrometers, respectively. Diffraction

Table 1. Cytotoxic activity of isolated compounds **1**–**4** against HeLa cancer cell line.

Test compounds	IC_{50} (µM)
1	7.3 ± 0.2
2	10.0 ± 1.7
3	7.8 ± 0.2
4	7.5 ± 0.2
Cisplatin	7.8 ± 0.3

Note: Data are reported as means ± SD for three replicates.

data for the crystal were collected on an Agilent SuperNova Dual diffractometer (Agilent Technologies, Santa Clara, CA, US) equipped with a graphite monochromated Mo-Kα radiation source ($\lambda = 0.71073$ Å) at 100(2) K. All reagents were of analytical quality and used without further purification unless otherwise specified. CC was performed with silica gel 60 (230–300 mesh, Merck, Darmstadt, Germany) via gradient elution. Analytical TLC was performed on precoated silica gel 60 F_{254} (Merck, Darmstadt, Germany) and methanolic $FeCl_3$ was used for detection of phenolic compounds.

3.2. Plant material

The stem bark of *C. teysmannii* was collected from the jungle in Landeh district of Sarawak, Malaysia, and was identified by Mr. Tinjan Anak Kuda, botanist from the Forest Department, Sarawak. Voucher specimen (UITM 3006) was deposited at the herbarium of Universiti Teknologi MARA, Sarawak.

3.3. Extraction and isolation

The air-dried and ground stem bark material of *C. teysmannii* (2.0 kg) was successively extracted twice (each for 72 h) by maceration in dichloromethane, and subsequently twice with EtOAc at room temperature. Evaporation of the solvents under reduced pressure by a rotary evaporator at 40°C yielded 298 and 35 g of dichloromethane and EtOAc extracts, respectively.

A portion of dichloromethane extract (100 g) was subjected to CC over silica gel packed in *n*-hexane and eluted with *n*-hexane-dichloromethane mixtures of increasing polarity, followed by increasing concentration of EtOAc in dichloromethane to give 20 fractions (CTDA1-20). Fraction CTDA14 was fractionated by Si gel CC (0–100% *n*-hexane–acetone) to give 20 fractions (CTDB1-20). Fractions CTDB14-15 were combined and further recrystallised in MeOH to afford caloteysmannic acid (1), as yellow cubic crystals (696 mg). From fractions CTDB4-7, isocalolongic acid (3, 1250 mg) was obtained. Meanwhile, fractions CTDA3-4 were combined and purified by Si gel CC (0–100% *n*-hexane–EtOAc) to yield stigmasterol (4, 7 mg). About 32 g of EtOAc extract was chromatographed on Si gel column (0–100% *n*-hexane–dichloromethane followed by 0–100% dichlorometane–EtOAc) to afford 20 fractions (CTEA1-20). Fractions CTEA4-5 were pooled and subjected to Si gel CC (0–100% *n*-hexane–acetone) to give 20 fractions (CTEB1-20). Fraction CTEB8 was rechromatographed over Si gel CC (0–100% *n*-hexane–EtOAc) to give 10 fractions (CTEC1-10). Fraction CTEC4 yielded calolongic acid (2, 8 mg).

3.4. Spectral data of compounds

3.4.1. Caloteysmannic acid (1)

Yellow cubic crystals; m.p., 159–161°C; $[\alpha]_D = -156.0°$ (MeOH, *c* 0.05); UV λ_{max} nm (EtOH) (log ϵ): 214 (0.78), 271 (1.75), 300 (0.48), 367 (0.15); IR ν_{max} (KBr) cm^{-1}: 3429, 3031, 2982, 2920, 1706, 1621, 1589, 1447, 1343, 1291, 1136, 1116, 820, 724; ^1H NMR (400 MHz, acetone-d_6): 12.96 (1H, s, 5-OH), 7.40 (2H, d, $J = 7.3$ Hz, H-2' & H-6'), 7.21 (2H, t, $J = 7.3$ Hz, H-3' & H-5'), 7.09 (1H, t, $J = 7.3$ Hz, H-4'), 6.49 (1H, d, $J = 10.4$ Hz, H-10), 5.53 (1H, d, $J = 10.4$ Hz, H-9), 5.09 (1H, t, $J = 8.0$ Hz, H-13), 4.62 (1H, qd, $J = 6.7, 3.1$ Hz, H-2), 3.34 (1H, dd, $J = 15.9, 8.5$ Hz, H-14), 3.12 (1H, dd, $J = 15.9, 7.3$ Hz, H-14), 2.62 (1H, qd, $J = 7.3, 3.1$ Hz, H-3), 1.42 (3H, s, H-16), 1.34 (3H, d, $J = 6.7$ Hz, H-11), 1.18 (3H, s, H-17), 1.09 (3H, d, $J = 7.3$ Hz, H-12); ^{13}C NMR (100 MHz, acetone-d_6): 201.4 (C-4), 173.3 (C-15), 161.6 (C-5), 159.6 (C-6a), 155.3 (C-10b), 143.9 (C-1'), 127.9 (C-3' & C-5'), 127.8 (C-2' & C-6'), 126.3 (C-9), 125.9 (C-4'), 115.6 (C-10), 111.8 (C-6), 101.6 (C-10a), 100.9 (C-4a), 78.3 (C-8), 76.5 (C-2), 44.0 (C-3), 36.4 (C-14),

35.0 (C-13), 27.6 (C-16), 27.3 (C-17), 15.8 (C-11), 9.0 (C-12); EIMS *m/z* (rel. int.): 422 ([M]$^{+\cdot}$ 17), 407 (100), 389 (8), 363 (15), 333 (12), 305 (7), 291 (30), 259 (8), 203 (14), 153 (7), 107 (9), 77 (6); HREI-MS: 422.17299 ([M]$^{+\cdot}$, $C_{25}H_{26}O_6^+$; calcd 422.17294).

3.4.2. *Calolongic acid (2)*

Yellow gum; $[\alpha]_D = -36.0°$ (MeOH, *c* 0.08); UV λ_{max} nm (CHCl$_3$) (log ϵ): 231 (0.65), 270 (1.42), 365 (0.16); IR v_{max} (KBr) cm^{-1}: 3436, 2930, 1718, 1618, 1351, 1282, 1189, 1125, 939, 823; EIMS *m/z* (rel. int.): 388 ([M]$^+$ 11), 373 (100), 327 (12), 313 (7), 301 (10), 287 (12), 271 (8), 257 (13), 229 (9), 215 (12), 43 (6).

3.4.3. *Isocalolongic acid (3)*

Yellow gum; $[\alpha]_D = -50.0°$ (MeOH, *c* 0.05); UV λ_{max} nm (EtOH) (log ϵ): 212 (1.06), 229 (0.99), 273 (2.96), 299 (1.05), 367 (0.32); IR v_{max} (KBr) cm^{-1}: 3428, 2958, 2931, 2874, 1702, 1621, 1589, 1455, 1445, 1309, 1140, 1117, 818; EIMS *m/z* (rel. int.): 388 ([M]$^+$ 12), 373 (100), 327 (12), 313 (7), 301 (10), 287 (12), 271 (8), 257 (14), 229 (9), 215 (13), 43 (7).

3.4.4. *Stigmasterol (4)*

Colourless needles; m.p., 164–166°C; IR v_{max} (KBr) cm^{-1}: 3424, 2942, 2868, 1668, 1460, 1376, 1052, 960; EIMS *m/z* (rel. int.): 412 ([M]$^{+\cdot}$ 22), 351 (7), 300 (11), 271 (19), 255 (20), 213 (12), 159 (23), 145 (20), 133 (26), 119 (21), 105 (36), 91 (38), 81 (56), 69 (55), 55 (100), 41 (49).

3.5. *Stock solution and cell culture*

Stock solutions of compounds **1–4** were prepared at concentration of 5 mg/mL in DMSO. The human cancer cell line, HeLa (cervical carcinoma) was obtained from the American Type Culture Collection (ATCC, USA). Cells were cultured in DMEM with 10% fetal bovine serum (FBS), 1% penicillin-streptomycin by using 25 mL flask in a 37°C incubator with 5% CO$_2$.

3.6. *Cytotoxic assay*

Cytotoxic activity of test compounds **1–4** against human HeLa cancer cell line was evaluated using the MTT method described in the literature (Mosmann 1983). Cisplatin was used as the positive control.

3.7. *DPPH assay*

Radical scavenging activity was determined via colorimetric method in 96-well microplate. The stock solution of sample was prepared in methanol at concentration of 1 mg/mL. Serial dilution of stock solution gave a series of concentrations at 240, 120, 60, 30, 15, 7.5 and 3.75 µg/mL. 100 µL of sample solutions were added with 100 µL of DPPH solution (2 mg/mL in methanol). After 30 min incubation in darkness at room temperature (25°C), the absorbance of the resulting solution was measured at 517 nm with a spectrophotometer. All tests were run in triplicate and averaged. Ascorbic acid was used as positive control in the assay.

4. Conclusion

Chemical study on the stem bark of *C. teysmannii* has resulted in the isolation of a new chromanone acid, caloteysmannic acid (**1**), along with three other known compounds, calolongic

acid (**2**), isocalolongic acid (**3**) and stigmasterol (**4**). All these compounds were found to show potent cytotoxic activity against HeLa cancer cell line, but with no significant activity observed in DPPH assay.

Supplementary material

Crystallographic data for the structure **1** have been deposited with the Cambridge Crystallographic Data Centre (CDCC), 12 Union Road, Cambridge, CB2 1EZ, UK (Fax: +44-(0)1223-336033 or e-mail: deposit@ccdc.cam.ac.uk or www://www.ccdc.cam.ac.uk) and are available on request by quoting the deposition number CCDC 1038299. Supplementary material related to the following articles is available online.

Acknowledgements

Note

1. Present address: Center for Natural Products and Drug Research, University of Malaya, 50603 Kulala Lumpur, Malaysia.

References

Cechinel VF, Meyre-Silva C, Niero R. 2009. Chemical and pharmacological aspects of the genus calophyllum. Chem Biodiv. 6(3):313–327, 10.1002/cbdv.200800082.

Cottiglia F, Dhanapal B, Sticher O, Heilmann J. 2004. New chromanone acids with antibacterial activity from *Calophyllum brasiliense*. J Nat Prod. 67(537):541.

Crane S, Aurore G, Joseph H, Mouloungui Z, Bourgeois P. 2005. Composition of fatty acids triacylglycerols and unsaponifiable matter in calophyllum calaba l. Oil from guadeloupe. Phytochemistry. 66(15):1825–1831, 10.1016/j.phytochem.2005.06.009.

Dziewulska-kułaczkowska A, Bartyzel A. 2013. Structural and physicochemical properties of 3-(3-carboxyphenyla-minomethylene)-2-methoxychroman-4-one. J Mol Struc. 1033:67–74, 10.1016/j.molstruc.2012.08.013.

Guerreiro E, Kunesch G, Polonsky J. 1973. Chromanones de l'écorce de calophyllum recedens. Phytochemistry. 12(1):185–189, 10.1016/S0031-9422(00)84644-0.

Gunatilaka AAL, De Silva AMYJ, Sotheeswaran S, Balasubramaniam S, Wazeer MIM. 1984. Terpenoid and biflavonoid constituents of calophyllum calaba and garcinia spicata from Sri Lanka. Phytochemistry. 23(2):323–328, 10.1016/S0031-9422(00)80326-X.

Ha LD, Hansen PE, Duus F, Pham HD, Nguyen L-HD. 2012. A new chromanone acid from the bark of calophyllum dryobalanoides. Phytochem Lett. 5(2):287–291, 10.1016/j.phytol.2012.02.003.

Hay AE, Guilet D, Morel C, Larcher G, Macherel D, Le Ray AM, Litaudon M, Richomme P. 2003. Antifungal chromans inhibiting the mitochondrial respiratory chain of pea seeds and new xanthones from calophyllum caledonicum. Plant Med. 69(12):1130–1135, 10.1055/s-2003-818004.

Huerta-Reyes M, Basualdo MdelC, Abe F, Jimenez-Estrada M, Soler C, Reyes-Chilpa R. 2004. Hiv-1 inhibitory compounds from calophyllum brasiliense leaves. Biol Pharm Bull. 27(9):1471–1475, 10.1248/bpb.27.1471.

Ibrahim SRM, Mohamed GA, Shaala LA, Banuls LMY, Van goietsenoven GV, Kiss R, Youssef DTA. 2012. New ursane-type triterpenes from the root bark of calotropis procera. Phytochem Lett. 5(3):490–495, 10.1016/j.phytol.2012.04.012.

Kanagalakshmi K, Premanathan M, Priyanka R, Hemalatha B, Vanangamudi A. 2010. Synthesis, anticancer and antioxidant activities of 7-methoxyisoflavanone and 2,3-diarylchromanones. Eur J Med Chem. 45(6):2447–2452, 10.1016/j.ejmech.2010.02.028.

Mosmann T. 1983. Rapid colorimetric assay for cellular growth and survival: application to proliferation and cytotoxicity assays. J Immunol Methods. 65:55–63.

Piccinelli AL, Kabani AO, Lotti C, Alarcon AB, Cuesta-Rubio O, Rastrelli L. 2013. A fast and efficient hplc-pda–ms method for detection and identification of pyranochromanone acids in calophyllum species. J Pharm Biomed Anal. 76:157–163, 10.1016/j.jpba.2012.12.028.

Plattner RD, Spencer GF, Weisleder D, Kleiman R. 1974. Chromanone acids in calophyllum brasiliense seed oil. Phytochemistry. 13(11):2597–2602, 10.1016/S0031-9422(00)86943-5.

Prasad J, Shrivastava A, Khanna AK, Bhatia G, Awasthi SK, Narender T. 2012. Antidyslipidemic and antioxidant activity of the constituents isolated from the leaves of calophyllum inophyllum. Phytomedicine. 19(14):1245–1249, 10.1016/j.phymed.2012.09.001.

Stout GH, Hickernell GK, Sears KD. 1968. Calophyllum products. Iv. Papuanic and isopapuanic acids. J Org Chem. 33(11):4191–4200, 10.1021/jo01275a039.

Stout GH, Sears KD. 1968. Calophyllum products. Iii. Structure of blancoic acids. J Org Chem. 33(11):4185–4190, 10.1021/jo01275a038.

Su X-H, Zhang M-L, Li L-G, Huo C-H, Gu Y-C, Shi Q-W. 2008. Chemical constituents of the plants of the genus calophyllum. Chem Biodiv. 5(12):2579–2608, 10.1002/cbdv.200890215.

Zhai B, Clark J, Ling T, Connelly M, Medina-Bolivar F, Rivas F. 2014. Antimalarial evaluation of the chemical constituents of hairy root culture of *Bixa orellana* L. Molecules. 19(1):756–766, 10.3390/molecules19010756.

ORIGINAL RESEARCH

In vitro cytotoxic activity of isolated compounds from Malaysian *Calophyllum* species

Chan Kiang Lim[1] · Subramaniam Hemaroopini[1] · Shu Ying Gan[1] · Siew Mian Loo[1] ·
Jo Ring Low[1] · Vivien Yi Mian Jong[2] · Hsien Chuen Soo[3] · Chee Onn Leong[4] ·
Chun Wai Mai[5] · Chin Fei Chee[5]

Abstract Cancer is a leading cause of death worldwide. In our continuing search for new anticancer agents, four Malaysian *Calophyllum* species, namely *C. castaneum*, *C. teysmannii*, *C. canum*, and *C. sclerophyllum*, had been phytochemically studied to give compounds **1–12**. All the isolated compounds were evaluated for their antiproliferative activity against nasopharyngeal (SUNE1, TW01, CNE1, HK1) and breast (HCC38, MDA-MB-231, MDA-MB-468, SKBR3) cancer cell lines via methyl thiazolyl tetrazolium cell viability assay. Among the tested compounds, isodispar B (**1**) showed a promising dose-dependent and a broad spectrum of cytotoxic effects on all the tested cancer cell lines; in particular, potent inhibitory activities were observed on nasopharyngeal cancer cell lines (SUNE1, TW01, CNE1, HK1), with IC_{50} values ranging from 3.8 to 11.5 µM. In comparison with 5-fluorouracil as positive control, compound **1** was found to exhibit at least sixfold much higher activity than the standard drug used against the nasopharyngeal cell lines. Compound **1** was later found to induce apoptotic cell death in nasopharyngeal

cancer cells, as evidenced by 'Cell Death Detection' ELI-SA[PLUS] kit, and exhibited good cancer-specific cytotoxicity when tested with noncancerous NP460 cells. Meanwhile, compounds **2–12** displayed moderate to weak activities against the tested cancer cell lines. The findings have highlighted the therapeutic potential of compound **1** against nasopharyngeal cancer.

Keywords *Calophyllum* · Antiproliferative activity · Apoptosis · Chromanone acids · Phenylcoumarins

Introduction

Plants from the genus *Calophyllum* are found to be a valuable source of bioactive chromanones, coumarins, xanthones, biflavonoids, and triterpenoids (Oliveira et al., 2014). Ever since the discovery of (+)-calanolide A as an anti-HIV agent from *C. lanigerum* in the early 1990s, there has been a growing interest shown by global scientists in *Calophyllum* species in the search for new chemotherapeutic leads from these plants due to their promising pharmacological properties. (+)-Calanolide A has been reported to exhibit potent activity against human immunodeficiency virus type-1 (HIV-1), and is currently tested in human clinical trials (Cragg and Newman, 2003). Apart from that, preliminary studies had also revealed that plants from this genus exhibited a wide range of biological activities, including antiviral (Ito et al., 1999; Brahmachari and Jash, 2014), cytotoxic (Mah et al., 2015), antimalarial (Hay et al., 2004), antibacterial, (Cuesta-Rubio et al., 2015) and antioxidant activities (Taher et al., 2010).

Cancer is a leading cause of death worldwide. According to estimates from the International Agency for Research on

✉ Chan Kiang Lim
cklim@utar.edu.my

1 Faculty of Science, Universiti Tunku Abdul Rahman, Jalan Universiti, Bandar Barat, Kampar, Perak, Malaysia

2 Centre for Applied Sciences, Faculty of Applied Sciences, Universiti Teknologi MARA, Jalan Meranek, Kota Samarahan, Sarawak, Malaysia

3 School of Medicine, International Medical University, Bukit Jalil, Kuala Lumpur, Malaysia

4 Department of Life Sciences, School of Pharmacy, International Medical University, Bukit Jalil, Kuala Lumpur, Malaysia

5 Department of Pharmaceutical Chemistry, School of Pharmacy, International Medical University, Bukit Jalil, Kuala Lumpur, Malaysia

Cancer, there were 14.1 million new cancer cases and 8.2 million cancer deaths reported in 2012, and the number of cancer deaths is expected to increase to 13.2 million by 2030 (GLOBOCAN, 2012). Although a number of plant-derived anticancer drugs such as vinblastine, vincristine, epipodophyllotoxin, and paclitaxel have been successfully developed over the years, the ability of cancer cells to develop resistance to the drugs during the course of treatment has evoked the need for a continuous search for new drugs with a better efficacy to overcome the drug-resistant problem (Cragg and Newman, 2003). In conjunction with this, investigation has been undertaken by our team on the four Malaysian *Calophyllum* species, namely *C. sclerophyllum*, *C. teysmannii*, *C. castaneum*, and *C. canum*. This work has successfully yielded 12 isolated compounds, including two phenylcoumarins, five chromanone acids, two xanthones, and three triterpenoids. *C. sclerophyllum* afforded isodispar B (**1**), 5,7-dihydroxy-6-(3-methylbutyryl)-4-phenylcoumarin (**2**), and friedelin (**3**); *C. teysmannii* gave caloteysmannic acid (**4**), calolongic acid (**5**), isocalolongic acid (**6**), and stigmasterol (**7**); *C. castaneum* yielded blancoic acid (**8**), isoblancoic acid (**9**), euxanthone (**10**), friedelinol (**11**), and friedelin (**3**); *C. canum* gave ananixanthone (**12**), euxanthone (**10**), friedelinol (**11**), and friedelin (**3**). All these compounds (Fig. 1) were screened for their antiproliferative activities against nasopharyngeal (SUNE1, TW01, CNE1, HK1) and breast (HCC38, MDA-MB-231, MDA-MB-468, SKBR3) cancer cell lines. Interestingly, some of these compounds, particularly with isodispar B (**1**), showed prominent and a broad spectrum of activity against the tested cancer cell lines. The present paper describes the bioactivity-screening results of isolated compounds **1–12** from the four *Calophyllum* species.

Materials and methods

Chemicals

All reagents were of analytical quality and used without further purification unless otherwise specified. Column chromatography (CC) was performed on silica gel 60 (230–300 mesh, Merck) and Sephadex LH-20 (GE Healthcare). Analytical thin-layer chromatography was performed on precoated silica gel 60 F_{254} (Merck). 5-Fluorouracil (purity ≥ 99 %) was purchased from Sigma-Aldrich.

Plant materials

The stem bark materials of *C. sclerophyllum*, *C. teysmannii*, *C. castaneum*, and *C. canum* were collected in April 2013, from the jungle in Landeh district of Sarawak, Malaysia,

and the authentication was carried out by Mr. Tinjan Anak Kuda, botanist from the Forest Department, Sarawak. Voucher specimens (UITM 3008, UITM 3006, UITM 3001, and UITM 3007) were deposited at the herbarium of Universiti Teknologi MARA, Sarawak.

Extraction

The air-dried and powdered stem bark material of *C. sclerophyllum* (1.5 kg), *C. teysmannii* (2.0 kg), *C. castaneum* (2.0 kg), and *C. canum* (2.6 kg) was separately extracted at room temperature with dichloromethane (2 × 10 L) for 72 h. Removal of the solvent under reduced pressure by a rotary evaporator at 40 °C yielded 52, 298, 41, and 125 g of dichloromethane extracts, respectively.

Isolation of compounds from *C. sclerophyllum*

About 50 g of dichloromethane extract was subjected to Si gel CC (40–63 μm, 8.5 × 50 cm, 600 g) packed in *n*-hexane and eluted with *n*-hexane-dichloromethane mixtures of increasing polarity (90:10, 80:20, 70:30, 60:40, 50:50, 40:60, 30:70, 20:80, 10:90, 0:100, each 1 L, 25 mL/min) followed by increasing concentration of acetone in dichloromethane (10:90, 20:80, 30:70, 40:60, 50:50, 60:40, 70:30, 80:20, 90:10, 100:0, each 1 L, 25 mL/min) to give 20 fractions (CSA1–20). From fractions CSA9–10, isodispar B (**1**, 121 mg) was obtained. Fractions CSA12–13 (3.9 g) were combined based on a similar TLC pattern (spots were detected on TLC under ultraviolet (UV) light and in an iodine chamber) and fractionated by Si gel CC (40–63 μm, 3.0 × 50 cm, 110 g) with a gradient of *n*-hexane–EtOAc (90:10, 80:20, 70:30, 60:40, 50:50, 40:60, 30:70, 20:80, 10:90, 0:100, each 0.5 L, 15 mL/min) to give 20 subfractions (CSB1-20). Subfractions CSB2–3 afforded friedelin (**3**, 107 mg). Meanwhile, fractions CSA15–17 (4.2 g) were pooled and subjected to Si gel CC (40–63 μm, 3.0 × 50 cm, 110 g), and eluted with *n*-hexane–acetone (90:10, 80:20, 70:30, 60:40, 50:50, 40:60, 30:70, 20:80, 10:90, 0:100, each 0.5 L, 15 mL/min) to give 20 subfractions (CSC1–20). Subfractions CSC12–14 yielded 5,7-dihydroxy-6-(3-methylbutyryl)-4-phenylcoumarin (**2**, 136 mg).

Isolation of compounds from *C. teysmannii*

About 100 g of dichloromethane extract was subjected to Si gel CC (40–63 μm, 8.5 × 50 cm, 600 g) packed in *n*-hexane and eluted with *n*-hexane–dichloromethane mixtures of increasing polarity (90:10, 80:20, 70:30, 60:40, 50:50, 40:60, 30:70, 20:80, 10:90, 0:100, each 1 L, 25 mL/min), followed by increasing concentration of EtOAc in dichloromethane (10:90, 20:80, 30:70, 40:60,

Fig. 1 Structures of isolated compounds **1–12**
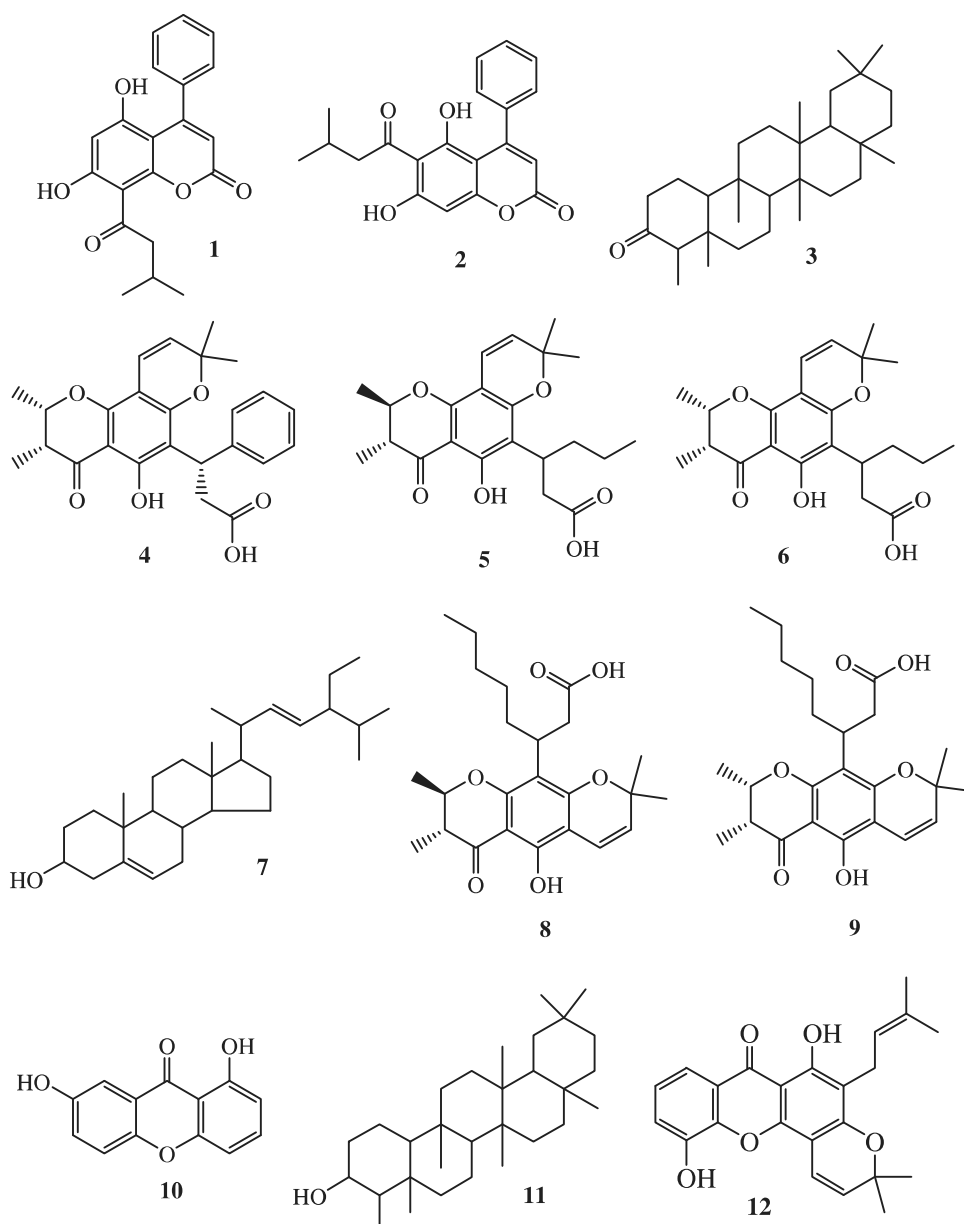
50:50, 60:40, 70:30, 80:20, 90:10, 100:0, each 1 L, 25 mL/min) to give 20 fractions (CTDA1–20). Fraction CTDA14 (6.2 g) was fractionated by Si gel CC (40–63 μm, 3.5 × 50 cm, 150 g) with a gradient of *n*-hexane–acetone (90:10, 80:20, 70:30, 60:40, 50:50, 40:60, 30:70, 20:80, 10:90, 0:100, each 0.5 L, 15 mL/min) to give 20 subfractions (CTDB1–20). Subfractions CTDB14–15 (0.75 g) were combined and further recrystallized in MeOH to afford caloteysmannic acid (**1**, 696 mg) as yellow cubic crystals. From subfractions CTDB4–7, isocalolongic acid (**3**, 1250 mg) was obtained. Meanwhile, fraction CTDA12 (4.8 g) was rechromatographed over Si gel CC (40–63 μm, 3.5 × 50 cm, 150 g) eluted with *n*-hexane–EtOAc (90:10,

80:20, 70:30, 60:40, 50:50, 40:60, 30:70, 20:80, 10:90, 0:100, each 0.5 L, 15 mL/min) to afford 20 subfractions (CTDC1–20). Subfraction CTDC14 (0.4 g) was further fractionated by Si gel CC (40–63 μm, 2.0 × 50 cm, 50 g) with a gradient of *n*-hexane–acetone (90:10, 80:20, 70:30, 60:40, 50:50, 40:60, 30:70, 20:80, 10:90, 0:100, each 0.25 L, 6 mL/min) to give 20 subfractions (CTDD1–20). Subfraction CTDD10 afforded calolongic acid (**2**, 9 mg). Fractions CTDA3–4 (0.5 g) were combined and purified by Si gel CC (40–63 μm, 2.0 × 50 cm, 50 g), and eluted with *n*-hexane–EtOAc (90:10, 80:20, 70:30, 60:40, 50:50, 40:60, 30:70, 20:80, 10:90, 0:100, each 0.25 L, 6 mL/min) to yield stigmasterol (**4**, 7 mg).

Isolation of compounds from *C. castaneum*

About 35 g of dichloromethane extract was subjected to Si gel CC (40–63 μm, 8.5 × 50 cm, 600 g) packed in *n*-hexane and eluted with *n*-hexane-dichloromethane mixtures of increasing polarity (90:10, 80:20, 70:30, 60:40, 50:50, 40:60, 30:70, 20:80, 10:90, 0:100, each 1 L, 25 mL/min), followed by increasing concentration of EtOAc in dichloromethane (10:90, 20:80, 30:70, 40:60, 50:50, 60:40, 70:30, 80:20, 90:10, 100:0, each 1 L, 25 mL/min) to give 20 fractions (CCA1–20). Fractions CCA8–9 (4.0 g) were combined and fractionated by Si gel CC (40–63 μm, 3.0 × 50 cm, 110 g) with a gradient of *n*-hexane-EtOAc (90:10, 80:20, 70:30, 60:40, 50:50, 40:60, 30:70, 20:80, 10:90, 0:100, each 0.5 L, 15 mL/min) to give 20 subfractions (CCB1–20). Subfractions CCB5–6 yielded friedelin (**3**, 163 mg) as colorless needle-like crystals. From subfraction CCB9, friedelinol (**11**, 74 mg) was obtained. Meanwhile, fractions CCA14–15 (4.8 g) were combined and purified by Si gel CC (40–63 μm, 3.0 × 50 cm, 110 g) and eluted with *n*-hexane-acetone (90:10, 80:20, 70:30, 60:40, 50:50, 40:60, 30:70, 20:80, 10:90, 0:100, each 0.5 L, 15 mL/min) to afford 20 subfractions (CCC1–20). Subfractions CCC9–10 (0.5 g) were combined and subjected to Si gel CC (40–63 μm, 2.0 × 50 cm, 50 g), eluted with *n*-hexane–acetone (90:10, 80:20, 70:30, 60:40, 50:50, 40:60, 30:70, 20:80, 10:90, 0:100, each 0.25 L, 6 mL/min) to give 20 subfractions (CCD1–20). Subfractions CCD11–14 (0.03 g) were pooled and purified by sephadex LH-20 CC (2.0 × 50 cm) eluted with dichloromethane–MeOH (10:90, 1 mL/min) to yield euxanthone (**10**, 15 mg). Subfractions CCC12–15 (0.8 g) were combined and rechromatographed over Si gel CC (40–63 μm, 2.0 × 50 cm, 50 g) with a gradient of *n*-hexane-acetone (90:10, 80:20, 70:30, 60:40, 50:50, 40:60, 30:70, 20:80, 10:90, 0:100, each 0.25 L, 6 mL/min) to give 20 subfractions (CCE1–20). Subfractions CCE9–10 yielded blancoic acid (**8**, 283 mg). Lastly, subfractions CCC17–18 (0.7 g) were combined and subjected to sephadex LH-20 CC (3.0 × 50 cm) eluted with dichloromethane–MeOH (10:90, 2 mL/min) to give isoblancoic acid (**9**, 427 mg).

Isolation of compounds from *C. canum*

About 120 g of dichloromethane extract was subjected to Si gel CC (40–63 μm, 8.5 × 50 cm, 600 g) packed in *n*-hexane and eluted with *n*-hexane-dichloromethane mixtures of increasing polarity (90:10, 80:20, 70:30, 60:40, 50:50, 40:60, 30:70, 20:80, 10:90, 0:100, each 1 L, 25 mL/min), followed by increasing concentration of acetone in dichloromethane (10:90, 20:80, 30:70, 40:60, 50:50, 60:40, 70:30, 80:20, 90:10, 100:0, each 1 L, 25 mL/min) to give 20 fractions (CDA1–20). Fractions CDA7–8 (6.5 g) were combined and fractionated by Si gel CC (40–63 μm, 3.5 × 50 cm, 150 g) and eluted with *n*-hexane-EtOAc (90:10, 80:20, 70:30, 60:40, 50:50, 40:60, 30:70, 20:80, 10:90, 0:100, each 0.5 L, 15 mL/min) to give 20 subfractions (CDB1–20). Subfractions CDB 5–6 afforded friedelin (**3**, 1062 mg). From subfractions CDB8–10, friedelinol (**11**, 125 mg) was obtained. Meanwhile, fractions CDA10–13 (7.2 g) were combined and purified by Si gel CC (40–63 μm, 3.5 × 50 cm, 150 g) with a gradient of *n*-hexane–EtOAc (90:10, 80:20, 70:30, 60:40, 50:50, 40:60, 30:70, 20:80, 10:90, 0:100, each 0.5 L, 15 mL/min) to give 20 subfractions (CDC1–20). Subfractions CDC9–11 (0.1 g) were pooled and rechromatographed over sephadex LH-20 CC (2.5 × 50 cm) eluted with dichloromethane–MeOH (10:90, 1 mL/min) to give ananixanthone (**12**, 21 mg) as yellowish needles. Fractions CDA15–18 (6.1 g) were combined and subjected to Si gel CC (40–63 μm, 3.5 × 50 cm, 150 g) and eluted with *n*-hexane–acetone (90:10, 80:20, 70:30, 60:40, 50:50, 40:60, 30:70, 20:80, 10:90, 0:100, each 0.5 L, 15 mL/min) to give 20 subfractions (CDD1–20). Subfractions CDD11–13 (0.1 g) were pooled and purified by sephadex LH-20 CC (2.5 × 50 cm) eluted with 100 % MeOH at 1 mL/min to yield euxanthone (**10**, 12 mg).

Cell lines and cell culture

The nasopharyngeal cancer cells (HK1, CNE1, TW01, and SUNE1) and breast cancer cells (HCC38, MDA-MB-231, MDA-MB-468, and SKBR3) were maintained in RPMI 1640 medium supplemented with 100 IU/mL of penicillin and 100 μg/mL of streptomycin (Sigma–Aldrich). The immortalized normal nasopharyngeal epithelial cells NP460 were kindly provided by Dr. George Tsao, Department of Anatomy, Hong Kong University. NP460 cells were maintained in keratinocyte-SFM containing epidermal growth factor (EGF 1-53) and bovine pituitary extract (BPE) (Invitrogen). All cells were maintained at 37 °C under 5 % CO_2 in a humidified incubator.

Cell proliferation assay

Inhibition of cell proliferation by the isolated compounds was determined by using the methyl thiazolyl tetrazolium (MTT) cell viability assay, as described previously with slight modification (Tan et al., 2013; Low et al., 2012). 5-Fluorouracil was used as a positive control in the assay. Briefly, all isolated compounds and positive control were reconstituted using dimethylsulfoxide (DMSO) (Sigma-Aldrich) to 100 mM and further diluted to the desirable concentrations using ultra purified sterile water just prior to the assays. Cancerous cells ($5 × 10^3$ cells/well) were plated in sterile 96-well plates for 24 h. Cells were treated with the

isolated compounds in a dose-dependent manner for 72 h. The cell growth and anticancer effects were recorded at a test wavelength of 570 nm and a reference wavelength of 630 nm using the Tecan® Infinite F200 plate reader. The results were compiled in a dose-response curve to enable the quantification of IC_{50}, or the concentration of the isolated compounds that inhibits cell proliferation by 50 %. In order to further assess the selectivity of the isolated compounds toward cancerous and noncancerous cells, the above process was also repeated on the noncancerous nasopharyngeal cells (NP460).

Detection of mode of cancer cells deaths by quantitative sandwich enzyme immunoassay (ELISA)

The degree of mode of cancer cell deaths induced by isodispar B (1) was quantified using the Cell Death Detection ELISA^{PLUS} kit (Roche Diagnostics) as per the manufacturer's instruction and as in our previous studies (Mai et al., 2009; Mai et al., 2014). Since nasopharyngeal cancer cells were most sensitive to the treatment, TW01, CNE1, HK1, and SUNE1 cells were seeded at a density of 5×10^3 cells/well on 96-well plates and treated with 1 % DMSO, 1 µM or 10 µM of isodispar B (1) for 3 days. The absorbances were measured at 405 nm using Tecan® Infinite F200 plate reader. Enrichment factors were calculated based on the absorbance of cells treated with compound 1 over absorbance of cells treated with 1 % DMSO.

Results and discussion

The structures of isolated compounds 1–12 (Fig. 1) were established by spectroscopic methods and comparison with literature data (Plattner et al., 1974; Guilet et al., 2001; Lin et al., 2006; Bayma et al., 1998; Dharmaratne et al., 2009; Sousa et al., 2012; Lim et al., 2015). Isolation of isodispar B (1) was previously reported from *C. dispar* (Guilet et al., 2001). Compound 1 has been shown to be a HIV transcription inhibitor by displaying anti-NF-κB and anti-Tat activities (Bedoya et al., 2005). It displayed cytotoxic activities against human SF-268, H-460, MCF-7, and KB cancer cell lines (Guilet et al., 2001; López-Pérez et al., 2005), and antifungal activities (Sandjo et al., 2012). 5,7-Dihydroxy-6-(3-methylbutyryl)-4-phenylcoumarin (2) was previously synthesized and assayed to show anti-inflammatory activity by inhibiting NO production in LPS-induced RAW 264.7 cells (Lin et al., 2006). Friedelin (3), stigmasterol (7), and friedelinol (11) were ubiquitous compounds commonly found in higher plants, which have been extensively studied to show antibacterial (Viswanathan et al., 2012), antifungal (Jain et al., 2001), and

cytotoxic (Csupor-Löffler et al., 2011; Shen et al., 2012) activities. Tesymannic acid (4) isolated from *C. teysmannii* was found to exhibit potent inhibitory activity against HeLa cancer cells (IC_{50} value of 7.3 µM) (Lim et al., 2015). Calolongic acid (5) and isocalolongic acid (6) previously isolated from *C. caledonicum* were both reported to exert strong antifungal activities against *Aspergillus fumigatus*, showing MIC_{80} values of 4 and 2 µg/mL, respectively (Hay et al., 2004). Blancoic acid (8) and isoblancoic acid (9) were previously isolated from *C. brasiliense* (Plattner et al., 1974) and, to our knowledge, there has been no biological activity result reported on these two compounds by far. Euxanthone (10) isolated from *Harungana madagascariensis* was strongly active against the Gram-positive *Bacillus megaterium* (Kouam et al., 2007), and was reported to inhibit HIV-1 reverse transcriptase (Reutrakul et al., 2006) and cytotoxic against human MCF-7, TK-10, and UACC-62 cancer cell lines (Pedro et al., 2002). Ananixanthone (12) previously isolated from *C. caledonicum* has been found to exhibit antifungal activity against *A. fumigatus* (Morel et al., 2002) and demonstrated anti-tobacco mosaic virus (anti-TMV) activities with inhibition rates above 10 % (Wu et al., 2013).

In this study, the in vitro antiproliferative activities of coumarins 1, 2, chromanone acids 4, 5, 6, 8, 9, xanthones 10, 12, triterpenoids 3, 7, 11, and positive control 5-fluorouracil were measured against a panel of nasopharyngeal (SUNE1, TW01, CNE1, HK1) and breast (HCC38, MDA-MB-231, MDA-MB-468, SKBR3) cancer cell lines. The cell viability was assessed using the MTT-dye reduction assay and the corresponding IC_{50} values were calculated as the concentrations of tested compounds leading to 50 % decrease of cell survival (Table 1).

The cytotoxic results indicated that most of the tested compounds showed selective antiproliferative activity against the tested cancer cell lines except for isodispar (1), which displayed a broad spectrum of antiproliferative activities (> 90 % inhibition) against all tested cancer cell lines. More interestingly, compound 1 exerted the highest cytotoxicity among the tested compounds, against nasopharyngeal cancer cell lines (SUNE1, TW01, CNE1, HK1), with IC_{50} values ranging from 3.8 to 11.5 µM (Table 1). This compound demonstrated a greater cytotoxic potency, with at least sixfold much higher activity than the positive control used in the assay. The IC_{50} values of compound 1 against normal nasopharyngeal epithelial cells, NP460, was about 3.8 to 11.5-fold higher than that of nasopharyngeal cancer cells (Table 2). The dose–response curves (Fig. 2a) showed that compound 1 exhibited lower average percentages of cell viability in all nasopharyngeal cancer cells at all concentrations as compared to the normal nasopharyngeal epithelial cells. The cytotoxic effects exhibited by compound 1 were also found to be dose-dependent.

Table 1 Antiproliferative activity of compounds **1–12** against a panel of cancer cell lines

Cell lines	IC$_{50}$ (µM)[a]												5-fluorouracil
	1	2	3	4	5	6	7	8	9	10	11	12	
SUNE1	3.84±0.70	>100	89.80±1.58	54.60±8.44	54.42±1.32	44.09±1.41	60.08±6.32	27.73±0.44	15.19±4.40	69.22±2.37	62.87±0.09	22.80±0.35	32.93±2.17
TW01	11.49±5.48	>100	>100	>100	>100	>100	77.43±3.09	49.54±1.97	24.87±1.68	>100	68.60±1.26	21.38±0.28	69.75±4.45
CNE1	9.74±0.99	>100	76.42±3.14	81.57±1.15	84.39±0.11	40.78±3.47	71.28±2.60	33.66±0.87	38.89±0.42	75.27±1.73	64.54±0.22	20.68±3.87	73.13±3.33
HK1	5.58±0.48	>100	81.68±1.32	65.99±8.13	75.93±1.10	71.89±0.66	55.43±0.22	48.96±0.22	25.86±2.22	66.15±1.31	55.28±2.32	29.45±1.76	>100
HCC38	56.73±3.88	>100	58.60±1.83	60.96±0.82	>100	>100	>100	>100	>100	71.84±4.70	>100	>100	63.30±5.60
MDA-MB-231	52.69±2.95	>100	>100	79.20±5.63	>100	>100	>100	>100	90.16±1.56	71.13±0.70	57.70±0.87	>100	33.25±1.11
MDA-MB-468	52.75±3.95	>100	20.56±3.79	53.14±2.95	>100	>100	99.80±1.50	>100	77.52±2.65	62.01±1.81	>100	>100	56.29±2.77
SKBR3	54.85±3.92	>100	58.07±8.86	54.04±2.93	>100	65.11±1.77	>100	>100	71.01±2.70	68.29±1.73	>100	>100	92.20±6.55

[a] Data are reported as means ± SD for minimum three independent experiments

Microscopic observation (Fig. 2b) showed no significant morphological change in NP460 cells treated with 10 µM of compound **1**, as compared to NP460 cells treated with negative control (1 % DMSO). These results further confirmed that compound **1** induced cancer-specific cytotoxicity, sparing the noncancer cells. In addition, a great reduction in the number of viable nasopharyngeal cancer cells treated with compound **1** was observed (Fig. 2b). Comparing with nasopharyngeal cancer cells treated with 1 % DMSO, cancer cells treated with compound **1** was shrunken and round in shape (Fig. 2b). This microscopic observation suggests that the shrunken and round-shaped cancer cells were the apoptotic bodies, which resulted from the preferred apoptotic program cell death (Ziegler and Groscurth, 2004; Elmore, 2007; Saraste and Pulkki, 2000). In order to confirm the mode of cell death as observed in Fig. 2b, nasopharyngeal cells were treated with 1 % DMSO, 1 and 10 µM of isodispar B (**1**) for 72 h. Apoptosis inductions by compound **1** were measured using the Cell Death Detection ELISA^{PLUS} (Roche, Germany). The results showed that compound **1** induced a significantly higher percentage of apoptosis ($p < 0.05$) as compared with cells treated with 1 % DMSO in all nasopharyngeal cancer cells. The effects were also dose-dependent. The apoptotic induction effects were most significant in SUNE1 cells, followed by HK1, CNE1, and TW01 (Fig. 3). These results correlated with the IC$_{50}$ induced by compound **1** on nasopharyngeal cancer cells, in which SUNE1 cells were also the most sensitive nasopharyngeal cancer cells (Table 2). Apart from that, ananixanthone (**12**) and isoblancoic acid (**9**) also displayed significant cytotoxicity against nasopharyngeal cancer cell lines with IC$_{50}$ values of less than 40 µM.

SAR study revealed that the presence of isovaleryl group at different key positions on coumarin nucleus imparts determinant effect on antiproliferative activities against the nasopharyngeal cancer cell lines. Compound **1** with an isovaleryl group linked at C-8 position showed potent inhibitory activities against the cancer cell lines. On the contrary, the presence of isovaleryl moiety at C-6 position in compound **2** was found to be totally devoid of activity against the same panel of cancer cell lines. In the present study, the biological role of isovaleryl group in compound **1** remained unknown. However, the presence of isovaleryl group was found to be essential for cytotoxicity. Apart from that, ananixanthone (**12**) was reported to trigger a much greater cytotoxic potency (IC$_{50}$ values of 20.7–29.5 µM) than euxanthone (**10**) (IC$_{50}$ values of 66.1 µM and above) against the nasopharyngeal cancer cell lines, suggesting the importance of prenyl and pyrano moieties in compound **12** for the studied effect on the cancer cell lines, and this was in agreement with the literature (Lim et al, 2011).
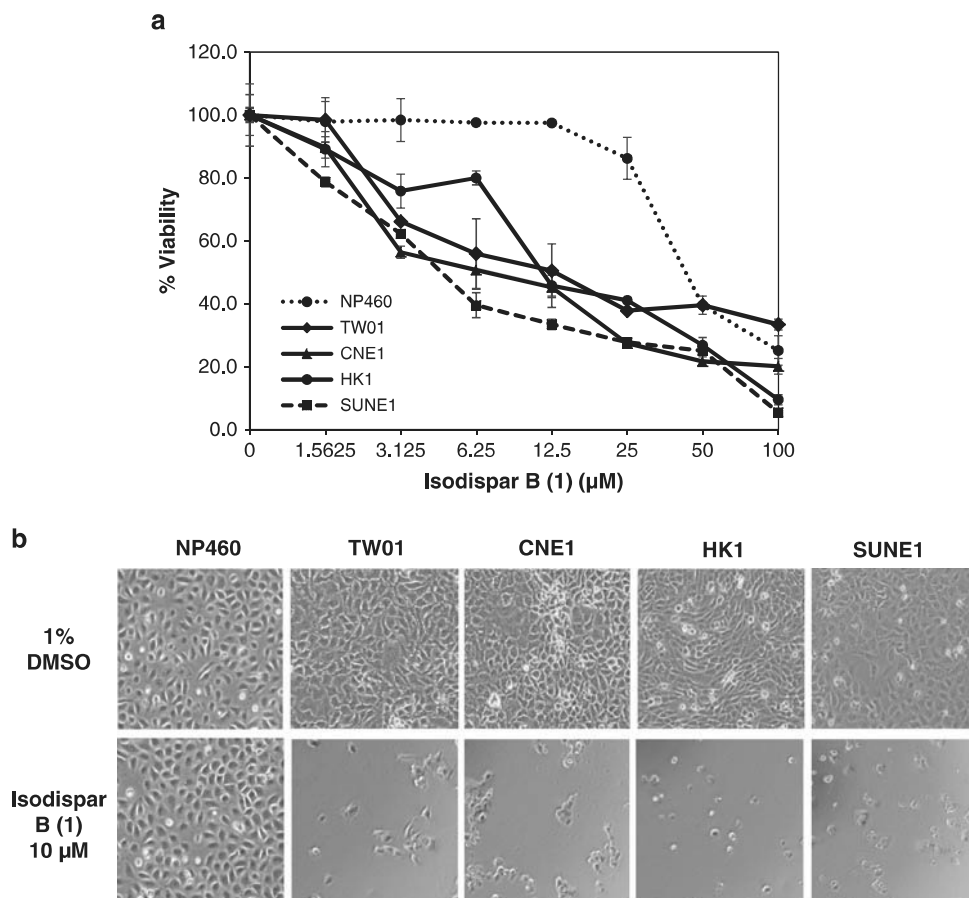
Among chromanone acids **4**, **5**, **6**, **8**, and **9** tested, isoblancoic acid (**9**) showed the highest cytotoxicity toward HK1, TW01, and SUNE1 cancer lines, giving IC$_{50}$ values below 30 μM. On the other hand, blancoic acid (**8**), which

Table 2 The selective ratios of isodispar B (**1**) in SUNE1, TW01, CNE1, and HK1

Cell lines		Isodispar B (**1**), IC$_{50}$ (μM)	Cancer selectivity ratio
Noncancerous	NP460	44.36 ± 4.59	—
Cancerous	SUNE1	3.84 ± 0.70	11.55
	TW01	11.49 ± 5.48	3.86
	CNE1	9.74 ± 0.99	4.56
	HK1	5.58 ± 0.05	7.95

Isodispar B (**1**) was tested in twofold dilution dose curves in all cell lines. The table lists the concentration (in μM) required to achieve 50 % inhibition of MTT cell viability (IC$_{50}$) for **1** in each cell line. The IC$_{50}$ in noncancer nasopharyngeal cells (NP460) was divided by the IC$_{50}$ in nasopharyngeal cancer cells (SUNE1, TW01, CNE1, or HK1) to obtain a cancer selectivity ratio for each compound. The higher the cancer selectivity ratio, the more the selectivity of **1** toward cancer cells than the noncancer cells
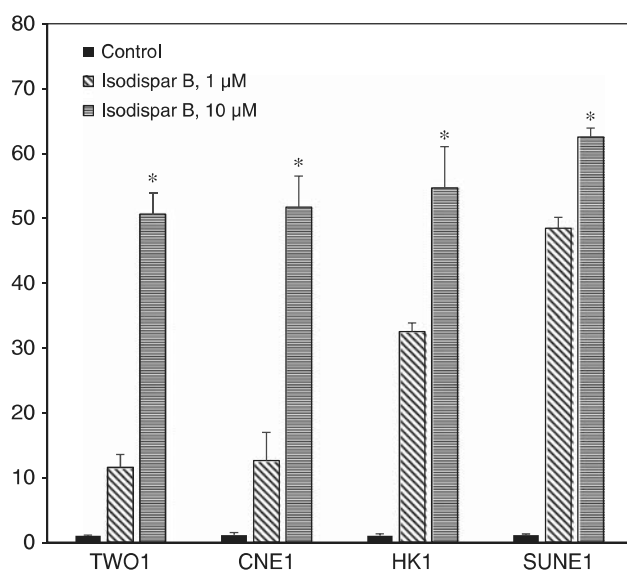
is the stereoisomer of compound **9**, exhibited a much weaker inhibitory activity against the cancer cell lines, indicating the substantial role played by the stereochemistry of compounds on growth inhibition. Compound **8** showed *trans*-2,3-dimethyl substitution on the chomanone ring, which was different from compound **9** with a *cis*-2,3-dimethyl substitution. In the case of triterpenoids **3**, **7**, and **11** tested, stigmasterol (**7**) with a steroidal skeleton demonstrated a more selective activity than those of friedelane triterpenoids **3** and **11** in the assay. In comparison with the phenolic compounds tested, friedelin (**3**) gave the highest inhibitory activity against MDA-MB-468 cancer cells with IC$_{50}$ values of 20.6 μM. However, these triterpenoids were not suitable for drug development because of their poor pharmacodynamic and pharmacokinetic properties.

Conclusions

Twelve chemical constituents, **1–12**, isolated from four Malaysian *Calophyllum* species were evaluated for their cytotoxic activity against a panel of nasopharyngeal (SUNE1, TW01, CNE1, HK1) and breast (HCC38,

Fig. 2 **a** The dose-response curve of isodispar B (**1**) against nasopharyngeal cancer cells (TW01, CNE1, HK1, and SUNE1) and noncancerous nasopharyngeal cells (NP460). Cell viability was determined 72 h after treatment using MTT assay. Points represent mean ± standard deviation from minimum three independent experiments. Statistical analysis was performed using one-way analysis of variance (ANOVA) post hoc Dunnett *t*-test using SPSS 18.0. Statistically significant differences (*p* < 0.05) are expressed as * as compared to control (1 % DMSO). **b** Morphological changes in all the cells upon treatment with **1** using inverted phase-contrast microscopy (10×) 72 h after treatment with 10 μM of **1**

Fig. 3 Apoptotic induction effect of isodispar B (**1**) on nasopharyngeal cancer cells (TW01, CNE1, HK1, and SUNE1). Cells were treated with compound **1** with 1 % DMSO, 1 or 10 µM for 72 h. Apoptosis induction by compound **1** was measured using the Cell Death Detection ELISA^{PLUS} (Roche, Germany). All data were reported as mean ± standard deviation from minimum three independent experiments. Statistical analysis was performed using one-way analysis of variance (ANOVA) post hoc Dunnett t-test using SPSS 18.0. Statistically significant differences ($p < 0.05$) are expressed as * as compared to control (1 % DMSO)

MDA-MB-231, MDA-MB-468, SKBR3) cancer cell lines, and were found to exhibit strong to weak inhibitory activities in the assay. Among these compounds, isodispar B (**1**) showed the most promising result; in particular, potent inhibitory activities were observed on nasopharyngeal cancer cell lines (SUNE1, TW01, CNE1, HK1), with IC$_{50}$ values ranging from 3.8 to 11.5 µM. This compound was found to induce apoptotic cell death in nasopharyngeal cancer cells and exhibited good cancer-specific cytotoxicity when tested with noncancerous NP460 cells. The findings in the present study might be important in development of a new drug lead against nasopharyngeal cancer.

Compliance with ethical standards

Conflict of interest The authors declare that they have no conflict of interests.

References

Bayma JC, Arruda MSP, Neto MS (1998) A prenylatedxanthone from the bark of *Symphonia globulifera*. Phytochemistry 49:1159–1160

Bedoya LM, Beltrán M, Sancho R, Olmedo DA, Sánchez-Palomino S, Olmo E, López-Pérez JL, Muñoz E, Feliciano AS, Alcamí J (2005) 4-Phenylcoumarins as HIV transcription inhibitors. Bioorg Med Chem Lett 15:4447–4450

Brahmachari G, Jash SK (2014) Naturally occurring calanolides: an update on their anti-HIV potential and total syntheses. Recent Pat Biotechnol 8:3–16

Cragg GM, Newman DJ (2003) Plants as a source of anti-cancer and anti-HIV agents. Ann Appl Biol 143:127–133

Csupor-Löffler B, Hajdú Z, Zupkó I, Molnár J, Forgo P, Vasas A, Kele Z, Hohmann J (2011) Antiproliferative constituents of the roots of *Conyza canadiensis*. Planta Med 77:1183–1188

Cuesta-Rubio O, Oubada A, Bello A, Maes L, Cos P, Monzote L (2015) Antimicrobial assessment of resins from *Calophyllum Antillanum* and *Calophyllum Inophyllum*. Phytother Res 29:1991–1994

Dharmaratne HRW, Napagoda MT, Tennakoon SB (2009) Xanthones from roots of *Calophyllum thwaitesii* and their bioactivity. Nat Prod Res A: Struct Synth 23:539–545

Elmore S (2007) Apoptosis: a review of programmed cell death. Toxicol Pathol 35:495–516

GLOBOCAN (2012) Cancer incidence and mortality worldwide: IARC CancerBase No. 11. http://globocan.iarc.fr. Accessed 16 July 2015

Guilet D, Séraphin D, Rondeau D, Richomme P, Bruneton J (2001) Cytotoxic coumarins from *Calophyllum dispar*. Phytochemistry 58:571–575

Hay AE, Hélesbeux JJ, Duval O, Labaïed M, Grellier P, Richomme P (2004) Antimalarial xanthones from *Calophyllum caledonicum* and *Garcinia vieillardii*. Life Sci 75:3077–3085

Ito C, Itoigawa M, Furukawa H, Tokuda H, Okuda Y, Mukainaka T, Okuda M, Nishino H (1999) Anti-tumor-promoting effects of 8-substituted 7-methoxycoumarins on Epstein-Barr virus activation assay. Cancer Lett 138:87–92

Jain SC, Singh B, Jain R (2001) Antimicrobial activity of triterpenoids from *Heliotropium ellipticum*. Fitoterapia 72:666–668

Kouam SF, Yapna DB, Krohn K, Ngadjui BT, Ngoupayo J, Choudhary MI, Schulz B (2007) Antimicrobial prenylatedanthracene derivatives from the leaves of *Harungana madagascariensis*. J Nat Prod 70:600–603

Lim CK, Subramaniam H, Say YH, Jong VY, Khaledi H, Chee CF (2015) A new chromanone acid from the stem bark of *Calophyllum teysmannii*. Nat Prod Res 29:1970–1977

Lim CK, Tho LY, Lim CH, Lim YM, Shah SAA, Weber JFF (2011) Synthesis and SAR study of prenylatedxanthone analogues as HeLa and MDA-MB-231 cancer cell inhibitors. Lett Drug Des Disc 8:523–528

Lin CM, Huang ST, Lee FW, Kuo HS, Lin MH (2006) 6-Acyl-4-aryl/alkyl-5,7-dihydroxycoumarins as anti-inflammatory agents. Bioorg Med Chem 14:4402–4409

López-Pérez JL, Olmedo DA, Olmo E, Vásquez Y, Solís PN, Gupta MP, Feliciano AS (2005) Cytotoxic 4-phenylcoumarins from the leaves of *Marila pluricostata*. J Nat Prod 68:369–373

Low SY, Tan BS, Choo HL, Tiong KH, Khoo AS, Leong CO (2012) Suppression of BCL-2 synergizes cisplatin sensitivity in nasopharyngeal carcinoma cells. Cancer Lett 314:166–175

Mah SH, Ee GCL, Teh SS, Sukari MA (2015) *Calophyllum inophyllum* and *Calophyllum soulattri* source of anti-proliferative xanthones and their structure–activity relationships. Nat Prod Res 29:98–101

Mai CW, Pakirisamy P, Tay EF, Subramaniam S, Shamsuddin ZH, Pichika MR (2009) Nasopharyngeal carcinoma cell proliferation and apoptosis induced by the standardised ethanolic extracts of *Mucuna bracteata*. Malays J Chem 11:143–148

Mai CW, Yaeghoobi M, Abd-Rahman N, Kang YB, Pichika MR (2014) Chalcones with electron-withdrawing and electron-donating substituents: anticancer activity against TRAIL resistant cancer cells, structure-activity relationship analysis and regulation of apoptotic proteins. Eur J Med Chem 77C:378–387

Morel C, Séraphin D, Teyrouz A, Larcher G, Bouchara JP, Litaudon M, Richomme P, Bruneton J (2002) New and antifungal xanthones from *Calophyllum caledonicum*. Planta Med 68:41–44

Oliveira MC, Lemos LMS, de Oliveira RG, Dall'Oglio EL, de Sousa Júnior PT, de Oliveira Martins DT (2014) Evaluation of toxicity of *Calophyllum brasiliense* stem bark extract by *in vivo* and *in vitro* assays. J Ethnopharmacol 155:30–38

Pedro M, Cerqueira F, Sousa ME, Nascimentoa MSJ, Pinto M (2002) Xanthones as inhibitors of growth of human cancer cell lines and their effects on the proliferation of human lymphocytes in vitro. Bioorg Med Chem 10:3725–3730

Plattner RD, Spencer GF, Weisleder D, Kleiman R (1974) Chromanone acids in *Calophyllum brasiliense seed oil*. Phytochemistry 13:2597–2602

Reutrakul V, Chanakul W, Pohmakotr M, Jaipetch T, Yoosook C, Kasisit J, Napaswat C, Santisuk T, Prabpai S, Kongsaeree P, Tuchinda P (2006) Anti-HIV-1 constituents from leaves and twigs of *Cratoxylum arborescens*. Planta Med 72:1433–1435

Sandjo LP, Foster AJ, Rheinheimer J, Anke H, Opatz T, Thines E (2012) Coumarin derivatives from *Pedilanthus tithymaloides* as inhibitors of conidial germination in *Magnaporthe oryzae*. Tetrahedron Lett 53:2153–2156

Saraste A, Pulkki K (2000) Morphologic and biochemical hallmarks of apoptosis. Cardiovasc Res 45:528–537

Shen T, Zhang L, Wang YY, Fan PH, Wang XN, Lin ZM, Lou HX (2012) Steroids from *Commiphora mukul* display antiproliferative effect against human prostate cancer PC3 cells via induction of apoptosis. Bioorg Med Chem Lett 22:4801–4806

Sousa GF, Duarte LP, Alcantara AFC, Silva GDF, Vieira-Filho SA, Silva RR, Oliveira DM, Takahashi JA (2012) New triterpenes from *Maytenus robusta*: structural elucidation based on NMR experimental data and theoretical calculations. Molecules 17:13439–13456

Taher M, Attoumani N, Susanti D, Ichwan SJA, Ahmad F (2010) Antioxidant activity of leaves of *Calophyllum rubiginosum*. Am J Appl Sci 7:1305–1309

Tan BS, Kang O, Mai CW, Tiong KH, Khoo AS, Pichika MR, Bradshaw TD, Leong CO (2013) 6-Shogaol inhibits breast and colon cancer cell proliferation through activation of peroxisomal proliferator activated receptor gamma (PPARgamma). Cancer Lett 336:127–139

Viswanathan MB, Ananthi JDJ, Kumar PS (2012) Antimicrobial activity of bioactive compounds and leaf extracts in *Jatropha tanjorensis*. Fitoterapia 83:1153–1159

Wu YP, Zhao W, Xia ZY, Kong GH, Lu XP, Hu QF, Gao XM (2013) Three new xanthones from the stems of *Garcinia oligantha* and their anti-TMV activity. Phytochem Lett 6:629–632

Ziegler U, Groscurth P (2004) Morphological features of cell death. News Physiol Sci 19:124–128

Original Research Article

Anti-obesity effect of phenylcoumarins from two Calophyllum spp in 3T3-L1 adipocytes

Siroshini Thiagarajan[1], Fui-Lu Yong[2], Hemaroopini Subramaniam[2], Vivien Yi-Mian Jong[3], Chan-Kiang Lim[2] and Yee-How Say[1]*

[1]Department of Biomedical Science, [2]Department of Chemical Science, Faculty of Science, Universiti Tunku Abdul Rahman (UTAR) Kampar Campus, Kampar, Perak, [3]Centre for Applied Sciences, Faculty of Applied Sciences, Universiti Teknologi MARA Samarahan Campus 2, Kota Samarahan, Sarawak, Malaysia

*For correspondence: **Email:** sayyh@utar.edu.my; **Tel:** +605-4688888 ext. 4505; **Fax:** +605-4661676

Abstract

Purpose: To evaluate the anti-obesity effects of five compounds isolated from Calophyllum andersonnii and Calophyllum sclerophyllum, viz, friedelin (CP1), friedelinol (CP2), isodispar B (CP3), 5,7-dihydroxy-6-(3-methybutyryl)-4-phenylcoumarin (CP4) and 5,7-dihydroxy-6-(2-methybutyryl)-4-phenylcoumarin (CP5) in 3T3-L1 mouse pre-adipocytes.
Methods: Maximum non-toxic doses (MNTDs) of CP1 - CP5 were obtained by conducting 3-(4,5-dimethylthiazol-2-yl)-2,5-diphenyltetrazolium bromide (MTT) assay. Intracellular lipid droplet accumulation was determined by Oil Red O (ORO) staining. The effects of CP1 - 5 on the expression of adipogenesis transcriptional factors, namely, C/ebpα, Pparγ1, aP2 and on cellular glucose uptake and adipokine (adiponectin, leptin, resistin) secretion were assessed by commercial colorimetric and ELISA kits, respectively.
Results: MNTDs for CP1-CP5 were 3.0, 1.4, 1.0, 29.0 and 25.0 µM, respectively. 3T3-L1 cells treated with CP1 - CP3 showed increased lipid accumulation (p < 0.05) and decreased glucose uptake (p < 0.05), compared with untreated cells; cells treated with CP4 and CP5 had opposite effects. Cells treated with CP4 and CP5 also showed downregulated Pparγ1, C/ebpα and aP2 expression (p < 0.05), compared with untreated cells. The anti-adipogenic property exerted by CP4 and CP5 manifested as increased secretion of adiponectin as well as reduced leptin and resistin levels.
Conclusion: CP4 and CP5 isolated from Calophyllum sclerophyllum show promising anti-obesity properties, and could serve as candidate hits for further investigation at in vivo level to provide additional mechanistic evidence.

Keywords: Phenylcoumarin, Calophyllum, Adipogenesis, Adipocyte, Adipokine, Obesity

INTRODUCTION

The genus *Calophyllum*, commonly known as "bintangor" or "penaga" in Malay, is a large group of tropical trees made up of around 200 different species [1]. Numerous *Calophyllum* species have been used in folk medicine. In Malaysia, the seed oil is used as a remedy for ulcer and rheumatism ailments. Moreover, Dweck and Meadows [2]

reported the wound-healing property of *Calophyllum* seed oil after applying on scars. An infusion of the leaves is used to treat inflamed eyes.

Further pharmacological research on this genus has further revealed a variety of biological activities exhibited by these plants, such as anti-HIV, antibacterial, antimalarial, antioxidant,

antitumor-promoting, and cytotoxic activities [3]. These biological activities have been attributed to phytochemicals such as xanthones, coumarins, chomanones (flavonoids, biflavonoids), terpenes and steroids [3].

Isolation of phytochemicals from *Calophyllum andersonnii* and *Calophyllum sclerophyllum* (native in the jungle of Landeh, Sarawak, Borneo Malaysia) yielded two classes, namely triterpenoids (friedelin, freidelinol) and coumarins (isodispar B, 5,7-Dihydroxy-6-(3-methybutyryl)-4-phenylcoumarin and 5,7-Dihydroxy-6-(2-methybutyryl)-4-phenylcoumarin)[4]. These phytochemicals could have potential adipogenic modulatory effects, as previous studies have shown that friedelin and freidelinol isolated from other plants have pro-adipogenic effects [5,6] while esculetin, a coumarin, has anti-adipogenic effect [7,8].

Therefore, the objective of this study was to investigate if the five triterpenoids and coumarins above would have the same pro-/anti-adipogenic effects on a differentiated mouse pre-adipocyte cell line, 3T3-L1. Adipogenic parameters assessed included intracelluar lipid droplet accumulation, glucose uptake, gene expression of adipogenic transcription factors and secretion of adipokines.

EXPERIMENTAL

Plant, isolation and characterization of compounds

Triterpenoids - friedelin (compound **3**) and friedelinol (compound **11**) were isolated from *Calophyllum andersonnii*, while coumarins - isodispar B (compound **1**), 5,7-Dihydroxy-6-(3-methybutyryl)-4-phenylcoumarin (compound **2**) and 5,7-Dihydroxy-6-(2-methybutyryl)-4-phenylcoumarin] were isolated from *Calophyllum sclerophyllum* [4] The detailed steps involved in the isolation and characterization of the compounds used in this study are as described previously [4]. Figure 1 shows the structure, codes and molecular weights of the five compounds.
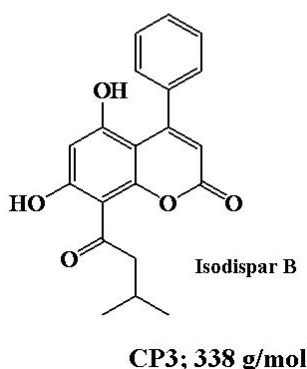
Cell culture

Mus musculus mouse fibroblast cell line 3T3-L1 (ATCC® CL-173™) was obtained from the American Type Culture Collection (Manassas, VA, U.S.A.). Methods to differentiate 3T3-L1 pre-adipocytes were achieved according to ATCC protocol. Seeded cells were maintained in pre-adipocyte expansion medium [90 % Dulbelcco's Modified Eagle's Medium (DMEM; Thermo Fischer Scientific PA, USA),

Triterpenoids

Frieddin

CP1; 426 g/mol

Friedelinol

CP2; 428 g/mol

Coumarins

Isodispar B

CP3; 338 g/mol

5,7-Dihydroxy-6-(3-methylbutyryl)-4-phenylcoumarin

CP4; 338 g/mol

5,7-Dihydroxy-6-(2-methylbutyryl)-4-phenylcoumarin

CP5; 338 g/mol
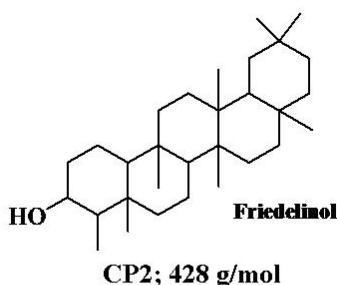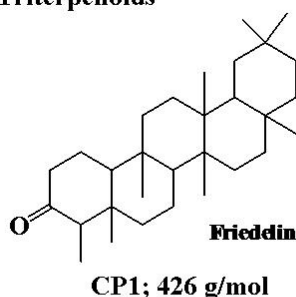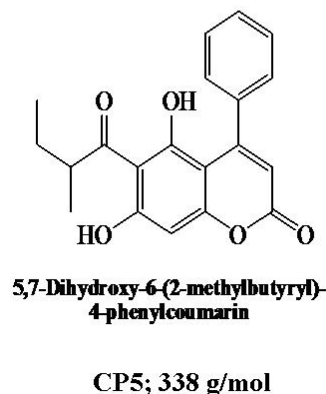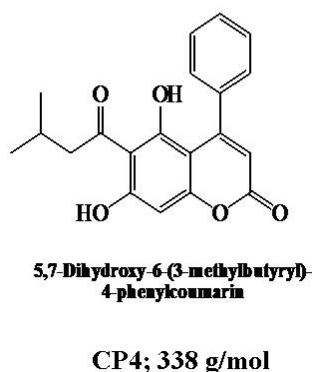
Figure 1: Structure, molecular weight (g/mol) and codes of five selected compounds used in this study

10 % Fetal Bovine Serum (FBS; Sigma-Aldrich, MO, USA)] by incubating them at 37 °C in a 5 % humidified CO_2 incubator for 48 h until 100 % confluence was achieved (day 0). To induce differentiation, cells were incubated with differentiation medium [90 % DMEM, 10 % FBS, 0.5 mM 3-isobutyl-1-methylxanthine (Merck KGaA, Germany), 0.25 µM dexamethasone (Merck KGaA, Germany), 1 µg/mL insulin (Nacalai Tesque, Japan) and 2 µM rosiglitazone (Nacalai Tesque, Japan)] for 72 h (day 3). Cells were then maintained in adipocyte maintenance medium (90 % DMEM, 10 % FBS and 1 µg/mL insulin) for another 2 d (day 5), which was subsequently changed every 2 d. At day 10, the cells were fully differentiated after induction and subsequent bioassays were performed.

Determination of maximum non-toxic dose (MNTD)

A total of 2500 3T3-L1 pre-adipocytes cells/well were plated in 96-well plates. At 70 % confluence, the cells were treated with the test compounds (0, 1.875, 3.75, 7.5, 15, 30 and 60 µM), dissolved in dimethyl sulfoxide (DMSO). Cell viability was assessed by 3-(4,5-dimethylthiazol-2-yl)-2.5-diphenyltetrazolium bromide (MTT) assay. The cells were incubated for 48 h at 37 ºC in humidified 5 % CO_2. After 48 h, cells were rinsed twice with phosphate buffer saline (PBS). Twenty microliters of 5 mg/mL MTT (Bio Basic Canada Inc, Canada) stock solution were added to each well, further incubated at 37 ºC for 4 h, before the addition of 100 µL DMSO to solubilize the purple formazan crystals. After 1 h of incubation, the absorbance was measured at 570 nm using a microplate reader (M200 Tecan, Switzerland). A graph of percentage of toxicity against the $\log_{10}$ concentration of phytochemicals was plotted to determine the MNTD or ½ MNTD of the compounds. MNTD was determined at the first *x*-intercept where the toxicity is 0 %, while ½MNTD was half of the MNTD selected. These dosages were then added together in the differentiation medium at day 0 of differentiation as described in 'Cell Culture'.

Determination of intracellular lipid droplet accumulation

Eight days (day 10) after the induction of differentiation, the cells were rinsed three times with PBS. After fixation with paraformaldehyde (Sigma-Aldrich, MO, USA) for 1 h, the cells were rinsed with PBS and then stained with freshly diluted ORO solution [3 parts 0.5 % ORO (R&M Chemicals, UK) in isopropyl alcohol and 2 parts of water] for 30 min. The cells were then rinsed twice with water and visualized and

photographed using an inverted phase contrast microscope (TS100, Nikon Eclipse, Japan). ORO stain was dissolved in isopropyl alcohol for quantitative analysis, and absorbance at 520 nm was measured using a microplate reader (M200, Tecan, Switzerland).

Glucose uptake assay

Glucose uptake was measured using glucose uptake assay kit (Abnova, Taiwan) according to manufacturer's instructions. First, 3T3-L1 cells were plated in 96-well plate and differentiated, and at day 10 the differentiated cells were starved for 12 h without the addition of FBS to the basic medium. The cells were then treated with insulin (100 nM), metformin (1 mM; Sigma-Aldrich, MO, USA), MNTDs of CP1-CP5 and 2-deoxyglucose (2-DG) (negative control), for 1 h. Cellular 2-DG uptake was then measured by monitoring OD ratio increase at 570/610 using a microplate reader. The OD ratio for 2-DG (negative control) was normalised at 1000 µM.

Measurement of adipokine concentration

After treatments, conditioned media were collected and cells were then rinsed with ice-cold PBS twice and lysed with 10 µL of lysis buffer [10 mM Tris/HCl, pH 7.8, 100 mM NaCl, 0.5 % (w/v) sodium deoxycholate, 0.05 % (v/v) nonidet-P40, 10 mM EDTA, 0.1 mM PMSF] added with 1 µL of protein inhibitor cocktail (Thermo Fischer Scientific PA, USA). Subsequently, concentrations of mouse leptin, resistin and adiponectin in the conditioned medium and cell lysates were determined using commercial ELISA kits (CUSABIO, China) according to manufacturer's instructions. Protein concentrations of media and cell lysates were also measured by bicinchoninic acid protein assay kit (Thermo Fischer Scientific PA, USA) and adipokine concentrations were normalized per total extracted proteins.

Determination of gene expression of adipogenesis markers

The gene expression of three common adipogenesis markers namely mouse nuclear receptor peroxisome proliferator-activated receptor gamma 1 (*Pparγ1*), CCAAT/enhancer binding protein-alpha (*C/ebpα*), and adipocyte fatty acid-binding protein (*aP2*) was assessed by semi-quantitative reverse transcription-polymerase chain reaction (RT-PCR). Total RNA was extracted from the 3T3-L1 adipocyte cells using EZ 10 Spin Column animal total RNA extraction kit (Bio Basic Canada Inc., Canada) according to manufacturer's instructions. RNA

purity and concentration were determined using a nanospectrophotometer (IMPLEM, Germany) at absorbance of 260 and 280 nm. The integrity of total RNA extracted was assessed by using 1 %(w/v) agarose gel electrophoresis and denaturing agent formamide. The primer sequences for RT-PCR were adopted from [8,9]. RT-PCR was performed using Realhelix™ RT-PCR Kit (Nanohelix, Korea) according to manufacturer's instructions on Bio-Rad CFX-96T RT-PCR machine following this protocol: 1 cycle of cDNA synthesis at 55 °C for 50 min; 1 cycle of initial-denaturation at 95 °C for 15 min; 30 cycles of denaturation at 95 °C for 20 s, annealing at 53, 57, 57 and 62°C for *C/ebpα, Pparγ1, aP2, β-actin,* respectively, for 40 s and extension at 72 °C for 40 s and a final cycle of post extension at 72 °C for 5 min. PCR products were resolved by 1.8 % agarose gel electrophoresis, stained with Gel Red® dye (Biotium, CA, USA) and visualized with BIO-RAD Gel Doc image analysis software (BIO-RAD Laboratories Inc., CA, USA). Densitometry was performed using NIH Image J software.

Statistical analysis

The results are expressed as mean ± standard error of the mean (SEM) of at least two independent experiments performed in at least triplicate, unless otherwise stated. Statistical analysis was performed using Student's *t*-test for comparison between two means using IBM SPSS Statistics software version 16.0 (IBM, NY, USA). A *p*-value < 0.05 was considered as statistically significant.

RESULTS

MNTD and ½ MNTD of the compounds

In the graph of cytotoxicity percentage in 3T3-L1 pre-adipocytes against log CP1-CP5 concentrations (Figure 2), the percentage of cytotoxicity for CP1, CP2 and CP5 showed fluctuations across concentrations while the percentage of cytotoxicity for CP3 and CP4 showed an increasing trend across concentrations.. However, cell death was not evident at concentrations below 3.75 µM, for CP1 and CP2; and at concentrations below 30 µM for CP3 and CP4 (Figure 2). MNTDs of CP1, CP2, CP3, CP4 and CP5 were 3.00, 1.44, 1.04, 29.0 and 25.0 µM, respectively, while their ½MNTDs were 1.50, 0.72, 0.52, 14.5 and 12.5 µM, respectively. Overall, cytotoxicity of CP3 was the highest, and triterpenoids CP1 and CP2 were up to 20-folds more cytotoxic than phenylcoumarins CP4 and CP5.

Phenylcoumarins inhibit intracellular lipid accumulation

As an evidence of adipogenesis, copious ORO dye stained material accumulated in differentiated 3T3-L1 adipocytes (positive control) while no staining was detected in 3T3-L1 preadipocytes (negative control, Figure 3A). Compared to the negative control, cells treated with MNTDs and ½ MNTDs of CP1 - CP3 showed higher accumulation of dye-stained material; CP4 and CP5 showed opposite effects (Figure 3A). A 100× magnification of the cells revealed larger adipocytes for CP1 - CP3 (indicating higher lipid droplet accumulation), while the opposite was observed for CP4 - CP5 (Figure 3B).

As shown in Figure 3C and D, there was almost 50 % less lipid accumulation in non-differentiated 3T3-L1 cells compared with differentiated cells. CP2 and CP3 at both doses significantly increased lipid accumulation compared with the positive control, while CP4 and CP5 at both doses decreased lipid accumulation of up to 0.7-fold, albeit with statistical significance for the latter compound. Taken together, this implies that CP4 and CP5 would indeed attenuate adipocyte differentiation.

Phenylcoumarins promote cellular glucose uptake in 3T3-L1 adipocytes

As shown in Figure 4, treatment with insulin and with insulin + metformin (a type II diabetes mellitus drug) significantly increased cellular uptake of glucose in 3T3-L1 adipocytes. Treatment with MNTDs of CP1, CP2 and CP3 significantly decreased cellular glucose uptake compared with insulin-treated cells. On the other hand, CP4 and CP5 significantly stimulated cellular glucose uptake compared with insulin-treated cells, but still the amount was still lesser than the synergistic effect of insulin + metformin (Figure 4). These indicate that phenylcoumarins CP4 and CP5 promote cellular glucose uptake in 3T3-L1 adipocytes, comparable with the effect of insulin.

Phenylcoumarins inhibit adipogenesis by reducing gene expression of *C/ebpα, Pparγ1* and *aP2*

As shown in Figure 5, cells treated with CP1, CP2 and CP3 presented significant increases in the expression of adipocyte-specific transcription factors when compared with the untreated cells.

Specifically, cells treated with CP2 had the highest expression of *C/ebpα* and *Pparγ1*. Adipocyte specific transcriptional factor, *aP2* showed the highest expression when cells were treated with CP1, which was about 18 % higher compared to the control (Figure 5). On the other hand, cells treated with CP4 and CP5 showed significant down-regulation of the expression of all three adipogenesis markers (Figure 5), implying that CP4 and CP5 attenuate adipocyte differentiation.

Phenylcoumarins from increase adiponectin and leptin secretion and decrease resistin secretion

As shown in Figure 6, differentiated 3T3-L1 adipocytes had increased secretions of adiponectin, leptin and resistin compared with undifferentiated pre-adipocytes. Cells treated with ½MNTD CP5 had the highest amount of adiponectin secretion in conditioned medium, consistent with the lowest amount of intracellular adiponectin (Figure. 6A). Leptin secretion in conditioned medium was the highest in cells treated with CP2 (½MNTD), while the same cells had among the lowest intracellular leptin concentration (Figure 6B). Cells treated with CP4 had the highest intracellular leptin concentration. As for resistin, cells treated with CP3 (½MNTD) had the highest secretion (2.5 times higher) compared with differentiated adipocytes, while the lowest for cells treated with CP5 (MNTD) (Figure 6C). For intracellular resistin concentration, cells treated with CP1 (MNTD)
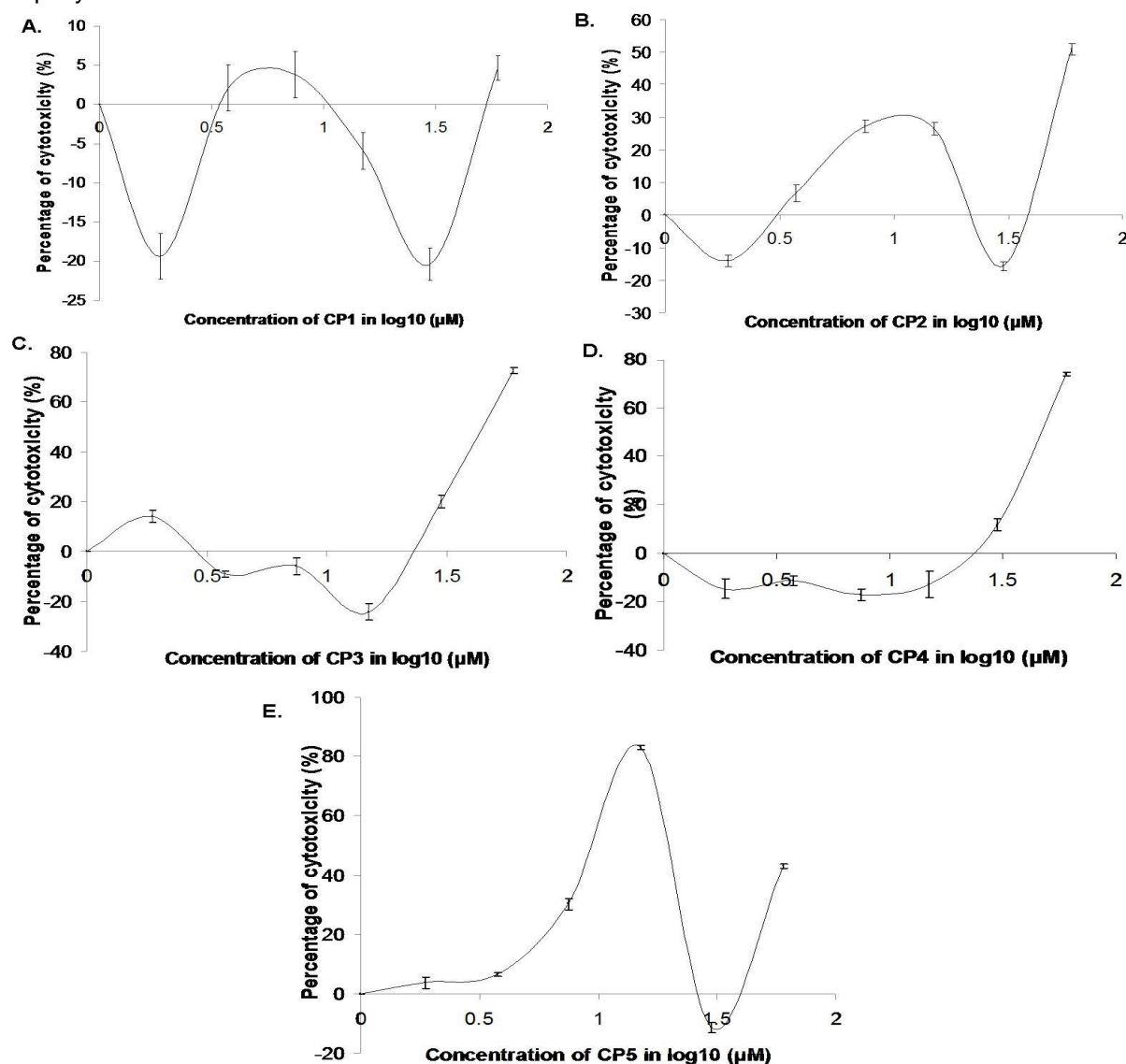
Figure 2: Maximum non-toxic dose (MNTD) and half maximum non-toxic dose (½ MNTD) of CP1 - CP5. Percentage of cytotoxicity of A. CP1; B. CP2; C. CP3; D. CP4; and E. CP4 on 3T3-L1 pre-adipocytes after incubation for 48 h, in two-fold dilution method with the range of 60 µM to 0 µM. MNTDs were determined where the graph intersects the *x*-axis, while ½MNTDs are half of the MNTDs obtained. Data are mean ± SEM of three independent experiments performed in five replicates
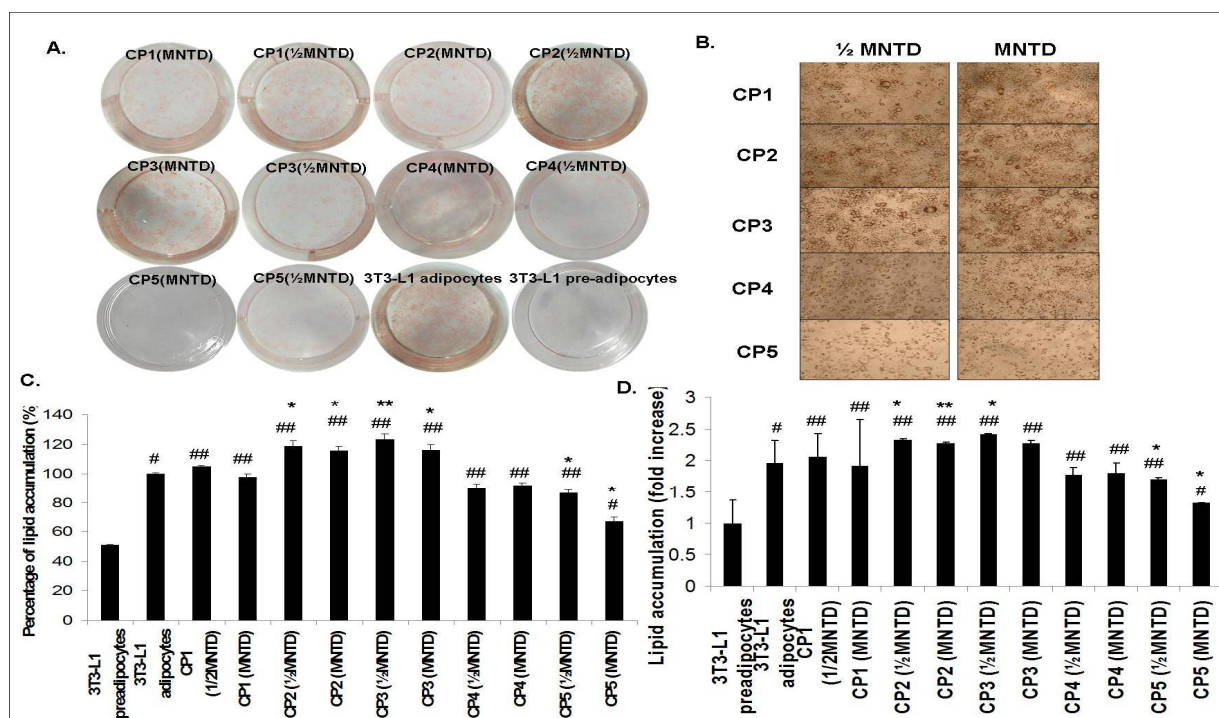
Figure 3: Intracellular lipid droplet accumulation in 3T3-L1 adipocytes. A = representative images after induction of differentiation with the differentiation cocktail along with the MNTDs and ½ MNTDs of CP1 - CP5. Red colour indicates ORO staining; the darker the stain, the higher the intracellular lipid droplet content. The amount of lipid accumulation were compared using the well of 3T3-L1 adipocytes (positive control); B = Representative fields with 100× magnification of the wells in A for CP1 - CP5, showing the sizes of the adipocytes; C = % of lipid accumulation in 3T3-L1 treated cells and controls; D = Fold increases of lipid accumulation in 3T3-L1 treated cells and controls. Results are presented as mean ± SEM (n = 3); *p < 0.05; **p < 0.01 compared with 3T3-L1 adipocytes; #p < 0.05; ##p < 0.01 compared to 3T3-L1 pre-adipocyte
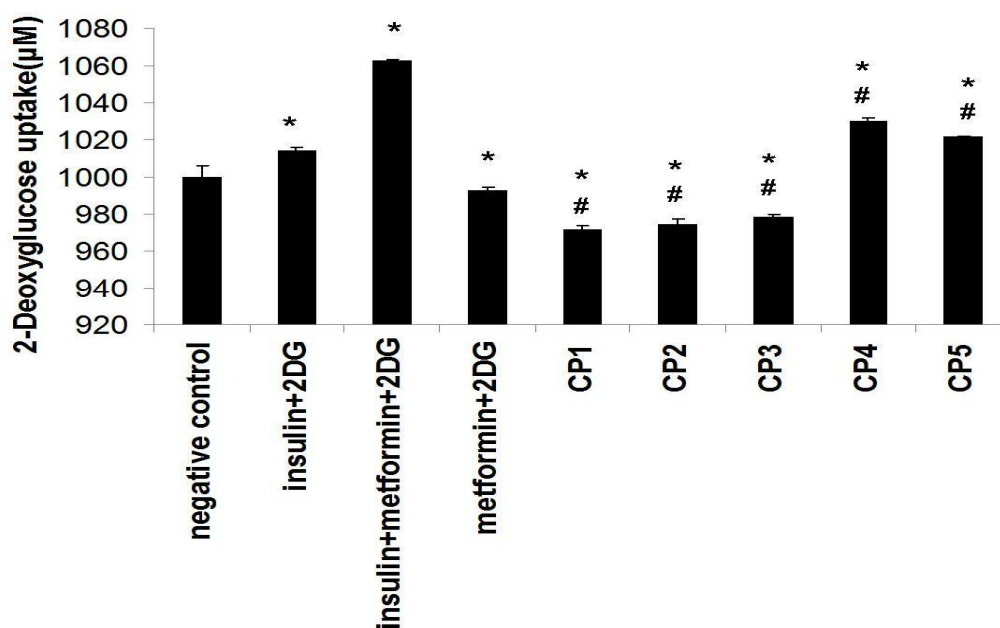
Figure 4: Effect of compounds CP1 - CP5 on cellular glucose uptake in 3T3-L1 adipocytes. Results are presented as mean ± SEM, (n = 3); *p < 0.05 compared with the negative control; #p < 0.05 compared with insulin-treated cells (positive control)
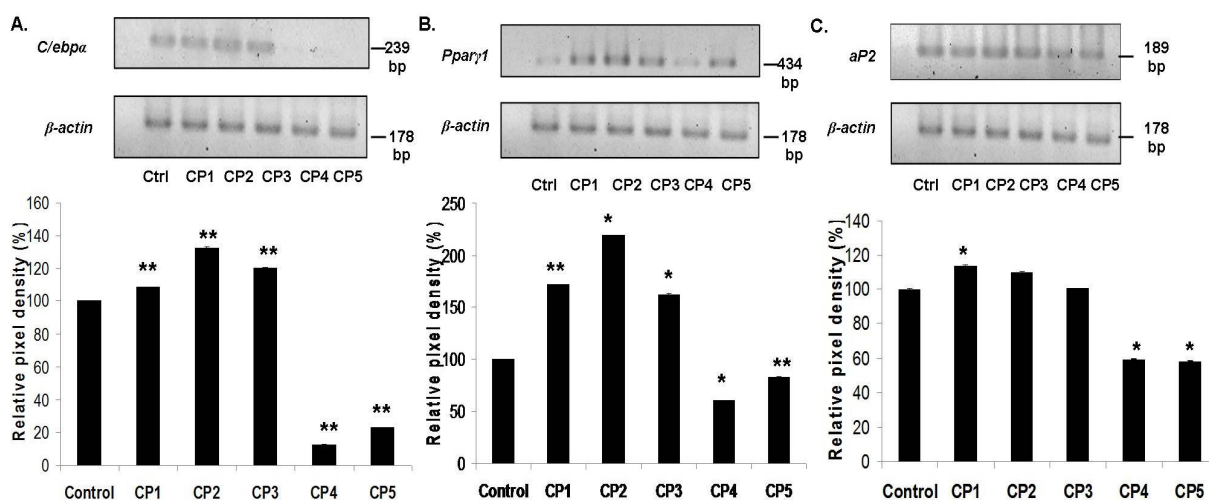
Figure 5: Effect of compounds CP1-CP5 on the expression of adipogenesis markers *C/ebpα*, *Pparγ1* and *aP2* in 3T3-L1 adipocytes. Total RNA was extracted from differentiated 3T3-L1 adipocytes treated with MNTDs of CP1-CP5 compounds and semi quantitative RT-PCR was performed for gene expression of A. *C/ebpα*; B. *Pparγ1* and C. *aP2*. Bar charts depict the densitometry as expressed as relative pixel density and expressed as ratio to *β-actin* (internal control not affected by compound treatment). Data are expressed as a percentage of control (set as 100 %) and values represent mean ± SEM (*n* = 3) of three independent experiments; *p < 0.05; **p <0.01 compared to the control
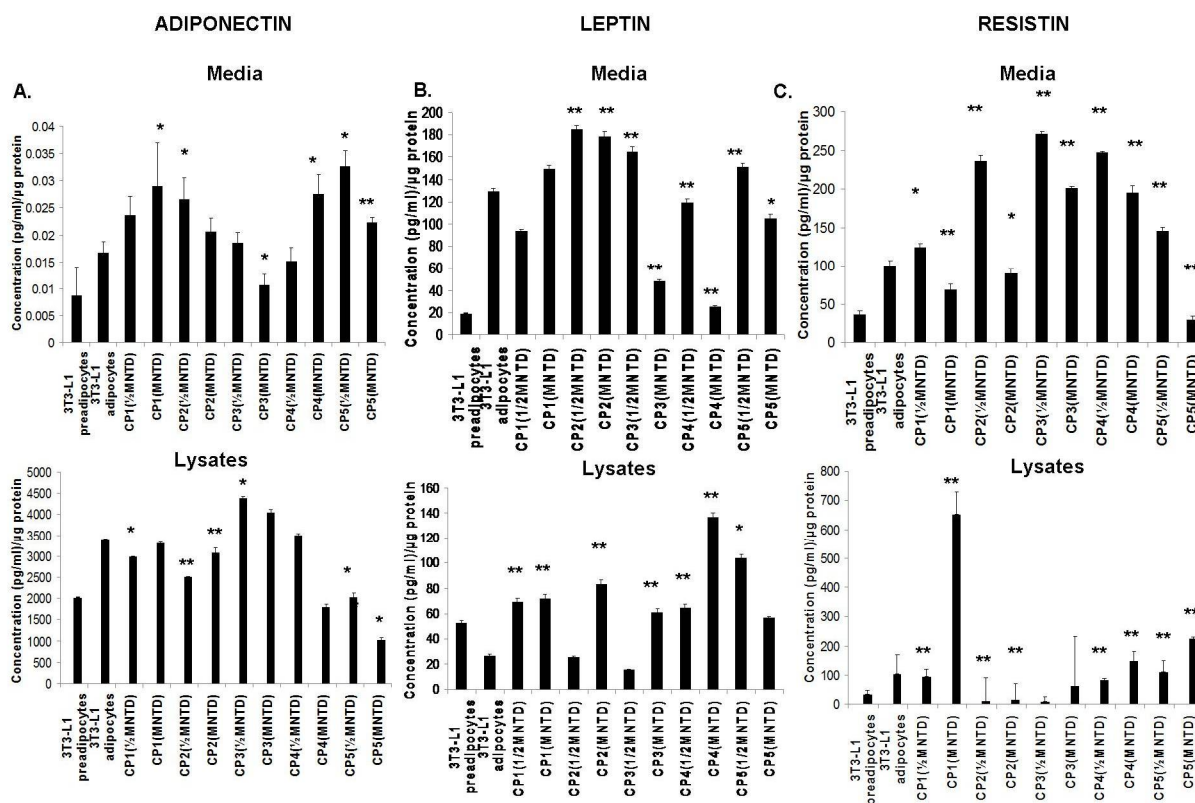
Figure 6: Extracellular secretions and intracellular concentrations of adiponectin, leptin and resistin treated or untreated with ½MNTD and MNTDs of CP1-CP5. Measurements of concentrations for A. Adiponectin; B. Leptin; C. Resistin, were conducted using commercial ELISA kits. Absorbance measurements were normalized per total extracted proteins. Data are expressed as concentration (pg/mL)/µg protein and values represent the mean ± SEM (*n* = 3) of three independent experiments; *p < 0.05, **p < 0.01 compared to 3T3-L1 adipocytes

showed 6.5 times higher level compared with differentiated adipocytes (Figure 6C).

DISCUSSION

Previously, it was shown that friedelin, a triterpenoid isolated from *Garcinia prainiana*, upregulated adipocyte differentiation and glucose uptake in 3T3-L1 adipocytes [6], while esculetin (a coumarin derivative), either naturally isolated from *Fraxinus rhynchophylla* [7] or chemically-synthesized [8], has anti-adipogenic effect. In this study, we found that the anti-adipogenic and pro-glucose uptake activities of CP4 and CP5 are consistent with the reduced expression of adipogenesis markers *Ppary1, C/ebpα, aP2*, increased secretion of adiponectin and reduced secretion of leptin and resistin.

It is widely reported that adipogenesis can be inhibited or promoted by various natural compounds [6-8]. Two out of three coumarins that showed anti-adipogenic activity are CP4 and CP5. Isodipar B (CP3), also a coumarin, however showed pro-adipogenic effect. This may be due to the structural differences within the coumarins, as reported in [7]. There were differences in the moiety of R-group added to coumarin, the backbone of the phytochemicals [6,10].

Methylbutyryl located on a different carbon might cause a difference in activity in adipocytes. In CP3, the R-group is located in C-8 of the coumarin backbone. These results therefore, suggest that methylbutyryl located in C-8 is important for exerting anti-adipogenic effect. For cells treated with CP1 and CP2, an induction in lipid accumulation was observed. Friedelin naturally isolated from *Garcinia prainiana* also exerted the same activity [6], albeit at a higher concentration of 10 µM (*vs*. 3 µM in our study).

Unlike friedelin from *Garcinia prainiana* which promoted cellular glucose uptake in 3T3-L1 adipocytes [6], our results showed the opposite effect. This discrepancy could be due to the higher dose used in our study. For the first time, we observed that treatment with CP4 and CP5 promoted 3T3-L1 adipocyte uptake of glucose, to the extent that it was even significantly higher than the positive control, insulin. Therefore, compounds CP4 and CP5 may imitate the action of insulin in stimulating cellular glucose uptake and it is speculated that these compounds may also reduce blood glucose level *in vivo*. Based on the above findings, it appears that our findings related to the effect of phenylcoumarins CP4 and CP5 on 3T3-L1 adipocytes were in agreement with two other reports [12,13] stating that

compound that inhibits adipocyte differentiation could also improve glucose uptake.

In this study, we also measured the gene expression of three common adipogenesis markers *C/ebpα*, *Ppary1* and *aP2* to see if their expression correlates with the adipocyte differention/lipid droplet accumulation as assessed by ORO staining. *C/ebpα* and *Ppary* activate transcriptional adipogenesis activity by binding to their genomic promoter region interchangeably [14]. Cells treated with CP1, CP2 and CP3 showed pro-adipogenic activity, by increasing *Ppary1, C/ebpα* and *aP2* expression. Conversely, CP4- and CP5-treated cells showed a reduction in the expression of *Ppary1, C/ebpα* and *aP2*. The findings are supported by previous studies which showed that the reduction in adipocyte differentiation and increase in cellular glucose uptake are also correlated with the downregulation of *C/ebpα*, *Ppary1* and *aP2* expression [8,15].

Besides playing a role as an energy depot, the adipose tissue also secretes adipokines that are metabolic regulators. Three adipokines assessed in this study – adiponectin, leptin and resistin, modulate adipogenesis and are correlated with body mass index and total body fat [16]). Plasma levels of leptin and resistin has been shown to be proportional to body fat mass [17,18], whereas plasma adiponectin level is negatively correlated with the percentage of body fat [19]. Therefore, we hypothesized that CP4 and CP5 compounds which show anti-adipogenic/pro-glucose uptake effects would also show increased adiponectin and decreased leptin and resistin secretions in 3T3-L1 adipocytes. However, we found that CP1 - CP4 (MNTD) compounds produced mixed effects on the secretions of these adipokines, which do not correlate with their adipogenic/glucose uptake properties shown earlier. This phenomenon could be due to the unassessed complex signaling pathways that modulate the secretion of these adipokines and adipogenesis/glucose uptake independently. Nevertheless, CP5 (MNTD) consistently produced increased adiponectin and reduced leptin and resistin secretions, compared with untreated cells. Similarly, ginsenoside has been shown to reduce 3T3-L1 adipocyte lipid accumulation and increase adiponectin expression [20], while *Lysimachia foenum-graecum* treatment increased adiponectin level while decreasing leptin and resistin levels in the plasma of treated mice [21].

CONCLUSION

Friedelin and friedelinol isolated from *Calophyllum andersonnii* promote adipogenesis by increasing intracellular lipid droplet accumulation and expression of adipogenesis-related genes including *Pparγ1, C/ebpα and aP2*, and also by decreasing cellular glucose uptake in 3T3-L1 adipocytes. On the other hand, 5,7-dihydroxy-6-(3-methybutyryl)-4-phenylcoumarin and 5,7-dihydroxy-6-(2-methybutyryl)-4-phenyl-coumarin isolated from *Calophyllum sclerophyllum* show promising anti-obesity properties by attenuating adipogenesis (decreasing intracellular lipid droplet accumulation and expression of *Pparγ1, C/ebpα* and *aP2*), and also by increasing 3T3-L1 adipocyte glucose uptake. Last but not least, 5,7-dihydroxy-6-(2-methybutyryl)-4-phenylcoumarin increases adiponectin and reduces leptin and resistin secretions from 3T3-L1 treated cells.

DECLARATIONS

Acknowledgement

Conflict of Interest

No conflict of interest associated with this work.

Contribution of Authors

The authors declare that this work was done by the authors named in this article and all liabilities pertaining to claims relating to the content of this article will be borne by them.

Open Access

REFERENCES

1. *Crane S, Aurore G, Joseph H, Mouloungui Z, Bourgeois P. Composition of fatty acids triacylglycerols and unsaponifiable matter in Calophyllum calaba l. Oil from guadeloupe. Phytochemistry 2005; 66: 1825–1831.*

2. *Dweck AC, Meadows T. Tamanu (Calophyllum inophyllum) - the African, Asian, Polynesian and Pacific Panacea. Int J Cosmetic Sci 2002; 24: 341-348.*

3. *Cechinel VF, Meyre-Silva C, Niero R. Chemical and pharmacological aspects of the genus Calophyllum. Chem Biodiv 2009; 6: 313–327.*

4. *Lim CK, Hemaroopini S, Gan SY, Loo SM, Low JR, Jong VYM, Soo HC, Leong CO, Mai CW, Chee CF. In vitro cytotoxic activity of isolated compounds from Malaysian Calophyllum species. Med Chem Res. 2016; 25: 1686-1694.*

5. *Lee I, Kim H, Youn U, Kim J, Min B, Jung H, Na M, Hattori M, Bae K. Effect of lanostane triterpenes from the fruiting bodies of Ganoderma lucidum on adipocyte differentiation in 3T3-L1 Cells. Planta Med 2010; 76: 1558-1563.*

6. *Susanti D, Amiroudine M, Rezali M, Taher M. Friedelin and lanosterol from Garcinia prainiana stimulated glucose uptake and adipocytes differentiation in 3T3-L1 adipocytes. Nat Prod Res 2013; 27: 417-424.*

7. *Shin E, Choi K, Yoo H, Lee C, Hwang B, Lee M. Inhibitory effects of coumarins from the stem barks of Fraxinus rhynchophylla on adipocyte differentiation in 3T3-L1 cells. Biol Pharm Bull 2010; 33: 1610-1614.*

8. *Kim Y, Lee J. Esculetin, a coumarin derivative, suppresses adipogenesis through modulation of the AMPK pathway in 3T3-L1 adipocytes. J Funct Foods 2015; 12: 509-515.*

9. *Nerurkar P, Lee Y, Nerurkar V. Momordica charantia (bitter melon) inhibits primary human adipocyte differentiation by modulating adipogenic genes. BMC Complement Altern Med 2010; 10: 34.*

10. *Song Y, Park H, Kang S, Jang S, Lee S, Ko Y, Kim G, Cho J. Blueberry peel extracts inhibit adipogenesis in 3T3-L1 cells and reduce high-fat diet-induced obesity. PLoS ONE 2013; 8: e69925.*

11. *Jain P, Joshi H. Coumarin: Chemical and pharmacological profile. J App Pharm Sci 2012; 2: 236-240.*

12. *Anand S, Muthusamy V, Sujatha S, Sangeetha K, Bharathi RR, Sudhagar S, Poornima DN, Lakshmi B. Aloe emodin glycosides stimulates glucose transport and glycogen storage through PI3K dependent mechanism in L6 myotubes and inhibits adipocyte differentiation in 3T3L1 adipocytes. FEBS Lett 2010; 584: 3170-3178.*

13. *Taher M, Mohamed AM, Tengku ZT, Susanti D, Ichwan S, Kaderi M, Ahmed Q, Zakaria Z. α-Mangostin improves glucose uptake and inhibits adipocytes differentiation in 3T3-L1 cells via PPARγ, GLUT4, and leptin expressions. Evid Based Complement Altern Med 2015; 2015: 740238.*

14. *Lee J, Ge K. Transcriptional and epigenetic regulation of PPARγ expression during adipogenesis. Cell Biosci 2014; 4: 29.*

15. Kowalska K, Olejnik A, Rychlik J, Grajek W. Cranberries *(Oxycoccus quadripetalus) inhibit lipid metabolism and modulate leptin and adiponectin secretion in 3T3-L1 adipocytes. Food Chem 2015; 185: 383-388.*

16. Makki K, Froguel P, Wolowczuk I. *Adipose tissue in obesity-related inflammation and insulin resistance: cells, cytokines, and chemokines. ISRN Inflamm 2013; 2013: 139239.*

17. Friedman J, Halaas J. *Leptin and the regulation of body weight in mammals. Nature 1998; 395: 763-770.*

18. Steppan CM, Bailey ST, Bhat S, Brown EJ, Banerjee RR, Wright CM, Patel HR, Ahima RS, Lazar MA. *The hormone resistin links obesity to diabetes. Nature 2001; 409: 307-312.*

19. Yamauchi T, Kamon J, Waki H, Terauchi Y, Kubota N, Hara K, Mori Y, Ide T, Murakami K, Tsuboyama-Kasaoka N, et al. *The fat-derived hormone adiponectin reverses insulin resistance associated with both lipoatrophy and obesity. Nat Med 2001; 7: 941-946.*

20. Yeo CR, Lee SM, Popovich DG. *Ginseng (Panax quinquefolius) reduces cell growth, lipid acquisition and increases adiponectin expression in 3T3-L1 cells. Evid Based Complement Alternat Med 2011; 2011: 610625.*

21. Seo JB, Choe SS, Jeong HW, Park SW, Shin HJ, Choi SM, Park JY, Choi EW, Kim JB, Seen DS, et al. *Anti-obesity effects of Lysimachia foenum-graecum characterized by decreased adipogenesis and regulated lipid metabolism. Exp Mol Med 2011; 43: 205-215.*

NATURAL PRODUCT COMMUNICATIONS

INFORMATION FOR AUTHORS

Full details of how to submit a manuscript for publication in Natural Product Communications are given in Information for Authors on our Web site http://www.naturalproduct.us.

Authors may reproduce/republish portions of their published contribution without seeking permission from NPC, provided that any such republication is accompanied by an acknowledgment (original citation)-Reproduced by permission of Natural Product Communications. Any unauthorized reproduction, transmission or storage may result in either civil or criminal liability.

The publication of each of the articles contained herein is protected by copyright. Except as allowed under national "fair use" laws, copying is not permitted by any means or for any purpose, such as for distribution to any third party (whether by sale, loan, gift, or otherwise); as agent (express or implied) of any third party; for purposes of advertising or promotion; or to create collective or derivative works. Such permission requests, or other inquiries, should be addressed to the Natural Product Inc. (NPI). A photocopy license is available from the NPI for institutional subscribers that need to make multiple copies of single articles for internal study or research purposes.

To Subscribe: Natural Product Communications is a journal published monthly. 2017 subscription price: US$2,595 (Print, ISSN# 1934-578X); US$2,595 (Web edition, ISSN# 1555-9475); US$2,995 (Print + single site online); US$595 (Personal online). Orders should be addressed to Subscription Department, Natural Product Communications, Natural Product Inc., 7963 Anderson Park Lane, Westerville, Ohio 43081, USA. Subscriptions are renewed on an annual basis. Claims for nonreceipt of issues will be honored if made within three months of publication of the issue. All issues are dispatched by airmail throughout the world, excluding the USA and Canada.

Cytotoxic Compounds from the Stem Bark of *Calophyllum soulattri*

Chan-Kiang Lim[a,*], **Subramaniam Hemaroopini**[a], **Yee-How Say**[b] and **Vivien Yi-Mian Jong**[c]

[a]*Department of Chemical Science, Faculty of Science, Universiti Tunku Abdul Rahman, Jalan Universiti, Bandar Barat, 31900 Kampar, Perak, Malaysia*

[b]*Department of Biomedical Science, Faculty of Science, Universiti Tunku Abdul Rahman, Jalan Universiti, Bandar Barat, 31900 Kampar, Perak, Malaysia*

[c]*Centre for Applied Sciences, Faculty of Applied Sciences, Universiti Teknologi MARA, Samarahan Campus 2, Jalan Meranek, 94300 Kota Samarahan, Sarawak, Malaysia*

cklim@utar.edu.my

Chemical investigation of the stem bark of *Calophyllum soulattri* resulted in the isolation of a new phloroglucinol, namely calosubellinone (**1**) along with two known compounds, garsubellin B (**2**) and soulattrone A (**3**). The structures of these compounds were established on the basis of spectroscopic methods. Compounds **1** and **2** displayed growth inhibitory activities against HeLa cancer cells comparable to the positive control cisplatin, with IC$_{50}$ values of 19.3 and 16.5 µM, respectively. In addition, compound **2** also showed antiproliferative activity against a MDA-MB-231 cancer cell line with an IC$_{50}$ value of 17.7 µM. Compounds **1** and **2** were found to exhibit good cancer-specific cytotoxicity when tested against noncancerous HEK293 cells. These findings have highlighted the therapeutic potential of compounds **1** and **2** as anticancer agents.

Keywords: *Calophyllum soulattri*, Calosubellinone, Garsubellin B, Cytotoxicity, HeLa, MDA-MB-231, LS174T, T98G.

The genus *Calophyllum,* belonging to the family Clusiaceae, is found to be abundant in bioactive chromanones, coumarins, xanthones, and triterpenoids [1], and a number of these compounds were reported to show interesting biological properties, such as antimalarial [2], anticancer [3], antiviral [4], antibacterial [5], antidiabetic [6], antifilarial [7] and antioxidant activities [8]. Previous phytochemical studies by Gwen and co-workers on *C. soulattri* reported the isolation of pyranocoumarins [9], xanthones [3, 10] and triterpenoids [9, 10]. Soulattrin, a linear pyranoxanthone isolated from stem bark of *C. soulattri,* was found to exhibit potent antiproliferative activities against HeLa (cervical), K562 (leukaemia), NCI-H23 (lung) and SNU-1 (stomach) cancer cell lines with IC$_{50}$ values of below 3.0 µM [3]. In pursuit of more biological active compounds from *C. soulattri*, we had also studied the stem bark extract of this plant which has led to the isolation of a new phloroglucinol, calosubellinone (**1**), and two known compounds, garsubellin B (**2**) and soulattrone A (**3**). Phloroglucinols **1** and **2** were reported for the first time from *Calophyllum* species.

A phytochemical study of the dichloromethane extract afforded two phloroglucinols, **1** and **2**, and a terpenoid **3**. Calosubellinone (**1**) was isolated via column chromatography (CC) as a yellow gum, giving a specific rotation, [α]$_D$ of +15.6° (EtOH, *c* 0.60) at room temperature. This compound showed a retention factor, R$_f$ value of 0.62 via a mobile phase of 8:1:1 *n*-hexane/CH$_2$Cl$_2$/EtOAc. The molecular formula C$_{31}$H$_{46}$O$_5$ was deduced from the EIMS ([M]$^+$·at *m/z* 498) and HR-EIMS ([M]$^+$·at *m/z* 498.33612). The IR spectrum displayed absorption bands at 3440 (O-H stretch), 2954 (C-H stretch), 1727 (C=O stretch) and 1149 (C-O stretch).

The ^{1}H and ^{13}C NMR spectra of **1** (Supplementary Figures S1 to S4) revealed resonances for the presence of three isoprenyl groups [δ$_H$ 4.90 (1H, t, *J* = 7.3 Hz, H-13), 2.06 (2H, m, H-12), 1.67 (3H, s, H-16) and 1.53 (3H, s, H-15); δ$_C$ 133.4 (C-14), 122.2 (C-13), 27.8 (C-12), 25.9 (C-16) and 18.0 (C-15)], [δ$_H$ 5.26 (1H, t, *J* = 7.3 Hz,
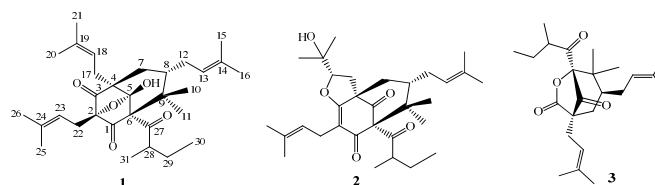
Figure 1: Structures of isolated compounds **1-3** from *C. soulattri*.

H-18), 2.40 (2H, m, H-17), 1.67 (3H, s, H-21) and 1.54 (3H, s, H-20); δ$_C$ 133.8 (C-19), 119.0 (C-18), 31.0 (C-17), 25.9 (C-21) and 17.8 (C-20)], [δ$_H$ 5.00 (1H, t, *J* = 7.3 Hz, H-23), 2.74 (1H, dd, *J* = 15.9, 7.3 Hz, H$_a$-22), 2.47 (1H, dd, *J* = 15.3, 7.3 Hz, H$_b$-22), 1.63 (3H, s, H-26) and 1.62 (3H, s, H-25); δ$_C$ 135.8 (C-24), 116.0 (C-23), 23.8 (C-22), 26.1 (C-26) and 18.0 (C-25)] and a 2-methyl-butanoyl group [δ$_H$ 2.94 (1H, sext, *J* = 6.7 Hz, H-28), 1.50 (2H, m, H-29), 0.91 (3H, t, *J* = 7.3 Hz, H-30) and 0.87 (3H, d, *J* = 6.7 Hz, H-31); δ$_C$ 217.5 (C-27), 45.8 (C-28), 24.7 (C-29), 16.1 (C-31) and 11.7 (C-30)]. The 10-oxatricyclo[3.3.1.1]decane-2,4-dione nucleus of **1** gave rise to the carbon resonances at δ$_C$ 209.2 (C-3), 206.9 (C-1), 108.0 (C-5), 97.3 (C-2), 70.4 (C-6), 54.9 (C-4), 44.1 (C-9), 41.1 (C-8) and 33.2 (C-7).

In the HMBC spectrum (Supplementary Figure S5), key correlations from the methylene protons H-17 to C-4 (δ$_C$ 54.9), and H-22 to C-1 (δ$_C$ 206.9), C-2 (δ$_C$ 97.3) and C-3 (δ$_C$ 209.2) suggested two isoprenyl groups were separately attached to the ring structure at carbon positions C-4 and C-2. While the HMBC correlations from OH to C-4 (δ$_C$ 54.9), C-5 (δ$_C$ 108.0) and C-6 (δ$_C$ 70.4) suggested the OH group to be attached to the acetal-type quaternary carbon C-5. Moreover, both the geminal dimethyl groups, H-10 and H-11 showed correlations with carbons C-6 (δ$_C$ 70.4), C-8 (δ$_C$ 41.1) and C-9 (δ$_C$ 44.1) indicating the two methyl groups to be linked to the quaternary carbon C-9. The 2-methylbutanoyl group was attached to the relatively deshielded methine carbon C-6 (δ$_C$ 70.4) due to the anisotropic effect of the adjacent keto carbonyl of the

2-methylbutanoyl group and the ring keto carbonyl group linked to it. Lastly, the third isoprenyl group was found to be attached to the remaining methine carbon C-8 in the ring. The relative configurations at the chiral carbons C-4, C-6 and C-8 were assumed to be analogous to those related carbons in compound **2**. Compound **1** was therefore established to be calosubellinone with its chemical structure being displayed in Figure 1. Compounds **2** and **3** were identified as garsubellin B and soulattrone A based on their NMR and MS data and comparison with the reported values [11, 12].

Compounds **1-3** were screened for their cytotoxic activities against four cancer cell lines, HeLa (cervical carcinoma), MDA-MB-231 (breast adenocarcinoma), LS174T (colorectal carcinoma), T98G (ganglioblastoma) and a normal human cell line, HEK293 (human embryonic kidney cells). The results of the assays of the isolates are displayed in Table 1. Compounds **1** and **2** were cytotoxic against the HeLa cancer cell line with IC_{50} values of 19.3 and 16.5 μM, respectively, comparable to the positive control cisplatin. Compound **2** also exhibited growth inhibitory activity against MDA-MB-231 cancer cells with an IC_{50} value of 17.7 μM. While compound **3** showed only weak activities against the four cancer cell lines.

Table 1: Growth inhibitory activities of compounds **1-3** and positive controls.

Compounds	IC_{50} (μM)[a]				
	HeLa	MDA-MB-231	LS174T	T98G	HEK293
Calosubellinone (**1**)	19.3±1.6	43.8±0.4	62.7±0.4	29.5±1.4	>200
Garsubellin B (**2**)	16.5±1.0	17.7±2.4	53.4±1.8	60.2±0.4	>200
Soulattrone A (**3**)	72.9±0.5	72.2±2.3	70.9±3.4	>100	>200
Cisplatin[b]	16.3±1.3	-	31.0±5.0	39.3±2.0	-
Doxorubicin[b]	-	4.2±0.4	-	-	-

[a]Data are reported as means ± SD for minimum three independent experiments.
[b]Positive controls.

When treated with noncancerous HEK293 cells, compounds **1** and **2** were found to exhibit good cancer-specific cytotoxicity against HeLa cells. The IC_{50} values for compounds **1** and **2** against normal human embryonic kidney cells, HEK293, were at least 10-fold higher than that for HeLa cancer cells. Further, compound **2** also showed good cancer-specific cytotoxicity against MDA-MB-231 cells.

Experimental

General: Melting points were determined on a Stuart SMP10 melting point apparatus (Barloworld Scientific Limited, Staffordshire, UK) and are uncorrected. Optical rotations were performed on a JASCO P-1020 polarimeter (JASCO, Tokyo, Japan). IR spectra were obtained in KBr using a Perkin–Elmer Spectrum RXI FTIR spectrophotometer (Perkin-Elmer, Waltham, MA, US). NMR spectra were measured on a JEOL JNM-ECX 400 MHz FTNMR spectrometer (JEOL, Tokyo, Japan) in CDCl₃ with TMS as the internal standard. Chemical shifts (δ) are reported in ppm and coupling constants (*J*) are expressed in Hertz. EIMS and HR-EIMS were acquired on an Agilent 5975C MSD (Agilent Technologies, Santa Clara, CA, US) and Thermo Finnigan MAT95XL (Thermo Fisher, Bremen, Germany) mass spectrometers, respectively. All reagents were of analytical quality and used without further purification unless otherwise specified. Column chromatography was performed with silica gel 60 (230–300 mesh, Merck, Darmstadt, Germany) via gradient elution and sephadex LH-20 (GE Healthcare, US) via isocratic elution. Analytical TLC was performed on precoated silica gel 60 F_{254} (Merck, Darmstadt, Germany).

Plant material: The stem bark of *C. soulattri* was collected from the jungle in Landeh district of Sarawak, Malaysia, and was identified by Mr. Tinjan Anak Kuda, botanist from the Forest Department, Sarawak. Voucher specimen (UITM 3010) was deposited at the herbarium of Universiti Teknologi MARA, Sarawak.

Extraction and isolation: About 1.5 kg of dried and ground stem bark material of *C. soulattri* was extracted twice, each time with 10 L of CH₂Cl₂ at room temperature for 72 h. The combined CH₂Cl₂ extract was concentrated under reduced pressure by using a rotary evaporator to give 24.8 g of dried CH₂Cl₂ extract. About 20 g of CH₂Cl₂ extract was subjected to silica gel CC (40-63 μm, 8.5 x 50 cm, 600 g) packed in *n*-hexane and eluted with *n*-hexane-CH₂Cl₂ mixtures of increasing polarity (90:10, 80:20, 70:30, 60:40, 50:50, 40:60, 30:70, 20:80, 10:90, 0:100), followed by increasing concentration of EtOAc in CH₂Cl₂ (10:90, 20:80, 30:70, 40:60, 50:50, 60:40, 70:30, 80:20, 90:10, 100:0) to give 21 fractions (HECA1-21). Fraction HECA3 (4.8 g) was purified via silica gel CC (40-63 μm, 3.5 x 50 cm, 150 g) packed in *n*-hexane and eluted with *n*-hexane-CH₂Cl₂ mixtures of increasing polarity (90:10, 80:20, 70:30, 60:40, 50:50, 40:60, 30:70, 20:80, 10:90, 0:100), followed by increasing concentration of EtOAc in CH₂Cl₂ (10:90, 20:80, 30:70, 40:60, 50:50, 60:40, 70:30, 80:20, 90:10, 100:0) giving rise to 20 fractions (HECC1-20). Subfractions HECC3-4 (1.8 g) were combined and purified further via Sephadex LH-20 packed column eluted with a mobile phase of 9:1 MeOH/CH₂Cl₂ to yield 10 subfractions (HECN1-10). Subfraction HECN4 (0.3 g) was selected and further subjected to Sephadex LH-20 column chromatography eluted with 9:1 MeOH/CH₂Cl₂ to give 26 subfractions (HECP1-26). Subfractions HECP24-26 yielded calosubellinone (**1**) as a yellow gum (75 mg). Fraction HECA9 (2.1 g) was fractionated via silica gel CC (40-63 μm, 3.5 x 50 cm, 150 g) packed in *n*-hexane and eluted with *n*-hexane-CH₂Cl₂ mixtures of increasing polarity (90:10, 80:20, 70:30, 60:40, 50:50, 40:60, 30:70, 20:80, 10:90, 0:100), followed by increasing concentration of EtOAc in CH₂Cl₂ (10:90, 20:80, 30:70, 40:60, 50:50, 60:40, 70:30, 80:20, 90:10, 100:0) to give 19 subfractions (HECE1-19). Subfraction HECE9 afforded garsubellin B (**2**) as a yellow solid (257 mg). Fraction HECA5 (1.8 g) was fractionated via silica gel CC (40-63 μm, 3.5 x 50 cm, 150 g) packed in *n*-hexane and eluted with same solvent system as above to give 13 subfractions (HECH1-13), in which subfractions HECH4-8 (0.75 g) were purified by using Sephadex LH-20 column eluted with 9:1 MeOH/CH₂Cl₂ to give 33 subfractions (HECQ1-33). Subfractions HECQ23-28 afforded soulattrone A (**3**) as white needles (17 mg).

Calosubellinone (1)

Yellow gum.
$[α]_D$: +15.6 (*c* 0.60, EtOH).
IR $υ_{max}$ (KBr): 3440, 2954, 1727 and 1149 cm⁻¹.
¹H NMR (400 MHz, CDCl₃): 8.11 (1H, s, 5-OH), 5.26 (1H, t, *J* = 7.3 Hz, H-18), 5.00 (1H, t, *J* = 7.3 Hz, H-23), 4.90 (1H, t, *J* = 7.3 Hz, H-13), 2.94 (1H, sext, *J* = 6.7 Hz, H-28), 2.74 (1H, dd, *J* = 15.9, 7.3 Hz, H_a-22), 2.47 (1H, dd, *J* = 15.3, 7.3 Hz, H_b-22), 2.40 (2H, m, H-17), 2.06 (2H, m, H-12), 1.87 (1H, dd, *J* = 14.0, 3.6 Hz, H_a-7), 1.67 (6H, s, H-16 & H-21), 1.63 (3H, s, H-26), 1.62 (3H, s, H-25), 1.54 (3H, s, H-20), 1.53 (3H, s, H-15), 1.50 (2H, m, H-29), 1.22 (3H, s, H-11), 1.21 (1H, m, H_b-7), 0.93 (1H, m, H-8), 0.92 (3H, s, H-10), 0.91 (3H, t, *J* = 7.3 Hz, H-30), 0.87 (3H, d, *J* = 6.7 Hz, H-31).
¹³C NMR (100 MHz, CDCl₃): 217.5 (C-27), 209.2 (C-3), 206.9 (C-1), 135.8 (C-24), 133.8 (C-19), 133.4 (C-14), 122.2 (C-13), 119.0 (C-18), 116.0 (C-23), 108.0 (C-5), 97.3 (C-2), 70.4 (C-6), 54.9 (C-4), 45.8 (C-28), 44.1 (C-9), 41.1 (C-8), 33.2 (C-7), 31.0 (C-17),

27.8 (C-12), 26.1 (C-26), 25.9 (C-16 & C-21), 24.7 (C-29), 23.8 (C-22), 23.0 (C-11), 18.0 (C-15 & H-25), 17.8 (C-20), 17.7 (C-10), 16.1 (C-31), 11.7 (C-30).

EIMS *m/z* (rel. int.): 498 ($[M]^{+\cdot}$ 2), 401 (17), 333 (43), 289 (11), 265 (31), 209 (17), 85 (23), 69 (100), 57 (54), 41 (37).

HREI-MS: 498.33612 ($[M]^{+\cdot}$, $C_{31}H_{46}O_5^{+\cdot}$; calcd 498.33453).

Cell culture: HeLa, MDA-MB-231 and LS174T cells were cultured in Dulbecco's Modified Eagle's Medium (DMEM) while T98G in Modified Eagle's Medium (MEM). The cancer cells were supplemented with 5% Fetal Bovine Serum (FBS) and 1% penicillin-streptomycin, and were maintained at 37 °C in 5% CO_2 incubator.

Cytotoxicity assay: Compounds **1-3** were tested on the cervical carcinoma (HeLa), breast adenocarcinoma (MDA-MB-231), colorectal carcinoma (LS174T), ganglioblastoma (T98G) cancer cell lines and human embryonic kidney (HEK293) normal cell line using the methyl thiazolyltetrazolium (MTT) cell viability assay as described previously by Mosmann [13]. Cisplatin and doxorubicin were used as positive controls.

Supplementary data: ^{1}H, ^{13}C, HMQC and HMBC NMR spectra for compound **1** are available.

References

[1]   Oliveira MC, Lemos LMS, de Oliveira RG, Dall'Oglio EL, de Sousa Júnior PT, de Oliveira Martins DT. (**2014**) Evaluation of toxicity of *Calophyllum brasiliense* stem bark extract by *in vivo* and *in vitro* assays. *Journal of Ethnopharmacology*, **155**, 30-38.

[2]   Hay AE, Hélesbeux JJ, Duval O, Labaïed M, Grellier P, Richomme P. (**2004**) Antimalarial xanthones from *Calophyllum caledonicum* and *Garcinia vieillardii*. *Life Sciences*, **75**, 3077-3085.

[3]   Mah SH, Ee GCL, Teh SS, Sukari MA. (**2015**) *Calophyllum inophyllum* and *Calophyllum soulattri* source of anti-proliferative xanthones and their structure–activity relationships. *Natural Product Research*, **29**, 98-101.

[4]   Brahmachari G, Jash SK. (**2014**) Naturally occurring calanolides: an update on their anti-HIV potential and total syntheses. *Recent Patents on Biotechnology*, **8**, 3-16.

[5]   Cuesta-Rubio O, Oubada A, Bello A, Maes L, Cos P, Monzote L. (**2015**) Antimicrobial assessment of resins from *Calophyllum antillanum* and *Calophyllum inophyllum*. *Phytotherapy Research*, **29**, 1991-1994.

[6]   Aminudin NI, Ahmad F, Taher M, Zulkifli RM. (**2015**) α-Glucosidase and 15-lipoxygenase inhibitory activities of phytochemicals from *Calophyllum symingtonianum*. *Natural Product Communications*, **10**, 1585-1588.

[7]   Jankiprasad, Naresh G, Gupta J, Bhattacharya SM, Rajendran SM, Shailendra K. Awasthi, Narender T. (**2013**) Antifilarial activity of constituents of *Calophyllum inophyllum* and their derivatives. *Natural Product Communications*, **8**, 803-804.

[8]   Taher M, Attoumani N, Susanti D, Ichwan SJA, Ahmad F. (**2010**) Antioxidant activity of leaves of *Calophyllum rubiginosum*. *American Journal of Applied Sciences*, **7**, 1305-1309.

[9]   Ee GCL, Mah SH, Teh SS, Rahmani M, Go R, Taufiq-Yap YH. (**2011**) Soulamarin, a new coumarin from stem bark of *Calophyllum soulattri*. *Molecules*, **16**, 9721-9727.

[10]   Mah SH, Ee GCL, Rahmani M, Taufiq-Yap YH, Sukari MA, Teh SS. (**2011**) A new pyranoxanthone from *Calophyllum soulattri*. *Molecules*, **16**, 3999-4004.

[11]   Fukuyama Y, Minami H, Kuwayama A. (**1998**) Garsubellins, polyisoprenylated phloroglucinol derivatives from *Garcinia subelliptica*. *Phytochemistry*, **49**, 853-857.

[12]   Nigam SK, Banerji R, Rebuffat S, Cesario M, Pascard C, Bodo B. (**1988**) Soulattrone A, a C_{24} terpenoid from *Calophyllum soulattri*. *Phytochemistry*, **27**, 527-530.

[13]   Mosmann T. (**1983**) Rapid colorimetric assay for cellular growth and survival: application to proliferation and cytotoxicity assays. *Journal of Immunological Methods*, **65**, 55-63.

Accounts/Reviews

Natural Product Communications
2017
Volume 12, Number 9

Contents

Continued inside backcover